University of Glasgow

Euston, Eloise (2023) *Investigating the physiological functions of free fatty acid receptor 4 in the lung and colon following synthetic agonist activation.* PhD thesis.

https://theses.gla.ac.uk/83457/

Investigating the physiological functions of free fatty acid receptor 4 in the lung and colon following synthetic agonist activation

Eloise Euston

BSc (Hons)

Submitted in fulfilment of the requirements for the Degree of

Doctor of Philosophy

School of Molecular Biosciences

College of Medical, Veterinary and Life Science

University of Glasgow

September 2022

Abstract

Free fatty acids not only function as dietary nutrients but act as signalling molecules by activating the free fatty acid family of G protein-coupled receptors. Following deorphanisation in 2005, FFA4 was found to be abundantly expressed in the colon where it was suggested to play a role in GLP-1 incretin secretion. This has been the basis for the development of synthetic FFA4 agonists as treatment for type 2 diabetes mellitus. Although more recently, the role of FFA4 in the lung, a tissue which also show high levels of FFA4 expression, has been investigated. Within the lung, FFA4 has been shown to exert anti-inflammatory effects in lung resident macrophages, as well as mediating airway smooth muscle relaxation. Therefore, FFA4 represents an attractive drug target for both metabolic diseases and inflammatory lung diseases. However, there is a substantial lack of FFA4 agonists reaching clinical trials due to a limited number of available agonists, issues with selectivity of drugs and poor pharmacokinetic and pharmacodynamic properties, which highlights the need for greater interest in the development and scientific research of these receptor agonists. This thesis aimed to extend on previous work performed in our lab, exploring the roles of FFA4 receptor agonists in airway smooth muscle relaxation and the previously undefined role that phosphorylation may play in airway smooth muscle relaxation. Additionally, the involvement of FFA4 in GLP-1 incretin secretion is a somewhat controversial topic, with reports suggesting that FFA4 is a primary mechanism in GLP-1 secretion and opposing reports suggesting that FFA4 has no involvement in the role of GLP-1 secretion from the colon. This thesis also aimed to answer the question of whether GLP-1 release is mediated by FFA4 activity.

To characterise signalling mechanisms for the mouse FFA4 receptor, functional assays were performed on cell lines which stably express the mouse ortholog of FFA4. Here it was confirmed that FFA4 primarily couples to Gαq/11 G proteins, with no evidence of Gαs or Gαi coupling in cell lines. Additionally, bias factor calculations were performed which indicated that carboxylic agonist, Agonist 2, displayed bias towards IP1 signalling pathways. Similarly, signalling mechanisms of phosphorylation deficient (PD) mouse FFA4 were also characterised using the same functional assays. Here, agonist activation of the PD-mFFA4 receptor

induced enhanced IP1 and pERK1/2 signalling but resulted in a loss β-arrestin2 coupling and receptor internalisation. Functional bias calculations revealed that several agonists acting on the PD-mFFA4 receptor display bias towards IP1 signalling, revealing a complex nature of signalling downstream of Gq:receptor coupling.

Functional experiments to assess the physiological roles of FFA4 in the lung and colon revealed some interesting results. Quantification of mouse lung airway diameter following FFA4 agonist addition to pre-contracted airways indicated a robust relaxation of airway smooth muscle. Furthermore, in a novel finding, there was an indication that airway relaxation was mediated in part by receptor phosphorylation. Additionally, to understand the contribution of FFA4 in GLP-1 release from the colon, experiments assessing GLP-1 release from primary colonic crypts following FFA4 agonist treatment were performed. Following 50 µM agonist treatment, GLP-1 secretion was significantly increased, exposing another physiological role of the FFA4 receptor.

These findings validate FFA4 as a novel drug target in the treatment of respiratory diseases such as asthma and chronic obstructive pulmonary disease and also in the treatment of metabolic diseases such as diabetes. Current drug therapies for these diseases can result in harmful side effects and may be ineffective on certain populations of patients, highlighting a clinical need for novel and safer therapeutics. Thus, research on novel FFA4 drugs is crucial to bring new drugs to clinic.

Table of Contents

List of Tables

List of Figures

List of Publications

Prihandoko, R., Kaur, D., Wiegman, C.H., Alvarez-Curto, E., Donovan, C., Chachi, L., Ulven, T., Tyas, M.R., **Euston, E**., Dong, Z., Alharbi, A.G.M., Kim, R.Y., Lowe, J.G., Hansbro, P.M., Chung, K.F., Brightling, C.E., Milligan, G. and Tobin, A.B. (2020) 'Pathophysiological regulation of lung function by the free fatty acid receptor FFA4', *Science Translational Medicine*, 12(557), pp. 1–14.

Acknowledgement

Firstly, I would like to thank my supervisors Andrew Tobin and Graeme Milligan for their support and encouragement during my studies. The opportunities that they have provided me have not only allowed me to learn some fantastic new skills but also further my personal development. Their help has been instrumental in the completion of my PhD and they have guided me through the challenges of working throughout a global pandemic. I would also like to thank all of the postdocs and technicians who have supported me in this process, in particular Rudi, Natasja, Gonzalo, Lisa and Colin, who have answered all my questions and have shown me many of the techniques I have used. Abdul and Zhaoyang, my FFA4 team, thank you so much for always being there and always being willing to help when one of us is in need. I could not have done it without you all.

I would also like to thank all of the friends that I have made along the way, the experience would not have been made so great without you all. In particular, I would like to thank the best role model/friend/biggest fan there is, Miriam. I would also like to thank Jose, Nini, Becca and Sarah for being the most supportive fellow PhD students and never failing to put a smile on my face. I would also like to thank Woroud for the best cuddles and coffee breaks when I need it the most. I hope that we all remain friends for life.

My family have been a massive part of my career progression. Thank you to my mum and dad for always encouraging me and supporting me in everything I do, I would not be where I am today without you both. An extra special thank you goes to the best companion, my puppy Colt. Thank you for keeping my knees warm in zoom meetings and my feet warm when writing my thesis, I'm not sure you'll ever understand how much you helped me through the writing process.

Lastly, my biggest thanks goes to my Fiancé Jamie. Thank you for believing in me when I haven't believed in myself, for allowing me to work all hours of the day and for helping me through all of the ups and downs that come with doing a PhD. I am forever grateful for you.

Author's Declaration

"I declare that, except where explicit reference is made to the contribution of others, this dissertation is the result of my own work and has not been submitted for any other degree at the University of Glasgow or any other institution."

September 2022

Eloise Euston

Definitions/Abbreviations

AC – Adenylyl cyclase

AMPK – Adenosine monophosphate protein kinase

APC – Antigen presenting cell

ASM – Airway smooth muscle

ATP – Adenosine triphosphate

BRET - Bioluminescence resonance energy transfer

BSA – Bovine serum albumin

cAMP – Cyclic adenosine monophosphate

CBCC - Crypt-based columnar cells

CCK - Cholecystokinin

CCL – C-C motif chemokine ligand

cGMP – Cyclic guanosine 3',5' monophosphate

CHO – Chinese hamster ovary

COPD – Chronic obstructive pulmonary disease

CRD – Cysteine rich domain

CT - Comparative cycle threshold

DAG - Diacylglycerol

DMEM – Dulbecco's Modified Eagle Medium

DMSO – Dimethyl sulfoxide

dNTP – Deoxynucleoside triphosphate

DPP-4 – Dipeptidyl peptidase-4

DTT – Dithiothreitol

EC50/80 – Effective concentration at 50/80% maximal response

ECL – Extracellular loop

EDTA – Ethylenediamine tetraacetic acid

EEC – Enteroendocrine cell

ELISA – Enzyme-linked immunosorbent assay

EP2 – Extracellular protein 2

EPAC – Exchange protein directly activated by cAMP

ERK – Extracellular signal-regulated kinases

eYFP – Enhanced yellow fluorescent protein

FBS – Fetal bovine serum

FFA1 – Free fatty acid receptor 1

FFA2 – Free fatty acid receptor 2

FFA3 – Free fatty acid receptor 3

FFA4 – Free fatty acid receptor 4

FRET – Fluorescence resonance energy transfer

GABA – Gamma-aminobutyric acid

GAIN – GPCR autoproteolysis-inducing domain

GAPDH – Glyceraldehyde 3-phosphate dehydrogenase

GDP – Guanosine-5'-diphosphate

GIP – Gastric inhibitory peptide

GLP-1 – Glucagon like peptide 1

GLUT4 – Glucose transporter type 4

GM-CSF - Granulocyte-macrophage colony-stimulating factor

GPCR – G protein-coupled receptor

GRK – G protein-coupled receptor kinase

GTP – Guanosine-5'-triphosphate

HA – Hemagglutinin

HBSS – Hanks' balanced salt solution

HEK – Human embryonic kidney

HRP – Horseradish peroxidase

HTRF – Homogenous time resolved fluorescence

IBMX – 3-isobutyl-1-methylxanthine

ICL – Intracellular loop

IFN - Interferon

IKK – Inhibitor complex of nuclear factor-KB kinase

IL – Interleukin

IP1 – Inositol monophosphate

IP3 – Inositol triphosphate

IP3R – Inositol triphosphate receptor

JNK – c-Jun N-terminal kinases

K$_{ATP}$ - ATP sensitive potassium channels

KO - Knockout

LABA – Long-acting β agonists

LAMA – Long-acting muscarinic antagonist

LDH – Lactate dehydrogenase

LPS – Lipopolysaccharide

MAPK – Mitogen-activated protein kinase

MLC – Myosin light chain

MLCK – Myosin light chain kinase

NAM – Negative allosteric modulator

NEP24 - Neutral endopeptidase 24.11

PAM – Positive allosteric modulator

PBS – Phosphate buffered saline

PCLS – Precision cut lung slice

PCR – Polymerase chain reaction

PD – Phospho-deficient

PDE - Phosphodiesterase

PFA - Paraformaldehyde

PGE2 – Prostaglandin E2

PH – Plextrin homology

PIP2 – Phosphatidylinositol 4,5 bisphosphate

PKA – Protein kinase A

PKC – Protein kinase C

PKG- cGMP-dependent protein kinase

PLC – Phospholipase C

PPAR – Peroxisome proliferator-activated receptor

PYY – Peptide YY

RIPA buffer – Radioimmunoprecipitation assay buffer

ROS – Reactive oxygen species

RT – Reverse transcriptase

RyR - Ryanodine receptor

SDS-PAGE – Sodium dodecyl sulphate-polyacrylamide gel electrophoresis

STC - Secretin tumour cell

T2DM – Type 2 diabetes mellitus

TAB1 – TGF-beta activated kinase binding protein 1

TAK1 – TGF-beta activated kinase 1

TBST – Tris-buffered saline (TBS) Tween

TLR – Toll-like receptor

TM - Transmembrane

TNF – Tumour necrosis factor

V1 – Vasopressin 1

V2 - Vasopressin 2

VDCC – Voltage-dependent calcium channel

VFD – Venus fly-trap domain

WT – Wild type

β2AR – ß2-adrenergic receptor

ß2AR-ßarr1 - ß2 adrenergic receptor-ß-arrestin1 complex

ß2V2 - ß2-adrenergic receptor - vasopressin 2 receptor chimera

Chapter 1　Introduction

1.1 G protein-coupled receptors

G protein-coupled receptors (GPCRs) are a superfamily of membrane-bound receptors that mediate intracellular signalling in response to various stimuli including light, hormones, odorants, neurotransmitters and growth factors (Zhang and Xie, 2012). GPCRs are involved in a diverse range of physiological processes and function through a common G protein dependant signalling mechanism (Nejat *et al.*, 2022).

The GPCR superfamily have ancient origins, with evidence suggesting that the gene families encoding for GPCRs were present around 1.2 billion years ago and were present within the last common eukaryotic ancestor (Gurevich and Gurevich, 2008; De Mendoza, Sebé-Pedrós and Ruiz-Trillo, 2014). Evolution of GPCRs from their common ancestor has resulted in the presence of over 800 receptors in the human genome, and thus GPCRs represent the largest family of cell membrane receptors (Venter et al., 2001; Fredriksson et al., 2003). GPCRs are present in eukaryotes including animals, plants, fungi and protozoa and share a common structure, consisting of 7 transmembrane (TM) α-helices, that has been conserved despite evolutionary divergence. The 7 TM α-helices are comprised of 25-35 hydrophobic residues, which allow helices to embed within the hydrophobic membrane. These α-helices are linked together by three intracellular loops (ICL) and three extracellular loops (ECL) (Rosenbaum, Rasmussen and Kobilka, 2009; Zhang, Zhao and Wu, 2015; Basith *et al.*, 2018). ICLs and ECLs contain more hydrophilic residues to facilitate interaction with the cytoplasm and extracellular fluid (Schiöth and Fredriksson, 2005; Zhang, Zhao and Wu, 2015; Sojka *et al.*, 2017). In addition, each receptor also possesses an N-terminal domain and a C-terminal tail, with the exception of the Gonadotropin-Releasing Hormone (GnRH) receptor which lacks a C-terminal tail (Flanagan and Manilall, 2017). While the transmembrane helices are conserved structurally, other structural regions vary as they participate in ligand-binding specificity and binding of downstream signalling partners (Katritch, Cherezov and Stevens, 2012; Basith *et al.*, 2018).

1.2 GPCR subfamily classification

Whilst there are a plethora of methods which are recognised to classify GPCRs based on evolutionary and sequence conservation, the two most accepted methods are described here. In the first, there are six classes of GPCR, class A-F, categorised based on functional properties and sequence (Attwood and Findlay, 1994). Class A is the most common group and these receptors are sometimes referred to as rhodopsin-like GPCRs. Class B characterises secretin and adhesion receptors, class C, the metabotropic glutamate family, gamma-aminobutyric acid (GABA) receptors, calcium-sensing receptors and taste receptors. In rodents, class C receptors also include taste type 1 and Vasopressin (V2) pheromone receptors which are not present in humans (Alexander *et al.*, 2019). Class D receptors encompass fungal mating pheromone receptors, class E, cyclic adenosine monophosphate (cAMP) receptors and class F contains frizzled receptors and smoothened receptors (Attwood and Findlay, 1994).

Throughout time, another method of classification for GPCRs termed the GRAFS system has been developed. This system divides receptors into five different groups based on a phylogenetic tree following phylogenetic sequencing of the human genome, namely, Glutamate (G), Rhodopsin (R), Adhesion (A), Frizzled/Taste2 (F), and Secretin (S). These five classes have little to no sequence homology between them (Fredriksson *et al.*, 2003). More recently, this system was able to distinguish differences between secretin and adhesion GPCRs, which in the earlier classification system were defined as both class B. The GRAFS systems is the most commonly used system nowadays and will be used throughout this thesis.

Of the approximately 800 GPCRs present in mammalian systems, at least 140 receptors are orphan receptors (Levoye *et al.*, 2006). Orphan receptors are a group of GPCRs where activating ligands are unknown and so these receptors are not classified. Orphan receptors are deorphanized when endogenous ligands are discovered, often through cell signalling assays, exploring expression relationships between the receptor and ligand or comparing function and sequence to already deorphanized receptors (Tang *et al.*, 2012). It is important

to characterise orphan GPCRs as they may provide drug targets and therapeutic benefits.

1.3 GPCR subfamily structural characteristics

Structural studies have identified that the most vital points of difference between receptor subfamilies include distinct ligand binding compartments and N-terminal domains. The sequences of ECLs (especially ECL2) differ between families since ECL2 is known to be responsible for ligand recognition and binding. The seven transmembrane domains also adopt different conformations in different receptors to facilitate different ligand binding modes (Zhang, Zhao and Wu, 2015; Basith *et al.*, 2018).

Glutamate receptors have large extended N-termini comprised of around 600 residues. Here, the ligand binds to a binding site in the Venus fly trap domain (VFD), using two large N-terminal lobes located in the extracellular domain (Kunishima *et al.*, 2000; Wu *et al.*, 2014). Rhodopsin-like GPCRs are grouped together by the identification of a DRY motif between TM3 and ICL2, and an NSxxNPxxY motif in TM7 (Fredriksson *et al.*, 2003; Rovati, Capra and Neubig, 2007; Nomiyama and Yoshie, 2015). Secretin receptors used to be classified as class B receptors along with adhesion receptors, however, more recently the identification of structural and residual differences in adhesion receptors has led to these receptors being reclassified into their own adhesion group. Adhesion receptors have long N-termini, a large portion of which consists of Ser/Thr glycosylation sites to facilitate the binding of extracellular matrix proteins (Fredriksson *et al.*, 2003; Vizurraga *et al.*, 2020). Adhesion GPCRs also have a conserved GPCR autoproteolysis-inducing (GAIN) domain within the N-terminus which works to cleave the N-terminus, resulting in the adhesion domain becoming non-covalently bound to the receptor (Araç *et al.*, 2012; Prömel, Langenhan and Araç, 2013; Vizurraga *et al.*, 2020). Ligands bind to these adhesion domains and stimulate intracellular responses. Frizzled/Taste2 receptors are the most recently discovered class of receptor. As with other classes of GPCR, frizzled receptors have long N-termini, however, they contain a cysteine rich domain (CRD) which facilitates Wnt ligand binding (Dann *et al.*, 2001; Nichols *et al.*, 2013; Agostino, Pohl and Dharmarajan, 2017). Conversely taste2 receptors differ as they don't have long N or C-termini, and instead

ligands bind to ECLs (Pronin *et al.*, 2004; Nordström *et al.*, 2009; Upadhyaya *et al.*, 2015). Lastly, secretin receptors are a class of receptors currently including 15 genes, which contain long N-termini stabilised by disulphide bonds (Harmar, 2001; Karageorgos *et al.*, 2018). Ligands for secretin receptors include large peptides that bind through hormone peptide-binding domains within the long N-termini (Figure 1-1) (Nordström *et al.*, 2009).

Glutamate

Rhodopsin

Adhesion

Frizzled

Secretin
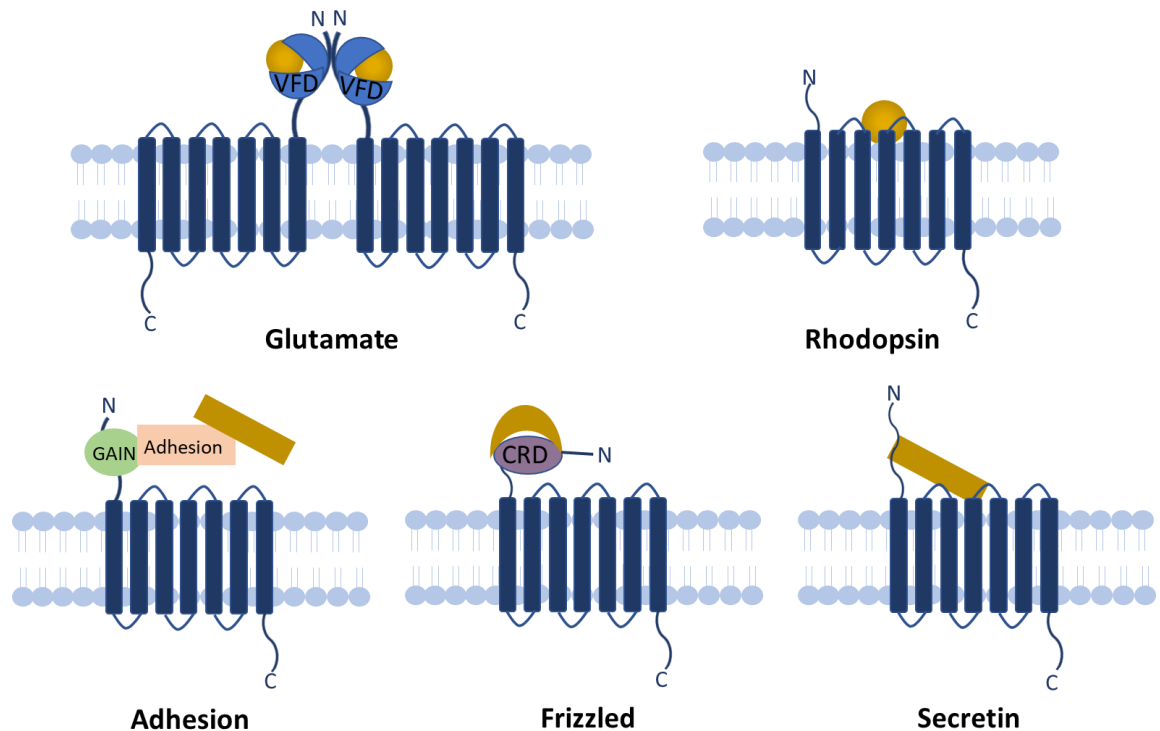
Figure 1-1: Classification of GPCR families based on structural features
G protein-coupled receptors share 7 transmembrane α-helices, however, extracellular regions differ between classes. Glutamate receptors possess Venus fly trap domains (VFD) on their N-termini to facilitate ligand binding, whereas ligand binding in rhodopsin-like receptors occurs in the transmembrane domains and so these receptors possess smaller N-termini. Adhesion receptors contain GPCR autoproteolysis-inducing (GAIN) domains which act to cleave N-termini allowing the non-covalent association of adhesion domains to which ligands bind. Frizzled receptors contain cysteine rich domains (CRD) within the N-terminus to facilitate ligand binding, whereas ligands bind to secretin receptors via hormone peptide binding domains within long N-termini. Ligands are shown in yellow.

1.4 GPCR canonical signalling

Binding of a ligand to an extracellular binding site initiates intracellular signal transduction by activation of associated guanine nucleotide-binding proteins (G proteins). G proteins are heterotrimeric proteins that consist Gα, Gβ and Gγ subunits (Lambright *et al.*, 1996). Within the human genome, there are 16 Gα, 5 Gβ and 12 Gγ proteins, and therefore diverse signalling can take place through

the formation of different G protein complexes (Gautam *et al.*, 1998; Hermans, 2003; Oldham and Hamm, 2008). While Gα subunits can signal as independent subunits, Gβ and Gγ subunits signal as a heterodimer (Gβγ) (Neer and Clapham, 1988). Furthermore, Gα subunits are classified into four functional families based on their signalling mechanisms and degree of sequence conservation: Gαs (Gαs(S), Gαs(XL) and Gαs(olf)), Gαi/o (Gαo, Gαi (1-3), Gαt, Gαz and Gαgust), Gαq/11 (Gαq, Gα11, Gα14 and Gα15/16), and Gα12/13 (Gα12 and Gα13) (Neer, 1995; Wettschureck and Offermanns, 2005; Syrovatkina *et al.*, 2016).

Upon the binding of a ligand to a receptor binding site, conformational changes are triggered within the receptor which facilitates the binding of the Gα subunit to the receptor intracellular domains (Hoffmann *et al.*, 2008; Latorraca, Venkatakrishnan and Dror, 2017). This promotes the exchange of guanosine diphosphate (GDP) for guanosine triphosphate (GTP) on the Gα subunit (Neer and Clapham, 1988; Oldham and Hamm, 2008; Weis and Kobilka, 2018). Subsequently, active GTP-bound G proteins dissociate into GTP-α and βγ subunits and transduce signals (Syrovatkina *et al.*, 2016). The Gα12/13 subunits have been shown to activate Rho GTPases, whereas Gαs stimulates adenylate cyclase (AC) which stimulates the production of cAMP from ATP which activates downstream protein kinases (Gilman, 1987; Fromm *et al.*, 1997; Gohla, Harhammer and Schultz, 1998; Wettschureck and Offermanns, 2005; Siehler, 2009; Kamato *et al.*, 2015; Guo *et al.*, 2022). Conversely, Gαi inhibits AC and associated cAMP production (Gilman, 1987; Luttrell, 2008; Kamato *et al.*, 2015). Lastly, Gαq activates phospholipase-C (PLC) leading to a release of intracellular Ca^{2+} and additionally feeds into the MAPK signalling pathway (Berridge, 1993; Exton, 1996; Wettschureck and Offermanns, 2005; Eishingdrelo, 2013; Kamato *et al.*, 2015). Additionally, Gβγ heterodimers can also act as scaffold proteins and signal by activating downstream effectors (Figure 1-2) (Dupré *et al.*, 2009).

GPCRs were once thought to only couple to one G protein pathway selectively upon agonist stimulation. However, GPCR biology is more complex than once thought, with receptors able to couple to multiple G protein subtypes (Wootten *et al.*, 2018).
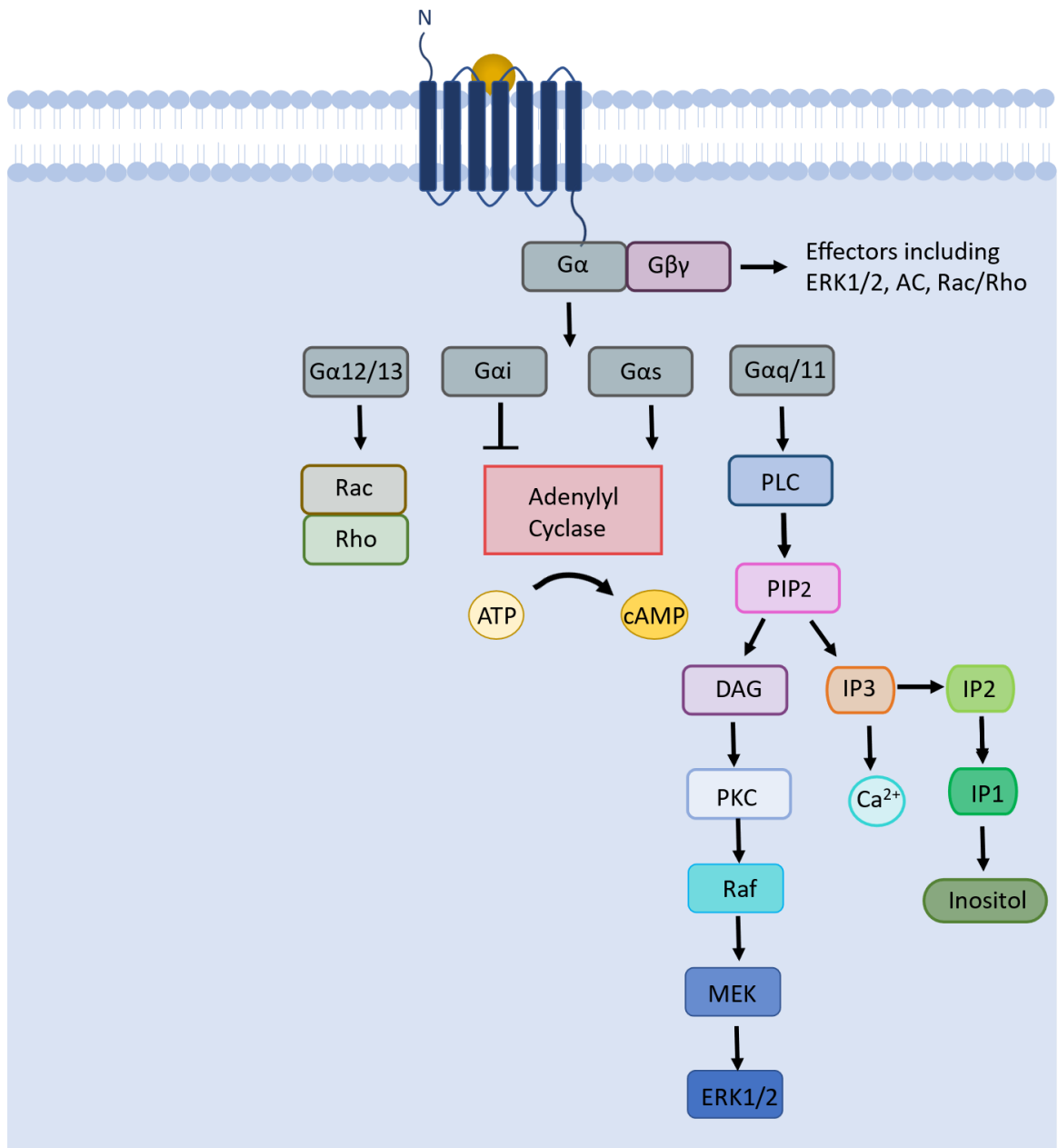
Figure 1-2: Signalling pathways following G protein coupling
G protein-coupled receptors couple to heterotrimeric G proteins. Following agonist stimulation, the exchange of guanosine diphosphate (GDP) for guanosine triphosphate (GTP) is facilitated on the Gα subunit, allowing Gα and Gβγ subunits to dissociate and activate downstream effectors. Gα subunits are categorised into four families: Gαs, Gαi/o, Gαq and Gα12/13. The Gα12/13 family activates Rho GTPases whereas Gαs and Gαi families regulate adenylate cyclase activity. The Gαq subunit stimulates phospholipase-C signalling leading to an increase of intracellular Ca^{2+} through IP3, which is then rapidly degraded to IP2, then IP1 before degrading to inositol in the inositol phosphate pathway. The PLC pathway also feeds into the MAPK signalling pathway. Additionally, Gβγ subunits can also activate effectors including ERK1/2, adenylyl cyclase and Rho GTPases.

1.5 GPCR β-arrestin signalling

1.5.1 GPCR phosphorylation

Kinases such as GPCR kinases (GRKs) phosphorylate serine/threonine residues in the C-terminal tail and/or intracellular loops of the GPCR in question in an agonist dependent process called homologous phosphorylation (Benovic *et al.*, 1989; Kelly, Bailey and Henderson, 2008; Tobin, 2008; Burns *et al.*, 2014). There are seven different GRK isoforms: GRK1-7. GRK1 and GRK7 are GRKs for visual GPCRs, located in vertebrate rod and cone photoreceptors respectively, with both also found in pinealocytes (Somers and Klein, 1984; Zhao *et al.*, 1999; Weiss *et al.*, 2001). Interestingly, GRK7 is absent in rodents with only the presence of GRK1 reported (Weiss *et al.*, 2001). There are also 5 non-visual GRKs which are categorised into two different groups: GRK2/3 and GRK4/5/6. GRK2 and GRK3 contain a pleckstrin homology (PH) domain which binds to dissociated Gβγ and phosphatidylinositol 4,5-bisphosphate (PIP2) to facilitate the movement of GRK2/3 to the plasma membrane from the cytosol (Tesmer *et al.*, 2005). The last group, GRK4/5/6 differs from GRK2/3 in a variety of ways. Whilst GRK2/3 are agonist dependent, GRK4/5/6 can phosphorylate residues independently from agonists (Li *et al.*, 2015). Additionally, GRK4/5/6 interact with the plasma membrane through interactions with charged regions within the membrane or additionally through palmitoylation and do not contain a PH domain (Gurevich *et al.*, 2012). Expression of GRK's varies within tissues, with GRK1 and 7 expressed in rod and cone cells, whereas GRK2/3/5/6 are expressed universally within mammalian tissues. However, GRK4 expression differs and is instead expressed within brain cerebellum, kidney and testis (Chaudhry and Bordoni., 2021). However, GRKs are not the primary mechanism of homologous phosphorylation in all receptors. This is the case in M1 and M3 muscarinic receptors which are phosphorylated by casein kinase 1α and casein kinase 2 respectively (Torrecilla *et al.*, 2007).

There is evidence that GRKs and other such kinases which phosphorylate receptors can phosphorylate different receptors in different locations, defining the so called phosphorylation barcode (Tobin, 2008). Different barcode patterns promote the binding of distinct downstream signalling partners. The identity of a phosphorylation barcode has been described in many receptors, including

ß2AR, where agonist isoproterenol stimulates phosphorylation at GRK2- and GRK6-specific sites whereas the agonist carvedilol stimulates phosphorylation at GRK6 specific sites. Experiments performed using these agonists demonstrated that siRNA knockdown of GRK2 promoted a reduction of β-arrestin2 recruitment, whereas this was not observed upon GRK6 knockdown (Nobles *et al.*, 2011). Evidence of a phosphorylation barcode has also been described for FFA4, the receptor of interest in this thesis, and this is described in Chapter 4.

1.5.2 Classes of arrestins

Following G protein activation, G proteins can become uncoupled from GPCRs by steric hindrance caused by arrestins binding to the receptor. This process is termed desensitisation and is an important process since prolonged signalling can be toxic to the cell (Rajagopal and Shenoy, 2018). The arrestin family comprises of four different types: arrestin 1-4 (Bond *et al.*, 2019). This includes two visual arrestins, arrestin 1 (visual arrestin) and 4 (cone arrestin) which are found within the eye (Wilden, Hall and Kuhn, 1986; Craft, Whitmore and Wiechmann, 1994) and two arrestins which are non-visual, arrestins 2 and 3 which are known as ß-arrestin1 (Lohse *et al.*, 1990) and ß-arrestin2 (Attramadal *et al.*, 1992) respectively. Additionally, two different types of arrestin-GPCR complex are described, class A and class B, depending on the affinity for the arrestin to the receptor. Class A receptors are known to form a transient interaction with arrestin whereas class B receptors are known to have a stronger affinity (Oakley *et al.*, 2000; Kahsai, Pani and Lefkowitz, 2018). This classification should not be confused with other GPCR family classifications and only differentiates receptors based on interactions with arrestins.

1.5.3 Receptor desensitisation and internalisation

ß-arrestin is recruited to a GPCR in a two-step process, where the arrestin recognises the sites of receptor phosphorylation but also transmembrane domains of the active GPCR conformation following agonist stimulation. This facilitates the conformational change of the arrestin, allowing binding to the GPCR with high affinity (Tobin, 2008; Lohse and Hoffmann, 2014). While ß-arrestin interaction with GPCRs is heavily dependent on interactions with the phosphorylated residues on intracellular residues within the GPCR,

phosphorylation independent coupling mechanisms have also been described. For example, the first 10 residues of ICL2 are involved in ß-arrestin binding in 5-HT2C and ß2AR (Marion *et al.*, 2006). In addition, it has been suggested that IL3 is involved in phosphorylation independent ß-arrestin binding in many receptors including vasopressin (V1) and lutropin receptors (Mukherjee *et al.*, 2002; Gurevich and Gurevich, 2006; Wu *et al.*, 2006). Binding of ß-arrestin to phosphorylated intracellular residues of the receptor results in steric hindrance of G protein binding to the receptor, thereby inhibiting activation and signalling of G proteins, resulting in receptor desensitisation. However, while homologous phosphorylation of GPCRs following ligand binding results in ß-arrestin recruitment and homologous desensitisation, receptor phosphorylation can also occur independently from ligand activation via second messenger kinases and tyrosine kinases in a process called heterologous phosphorylation, which directly uncouples the receptors from their G proteins in heterologous desensitisation events (Burns *et al.*, 2014).

ß-arrestins are not only involved in desensitization but also in the endocytosis, trafficking and signalling events of GPCRs (Thomsen *et al*, 2016). Binding of ß-arrestin can cause internalisation of the GPCR into clathrin coated pits by interacting with the endocytotic machinery that includes proteins such as clathrin and AP-2. The GPCR-ß-arrestin complex recruits AP-2 and clathrin to the membrane to internalise the receptor into clathrin coated pits (Figure 1-3) (Goodman *et al.*, 1996; Laporte *et al.*, 1999; Bond *et al.*, 2019). Two different methods of internalisation can occur dependent on the type of receptor-ß-arrestin interaction. ß-arrestins which weakly interact with receptors can dissociate as the clathrin coated pit pinches off and detaches from the plasma membrane via the action of dynamin. Alternatively, where interactions are stronger, ß-arrestin can remain attached to the GPCR and ß-arrestins which are internalised into endosomes act as adaptor proteins and scaffolding proteins by interacting with many different signalling molecules (Laporte *et al.*, 1999; Thomsen *et al.*, 2016). After ß-arrestin dissociation, the GPCR is dephosphorylated and degraded or recycled to the plasma membrane for further signalling (Thomsen *et al.*, 2016).
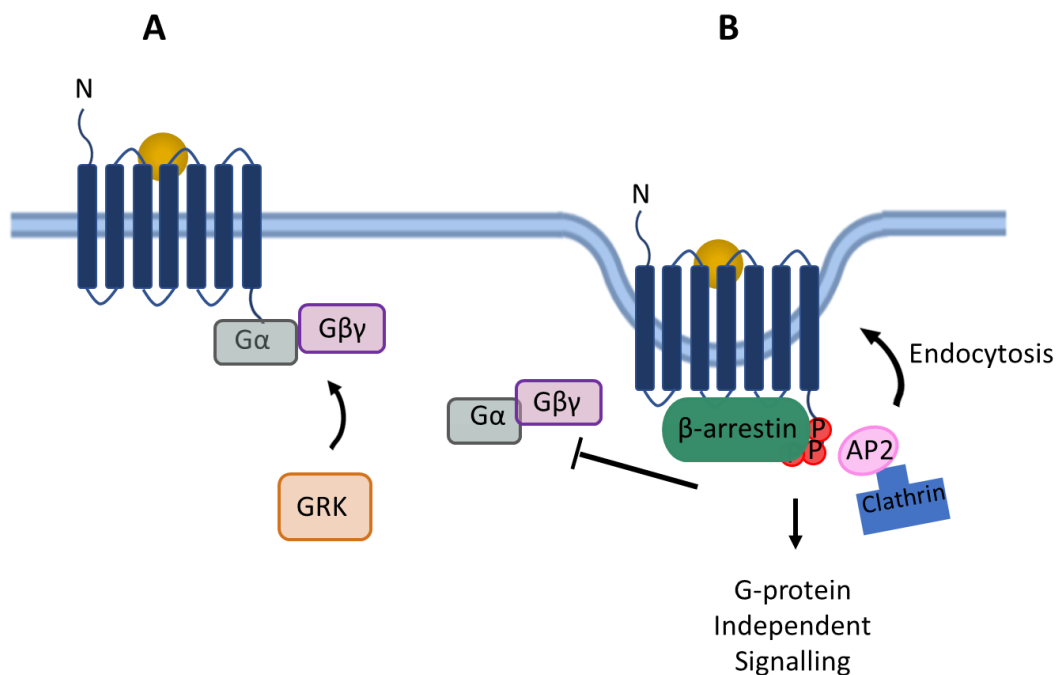
Figure 1-3: β-arrestin mediated receptor desensitisation, internalisation and signalling
(A) Following agonist binding and G protein signalling, kinases such as G protein-coupled receptor kinases (GRKs) phosphorylate intracellular residues of the activated GPCR. **(B)** β-arrestin is recruited to the receptor and this sterically hinders G protein binding and activation. Additionally, adaptor proteins including AP-2 and clathrin are recruited to the arrestin to initiate receptor internalisation into clathrin coated pits. β-arrestin also acts as a scaffold protein in G protein independent signalling.

1.5.4 β-arrestin-GPCR complexes

In 2014, Shukla and colleagues purified and determined the crystal structure of the ß2 adrenergic receptor-ß-arrestin1 (ß2AR-ßarr1) complex using single particle negative stain electron microscopy. Here, two differing conformations of receptor-arrestin complex were visualised: the core conformation and the tail conformation. Binding and interactions of these complexes were described using hydrogen-deuterium exchange mass spectrometry (HDXMS) and by the application of chemical cross-linking (Shukla *et al.*, 2014). The tail conformation arises when arrestins bind to the phosphorylated C-terminal tail of the GPCR and the core conformation arises when the arrestin binds to the C-terminal tail as well as the hydrophobic core region. In the core conformation, G protein binding to the GPCR is sterically hindered (Shukla *et al.*, 2014; Szczepek *et al.*, 2014; Kang *et al.*, 2015; Thomsen *et al.*, 2016). It is now known that different conformations give an insight into ß-arrestin function, more specifically how they regulate different processes. The tail conformation is said to be involved in internalisation of the receptor and the core conformation in desensitisation.

However, the exact function of the receptor-arrestin complex is dependent on the strength of receptor interaction (Goodman *et al.*, 1996; Laporte *et al.*, 1999; Thomsen *et al.*, 2016). It is now known that class A receptors, such as ß2-adrenergic receptor (ß2AR), that have weaker interactions with ß-arrestin mediate desensitisation via the core conformation and class B receptors, such as vasopressin type 2 receptor, that have stronger interaction with GPCRs mediate internalisation and signalling via the tail conformation (Cahill *et al.*, 2017).

In addition, the tail conformation suggests that it is possible for both arrestins and G proteins to bind as ICL1,2 and 3 are exposed, thereby, facilitating binding of G proteins also. There is a possibility that G protein internalisation and signalling could thus occur, and this has been demonstrated in ß2-adrenergic vasopressin 2 (ß2V2) chimera and V2 receptors. These receptors were shown to interact with Gαs G proteins in the core conformation while interacting with ß-arrestin in the tail conformation, subsequently allowing receptor internalisation at the same time as G protein signalling (Thomsen *et al.*, 2016).

1.6 GPCR ligands

The pharmacological characteristics of a ligand describe how it will act upon a receptor. Measurable qualities of drugs include affinity, efficacy and drug potencies. Affinity is described as the strength of ligand binding to the receptor site whereas efficacy is a biological measure, describing the maximal response of the receptor to produce the desired biological effect following ligand binding (Strange, 2008). Affinity can be estimated by measuring ligand binding using fluorescent or radiolabelled ligands, however, labelled ligands may not have been developed for the desired receptor and so potencies are often measured instead (Rosenkilde and Schwartz, 2000; Milligan, *et al.*, 2017). The potency of a ligand is described as the concentration of a drug required to produce 50% of that drug's maximal effect (EC50) (Weatherall, 1966; Salahudeen and Nishtala, 2017). Potencies and efficacies or maximal responses are often measured by a variety of different functional assays, however, values can differ between assays due to a number of factors including levels of signal amplification in assays and differences in receptor expression in cell lines used (Leroy *et al.*, 2007).

Depending on the binding properties of ligands they can be classified into three groups: orthosteric, allosteric and bitopic ligands. Orthosteric ligands bind to the same binding sites as the endogenous, natural ligand and can be categorised as full, partial, or inverse agonists or neutral antagonists based on pharmacological properties (Figure 1-4A) (Roche, Gil and Giraldo, 2013). Agonists are ligands which have affinity and efficacy for the receptor whereas antagonists have affinity and bind to the receptor but do not have efficacy to activate the receptor (Salahudeen and Nishtala, 2017). Allosteric ligands differ in that they bind to allosteric sites which are distinct from endogenous ligand binding sites. This makes the pharmacology of allosteric ligands more complex. In receptors which have multiple binding sites, allosteric modulators can display cooperativity with orthosteric ligands. This cooperativity can be the form of increasing or decreasing the affinity of an orthosteric ligand upon binding of the allosteric modulator to a second binding site (Bridges and Lindsley, 2008). Therefore, allosteric ligands can be also categorised based on their properties into neutral allosteric antagonists, and positive and negative allosteric modulators (PAMs and NAMs) depending on whether the agonist increases or decrease the ligand activity at the orthosteric binding site (Figure 1-4B,C) (Roche, Gil and Giraldo, 2013; Christopoulos, 2014). While orthosteric binding sites for many GPCR families are conserved leading to challenges in selectivity for one family member over another, allosteric modulators can target regions which are not conserved and may prove to be advantageous over orthosteric ligands (Gao and Jacobson, 2013). Lastly bitopic ligands have the ability to engage with both endogenous and allosteric binding sites. This enhances ligand specificity and may improve pharmacological properties including affinity for the receptor by binding to two binding sites and additionally selectivity by the possession of the allosteric site (Valant *et al.*, 2012). While different orthosteric ligands can display different efficacies for functional responses, called ligand bias, both bitopic and allosteric ligands show promise in coordinating ligand bias due to the possibility of distinct receptor conformations being formed when ligands bind to separate binding sites (Lane, Sexton and Christopoulos, 2013; Fronik, Gaiser and Sejer Pedersen, 2017).
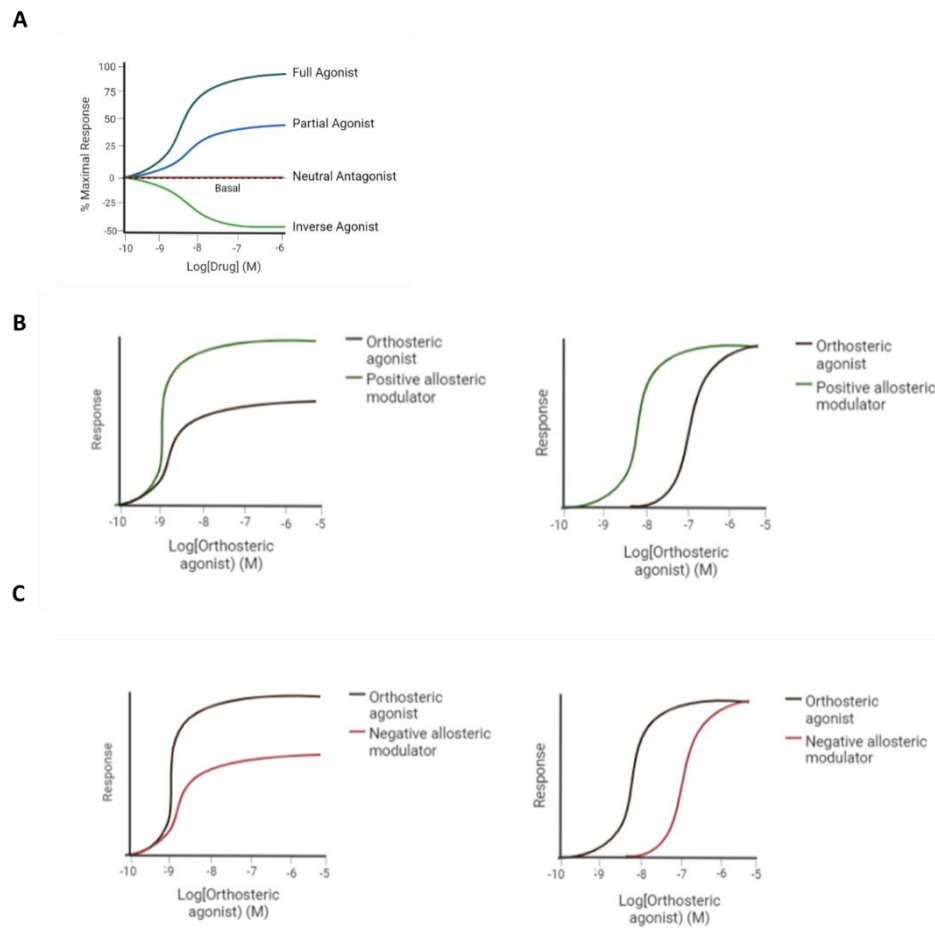
Figure 1-4: Pharmacology of GPCR ligands
Orthosteric agonists can produce different concentration response curves dependent on agonist efficacy. Full agonists produce maximal responses at the receptor, whereas partial agonists produce submaximal responses. Neutral antagonists produce no receptor response, however, inverse agonists induce a decrease in response compared to basal activity, assuming the receptor shows measurable constitutive activity **(A)**. Positive and negative allosteric modulators (PAMs and NAMs respectively) affect potencies and maximal receptor responses. **(B)** Incubation with PAMs increases potency and/or maximal response of the orthosteric agonist, whereas **(C)** incubation of NAMs reduces potency and/or maximal response of orthosteric agonist.

1.6.1 Biased agonism

In recent years it has become clear that the idea that one G protein binding exclusively to a GPCR is oversimplified. GPCRs can couple to multiple different G proteins and arrestins and signal through different pathways. For example, the β2AR's were thought to exclusively couple to Gαs G proteins, however, it was later shown that the receptor actually differentially couples to Gαi and Gαq G proteins (Tate *et al.*, 1991; Bylund *et al.*, 1994; Wenzel-Seifert and Siefert, 2000). With the knowledge that agonists can couple to more than one pathway, the idea of biased agonism was hypothesised. Biased agonism refers to the preferential activation of one signalling pathway over another pathway (Jarpe *et*

al., 1998; Hodavance *et al.*, 2016). This can refer to the preferential activation of one G protein-coupled pathway over another or ß-arrestin coupled pathways over G protein pathways or vice versa (Hodavance *et al.*, 2016). In order to elicit biased signalling, biased ligands are thought to induce receptors to adopt distinct conformations, locking the receptor in a preferential coupling pattern (Kenakin and Morgan, 1989; Kenakin and Miller, 2010; Yang, Hou and Tao, 2021). A phosphorylation barcode theory has been proposed that could explain properties of some biased agonists. This theory suggests that different ligands binding to a receptor can result in different phosphorylation patterns, and therefore, this could influence interactions with ß-arrestins and binding of differing signalling partners (Tobin, 2008; Butcher *et al.*, 2011).

Biased signalling could result in physiological benefits. For example, novel drugs could be designed to activate specific therapeutically beneficial pathways while inhibiting pathways that lead to deleterious or adverse responses, resulting in the generation of more targeted and safer therapeutic drugs (Hodavance *et al.*, 2016). These effects have already been identified for some receptors. For example in muscarinic M1 receptors, phosphorylation/ß-arrestin pathways were demonstrated to minimise adverse responses (Bradley *et al.*, 2020) while providing neuroprotective effects (Scarpa *et al.*, 2021). Therefore, harnessing these effects by using phosphorylation/ß-arrestin biased M1 agonists may provide novel disease-modifying and safer therapies in neurodegenerative diseases such as Alzheimer's Disease (Scarpa *et al.*, 2021).

1.7 GPCRs in drug discovery

GPCRs account for over 30% of targets of all prescription drugs, making them the largest class of receptors validated as targets in the drug discovery industry (Santos *et al.*, 2016). There are several factors which contribute to their success as drug targets, including their presence as the largest group of membrane located receptors in the human body regulating a vast array of biological processes (Rask-Andersen, Masuram and Schiöth, 2014). Transmembrane proteins also make good drug targets as drugs do not need to traverse the plasma membrane to reach their targets (Hauser *et al.*, 2017; Sriram and Insel, 2018). Therefore, it is no surprise that GPCRs continue to be the focus of many drug discovery programmes.

Many successful disease therapies have been developed that target GPCRs, including the treatment of obesity and diabetes, cardiovascular disease and neurological diseases (Hauser *et al.*, 2017). There are many naturally occurring agonists approved for treatment. One example includes epinephrine, the endogenous ligand for ß2AR, which is used to relieve symptoms from allergic reactions such as anaphylaxis (Ring, Klimek and Worm, 2018). We can directly modulate receptor activity with synthetic ligands also. Salmeterol is a synthetic agonist which acts also upon the ß2AR and is used as a treatment in asthma to relax constricted airways (Holdcroft, 1994; Wendell, Fan and Zhang, 2020). In addition, numerous drugs can modulate receptor signalling indirectly by activating proteins that are upstream or downstream of GPCRs. An example of this type of drug is serotonin reuptake inhibitors which block uptake of monoamine neurotransmitters and are commonly used as antidepressants as they increase serotonin levels within the brain (Sriram and Insel, 2018; Mantas *et al.*, 2022).

Despite GPCRs accounting for a wide proportion of drug targets, only around 12% of GPCRs have approved drugs targeting them (Sriram and Insel, 2018). Therefore, more research is required in order to develop appropriate drugs for these GPCRs to increase the number of available drug therapies. Amongst these receptors which have not yet been exploited for their therapeutic potential are the free fatty acid receptor family.

1.8 Free fatty acid receptors

1.8.1 Free fatty acids

Fatty acids are key sources of energy in the body as they are vital dietary sources as well as cellular structural elements. Fatty acids are usually found in their esterified form, but if unesterified they are named free fatty acids. The body is capable of synthesising all fatty acids which are not essential. Essential fatty acids however, must be obtained from the diet (Engelking, 2015). Fatty acids can be biosynthesised from carbohydrates through glycolysis in which acetyl coA is produced. Acetyl coA is then converted to fatty acids through fatty acid synthetases (Galli and Risé, 2006; Engelking, 2015; Kimura *et al.*, 2020).

These fatty acids can then be stored as triglycerides in adipocytes (Guilherme *et al.*, 2008; Kimura *et al.*, 2020). Release of free fatty acids occurs during lipolysis in adipose tissues, a process resulting in the hydrolysis of triglycerides to free fatty acids and glycerol which can be used as an energy source for tissues and organs of the body (Galli and Risé, 2006). These free fatty acids can then circulate around the body bound by plasma albumin (Kimura *et al.*, 2020).

Free fatty acids can be monounsaturated, polyunsaturated or saturated depending on the number of carbon to carbon double bonds in the carbon chain. An example of a monounsaturated free fatty acid is oleic acid, while examples of polyunsaturated free fatty acids include linoleic acid and docosohexanoic acid. Examples of saturated fatty acids include stearic acid and palmitic acid (Galli and Risé, 2006). Free fatty acids are classified into three groups: short chain fatty acids (C1-C6), medium chain fatty acids (C7-C12) and long chain fatty acids with >C12 (Hara *et al.*, 2014) .

Free fatty acids are key regulators in metabolism and are released from triglycerides upon hydrolysis during periods of fasting. It is also well known that free fatty acids are involved in the structural support of cellular membranes, with fatty acids being integral components in phospholipids, sphingolipids, lipoproteins and glycolipids (Sieber and Jehle, 2014). In addition to their functions of dietary nutrients and cellular components, free fatty acids have proven ability to act as signalling molecules by activating the free fatty acid family of G protein-coupled receptors. As free fatty acid receptors are expressed on immune cells, links are being made between these receptors and treatments for inflammatory metabolic and respiratory diseases (Alvarez-Curto and Milligan, 2016; Coope, Torsoni and Velloso, 2016; Prihandoko *et al.*, 2020).

1.8.2 Free fatty acid receptor families

Free fatty acid receptors are a family of GPCRs which are activated by free fatty acids. There are four known receptors within this family: free fatty acid receptor 1 (FFA1/GPR40), free fatty acid receptor 2 (FFA2/GPR41), free fatty acid receptor 3 (FFA3/GPR43) and free fatty acid receptor 4 (FFA4/GPR120). These receptors are part of the rhodopsin-like family of GPCRs (Ichimura *et al.*, 2014).

FFA1, 2 and 3 were identified by Sawzdargo *et al.*, (1997) when classifying subtypes of the human galanin receptor, where genes corresponding to these receptors were identified on the chromosome 19q13.1. Ligand screening experiments led to the deorphanisation of FFA1 in 2003, concurrent with the discovery that FFA1 was activated upon binding of long chain free fatty acids (Briscoe *et al.*, 2003). Similarly, FFA2 and 3 were deorphanised in 2003 when short chain fatty acids were found to activate these receptors (Brown *et al.*, 2003; Le Poul *et al.*, 2003; Nilsson *et al.*, 2003). FFA4, however, was identified later in 2003 by Fredriksson *et al.*, in genomic sequencing experiments and was subsequently deorphanised in 2005 by Hirasawa *et al.*, upon finding that long chain unsaturated free fatty acids activated the receptor. Following the deorphanisation of the free fatty acid receptors, their names were systematically changed from the GPR receptor classification to FFA1-4 receptors that we use today (Stoddart, Smith and Milligan, 2008; Davenport *et al.*, 2013).

1.8.3 FFA1

FFA1 is expressed in many tissues including the central nervous system, human brain, liver and skeletal muscle. However, FFA1 is most highly expressed in β-cells of the islets of Langerhans in the pancreas (Briscoe *et al.*, 2003; Itoh *et al.*, 2003; Kotarsky *et al.*, 2003; Zamarbide *et al.*, 2014). FFA1 couples to Gαq/11, Gαs, Gαi/o and β-arrestin2 pathways but signals primarily through Gαq/11 G proteins via which it stimulates insulin secretion (Itoh *et al.*, 2003; Kotarsky *et al.*, 2003; Fujiwara, Maekawa and Yada, 2005; Shapiro *et al.*, 2005; Shimpukade *et al.*, 2012; Hauge *et al.*, 2015; Mancini *et al.*, 2015). Therefore, it is not surprising that FFA1 is an attractive drug target for diabetes, and as a result many FFA1 compounds have been developed as potential therapeutics for type 2 diabetes mellitus (T2DM). One such drug is TAK875 (Takeda) which did enter clinical trials but was withdrawn at Phase III due to potential liver toxicity (Kaku, Araki and Yoshinaka, 2013; Defossa and Wagner, 2014; Otieno *et al.*, 2018; Shavadia *et al.*, 2019).

1.8.4 FFA2/FFA3

FFA2 and FFA3 are both activated by short chain free fatty acids with chain lengths between C1 and C6. Despite this, FFA2 and FFA3 are preferentially

activated by chain lengths of different sizes, meaning that some agonists preferentially activate one receptor over another or have different potencies at different receptors. FFA2 is more responsive to carbon chains C2 ≈ C3 > C4 > C5 ≈ C1, whereas FFA4 is more responsive to C3 ≈ C4 ≈ C5 > C2 > C1 (Hudson, Smith and Milligan, 2011).

FFA2 is highly expressed in adipose tissue, immune cells including neutrophils, enteroendocrine cells within the gut and β cells of pancreatic islets (Brown *et al.*, 2003; Le Poul *et al.*, 2003; Karaki *et al.*, 2008; Kebede *et al.*, 2009; Tolhurst *et al.*, 2012). Additionally, FFA2 along with FFA3, is expressed within myenteric neurones of the gut to increase transit (Barki *et al.*, 2022). Therefore, FFA2 modulation could be of use as a therapeutic target in diseases which have alterations in the immune system, particularly neutrophils, such as inflammatory bowel disease and also in metabolic diseases such as diabetes. Similarly, FFA3 is also expressed in the gut, pancreatic β cells and adipose tissues, with expression also detected within the spleen and neurons (Brown *et al.*, 2003; Le Poul *et al.*, 2003; Tazoe *et al.*, 2009; Barki *et al.*, 2022). Thereby, FFA3 has also been described as a potential drug target in the treatment of obesity and metabolic diseases.

Despite similarities in tissue expression and activating ligands, FFA2 receptors couple to Gαq/11 and Gαi/o G proteins and β-arrestin2, whereas FFA3 appears to signal exclusively via Gαi/o pathway (Le Poul *et al.*, 2003; Nilsson *et al.*, 2003; Hudson *et al.*, 2012).

1.9 Free Fatty Acid Receptor 4

1.9.1 Expression

FFA4, which is the receptor of primary interest in this thesis, is expressed in: enteroendocrine cells of the colon, the pancreas, adipose tissues, brain, thymus, skeletal muscle, lung and spleen (Hirasawa *et al.*, 2005; Miyauchi *et al.*, 2009). Additionally, high expression has been detected in CD11c macrophages and primary peritoneal macrophages (Oh *et al.*, 2010). Patterns of expression in tissues can differ between species and so care must be taken when translating results into humans (Cornall *et al.*, 2014).

Many of the previous studies on physiological functions of FFA4 were centred on responses associated with food intake in tissues including the colon and pancreas. The regulation of FFA4 in glucose homeostasis in these tissues highlighted the receptor as a key target for the treatment of T2DM (Hirasawa *et al.*, 2005). However, interestingly non-metabolic functions of FFA4 are emerging, with FFA4 expression also described in the lung, a tissue which has no association with food intake (Prihandoko *et al.*, 2020). The roles of FFA4 within the lung are described later in Part 1.11.

1.9.2 Signalling

Despite the broad variation in tissue expression, functions of FFA4 within these different tissues is facilitated by the activation of the same three intracellular signalling pathways (Figure 1-5). Activation of the FFA4 receptor primarily results in the coupling to Gαq/11 pathways resulting in the elevation of Ca^{2+} and inositol phosphate levels and the phosphorylation of ERK1/2 (Hirasawa *et al.*, 2005; Briscoe *et al.*, 2006; Alvarez-Curto *et al.*, 2016). While there has been no evidence of Gαi coupling in cell line studies, FFA4-mediated Gαi signalling in the pancreas and stomach has been detected. Upon increased levels of glucose in the pancreas, somatostatin secretion is reduced and release of ghrelin from the stomach is promoted under Gαi coupled pathways (Engelstoft *et al.*, 2013; Stone *et al.*, 2014).

Additionally, FFA4 couples to ß-arrestin2 leading to internalisation of an FFA4-ß-arrestin complex. ß-arrestin has also been described to stimulate the MAPK signalling pathway, although the involvement of ß-arrestin2 in this pathway for the FFA4 receptor has been disputed (Alvarez-Curto *et al.*, 2016). In macrophages, anti-inflammatory effects are elicited by FFA4-ß-arrestin complexes. FFA4 associated ß-arrestins interact with the transforming growth factor beta (TGF-ß)-activated kinase 1 binding protein 1 (TAB1), hindering interactions between TAB1 and TGF-ß-activated kinase 1 (TAK1), ultimately inhibiting NF-κB and JNK cascades and the resulting inflammatory responses (Figure 1-5) (Oh *et al.*, 2010).

Furthermore, Gαq/11 inhibits nuclear factor kappa-light-chain-enhancer of activated B cells (NF-KB) signalling via extracellular signal-regulated kinases 1/2

(ERK1/2)-dependent prostaglandin E2 (PGE2) synthesis. The inhibition of NF-KB signalling also inhibits associated inflammatory effects (Liu *et al.*, 2014).
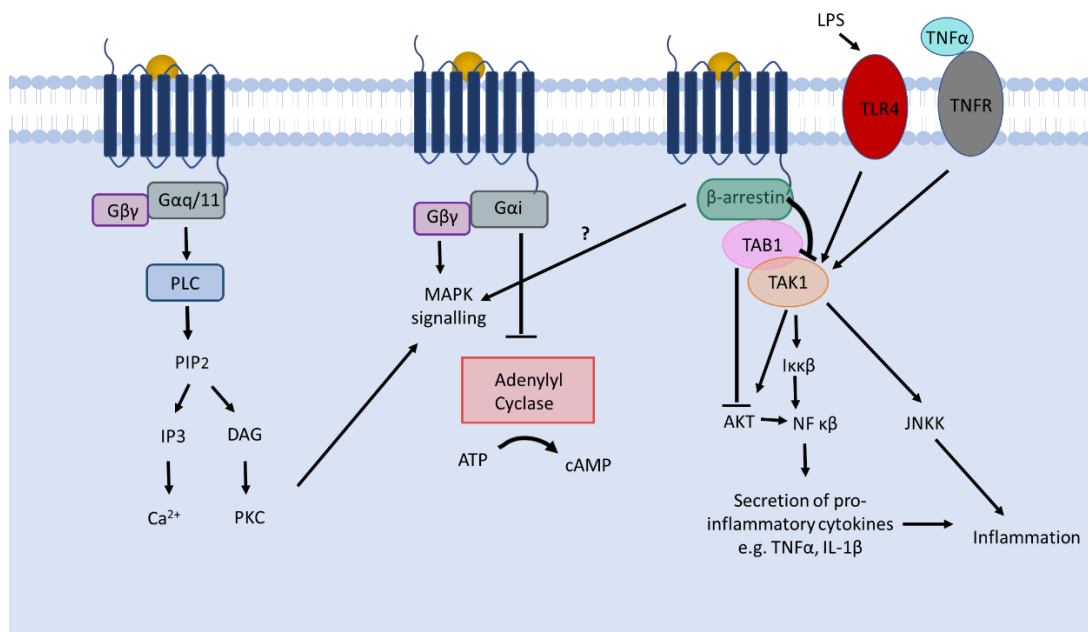
Figure 1-5: Signalling pathways of FFA4
Free fatty acid receptor 4 (FFA4) signals via Gαq/11 and Gαi G protein signalling, in addition to coupling to β-arrestin2. Ligands (yellow) bind to FFA4 and this stimulates G protein binding to the GPCR. G proteins are activated by exchange of GDP for GTP, causing α and βγ subunits to dissociate and signal**.** Gαq/11 stimulates phospholipase-C (PLC) which cleaves phosphoinositol 4,5-bisphosphate (PIP2) to produce diacylglycerol (DAG) and inositol triphosphate (IP3). IP3 stimulates calcium release from the sarcoplasmic reticulum in muscle or endoplasmic reticulum in other tissues. DAG activates protein kinase C (PKC) which feeds into mitogen-activated protein kinase (MAPK) signalling. Gαi signals to inhibit adenylyl cyclase (AC) which is stimulated by Gαs signalling. The βγ subunit in Gαi signalling pathway also initiates MAPK signalling, and while many receptors also stimulate MAPK signalling through β-arrestin pathways, this has been disputed in FFA4. FFA4 also exhibits anti-inflammatory properties in macrophages. The β-arrestin2 signalling pathway inhibits inflammation by inhibiting interactions between TGF-beta activated kinase binding protein 1 (TAB1) and TGF-beta activated kinase 1 (TAK1), the latter of which is activated by Toll Like Receptor 4 (TLR4) and tumour necrosis factor α receptor (TNFR), stimulated by lipopolysaccharides (LPS) and TNFα respectively. TAK1 induces phosphorylation of IKKβ and NFκB, leading to inflammation. Blocking actions of TAK1 leads to anti-inflammatory effects.

1.9.3 FFA4 isoforms and orthologs

There are two different isoforms of FFA4 in human, the long isoform and the short isoform. The short isoform is comprised of 361 amino acids, however, a splice variant also exists in which there are an extra 16 amino acids present within ICL3 and this isoform is named the long isoform (Figure 1-6) (Moore *et al.*, 2009). There are differences in expression patterns of these isoforms with both long and short isoforms being present in the human colon, with no evidence to suggest that the long isoform exists within any other species but humans at this time (Moore *et al.*, 2009; Galindo *et al.*, 2012; Song *et al.*, 2015; Moniri, 2016).

Differences in signalling between the two isoforms have also been described. The FFA4 short isoform is the most commonly described form and signals as detailed in Part 1.9.2, primarily through Gαq/11 signalling but signalling has also been described for Gαi G proteins and through ß-arrestin2 coupling. The long isoform differs and does not appear to couple to G protein dependent pathways, instead coupling exclusively to ß-arrestin2 (Watson, Brown and Holliday, 2012). However, the functions of this natively expressed, ß-arrestin2 biased isoform of the receptor are unknown.
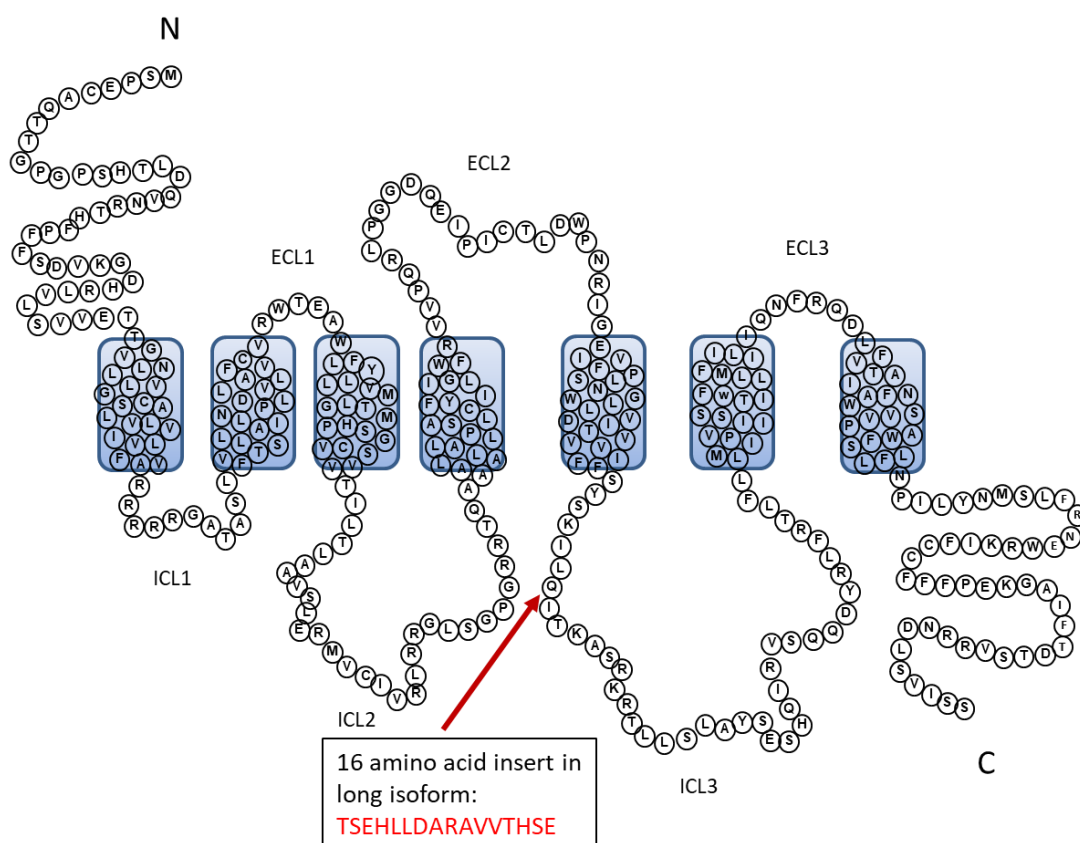
Figure 1-6: Primary amino acid sequence of FFA4 short isoform
Amino acid residues from the FFA4 short form isoform are displayed as a snake plot. The location of a 16 amino acid insertion in the third extracellular loop, which forms the FFA4 long isoform, is marked.

As many GPCRs are present in different species, differences in species orthologs must also be considered. Species orthologs have the ability to bind and respond to similar endogenous ligands, although it is possible for the pharmacology of ligands to vary (Milligan, 2009; Hudson, Murdoch and Milligan, 2013). Pharmacology of FFA4 agonists at both human and mouse orthologs is similar, however, selectivity over FFA1 is reduced in mouse orthologs and so this must be

considered if using agonists that respond to both FFA4 and FFA1 (Hudson *et al.*, 2013; Hudson, Murdoch and Milligan, 2013).

1.9.4 FFA4 agonists and antagonists

FFA4 receptors are endogenously activated by long chain free fatty acids. However, with the idea that modulating the activity of FFA4 may be therapeutically beneficial, a range of synthetic agonists have been developed. Many of these are agonists were developed with the view of a therapy for T2DM. Given that FFA1 and FFA4 share similarity in activating ligands, it comes as no surprise that many early agonists were recognised by FFA1 also. Synthetic agonist GW9508 was found to be selective for both FFA4 and FFA1 receptors, activating both receptors to produce a Ca^{2+} response resulting in glucose-sensitive insulin secretion. However, GW9508 was 100-fold less selective for FFA4 than FFA1 (Briscoe *et al.*, 2006). In an attempt to characterise agonists which were selective to FFA4 only, Suzuki *et al.*, (2008) synthesised and screened both novel and previously developed ligands. A peroxisome proliferator-activated receptor γ (PPARγ) active molecule was selected and modified, named 4-{4-[2-(phenyl-pyridin-2-yl-amino)-ethoxy]-phenyl}-butyric acid or more commonly known as NCG21. This compound showed a 10-fold selectivity for FFA4 over FFA1. PPARs are activated by fatty acids and it has been shown that PPARγ is involved in metabolic processes such as the synthesis of fatty acids. PPARγ has also been shown to activate FFA4, so it is unsurprising that chemically modifying these agonists results in potent activation of FFA4 (Varga, Czimmerer and Nagy, 2011; Grygiel-Górniak, 2014). However, with the knowledge that this compound was still an activator of FFA1 it was clear that novel FFA4 compounds which were more selective and potent were needed (Suzuki *et al.*, 2008).

Shimpukade *et al.*, (2012) screened a variety of compounds in ß-arrestin2 bioluminescence resonance energy transfer (BRET) assays which were previously developed for the FFA1 receptor. Compounds which displayed activity at FFA4 and selectivity over FFA1 were then optimised and using this method it was discovered that the *ortho*-biphenyl ligand 4-{[4-fluoro-4′-methyl(1,1′-biphenyl)-2-yl]methoxy}-benzenepropanoic acid, TUG-891, was more selective and potent for FFA4 than previous ligands. This agonist has now been extensively researched

and is perhaps the most well characterised FFA4 agonist. TUG-891 has been shown to be a potent molecule at human and mouse FFA4, although it does also result in activation of FFA1 in a species-specific manner as described in Part 1.9.3 (Hudson *et al.*, 2013). Compound A, another carboxylic compound was developed by Merck in 2014. Subsequent testing by Oh et al., (2014) revealed that in intracellular Ca^{2+} assays, Compound A showed little activity at FFA1. Additionally, Metabolex also developed a number of FFA4 agonists including Metabolex-36 which shows over 100-fold selectivity over FFA1 and Compound B (Agonist 2) which shows over 1000-fold selectivity over FFA1 (Engelstoft *et al.*, 2013).

These synthetic agonists described contain carboxylic groups, mimicking those of endogenous agonists. Mutational analysis of the orthosteric binding site of FFA4 identified that Arg99 was an important residue in the binding of carboxylic residues of free fatty acids and synthetic ligands (Shimpukade *et al.*, 2012). However, a series of non-carboxylic compounds have been also developed including GSK137647A and TUG-1197. GSK137647A is a sulfonamide FFA4 agonist, showing 50-fold greater selectivity for FFA4 than FFA1, however issues with agonist solubility may limit use in *in vivo* settings (Sparks *et al.*, 2014). TUG-1197 is a nonacidic benzosultam ligand and is described to show little activity at FFA1 (Azevedo *et al.*, 2016).

There have only been a handful of antagonists described for FFA4 including, 4-methyl-N-9H-xanthen-9-yl-benzenesulfonamide or AH7614 as it is commercially known and chemically similar 4-methyl-N-(9H-thioxanthen-9-yl)benzenesulfonamide or TUG-1506 (Sparks *et al.*, 2014; Watterson *et al.*, 2017). Both of these antagonists are non-competitive allosteric antagonists, which block FFA4 activity. Additionally, these antagonists are selective for FFA4 and do not block FFA1 agonist responses. FFA4 agonist and antagonist chemical structures are displayed in Table 1-1.
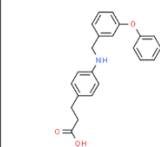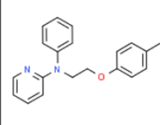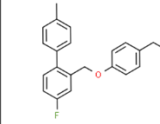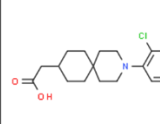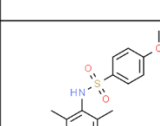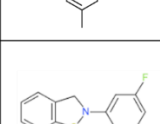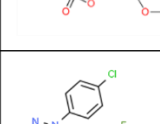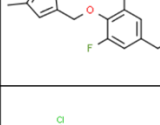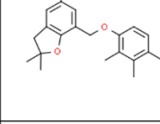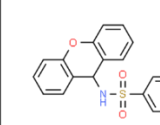
Compound	Chemical Structure	Chemical Formula	Selectivity
GW9508		**3**-{4-[(3-phenoxybenzyl)amino]phenyl}propanoic acid	FFA1/FFA4
NCG21		4-(4-{2-[phenyl(2-pyridinyl)amino]ethoxy}phenyl)butanoic acid	FFA4/FFA1
TUG-891		4-[(4-fluoro-4'-methyl[1,1'-biphenyl]-2-yl)methoxy]-benzenepropanoic acid	FFA4/FFA1
Compound A		3-[2-chloro-5-(trifluoromethoxy)phenyl]-3-azaspiro[5.5]undecane-9-acetic acid	FFA4
GSK137647A		4-methoxy-N-(2,4,6-trimethylphenyl)benzenesulfonamide	FFA4
TUG-1197		2-(3-(pyridin-2-yloxy)phenyl)-2,3-dihydrobenzo[d]isothiazole 1,1-dioxide	FFA4
Metabolex-36		3-(4-{[1-(4-chlorophenyl)-3-methyl-1H-pyrazol-5-yl]methoxy}-3,5-difluorophenyl)-2-methylpropanoic acid	FFA4
Compound B (Agonist 2)		3-{4-[(5-chloro-2,2-dimethyl-2,3-dihydro-1-benzofuran-7-yl)methoxy]-2,3-dimethylphenyl}propanoic acid	FFA4
AH7614		4-methyl-N-9H-xanthen-9-yl-benzenesulfonamide	FFA4
TUG-1506		4-methyl-N-(9H-thioxanthen-9-yl)benzenesulfonamide	FFA4

Table 1-1: Structures and chemical names of FFA4 compounds
Images of chemical structures from Chem spider.

Pharmacological research on the FFA4 receptor has been hindered by a lack of suitable agonists (Milligan *et al.*, 2017). Despite strenuous efforts, few FFA4 agonists are available and many of those that are have poor potency.

Additionally, only orthosteric agonists have been produced and we have not yet been able to exploit the potential therapeutic benefits which positive allosteric modulators offer. Perhaps for these reasons, there are very few FFA4 agonists which have made it to clinical trial. However, KDT501, an agonist chemically derived from natural hops has been characterised in phase II clinical trials where this drug increased adiponectin levels which promotes metabolic homeostasis (Konda *et al.*, 2014; Finlin *et al.*, 2017). Clearly there is potential therapeutic benefit in the modulation of FFA4 in metabolic diseases, and therefore there is a great need to develop and characterise more FFA4 agonists, not only for use as a drug target in metabolic diseases but also to explore newly emerging settings such as respiratory disease.

1.10   FFA4 in the colon

1.10.1   Background

In 2005, along with the discovery that FFA4 was a receptor that responded to long chain free fatty acids, Hirasawa *et al.*, (2005) showed localisation of FFA4 within the colon. High levels of expression have been shown within enteroendocrine cells (EECs) which are sparsely scattered throughout the gastrointestinal tract (Liddle, 2018). Within the colon, there are 4 layers: mucosa, submucosa, muscular layer and serosa (Rao and Wang, 2010; Kieffer and Epstein, 2022). Epithelial layers, which contain EECs, are present within mucosal layers which are important for the absorption of nutrients and contain villi to increase surface area to maximise absorption (Kiela and Ghishan, 2016). EECs form only 1% of the cells within the gut epithelium but are very important in the release of gastrointestinal hormones which regulate a variety of functions (R. Latorre *et al.*, 2016). Hormones secreted include glucagon-like peptide 1 (GLP-1), peptide YY (PYY), gastric inhibitory peptide (GIP), cholecystokinin (CCK), somatostatin and ghrelin. However, EECs are comprised of different cell types, each of which preferentially secrete a subtype of hormones or peptide. Within the stomach, the D subset of cells secrete somatostatin and A cells secrete ghrelin. K cells of the small intestines contain gastric GIP (Parker *et al.*, 2009; Lu *et al.*, 2012; Engelstoft *et al.*, 2013; Egerod *et al.*, 2015), intestinal I cells secrete CCK and L cells secrete PYY and GLP-1 (Reimann *et al.*, 2008).

EECs secrete peptide hormones following stimuli, with most peptide hormones released in response to food intake. Absorption of nutrients into the blood stream can result in peptide hormone release in a variety of different ways. Nutrients can interact with the surface of the EEC and most EECs sense nutrients through possession of microvilli which expand to the gut lumen (Liddle, 2018). However, some nutrients, including glucose require to be transported across the surface of the EEC in order to promote the release of gut hormones (McCauley, 2020). Additionally, hormones can be secreted upon stimulation of free fatty acid receptors, following binding of free fatty acids (Latorre *et al.*, 2016). The relative contributions of FFA4 on the secretions of these hormones is described in more detail in Chapter 6.

1.10.2   Overview of metabolic disease

Diabetes mellitus is prevalent worldwide with 537 million adults facing the disease in 2021, with around 90% of these cases expected to be T2DM cases. By 2030, this number is expected to rise to 643 million patients worldwide (International Diabetes Federation, 2021). T2DM is characterised by insulin insensitivity and dysfunction of ß cells of the pancreas (Saisho, 2015). Insulin insensitivity is described by improper function of insulin receptors, where in a healthy individual the release of insulin promotes glucose storage as glycogen in muscle and liver and as triglycerides in adipose tissue (Jensen *et al.*, 2011; Lankatillake, Huynh and Dias, 2019; Sanches *et al.*, 2021). However, insulin insensitivity results in a lack of glucose storage in liver, muscle and adipose tissues resulting in an excess of glucose in the bloodstream. As there is a lack of glucose within tissues, the liver believes the body is starved of glucose and converts glycogen to glucose for release into the bloodstream. This leads to elevation of glucose in the bloodstream leading to hyperglycaemia and glycosuria (Hatting *et al.*, 2018). To compensate for the high levels of glucose within the blood, the ß-cells of the pancreas secrete more insulin. However, eventually ß cells become dysfunctional and insulin secretion cannot cope with the demand for glucose production (Prentki and Nolan, 2006). Ultimately, the body is unable to maintain glucose homeostasis and cannot transport glucose around the body to liver, muscle and adipose tissues (Stanford and Goodyear, 2014). Pre-disposition factors for insulin resistance and T2DM include obesity, smoking and lack of physical activity. Additionally, diabetes is more frequent in

those over the age of 40 years old, however, incidences are increasing in younger age groups. Genetic factors can also contribute, with higher incidences seen in high-risk ethnic groups including Native American, African American and Asian groups (Chen, Magliano and Zimmet, 2012).

Additionally, T2DM is directly correlated with obesity. Obesity is characterised by an excess of fat storage as a result of a prolonged excess food intake. Obesity leads to an increase in excess free fatty acids which may lead to disruption of β-cell function and the development of diabetes (Shimabukuro *et al.*, 1998; Redinger, 2007). Obesity is also a chronic inflammatory disease triggering changes in many inflammatory markers including monocytes, lymphocytes, and neutrophils. Additionally, adipocytes release pro-inflammatory cytokines during obesity which contributes to the low grade inflammation (Deepesh and Anis, 2021). Macrophages also increase in number and change phenotype from M2 anti-inflammatory to M1 pro-inflammatory phenotypes (Zatterale *et al.*, 2020).

1.10.3   Current therapeutic opportunities in metabolic disease by targeting FFA4

Current treatments for T2DM work to enhance insulin secretion or improve sensitivity to insulin. The most widely used treatment is Metformin, which activates adenosine monophosphate protein kinase (AMPK) and promotes glucose uptake (Zhou *et al.*, 2001; Majumdar and Inzucchi, 2013; Marín-Peñalver *et al.*, 2016). Additional drugs may also be prescribed if Metformin does not lower blood glucose levels, some of which include GLP-1 receptor agonists which stimulate GLP-1 release, sulfonylureas which stimulate insulin secretion from β cells of the pancreas by regulating ATP-sensitive potassium channels and dipeptidyl peptidase-4 (DPP-4) inhibitors which inhibit the action of DPP-4, an enzyme which inhibits release of GLP-1 and GIP incretins (Majumdar and Inzucchi, 2013; Marín-Peñalver *et al.*, 2016). In addition to drug therapies, improved diet and exercise are also advised (Marín-Peñalver *et al.*, 2016). Prescribed drugs can however cause side effects including hypoglycemia and weight gain (Watterson *et al.*, 2014). Additionally, in 2017, T2DM was responsible for over 1 million deaths worldwide and so while there are current therapies, there is an obvious need for more effective therapies without adverse side effects (Khan *et al.*, 2020).

Free fatty acid receptors have gathered considerable interest in recent years as possible drug targets for metabolic diseases, due to their co-localisation in tissues responding to food intake such as the colon and the pancreas. Previously, FFA1 synthetic agonist treatment has been shown to improve glycaemic control and insulin secretion following treatment *in vivo* (Itoh *et al.*, 2003; Ghislain and Poitout, 2017). However, as earlier described in Part 1.8.3, FFA1 agonist TAK-875 failed clinical trials due to liver toxicity concerns, again highlighting the imperative need for the development of safer therapies (Kaku, Araki and Yoshinaka, 2013; Defossa and Wagner, 2014; Otieno *et al.*, 2018; Shavadia *et al.*, 2019). Given that FFA4 is also linked to regulation of glucose homeostasis, there is compelling evidence that FFA4 may provide a novel drug target for T2DM diabetes (Suckow *et al.*, 2014).

With the suggestion that FFA4 is co-expressed in EECs that regulate the release of metabolic hormones upon intake of food, links have been made between FFA4 and metabolic diseases such as diabetes and obesity (Alvarez-Curto and Milligan, 2016; Milligan *et al.*, 2017). FFA4 may promote the release of the incretin GLP-1 which stimulates insulin release, and furthermore FFA4 regulates inhibition of somatostatin release, the action of which promotes glucagon and insulin release (Hirasawa *et al.*, 2005; Croze *et al.*, 2021). Additionally, FFA4 has clinical implications in obesity, given that a variant of FFA4 containing a p.R270H mutation which inhibits FFA4 activity has been linked to an increased risk of obesity in European populations. This suggested that FFA4 is involved in regulation of body weight (Ichimura *et al.*, 2012). Further evidence supporting this indicated a role for FFA4 in satiety through the promotion of PYY secretion, a hormone which has been shown to reduce food intake in both mouse and human subjects (Moodaley *et al.*, 2017). Additionally, anti-inflammatory effects of FFA4 through β-arrestin pathways signalling may be beneficial in reduction of low grade inflammation experienced in obesity (Oh *et al.*, 2010). Therefore, FFA4 represents an attractive novel drug target for metabolic disease, however as described previously in Part 1.9.4, few FFA4 synthetic agonists have reached clinical trial in these areas. Therefore, development and characterisation of FFA4 agonists is vital in exploiting the therapeutic potential of FFA4 agonists in metabolic diseases.

1.11   FFA4 in the lung

1.11.1   Background

In addition to demonstrating FFA4 expression within colon tissues, Hirasawa *et al.*, (2005) also demonstrated that FFA4 was highly expressed in both human and mouse lung tissue. However, the physiological role of FFA4 within the lung was not investigated until Prihandoko *et al.*, (2020) unravelled the roles of FFA4 in airway smooth muscle (ASM) relaxation. Additionally in 2017, Lee *et al.*, discovered that ω-3 polyunsaturated fatty acids, natural ligands for FFA4, stimulated airway recovery in epithelial club cells. These two studies indicate that FFA4 may be a good drug target for respiratory disease.

The lung is composed of two halves, the right half containing three lobes and the left half containing two lobes, however, the lungs are part of a large and complex respiratory system (Chaudhry and Bordoni., 2021). The respiratory system is separated into conducting and the respiratory sections. The conducting section facilitates movement of air in and out of the lungs and is composed of nasal cavities, nasopharynx, larynx, trachea, bronchi and bronchioles. The respiratory section, often called lung parenchyma maintains gas exchange and is composed of bronchioles, alveolar ducts and sacs, and alveoli (Figure 1-7) (Khan and Lynch., 2022).
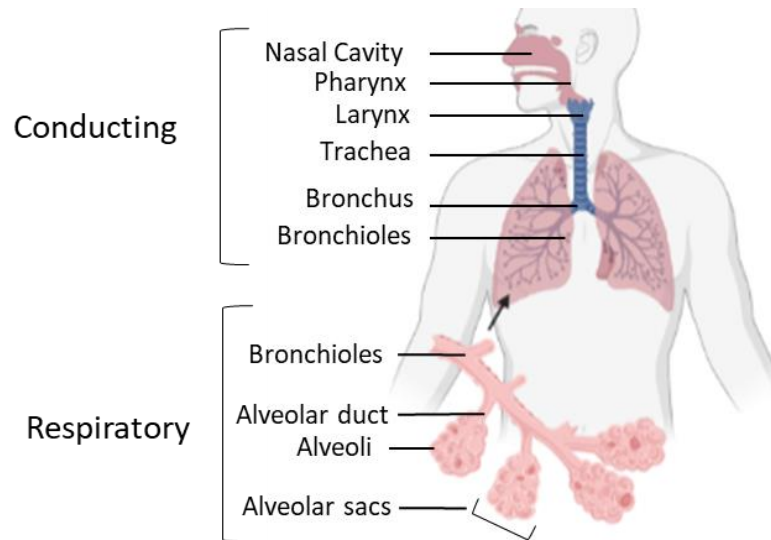
Figure 1-7: Lung anatomy
Within the respiratory system there are two portions, the conducting and the respiratory portions. The conducting section facilitates movement of air in and out of the lungs and the respiratory portion facilitates the exchange of gas inwards and outwards of the lung. The conducting proportion comprises of nasal cavities, nasopharynx, larynx, trachea, bronchi and bronchioles. The respiratory portion is comprised of bronchioles, alveolar ducts and sacs, and alveoli. Image created using Biorender.

There are four layers within the respiratory system: respiratory mucosa, submucosa, cartilage and muscular layer and adventitia. Epithelial layers are present within mucosal layers, functioning to prevent pathogen invasion (Larsen, Cowley and Fuchs, 2020). Epithelia of the respiratory parenchyma contain goblet cells which secrete mucus to act as a barrier for pathogens, while ciliated cells move mucus upwards to force pathogens out of the body. Deeper into the respiratory system, epithelial cells change from ciliated epithelium to non-ciliated epithelial cells called clara cells (Kia'i and Bajaj, 2022). FFA4 has been shown to reside in the lung epithelium, specifically within clara cells (Prihandoko *et al.*, 2020). FFA4 is also present in immune cell populations including lung resident macrophages where FFA4 plays anti-inflammatory roles (Oh *et al.*, 2010; Prihandoko *et al.*, 2020). Additionally, FFA4 has been detected in lung ASM (Prihandoko *et al.*, 2020).

1.11.2   Respiratory disease

Asthma and chronic obstructive pulmonary disease (COPD) are both respiratory diseases that involve lung inflammation and constriction of the airways. Asthma is one of the most common and prevalent diseases worldwide, with 262 million asthma sufferers reported globally in 2019 (Abbafati *et al.*, 2020). There is a

broad spectrum of different pathologies in asthma, which can be categorised based on differing disease stimuli, symptom onset and pathophysiology. These include allergic asthma, non-allergic asthma, seasonal and exercise induced asthmas, and adult and child onset asthma (Romanet-Manent *et al.*, 2002; Choi *et al.*, 2012; Trivedi and Denton, 2019). The most common form of asthma is allergic asthma, which is caused by environmental allergies including pollen and house dust mites. Common to all forms of asthma are symptoms including tightness of chest, shortage of breath, airway hyperresponsiveness and coughing (Barnes, Rodger and Thomson., 2009). These symptoms are induced by obstruction of airways and chronic inflammation (Barnes, 2008).

COPD is also a debilitating respiratory disease of the small airways, resulting in high rates of morbidity, and is currently the fourth most common cause of death worldwide (Barnes, 2016). In 2016, around 251 million people had been diagnosed with COPD worldwide but this number is expected to be far greater as many patients have been misdiagnosed or remain undiagnosed (Vos *et al.*, 2016). COPD often affects people over the age of 35 and is caused by exposure to pollutants such as cigarette smoke, inducing symptoms such as a chronic cough, breathlessness, production of atypical sputum, fibrosis of the lung and irreversible emphysema. A progressive reduction in lung function follows which leads to physical decline and may ultimately lead to death (Bhatia and Fromer, 2011).

1.11.3   Lung inflammation in asthma and COPD

In both asthma and COPD, disease pathophysiology is heavily influenced by inflammation. However, inflammation in both diseases differs. In allergic asthma, inflammation is driven by a T helper 2 (Th2) response that induce pathophysiological responses as a result of these immune responses, including contraction of smooth muscle, mucus hypersecretion, bronchial hyperresponsiveness and airway remodelling (Figure 1-8) (Bosnjak *et al.*, 2011; Lambrecht, Hammad and Fahy, 2019).
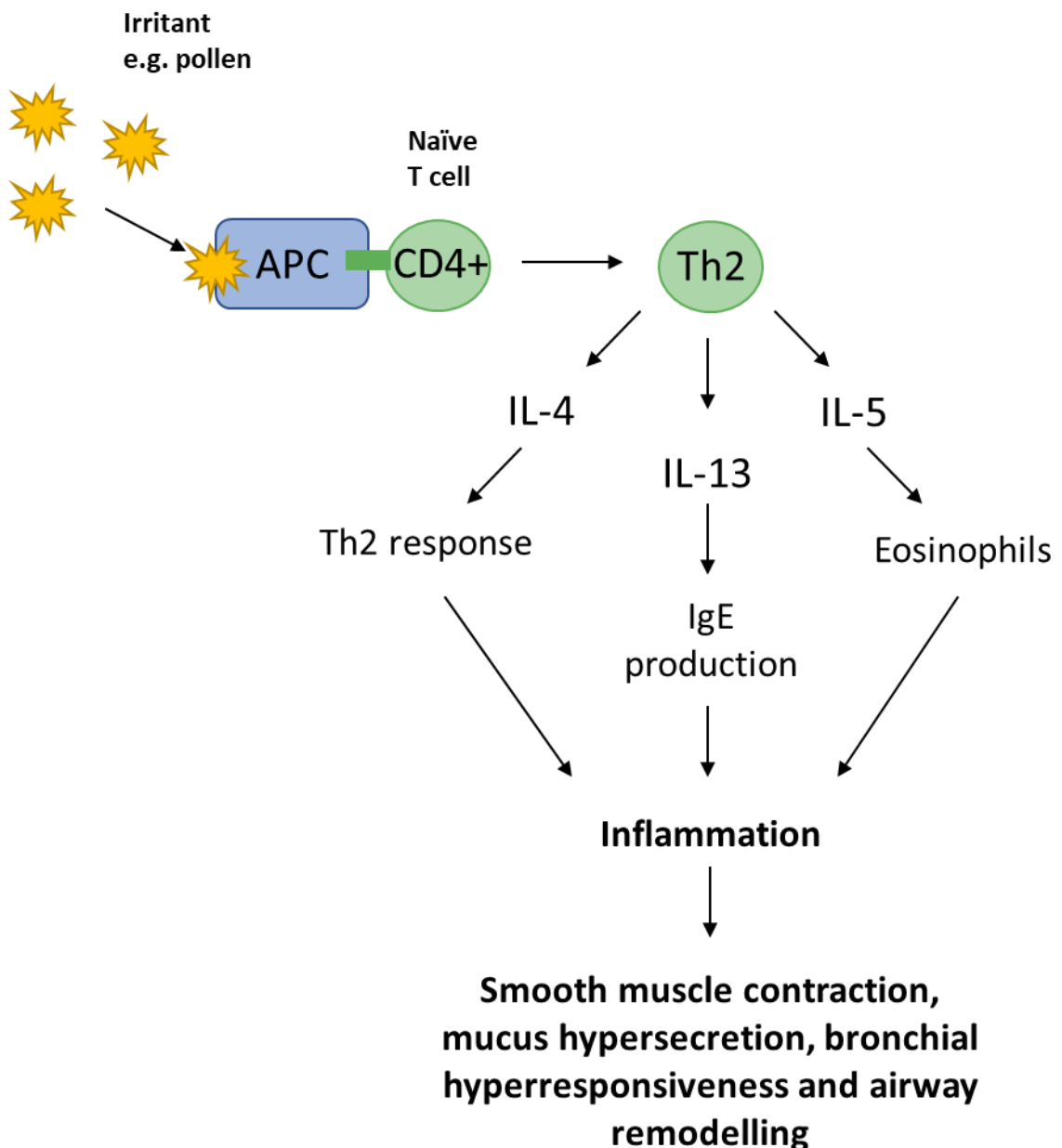
Figure 1-8: Inflammation in allergic asthma
In primary sensitising events, which usually occur during childhood, irritation with allergenic stimuli causes antigen presenting cells (APCs) to interact with CD4+ T cells (Bosnjak *et al.*, 2011; León and Ballesteros-Tato, 2021). This promotes the differentiation of these cells into Th2 helper cells. Following a second exposure to an allergen, these Th2 helper cells become activated and travel to airways where Th2-associated cytokines, such as IL-4, IL-13, and IL-5 are released (Seumois *et al.,* 2014) . IL-4 promotes further differentiation of naïve T cells to Th2 cells, IL-13 is a pro-inflammatory cytokine which stimulates IgE production from B cells and IL-5 promotes release of eosinophils which further promote inflammation by the release of pro-inflammatory mediators (May and Fung, 2015; Hassani and Koenderman, 2018; Russkamp *et al.,* 2019). Mast cells are also activated resulting in release of inflammatory mediators. The resulting immune responses contribute to the allergic physiological symptoms associated with asthma.

In COPD, the inflammatory response is complex and differs vastly from asthma. Following response to stimuli including inhaled cigarette smoke, lung epithelium releases inflammatory mediators and reactive oxygen species (ROS). This activates macrophages causing them to release a variety of chemokines and

cytokines in turn recruiting monocytes, neutrophils and lymphocytes. Membrane wall degrading serine proteases and reactive oxygen species are also secreted from macrophages. Additionally, eosinophils are involved in the immune response also, promoting emphysema (Barnes, 2016). Collectively, these immune cells and mediators contribute to physiological symptoms associated with COPD (Figure 1-9).
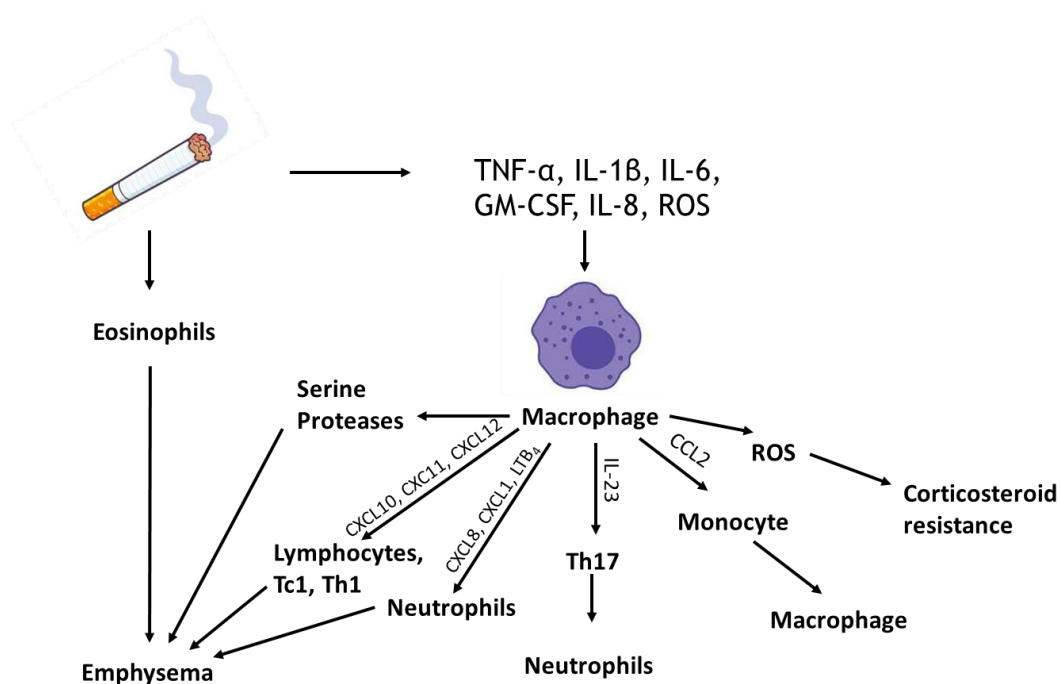
Figure 1-9: Inflammation in COPD
In response to stimuli such as cigarette smoke and pollution, epithelial cells release TNF-α, IL-1β, IL-6, granulocyte-macrophage colony-stimulating factor (GM-CSF) and IL-8. Macrophages are activated by release of these inflammatory mediators and reactive oxygen species (ROS) (Barnes, 2016). Activated macrophages secrete CCL2 to recruit monocytes which differentiate into macrophages (Traves *et al.*, 2002; Barnes, 2016). Additionally, macrophages stimulate chronic inflammation by secreting chemokines and cytokines which attract neutrophils, monocytes and Th17. Chemotactic factors such as IL-8 guide the neutrophils into the respiratory tract where they promote mucus hypersecretion and secrete serine proteases, resulting in the destruction of alveolar walls, leading to irreversible emphysema. Macrophages can also directly secrete these alveoli destructing enzymes, and additionally secretion of reactive oxygen species which contributes to resistance to corticosteroids, drugs commonly taken to reduce inflammation in COPD (Barnes, 2016). Lymphocytes and eosinophils can also be secreted during disease pathogenesis. Lymphocytes, including Th1 and Tc1 T cells, are increased upon disease onset by activation of CXCR3 by chemokines secreted by macrophages and lung epithelium. Release of IFN-γ from lymphocytes promotes further release of chemokines, perforin and granzyme B which contribute to airway emphysema. Eosinophils which are most commonly found in asthma patients can also be increased in COPD patients, although mechanisms for eosinophil accumulation are not certain.

Inflammation in respiratory diseases is a primary cause for the narrowing of the airway which results in symptoms such as shortness of breath, tightness of chest and coughing (Lambrecht, Hammad and Fahy, 2019). It is possible that the

inhibition of the TAB1/TAK1 interaction in the ß-arrestin signalling pathway of FFA4 may be able to alleviate some of the inflammatory processes and associated symptoms of asthma and COPD, although this is a poorly researched topic.

1.11.4   Smooth muscle contraction and relaxation in lung airways

Smooth muscle which is present throughout the body has the ability to contract and relax. As previously described, most of the discomfort in respiratory diseases comes from the restriction of airways which can lead to hyperresponsiveness. Airway smooth muscle (ASM) contraction and relaxation are complex processes regulated by a variety of different intracellular signalling pathways. Receptors involved in ASM contraction include M3 muscarinic receptors and tachykinin. These receptors signal through Gq protein pathways resulting in inositol triphosphate (IP3) production and release of Ca^{2+} from the sarcoplasmic reticulum (Gosens *et al.*, 2006; Mizuta *et al.*, 2008; Bradley *et al.*, 2016). This mechanism is mediated by the activation of inositol triphosphate receptors (IP3R) and ryanodine receptors (RyR), and results in activation of calmodulin and myosin light chain kinase (MLCK) (Somlyo and Somlyo, 2003; Kim *et al.*, 2016). The resulting phosphorylation of MLC results in interaction with myosin and actin to facilitate cross-bridge cycling in contractile events (Somlyo and Somlyo, 2003; Kim *et al.*, 2016; Hafen and Burns, 2022). Contraction can also occur independently of calcium through a RhoA GTPase pathway where Rho-kinase phosphorylates MLC (Somlyo and Somlyo, 2003). In addition, calcium release produces oscillations within ASM cells, which can be directly related to the size of airway contraction (Perez and Sanderson, 2005).

Smooth muscle relaxation occurs following inhibition of contraction by removal of stimulus or use of vasodilator. The process usually occurs by the dephosphorylation of MLC by MLC phosphatases and by depletion of intracellular calcium (Webb, 2003). There are a variety of molecular mechanisms which regulate ASM relaxation. Relaxation of ASM is as a result of increased cAMP which results in the inhibition of the previously mentioned MLCK and dephosphorylation of MLC (Billington *et al.*, 2013). Additionally, mechanisms have been described for the role of nitric oxide in ASM relaxation. Nitric oxide

produced in endothelial cells activates guanylate cyclase in smooth muscle cells. This results in cyclic guanosine 3',5' monophosphate (cGMP) production which activates effector proteins such as cGMP-dependent protein kinase or protein kinase G (PKG), phosphodiesterase's (PDE) and ion channels which stimulate smooth muscle relaxation (Carvajal *et al.*, 2000; Perez-Zoghbi, Bai and Sanderson, 2010).

Recently, FFA4 expression has been identified in ASM and activation of FFA4 has been shown to result in ASM relaxation (Prihandoko *et al.*, 2020). Efforts by Prihandoko *et al.*, (2020) revealed that upon FFA4 agonist stimulation, Prostaglandin E2 (PGE2) is released which may result in smooth muscle relaxation. Subsequently, it was identified that following FFA4 agonist stimulation, COX-2 transcription was increased. COX-2 leads to production of PGE2, which binds to EP4 receptors resulting in increased cAMP production through a Gs coupled pathway. The resulting cAMP acts to inhibit MLCK, resulting in smooth muscle relaxation (Ruan, Zhou and Chan, 2011; Billington *et al.*, 2013; Prihandoko *et al.*, 2020). However, the relative contributions that this may have on FFA4 mediated smooth muscle relaxation and the definitive mechanism by which this occurs is unknown. The role of FFA4 activation in ASM relaxation will be discussed in detail in Chapter 5.

1.11.5   Treatments for respiratory diseases

Treatments for asthma and COPD mainly comprise of orally inhaled drugs. Although these pathologies seem similar in terms of symptoms, their pathogeneses are very different, and therefore proper diagnosis is required for prescription of effective treatments. Inflammation that results in COPD involves infiltration with macrophages, neutrophils and T lymphocytes, however, in allergic asthma, inflammation is caused by an allergic reaction due activation of mast cells and T lymphocytes which results in recruitment of eosinophils. The blockage of the airways is almost completely reversible in asthma, however, in COPD it is irreversible (Bhatia and Fromer, 2011). In some cases, patients may have hallmarks of both asthma and COPD and this is called asthma-COPD overlap. The latter disease usually involves COPD patients who have increased eosinophils and respond well to bronchodilators and corticosteroid therapies, hallmarks that are shared with asthma patients (Barnes, 2019).

Due to molecular differences in these diseases, a treatment for asthma may not necessarily be an effective treatment for COPD. Thus a specific diagnosis is crucial for the prescription of the most appropriate medications (Bhatia and Fromer, 2011). Currently there are no therapies available which cure or slow the progression of asthma and COPD; however, therapies are available which manage disease symptoms. The most commonly prescribed drugs are long-acting β2-agonists (LABA), long acting muscarinic agonists (LAMA) and corticosteroids (Page and Cazzola, 2014). LABAs and LAMAs are bronchodilators which act as airway relaxants and are a largely effective treatment in the relief of breathing difficulty (Barnes, 2010). Corticosteroids can be used in combination with bronchodilators to reduce inflammation (Barnes, 2012) but steroid therapy is not without risk as some patients suffer from deleterious side effects including osteoporosis and cataracts (Dahl, 2006). Asthma patients are prescribed inhaled corticosteroids but if symptoms persist, LABAs can be prescribed. Patients with severe symptoms may be prescribed other drugs including LAMAs and oral corticosteroids. COPD patients are usually prescribed LABAs and LAMAs to relieve symptoms. However, if disease symptoms persists corticosteroids and additional drugs including phosphodiesterase 4 inhibitors may be prescribed (Bhatia and Fromer, 2011; Barnes, 2018). Patients suffering from asthma-COPD overlap require LABAs, LAMAs and inhaled corticosteroids in combination (Barnes, 2018). Some patients may develop resistance to corticosteroids resulting in a chronic form of the disease (Barnes, 1998). Additionally, these therapies are unable to act on the irreversible emphysema which is seen in COPD. Due to increasing numbers of patients suffering from these diseases, it is clear that pre-existing drug therapies do not effectively manage symptoms and novel drug therapies need to be considered to better manage respiratory diseases. FFA4 agonists represent a novel therapy due to their anti-inflammatory and broncho-dilating properties.

1.12   Thesis aims

Despite pre-existing therapies for metabolic diseases such as diabetes and respiratory diseases including asthma and COPD, these diseases are still very prevalent worldwide and affect the lives of millions of people. Drug therapies can result in harmful side effects and may be ineffective on certain populations of patients, highlighting a clinical need for novel and safer therapeutics. FFA4 provides a novel therapeutic target for T2DM based on its involvement in regulation of glucose homeostasis. Additionally, anti-inflammatory effects exerted by FFA4-mediated ß-arrestin-dependent signalling pathways may be able to alleviate low grade inflammation in obesity. These anti-inflammatory effects may also be beneficial in the relief of inflammation contributing to asthma and COPD symptoms. FFA4 has also been proven to relax ASM which may be useful in treatment of bronchoconstriction in these respiratory diseases.

Previously developed drugs have been unsuitable for clinical treatment due to poor selectivity, potency and insolubility. There has also been a lack of consistency across the pharmacological data collected for FFA4 ligands due to inconsistencies of the assay systems used. Therefore, the general aims of this thesis are to:

- Test FFA4 compounds in pharmacological assays to detect changes in inositol monophosphate (IP1), cAMP, pERK1/2 levels and ß-arrestin2 coupling in Chinese Hamster Ovary (CHO) or human embryonic kidney (HEK) cells to characterise ligand properties and directly compare to one another.

- Characterise the effects of FFA4 agonists on ASM relaxation in C57BL/6 mice containing an FFA4-HA tag or an FFA4 KO mutation.

- Characterise the effects of FFA4 compounds on GLP-1 secretion from primary colonic crypts within the colon in C57BL/6 mice containing an FFA4-HA tag or an FFA4-KO mutation.

Additionally, the definitive roles of phosphorylation of FFA4 and the physiological outcomes of FFA4-mediated phosphorylation-dependent pathways

are unknown. Therefore, experiments will also be conducted in CHO and HEK cell lines and C57BL/6 mice expressing a phosphorylation-deficient (PD) mutant form of the FFA4 receptor, whereby intracellular phosphorylation sites were removed resulting in an inability to couple to phosphorylation-dependent signalling pathways. These experiments will help to determine the relative contributions of phosphorylation-dependent signalling pathways on the physiological functions of FFA4.

It is hoped that further characterisation of FFA4 compounds may result in the development of safer and novel drug therapies for the treatments of metabolic and respiratory diseases.

Chapter 2   Materials and methods

2.1 Materials

2.1.1 Reagents

2X Laemlli buffer (Invitrogen, P/N: LC2676)

5X Reaction buffer (Invitrogen, P/N 28025013)

Carbachol (Sigma-Aldrich, P/N: PHR1511)

Coelenterazine-h (Nanolight Technology, P/N: 301)

Collagenase XI (Merck, P/N: C7657)

DNase amplification grade, 10X DNase I reaction buffer and DNase I stop solution (Sigma-Aldrich, P/N: AMPD1-1KT)

Deoxynucleoside triphosphate (dNTP) (New England Biolabs, P/N N0447S)

Dithiothreitol (DTT) (Invitrogen, P/N: D1532)

Dulbecco's phosphate buffered saline (PBS) (Thermo Fisher Scientific, P/N: 14190094)

Ethylenediamine tetraacetic acid (EDTA) (Invitrogen, P/N: 15575-038I)

Fatty acid free bovine serum albumin (BSA) (Merck, P/N: 10775835001)

Foetal bovine serum (FBS) (Thermo Fisher Scientific, P/N: 10500064)

Forskolin (Sigma-Aldrich, P/N: F3917)

Fura 8-AM (Stratech Scientific Limited, P/N: 21056-AAT)

Goat serum (Sigma-Aldrich, P/N: G9023)

Hank's balanced salt solution (HBSS) (Thermo Fisher Scientific, P/N: 14025-050)

High glucose DMEM (Thermo Fisher Scientific, P/N: D6546)

Hygromycin B solution (Santa Cruz Biotechnologies, P/N: sc-29067)

IBMX (3-isobutyl-1-methylxanthine) (Invitrogen, P/N: PHZ1124)

Igepal CA360 (Thermo fisher Scientific, P/N: J61055.AE)

Immobilon western chemiluminescent horseradish peroxidase (HRP) substrate (Millipore, P/N: WBKLS0100)

L-Glutamine (Gibco, P/N: 25030081)

Lipofectamine 2000 (Thermo Fisher Scientific, P/N: 11668019)

Matrigel (Corning, P/N: 356234)

MMVL reverse transcriptase enzyme (Invitrogen, P/N 28025013)

Nutrient mixture F-12 ham with L-glutamine and sodium bicarbonate (Sigma, P/N: N6658)

Opti-MEM (Thermo Fisher Scientific, P/N: 31985062)

Penicillin-Streptomycin (Pen-Strep) (10,000U/mL) (Thermo Fisher Scientific, P/N: 15140122)

Pierce™ coomassie plus (Bradford) assay reagent bradford reagent (Thermo Fisher Scientific, P/N: 23238)

Precision plus protein all blue prestained protein standards (Bio-Rad, P/N: 1610373)

Random hexamers (Invitrogen, P/N: N8080127)

Sodium propionate (C3) (Sigma-Aldrich, P/N: P1880)

Fast sybr green (Thermo Fisher Scientific, P/N: 4385612)

Triton X-100 (Sigma, P/N: T9284)

Tween-20 (Sigma, P/N: P7949)

UltraPure™ low melting point agarose (Invitrogen, P/N: 16520050)

Vectashield mounting media (2bscientific, P/N H-1200-10)

2.1.2 Solutions

1X Tris-buffered saline-Tween (TBST) (pH7.4) – 20 mM Tris-HCl, 137 mM NaCl, 0.1% Tween20 (v/v)

138 buffer - 10 mM HEPES, 138 mM NaCl, 4.5 mM KCl, 4.2 mM $NaHCO_3$, 1.2 mM NaH_2PO_4, 2.6 mM $CaCl_2$, 1.2 mM $MgCl_2$

Blocking buffer immunohistochemistry – TBS with 0.1% (v/v), 10% goat serum (v/v) and 1% BSA (w/v)

Colonic crypt lysis buffer - 50 mM Tris-HCl, 150 mM NaCl, 0.5% sodium deoxycholate (w/v), 1% Igepal CA-630 (v/v)

HEPES buffer (pH7.4) - 10 mM HEPES, 135 mM NaCl, 10 mM glucose, 5 mM KCl, 2 mM $CaCl_2$, and 1 mM $MgCl_2$

Radioimmunoprecipitation assay buffer (RIPA) buffer – 25 mM Tris-HCl, 150 mM NaCl, 5 mM EDTA, 1% Triton X-100 (v/v), 1% sodium deoxycholate (w/v), 0.1% SDS (v/v), 1 tablet protease inhibitor (Sigma-Aldrich, P/N: 11836170001)

Transfer buffer - 25 mM Tris-base, 192 mM glycine, and 20% methanol (v/v)

Tris-Glycine SDS running buffer– 5 mM Tris-Cl, 250 mM glycine, 0.1% SDS (v/v)

Wash buffer immunohistochemistry- TBS with 0.1% (v/v)

2.1.3 FFA4 pharmacological reagents

Compound	Supplier
TUG-891	Tocris (P/N: 4601)
Agonist 2 (Compound B)	MedChemExpress (P/N: 1234844-11-1)
GSK137647A	Tocris (P/N:5257)
TUG-1197	Kind gift from Trond Ulven, University of Copenhagen
Compound A	Merck (P/N: 349085-82-1)
Modulator 1	MedChemExpress (P/N: 1050506-75-6)
Modulator 2	MedChemExpress (P/N: 1050506-87-0)

Table 2-1: Product number and suppliers of FFA4 compounds

Structures and chemical formulas of FFA4 compounds are displayed in Table 1.1 of Chapter 1 Part 1.9.4.

2.1.4 Kits

CisBio cAMP (P/N: 62AM4PEC)

CisBio IP1 (P/N: 62IPAPEC)

CisBio phospho-ERK (Thr202/Tyr204) kit (P/N: 64AERPEH)

GLP-1 enzyme-linked immunosorbent assay (ELISA) kit from Millipore (P/N: EGLP-35K)

PYY ELISA kit from Phoenix Europe (P/N: EK-059-03)

Qiagen RNeasy plus mini kit (P/N: 74134)

2.2 Methods

2.2.1 Cell culture

2.2.1.1 Stable transfection of cell lines

All cell culture procedures were performed using aseptic techniques in class 2 biological safety cabinets. All cell lines were maintained in 37°C incubators, supplied with 5% CO_2.

Murine FFA4 (mFFA4) receptors were stably transfected into Chinese hamster ovary (CHO) cells using the Flp-In system. This contains a Flp Recombination Target (FRT) site that facilitates stable integration of a DNA plasmid in the pcDNA5/FRT/TO vector, which occurs upon co-transfection of the Flp recombinase-encoding pOG44 vector. Cells were co-transfected with FFA4 receptor, with enhanced yellow fluorescent protein (eYFP) C-terminal tag and an N-terminal FLAG epitope tag, in the pcDNA5 FRT/TO expression vector and pOG44 Flp-In recombinase vector at a ratio of 1:9 (Hudson *et al.*, 2013; Prihandoko *et al.*, 2016). Construct and vector were incubated for 15 min in 500 µL of Opti-MEM with 10 µL of Lipofectamine 2000 at room temperature. Non-transfected cells in a 10 cm dish were serum starved for at least 5 hours, before addition of transfection mixture containing construct and vector. Cells were incubated overnight at 37°C, 5% CO_2. Subsequently the medium was changed to complete growth medium containing hygromycin B. Selection for transfected cells was by addition of hygromycin B since the pcDNA5/FRT/TO plasmid imparts hygromycin resistance. Medium was changed every 2 days until wells were confluent. Cells were then washed with 2 mL PBS/1 mM EDTA and detached from 10 cm dishes by incubation with 0.5 mL PBS/1 mM EDTA for 5 min. Detached cells were diluted with appropriate medium and transferred to new T25 flasks containing fresh complete medium.

2.2.1.2 Maintenance of cell lines

Three CHO cell lines were used, one which had not been transfected, one which stably expressed FFA4 receptor and one which stably expressed a PD form of the FFA4 receptor. The two stable cell lines were cultured in F12 ham medium supplemented with 10% FBS (v/v), 100 units/mL penicillin, 100 µg/mL streptomycin and 400 µg/mL hygromycin B (v/v). The non-transfected cell line was cultured in F12 ham medium supplemented with 10% FBS (v/v), 100 units/mL penicillin and 100 µg/mL streptomycin only.

Human embryonic kidney (HEK) cells were also utilised, both non-transfected and additionally FFA1 T-rex Flp-In cells, containing mouse FFA1 with a C-terminal eYFP tag (generated by Brian Hudson, University of Glasgow) (Hudson *et al.*, 2013). T-rex Flp-In cell lines were cultured in Dulbecco's modified eagle medium (DMEM) supplemented with 10% FBS (v/v), 100 units/mL penicillin, 100 µg/mL streptomycin and 400 µg/mL hygromycin B (v/v). As T-rex Flp-In cell lines confer doxycycline-inducible expression of the receptor of interest, experiments performed using these cells were conducted after 24 hours of treatment with 100 ng/ml doxycycline to induce FFA1 receptor expression. Non-transfected cells were cultured in DMEM supplemented with 10% FBS (v/v), 100 units/mL penicillin and 100 µg/mL streptomycin.

Cell lines grown to confluence were passaged every 3-4 days by aspirating cell culture medium and washing cells in sterile 1X PBS supplemented with 1 mM EDTA. Following this, cells were incubated with PBS/1 mM EDTA for 5 min at 37°C, 5% CO_2 to detach the cells from the culture vessel. Detached cells were diluted with appropriate medium and transferred to a sterile flask containing fresh cell culture medium.

2.2.1.3 Cryopreservation of cells

Cells were grown to 80% confluency before aspiration of cell culture medium. Cells were washed in 5 mL sterile PBS/1 mM EDTA before incubation with 2 mL PBS/1 mM EDTA for 5 min at 37°C at 5% CO_2 to detach cells from the culture vessel. Detached cells were diluted with appropriate medium and transferred to a sterile falcon tube for centrifugation at 1000 x g for 5 min. Medium was

aspirated and cells resuspended in 1 mL freezing medium (10% DMSO-FBS). Cells were transferred to a cryotube and frozen at -80°C before storage in liquid nitrogen.

2.2.1.4 Receptor internalisation

eYFP tagged cells (CHO/HEK) were seeded at 3×10^5 cells/well and grown overnight on 30 mm round coverslips in a 6 well plate before serum starvation for 5 h. Cells were subsequently treated for 30 min with 10 µM compound before fixation with 4% paraformaldehyde (PFA) (v/v) for 30 min at 4°C. Coverslips were washed 4 times for 10 min each with 1 mL PBS. Coverslips were mounted on glass slides using Vectashield mounting media containing DAPI. Cells were imaged were imaged on an LSM 880 confocal laser scanning microscope (Zeiss) using a x20 objective.

2.2.2 Immunoblotting

2.2.2.1 Agonist stimulation in cells

CHO cells which were either non-transfected, stably expressing mFFA4 or stably expressing PD-mFFA4 were plated into a 6 well plate and left to grow for 3-4 days before serum starving for at least 5 h in 1 mL serum free medium. Cells were treated with either 0.01% DMSO vehicle (v/v), 10% FBS (v/v), 1 µM or 10 µM of FFA4 compound in 0.01% DMSO (v/v) for 5 min at 37°C. Medium was removed and cells were lysed for western blot preparation.

2.2.2.2 Western blot sample preparation

Cells in 6 well plates were lysed in 250 µL/well of RIPA buffer for 30 min on ice. Lysates were centrifuged at 21,000 x g, 4°C for 10 min to remove cell debris. The supernatants were retained and used for subsequent experiments.

2.2.2.3 Protein quantification

Protein in cell lysates was quantified using a bradford assay. Firstly, 990 µL of dH_2O, 10 µL of lysate/RIPA control and 1 mL of bradford reagent were added to 3 mL cuvettes. Absorbance at a wavelength of 595 nm was measured in a spectrophotometer (Eppendorf BioPhotometer) and concentrations interpolated

from a standard curve created by measuring the absorbance of standards with known concentration.

2.2.2.4 SDS-PAGE

Lysates were added to an equal volume of 2X laemmli buffer and heated at 65°C for 5 min to denature proteins. Protein samples were then resolved using sodium dodecyl sulphate polyacrylamide gel electrophoresis (SDS-PAGE). To a 10% SDS-PAGE gel, 10 µg of protein per lane was loaded and gels were run for 40-50 min at 200 V in 1X Tris-Glycine running buffer.

2.2.2.5 Western blot

SDS-PAGE gels were transferred onto nitrocellulose membrane in a semi-dry transfer Transblot machine (BioRad) at 25 V for 1 h. Membranes were then blocked with 5% non-fat milk powder (w/v) made up in TBST pH7.4 for 1-3 h at room temperature. Membranes were incubated overnight at 4°C in primary antibody (Table 2-2), made up in 5% non-fat milk powder (w/v) diluted in TBST.

Antibody	Dilution	Species	Catalog Number	Company
pERK1/2	1:1000	Rabbit	9101S	Cell Signalling Technology
tERK1/2	1:1000	Rabbit	9102S	Cell Signalling Technology
p-mFFA4	1:2000	Rabbit	In-house	(Prihandoko *et al.*, 2016)
GAPDH	1:5000	Rabbit	2118L	Cell Signalling Technology
GFP	1:1000	Mouse	1218	Abcam

Table 2-2: Primary antibodies for western blot

Membranes were washed 3x in TBST for 15 min each before addition of relevant secondary antibody (Table 2-3). LI-COR secondary antibody incubation was performed in the dark.

Antibody	Dilution	Host Species	Catalog Number	Company
IRDye 800CW Anti-Rabbit IgG (H+L)	1:5000	Donkey	926-32213	LI-COR Biotechnology
Anti-rabbit (HRP)	1:2000	Goat	65-6120	Thermo-Fisher Scientific
IRDye 800CW Anti-Mouse IgG (H + L)	1:5000	Donkey	926- 32212	LI-COR Biotechnology

Table 2-3: Secondary antibodies for western blot

Membranes were washed 3x in TBST for 15 min before development. This stage was carried out in the dark for membranes probed with LI-COR antibodies. Membranes were either developed by Immobilon western chemiluminescent HRP substrate and FFA4 bands detected on X-ray films using Xomat machinery or using the LI-COR development system with LI-COR secondary antibodies for all other proteins.

2.2.3 Pharmacological assays

2.2.3.1 pERK1/2 assay

pERK1/2 assays were performed as instructed in the CisBio phospho-ERK (Thr202/Tyr204) kit. All cells were plated out at 35,000 cells/well in 96 well plates and grown overnight. Cells were washed 2x with 100 μL F12 ham serum free medium and serum starved for 5 h with 90 μL of serum free medium, 80 μL for antagonist experiments.

Following serum starvation, 10 μL of serially diluted FFA4 agonists in serum free medium were added to cells so that the final concentration of agonist ranged from 0.1 nM to 3.16 μM. Cells were preincubated with antagonist for 30 min for experiments containing these, incubated with agonist for 5 min for dose response experiments, and agonist treatment for the time course was over 60 min. Medium was removed and cells were lysed in 50 μL of lysis buffer (prepared according to the manufacturer's instructions) for 30 min by shaking plates at 600 rpm at room temperature.

2.2.3.2 IP1 assay

IP1 assays were performed as instructed in the CisBio kit. All cells were plated out at 35,000 cells/well and grown overnight. After a 30 min incubation in stimulation buffer, 10 μL of serially diluted FFA4 agonists in serum free medium were added to cells for 1 h, so that the final concentration of compound ranged from 0.1 nM to 3.16 μM. Following agonist incubation, medium was removed and 50 μL of lysis buffer was added to each well. To lyse cells, the plate was shaken at 600 rpm at room temperature for 30 min.

2.2.3.3 cAMP assay

cAMP assays were performed as instructed in the CisBio kit to examine Gαs and Gαi coupled signaling. All cells were plated out at 35,000 cells/well and grown overnight. Stimulation buffer was made up with the addition of 0.5 mM IBMX, a non-selective phosphodiesterase inhibitor.

Gαs signalling: After a 15 min incubation in 90 μL stimulation buffer, 10 μL of serially diluted FFA4 agonists or forskolin in serum free medium were added to cells for 1 h 45 min, so that the final concentration of compound ranged from 0.1 nM to 3.16 μM. Following agonist incubation, medium was removed and 50 μL of lysis buffer was added to each well. To lyse cells, the plate was shaken at 600 rpm at room temperature for 30 min before freezing at -20°C.

Gαi signalling: After a 15 min incubation in 90 μL stimulation buffer, 10 μL of serially diluted FFA4 agonists in serum free medium and EC80 forskolin concentration (calculated on GraphPad Prism using values from Gαs experiments) were co-incubated on cells for 1 h 45 min. Following agonist

incubation, medium was removed and 50 μL of lysis buffer was added to each well. To lyse cells, the plate was shaken at 600 rpm at room temperature for 30 min before freezing at -20°C.

2.2.3.4 Pharmacological assay quantification

Following all assays in section 2.2.3, 16 μL of cell lysate and 4 μL of a 1:1 mixture of cryptate and d2 antibodies were added to each well of a 384 well optiplate (PerkinElmer). The cryptate antibody is a specific antibody which is labelled with Eu^{3+}-cryptate and acts as a donor with emission at 620 nm. The second specific antibody is labelled with d2 and acts as the acceptor antibody with emission at 665 nm. One antibody binds to the phosphorylated motif on the protein and the second binds the protein independently of its phosphorylation state. In pERK1/2 Assays, when both antibodies come into contact with phosphorylated ERK1/2, the Eu^{3+} cryptate and d2 are in close proximity and initiate a fluorescence resonance energy transfer (FRET) signal which is proportional to the phosphorylation of ERK1/2. cAMP and IP1 assays differ slightly in that they are competition binding assays and production of cAMP/IP1 outcompetes labelled cAMP/IP1 causing a decrease in signal.

Optiplates were shaken for the time stated on respective kits. Plates were read on CLARIOstar (BMG biotech) at wavelengths 665 nm and 620 nm. Readings for pERK1/2 assays were calculated as a % maximal response normalised to TUG-891 or the respective positive control as stated in each figure. Data was plotted as a concentration response curve on GraphPad Prism. Readings for IP1 and cAMP assays were plotted on GraphPad Prism as a concentration response curve and then subsequently values were inverted and then normalised to the % maximal response of TUG-891 or respective positive control as indicated in each figure.

2.2.3.5 Bioluminescence resonance energy transfer (BRET) β-Arrestin2 recruitment assay

HEK293 cells were seeded at 2 million cells per 10 cm petri-dish and incubated 37°C at 5% CO_2. One day later, transfection of cells with 1:4 ratio of FLAG-FFA4-eYFP and ß-arrestin-2 fused with Renilla-luciferase (ß-arrestin-2- RLuc) in 500 μL of Opti-MEM using Lipofectamine 2000 transfection reagent was performed (Butcher *et al.*, 2014; Hudson *et al.*, 2014). Cells were plated into white bottom

96 well plates and left to grow overnight. Cells were washed 2x in 200 µL 1X HBSS before 30 min incubation in 80 µL HBSS. Following HBSS incubation, 10 µL of 50 µM Renilla-luciferase substrate coelentrazine-h was added to each well for a 10 min incubation period. Half log serial dilutions of FFA4 agonists and forskolin were set up ranging from 0.1 nM to 3.16 µM and 10 µL of compound was added to wells for 5 min. Plates were read on a CLARIOstar plate reader at a wavelength of 475-30/520-30 nm. Readings were calculated as a % maximal response normalised to TUG-891 or respective positive control as indicated in each figure. Data was plotted as a concentration response curve on GraphPad Prism.

2.2.1 Bias Calculations

Data obtained from functional signalling assays were fit to a four parameter model to determine maximal and minimal responses and EC50 concentrations.

To acquire a measure of bias, concentration response curves were fitted to a modified operational model of agonism, based on the Black and Leff operational model of agonism (Black et al., 1985). This modified model described by Kenakin *et al.*, (2012) is defined as follows:

$$Y = basal + \frac{(Emax - basal)(\frac{\tau}{K_A})^n[A]^n}{[A]^n(\frac{\tau}{K_A})^n + (1 + (\frac{A}{K_A})^n)}$$

where basal is the level of response in absence of agonist, Emax is the maximal response of the system, K_A the equilibrium dissociation constant of the agonist, [A] the agonist concentration, τ is an index of the signalling efficacy of the agonist and n is the slope of the transducer function that links occupancy to response. Analysis assumed that Emax and n were shared between all agonists, however the transduction coefficient $log(\frac{\tau}{K_A})$, was estimated as a unique measure of activity for each agonist and thus used as an estimate of pathway bias.

However, to cancel out system bias, $log(\frac{\tau}{K_A})$ values for test compounds were normalised to $log(\frac{\tau}{K_A})$ for the reference ligand TUG-891:

$$\Delta log\left(\frac{\tau}{K_A}\right) = log\left(\frac{\tau}{K_A}\right) of\ test\ compound - log\left(\frac{\tau}{K_A}\right) of\ TUG-891$$

Subsequently, to determine a measure of bias, $\Delta log\left(\frac{\tau}{K_A}\right)$ were expressed as ratios for one pathway over another:

$$\Delta\Delta log\left(\frac{\tau}{K_A}\right) = \Delta log\left(\frac{\tau}{K_A}\right) of\ pathway\ 1 - log\left(\frac{\tau}{K_A}\right) of\ pathway\ 2$$

2.2.2 Experimental animals

Four types of mice were used: Wild type (WT) C57BL/6 (WT-FFA4), C57BL/6 mice where FFA4 possessed a hemagglutinin (HA) tag (WT-FFA4-HA), C57BL/6 mice where FFA4 has phosphorylation deficient (PD) mutations (PD-FFA4-HA) and C57BL/6 mice where FFA4 contains a ß-galactosidase knockout (FFA4-KO). Animals are described in more detail in Chapter 5. All animals were housed in a regulatory unit under 12 hour light/dark cycles, at room temperature and were fed normal chow. Both male and female adult mice were used for experimental procedures. Mice were genotyped by Transnetyx.

Since experiments were performed *ex vivo* using tissue or to obtain primary cells and no experiments were performed *in vivo*, only a Home Office breeding license (PP0894775) was required for experiment and not a Home Office personal license. Authorised personnel carried out humane killing of all animals and the 3R's (Replacement, Reduction and Refinement) were considered at all times to adhere with ethical standards. To ensure that the use of animals was kept to a minimum, preliminary experiments were performed on n=3/4 animals and power calculations were performed on experiments which did not reach significance to determine whether further experiments should be performed in future to reach significance. Additionally, if multiple tissues could be removed from one mouse, this was done to ensure that number of animals was kept to a minimal.

2.2.3 Quantitative real time polymerase chain reaction (qRT-PCR)

2.2.3.1 RNA extraction from tissue

RNA was extracted from tissue using Qiagen RNeasy plus mini kit as per manufacturer's instructions. Briefly, colon and lung tissues from mice were homogenised in RLT Buffer. Homogenates were then centrifuged at 8,000 x g for 30 sec in a gDNA eliminator spin column. Flow-through was collected and mixed with 70% ethanol, then applied to an RNeasy mini spin column and centrifugated at 8000 x g for 15 sec at room temperature. Thereafter, flow-through was discarded and the column was washed with wash buffers before RNA was eluted in 20 µL nuclease-free water. RNA concentration determined using a Nanodrop-1000 spectrophotometer by measuring absorbance at 260 nm.

DNAse digest was performed to ensure RNA samples extracted from tissue in RNA isolation were free of DNA contaminants. The reaction was set up with the following components: 1 µg of RNA in 8 µL nuclease free water and 2 µL of a 1:1 mixture of DNase amplification grade and 10X DNase I reaction buffer. This mixture was incubated at room temperature for 15 min before 1 µL of DNase I stop solution was added to halt the reaction.

2.2.3.2 Reverse transcriptase PCR

RNA from DNase digest was incubated in a thermocycler for 10 min at 65°C. A PCR master mix composed of 4 µL of 5X reaction buffer, 2 µL of 100 mM DTT, 1 µL of 50 ng/µL random hexamers, 1 µL of 10 mM dNTP and 1 µL of nuclease free water was prepared per 1 reaction. This PCR master mix and 200 U of MMVL reverse transcriptase enzyme was added to DNase digested RNA. PCR tubes were incubated for 10 min at 25°C, 37°C for 1 h and 70°C for 15 min. cDNA was diluted to a final volume of 100 µL with nuclease free water.

2.2.3.3 q-PCR

A q-PCR master mix composed of 10 µL fast sybr green, 5 µM forward primer and 5 µM reverse primer, was prepared and made up to 16.8 µL with nuclease free H_2O. Details of the qPCR primers are listed in (Table 2-4).

Primer	Sequence	Company
mFFA4 Forward Primer	GGCACTGCTGGCTTTCATA	Eurofins
mFFA4 Reverse Primer	GATTTCTCCTATGCGGTTGG	
mFFA1 Forward Primer	TTTCTGCCCTTGGTCATCAC	Eurofins
mFFA1 Reverse Primer	TTTCTGCCCTTGGTCATCAC	
HA Forward primer	GTGGTGGCCTTCACGTTTGC	Eurofins
HA Reverse primer	AGCGTAATCTGGAACATCGTAAGGGTA	
mGAPDH Forward Primer	CGGATTTGGCCGTATTGGG	Eurofins
mGAPDH Reverse Primer	CTCGCTCCTGGAAGATGG	

Table 2-4: qPCR primers

16.8 µL of master mix was added to each well of a 96 well PCR plate (Biorad) followed by 3.2 µL of cDNA to each well. Plates were sealed with a polypropylene plate seal and run in a BioRad CFX96 PCR instrument using the cycling parameters in Table 2-5. Step 2 was repeated for 44 cycles.

Stage	Temperature (°C)	Time (sec)
1 – Preheating	95	20
2- Denaturing	95	1
Annealing and Extension	60	20
Melt Curve – Heating	95	15
Annealing	60	60
Heating	95	15

Table 2-5: qPCR reaction scheme

Comparative cycle threshold (Ct) values were obtained using QuantStudioTM design and analysis software (Thermo Fisher Scientific). ΔCt values were calculated by subtracting the Ct value of the target gene from the Ct value of a GAPDH housekeeping gene. ΔΔCt values were calculated by subtracting the ΔCt value of the target gene from the ΔCt value of a reference condition (eg. WT tissue). $2^{-\Delta\Delta CT}$ were calculated and plotted on GraphPad Prism to indicate fold change of a gene to the reference. In experiments using FFA1 primers, data was normalised to WT tissue where FFA4 expression had been quantified using FFA4 primers to determine relative expression of FFA1 in comparison to FFA4.

2.2.4 *Ex vivo* precision cut lung slices

C57BL/6 mice (WT-FFA4-HA, PD-FFA4-HA or FFA4-KO) aged between 8 and 12 weeks were humanely killed and dissected to expose trachea. To inflate the lung, 2% agarose (w/v) was inserted into the lung using a 1 mL syringe via a 22g cannula (Vasovix Braun) inserted into the trachea. Once agarose had set, lungs were removed and sliced into 200 μm horizontal sections in a Vibrating blade

microtome (Leica VT1000 S). Slices were removed and placed into ice cold 1X HBSS before culturing in warmed DMEM. After overnight incubation of lung slices, precision cut lung slice experiments were performed on a Zeiss EVOS FL Auto 2 microscope. To contract airways, lung slices were stimulated with 100 µM of carbachol for 20 min. To determine agonist effect on contracted airways, lung slices were then stimulated with 50 µM of FFA4 agonist for a further 20 min. Images were taken at an objective of 20x LWD and analysed using Zen lite software (Zeiss). Airway luminal area size was measured at stated time points and expressed as airway luminal area as a % of baseline area to measure relative contraction and relaxation.

2.2.5 Immunohistochemistry

Lungs dissected from mice were fixed in 4% PFA overnight. Samples were processed in paraffin wax and sliced at 5 µm thickness. Antigen retrieval was performed using sodium citrate buffer pH 6 and boiling for 1 min 40 s at 125°C. Slides were then incubated in blocking buffer for 2 h at room temperature. Primary antibody (Table 2-6) made up in blocking buffer was incubated overnight at 4°C.

Antibody	Dilution	Species	Catalog Number	Company
HA	1:250	Rat	11867423001	Sigma-Aldrich
CC10	1:350	Mouse	365992	Santa Cruz Biotechnology
Alpha-actin	1:350	Mouse	A5228	Sigma-Aldrich

Table 2-6: Primary antibodies used in lung immunohistochemistry

Samples were washed 3x for 15 min in wash buffer before 2 h incubation with relevant secondary antibody (Table 2-7) at room temperature.

Antibody	Dilution	Catalog Number	Company
Goat Anti-rat IgG (H+L), (Alexa Fluor® 647 Conjugate)	1:400	4418	Cell Signalling Technology
Goat Anti-mouse IgG (H+L), (Alexa Fluor® 488 Conjugate)	1:400	4408	Cell Signalling Technology

Table 2-7: Secondary antibodies used in lung immunohistochemistry

Samples were again washed 3x for 15 min in wash buffer before mounting with coverslips using Vectashield mounting media containing DAPI before imaging on LSM 880 confocal laser scanning microscope (Zeiss).

2.2.6 Colonic crypt isolation

Following the dissection of colon from mice, the colon was pinned onto sylgard and longitudinally cut on ice cold PBS solution. Muscle layers were removed from the colon and remaining epithelial layers were cut into pieces. Colon epithelial pieces were washed three times in PBS before digestion in 0.3 mg/mL collagenase XI for 10 min at 37°C. Collagenase was removed and then centrifuged at 1500 x g for 3 min to pellet isolated colonic crypts. The digestion process was repeated 3 times on remaining undigested epithelium until the epithelium was completely digested. Colonic crypts were resuspended in high glucose DMEM supplemented with 10% FBS, 1% glutamine and 1% penicillin/streptomycin and plated out onto matrigel coated wells before overnight incubation at 37°C.

2.2.7 Colonic crypt secretion assay

Following overnight incubation of isolated colonic crypts, wells were washed three times each with 138 buffer. Compounds: 10 µM sodium propionate (C3), 10 µM TUG-891, 10 µM GSK137647A and 0.1% DMSO were made up in 138 buffer supplemented with 0.1% fatty acid free BSA was incubated on crypts for 2 h before secretion buffer was removed and cells lysed in lysis buffer. Secretion buffer supernatants and cell lysates were centrifuged 13,000 x g at 4°C for 15 min to remove cell debris.

Samples were assayed according to manufacturer's instruction from GLP-1 ELISA Kit or PYY ELISA Kit. Briefly, in the GLP-1 assay standards and samples were incubated overnight at 4°C on an ELISA plate coated with anti-GLP-1 antibody. Secretion supernatants were assayed undiluted and lysates were diluted 1 in 20. The following day, plates were washed before incubation with detection conjugate for 2 h. After washing, substrate was added and the plates incubated in the dark for 20 min before stop solution was added. Fluorescence was read on a CLARIOstar reader at 355 nm/460 nm.

In the PYY ELISA, standards, primary antibody, biotinylated peptide and samples were added to the immunoplate and incubated for 2 h. Secretion supernatants were assayed undiluted and lysates were diluted 1 in 20. Following washing stages SA-HRP was added to wells and the plate incubated for 1 h. TMB substrate was added to each well and incubated for 1 h in the dark before the reaction was terminated by addition of 2N HCl. Absorbance measurements were read at 450 nm on the Omega Polarstar plate reader (BMG Biotech).

Concentrations of PYY and GLP-1 in each well of 96 well ELISA plates were calculated by interpolating data from standard curves, created using standards of known GLP-1 or PYY concentrations provided in ELISA kits. Concentrations were then multiplied by volumes in wells and dilution factors to calculate true concentrations in cell lysates and supernatants. To determine % secretion of GLP-1 and PYY from cells, average concentration values in supernatant from three technical replicates were divided by the average total concentration of GLP-1 or PYY (concentration in cell lysis + cell supernatant) and multiplied by 100. Data was then normalised to a DMSO control to calculate fold increase

values. Data was calculated for each individual mouse and was plotted on GraphPad prism.

2.2.8 Calcium imaging

Following isolation of colonic crypts, crypts were distributed into 6 well plates containing 13 mm 0 thickness coverslips (VWA, P/N: 631-0148) and incubated overnight. The following day, 3 µM Fura 8-AM was incubated on coverslips for 20 min at 37°C in the dark. Coverslips containing clusters of colonic crypts were then placed in a recording chamber and mounted onto an invert fluorescent microscope (Nikon TE2000-E; Nikon Instruments, Melville, NY). Colonic crypts were randomly selected for imaging with oil-immersion super fluor objective lens (x40) and HEPES buffer was continuously perfused into the chamber at room temperature until Fura-8 ratio was stable. FFA4 compound TUG-891 was diluted in HEPES buffer and added into the chamber. Once the Fura-8 ratio had returned to basal, 5 µM of Ca^{2+} ionophore ionomycin was applied to colonic crypts as a positive control.

Crypts were excited at 355 nm and 415 nm and sequential fluorescent image pairs were recorded at 525 nm and imaged using MetaFluor imaging software (Molecular Devices). Free intracellular Ca^{2+} signal was expressed at a ratio of 355:415 nm and change of ratio was calculated by subtracting baseline values from peak TUG-891 responses in each individual cell. Since not all cells responded to TUG-891 treatment, a result which would be expected when FFA4 is not expressed in every cell type within colonic crypts, data is expressed as % of number of cells responding in each mouse.

2.2.9 Statistical analysis

To attain statistical measures, at least three biological replicates were measured in each experiment. Statistical analyses were performed using GraphPad Prism software on values of biological replicates. For statistical analysis performed on differences between groups, data were assumed to be normally distributed and comparisons were made using parametric tests. For groups of two, either unpaired t-tests or paired t-tests were performed. Unpaired t-tests were carried out when analysis was performed on two independent groups, whereas paired t-

tests were performed when two measurements were performed on the same animal. In experiments where three or more groups were being analysed (i.e three or more drugs) one-way analysis of variance (ANOVA) was performed. Dunnett's multiple-comparisons post hoc corrections were used following one-way ANOVA when comparing the mean of every group to one reference mean. For data comparing three or more groups where different measurements were taken of the same attribute, a repeated measures one-way ANOVA was performed. Here, Geisser-Greenhouse post-hoc corrections were performed.

2.2.10   Power Calculations

Power calculations were performed on preliminary data in Chapter 5 and 6 to determine minimum number of experimental animals required for meaningful effect sizes to be detected in future experiments. Statistical analysis was performed on experiments as indicated in part 2.2.9. Using Mini-Tab software, standard deviation of control conditions following analysis of data in GraphPad Prism was input into sample size calculators corresponding to correct statistical analyses. Targeted power was set to 80%, a standardised accepted power value in scientific literature (Charan and Kantharia, 2013). The level of significance to detect a meaningful effect size was set to $p < 0.05$. Meaningful effect sizes in PCLS experiments in Chapter 5 were set to a difference of 40% between contracted and relaxed airways, based on previous experiments performed by Prihandoko *et al.*, (2020). Meaningful effect sizes in colonic crypt secretion experiments for PYY and GLP-1 in Chapter 6 were set to a mean difference 0.75 fold change or 75% increase between PYY/GLP-1 secreted in vehicle and drug treated crypts, a value estimated based on previous experiments performed by Psichas *et al.*, (2015) and Bolognini *et al.*, (2019). Analysis revealed that sample sizes to reach desired power in PCLS experiments in Chapter 5 would be 4 experimental animals and in Chapter 6 colonic crypt experiments to assay release of GLP-1 would require 9 experimental animals, whereas assays for PYY secretion would require a total of 51 animals. It should be noted that sample size calculators calculate minimum numbers of animals to be significant and this can result in calculation of an inappropriately high number of animals which may result in false positive values of data that would be considered non-significant otherwise. Further experiments should be conducted adhering to the principles of the 3Rs and therefore data may be deemed non-significant if upon repeat

power calculation values remain inappropriately high. Many researchers use at least 6-10 animals as a maximum number per experiment, and thus we have considered that approximately 10 animals may be the maximal number of biological repeats in future experiments (Charan and Kantharia, 2013; Bonapersona *et al.*, 2020).

Chapter 3   Pharmacological evaluation of FFA4 agonists

3.1 Introduction

Although the FFA4 receptor is considered to primarily couple to $G\alpha q/11$ heterotrimeric G proteins, where receptor activation results in elevated levels of inositol phosphates and subsequent increases in intracellular Ca^{2+} levels, there is also evidence that this receptor can couple to $G\alpha i$ G proteins (Hirasawa *et al.*, 2005; Briscoe *et al.*, 2006; Engelstoft *et al.*, 2013; Stone *et al.*, 2014; Alvarez-Curto *et al.*, 2016). These studies, however, have been conducted in a range of recombinant and endogenous systems that make comparisons of the efficacy and potency of various FFA4 ligands challenging. As such, it is unclear if different orthosteric FFA4 agonists might show ligand bias.

Here I address the efficacy and potency of five orthosteric FFA4 agonists, TUG-891, TUG-1197, Compound A, GSK137647A and Agonist 2 (otherwise known as Compound B), in pERK1/2, inositol phosphate, ß-arrestin and receptor internalisation assays to determine the potential bias of FFA4 in Gq and ß-arrestin2 pathways and downstream of Gq protein:receptor coupling. In this way I assess the potential of generating biased ligands to this receptor which may have clinical implications given that FFA4 has been shown to elicit anti-inflammatory properties in macrophages though ß-arrestin signalling and there are suggestions of incretin release following Gq coupled signalling (Hirasawa *et al.*, 2005; Oh *et al.*, 2010). Therefore, biased ligands may have potential as drug therapies in areas such as inflammatory and metabolic diseases.

3.2 Aims

The aims of this chapter were to:

- Optimise a cell culture system to analyse mFFA4 function

- Assess mFFA4 receptor activation upon stimulation with FFA4 agonists

- Assess mFFA4 coupling to G protein and β-arrestin2 signalling pathways following FFA4 agonist stimulation

- Investigate selectivity of FFA4 agonists

3.3 Results

3.3.1 Expression of mFFA4 in stably transfected and non-transfected CHO cells

CHO cells, stably expressing mFFA4 construct were generated using the Flp-In expression system, where a plasmid encoding for the short isoform of mouse FFA4 was utilised. An eYFP tag was fused to the C-terminus of the receptor sequence, facilitating the detection of receptor. In the stably expressed mFFA4 Flp-In CHO cell line, receptor expression was confirmed using confocal microscopy by the presence of eYFP which denotes mFFA4-eYFP (Figure 3-1A). The receptor appeared to be more localised to the cell membrane, which is justifiable considering FFA4 is a transmembrane GPCR. Expression of eYFP tagged receptor was not evident in non-transfected cell lines providing confirmation of mFFA4 expression in the stably transfected cell line. To further confirm the presence of mFFA4 in the stably transfected cell line, protein samples were resolved on an SDS-PAGE gel and western blots performed (Figure 3-1B). The eYFP antibody used detected a band at around 75kDa in mFFA4 CHO cells which again confirmed presence of mFFA4. The size of this band was considerably higher than the stated molecular weight of FFA4 of 45kDa (Prihandoko *et al.*, 2016), however, when we take into consideration the molecular weight of the eYFP tag (27kDa) then this molecular weight was convincingly that of mFFA4-eYFP.
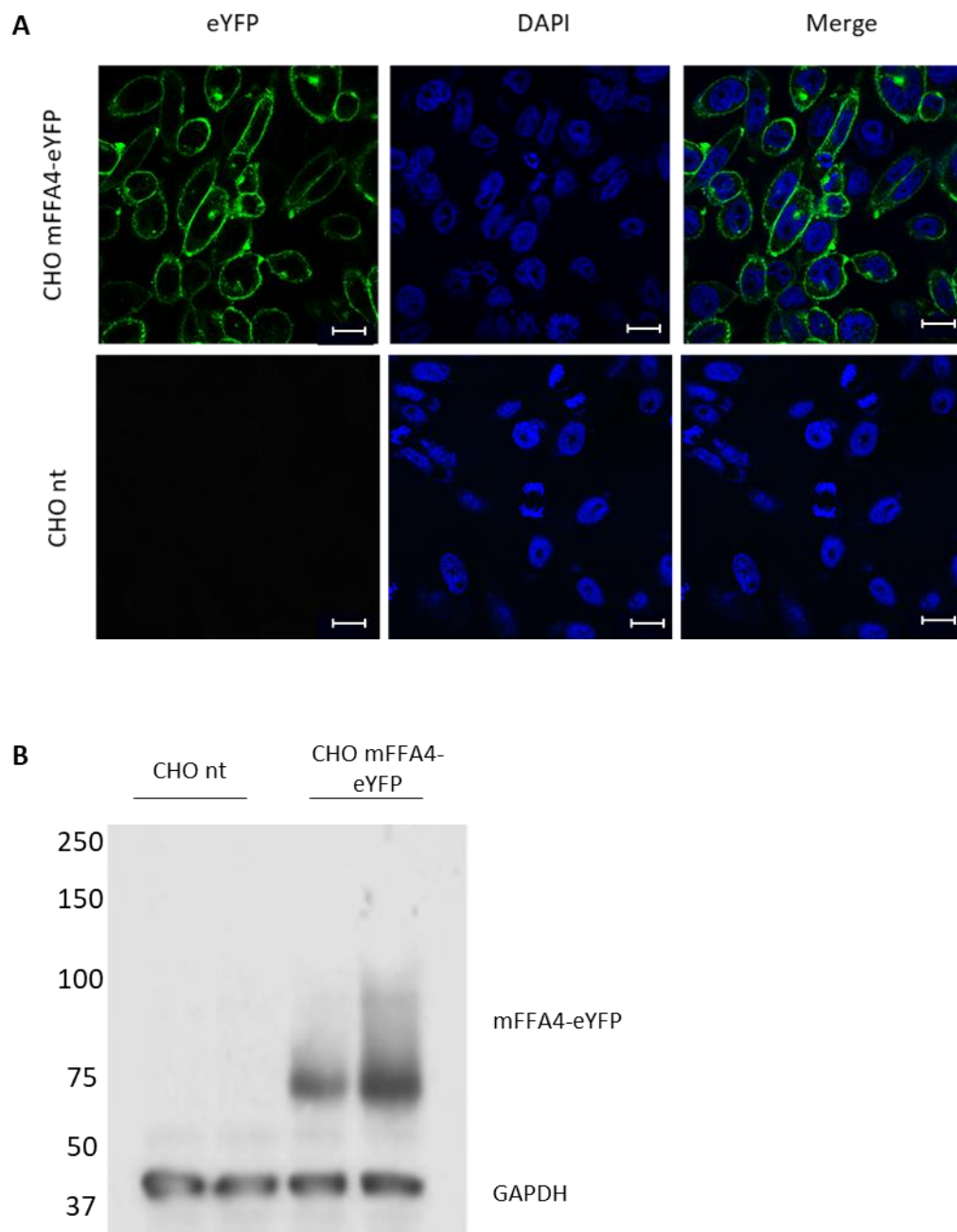
Figure 3-1: Expression of mFFA4 in stably transfected CHO cells
(A) Representative images of immunocytochemical staining to show expression of mFFA4-eYFP (green) colocalised with cell nuclei (DAPI, blue). Scale bar represents 10 µm, n=3. **(B)** Western blot analysis using anti-eYFP and GAPDH antibody to confirm presence of eYFP tagged receptor. Nt=non-transfected. Images are representative of three individual experiments (n=3), samples were assayed in duplicate.

3.3.2 Canonical signalling of mFFA4 agonists

GPCRs are known to promote the phosphorylation of ERK1/2 through G protein dependent and independent pathways (Shenoy *et al.*, 2006). Since FFA4 stimulates phosphorylation of ERK1/2, largely via Gq signalling pathways, measuring the activity of this pathway was used as an output of general receptor

activation and additionally facilitated assessment of mFFA4 pERK1/2 signalling capacity (Hirasawa *et al.*, 2005; Briscoe *et al.*, 2006; Alvarez-Curto *et al.*, 2016). Firstly, to assess whether a range of FFA4 agonists were able to activate the receptor, protein samples prepared from mFFA4 stably transfected and non-transfected CHO cells which had been stimulated with agonist for optimal incubation time, 5 minutes (Hudson *et al.*, 2013), were assayed in western blots to assess for phosphorylation of ERK1/2 (Figure 3-2). Phosphorylation of ERK1/2 and thus receptor activation was detected at both maximal (10 µM) and sub maximal (1 µM) concentrations (Hudson *et al.*, 2013) of all compounds, except Modulator 1 and Modulator 2 (Figure 3-2A), in comparison to non-transfected controls and positive FBS controls (Figure 3-2B). Therefore, these FFA4 agonists demonstrated ability to activate the mFFA4 receptor and induce mFFA4 mediated phosphorylation of ERK1/2. Since Modulator 1 and Modulator 2 showed poor activity in comparison to other compounds, these two compounds were excluded from further study.
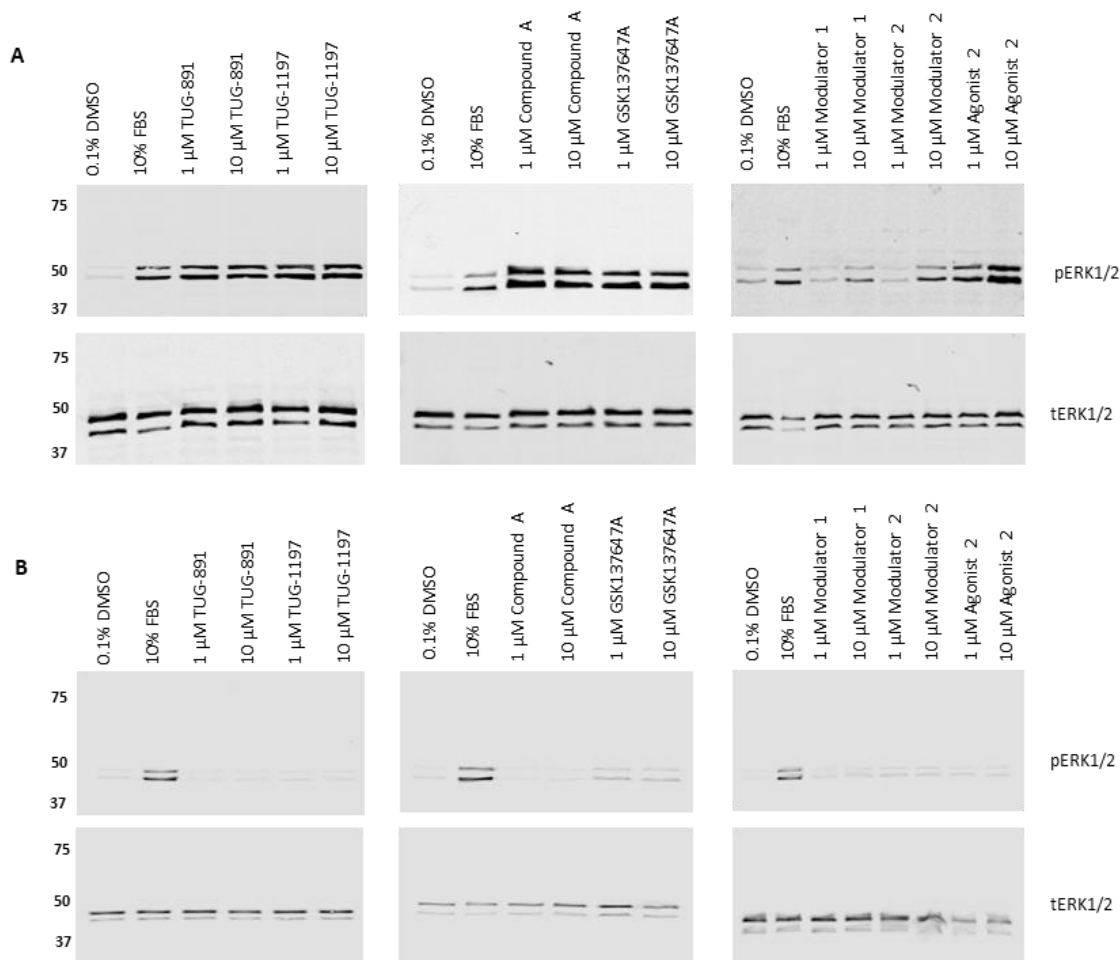
Figure 3-2: Activation of mFFA4 using FFA4 agonists
Western blot analysis using pERK1/2 antibody or tERK1/2 antibody following 1 µM or 10 µM treatment with various FFA4 agonists. **(A)** Lysate (10 µg) from Flp-In CHO cells stably expressing mFFA4 **(B)** Lysate (10 µg) from non-transfected cells. Images are representative of three individual experiments (n=3).

With the knowledge that a pool of agonists induced the activation of the mFFA4 receptor, these agonists were tested in a quantitative pERK1/2 HTRF assay which detects phosphorylation of ERK1/2. The optimal incubation time of agonists needed to elicit a maximal response was quantified in a pERK1/2 time course (Figure 3-3A). The maximal response for all agonists occurred at 5 min, and then decreased gradually until basal levels were reached at 60 min. Interestingly, for one agonist, Agonist 2, this was not the case. Agonist 2 appeared to reach a basal level more slowly suggesting possible differences in signalling mechanisms for this agonist.

A concentration response curve for the phosphorylation of ERK1/2, allowed potency (pEC50) and efficacy (% Emax) of FFA4 agonists to be quantified.

Following treatment of cells with agonist for 5 min, all agonists assayed initiated the phosphorylation of ERK1/2 (Figure 3-3B) consistent with the western blot data. Synthetic agonist TUG-891 was used as a reference ligand, a ligand which is largely considered to be the gold standard synthetic ligand for FFA4. Natural free fatty acids are generally not used as a reference since there is a range of long chain fatty acids which activate the receptor and uncertainty surrounds which ligand is the true endogenous ligand for FFA4. Additionally, TUG-891 shows no stimulus bias in comparison to endogenous ligands and so is an ideal reference ligand (Butcher *et al.*, 2014). Potencies of all agonists were similar to or significantly lower than that of TUG-891, whereas the efficacy of all agonists investigated was found to be significantly increased from TUG-891 (Table 3-1). In particular, the potency of GSK137647A appeared to be particularly low compared to that of TUG-891. However, while this value is actually higher than stated in literature, potency values for all compounds differed from literature values. Basal levels of ERK1/2 phosphorylation were detected in non-transfected CHO cells, providing further confirmation that agonist induced phosphorylation of ERK1/2 was indeed an FFA4 agonist mediated effect (Figure 3-3C).

A

B

C
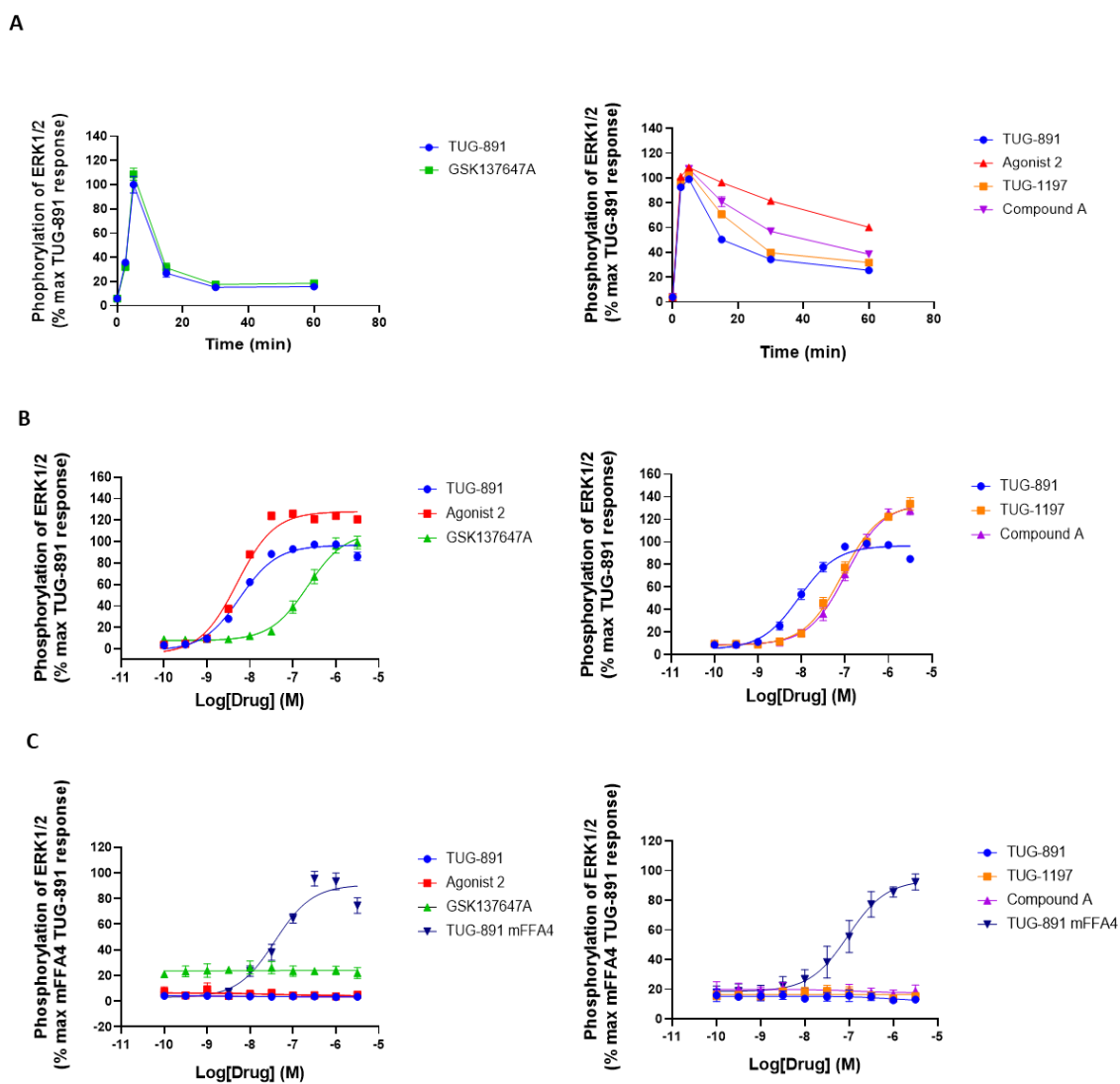
Figure 3-3: FFA4 mediated phosphorylation of ERK1/2
Agonist-induced phosphorylation of ERK1/2 was measured in **(A,B)** Flp-In CHO cells stably expressing mFFA4 or **(C)** non-transfected CHO cells following treatment with various FFA4 agonists. **(A)** Cells were stimulated with constant concentration (10 μM) of FFA4 agonists in 60 min time-course. **(B,C)** Cells were treated at range of concentrations for 5 min to produce a concentration response curve. TUG-891 was used as the reference ligand. Results are mean ± S.E.M of three independent experiments (n=3).

Ligand	pEC50		Reported pEC50	% Emax compared to TUG-891	
	Mean ± S.E.M	P Value		Mean ± S.E.M	P Value
TUG-891	8.2 (±0.1)		7.77 (±0.09) (Hudson *et al.*, 2013)	94.5 (±1.5)	
Agonist 2	8.3 (±0.1)	0.9 (ns)	ND	127.9 (±1.8)	<0.0001 (****)
TUG-1197	7.0 (±0.1)	<0.0001 (****)	ND	133.1 (±2.7)	<0.0001 (****)
Compound A	7.0 (±0.1)	<0.0001 (****)	7.62 (±0.11) (Oh *et al.*, 2014)	134.5 (±3.2)	<0.0001 (****)
GSK137647A	6.7 (±0.1)	<0.0001 (****)	6.20 (±0.17) (Sparks *et al.*, 2014)	109.1 (±4.3)	0.02 (*)

Table 3-1: Phosphorylation of ERK1/2 in mFFA4 CHO cells following FFA4 agonist treatment
Results are mean ± S.E.M of three independent experiments (n=3). Statistical analysis performed was one-way ANOVA (Dunnett's multiple comparisons), ns = non-significant, *=P<0.05, ****=P<0.0001. ND = not determined.

It is understood that FFA4 couples strongly to Gαq/11 G proteins, a good measure for which is detection of inositol phosphate (IP1) accumulation, a product of the inositide signalling pathway which is activated upon Gq/11 signalling (Alvarez-Curto *et al.*, 2016). To understand if activated receptor signals through Gq/11 coupled pathways and additionally if phosphorylation of ERK1/2 is largely Gq coupled as reported by Alvarez-Curto *et al.*, (2016), Gq inhibitor FR900359 was pre-incubated on mFFA4 CHO cells for a period of 30 min before agonist stimulation (Figure 3-4A). Following antagonist incubation at 1 µM, a statistically significant decrease in TUG-891 efficacy (P=0.0004) was observed, implying an mFFA4 coupling to Gq/11 signalling and additionally suggesting that mFFA4-mediated pERK1/2 pathways are largely Gq coupled (Figure 3-4A, Table 3-2). The same decrease of maximal response was not evident at 100 nM FR900359 suggesting 1 µM of this compound to be the optimal concentration for Gq inhibition, consistent with concentrations used by other

groups in cellular based assays (Schrage *et al.*, 2015; Marsango *et al.*, 2022). However, a response to TUG-891 was still evident in this experiment, which could suggest an additional signalling mechanism in the pERK1/2 pathway, although this is further elucidated in Chapter 4.

Upon treatment of FFA4 agonists in a concentration response curve, IP1 accumulation was detected for all agonists in mFFA4 CHO cells demonstrating Gq coupling abilities (Figure 3-4B) in comparison to non-transfected CHO cells (Figure 3-4C). While no agonist produced a significantly higher % Emax than TUG-891, agonist potency values varied (Table 3-3). Compound A had a similar potency and efficacy to that of TUG-891, however Agonist 2 evoked a response which was significantly more potent (P=0.02). Neither GSK137647A nor TUG-1197 reached a peak response in concentration response curves, likely due to lower pEC50 values, demonstrating that these compounds were not potent activators of Gq/11 coupled signalling.
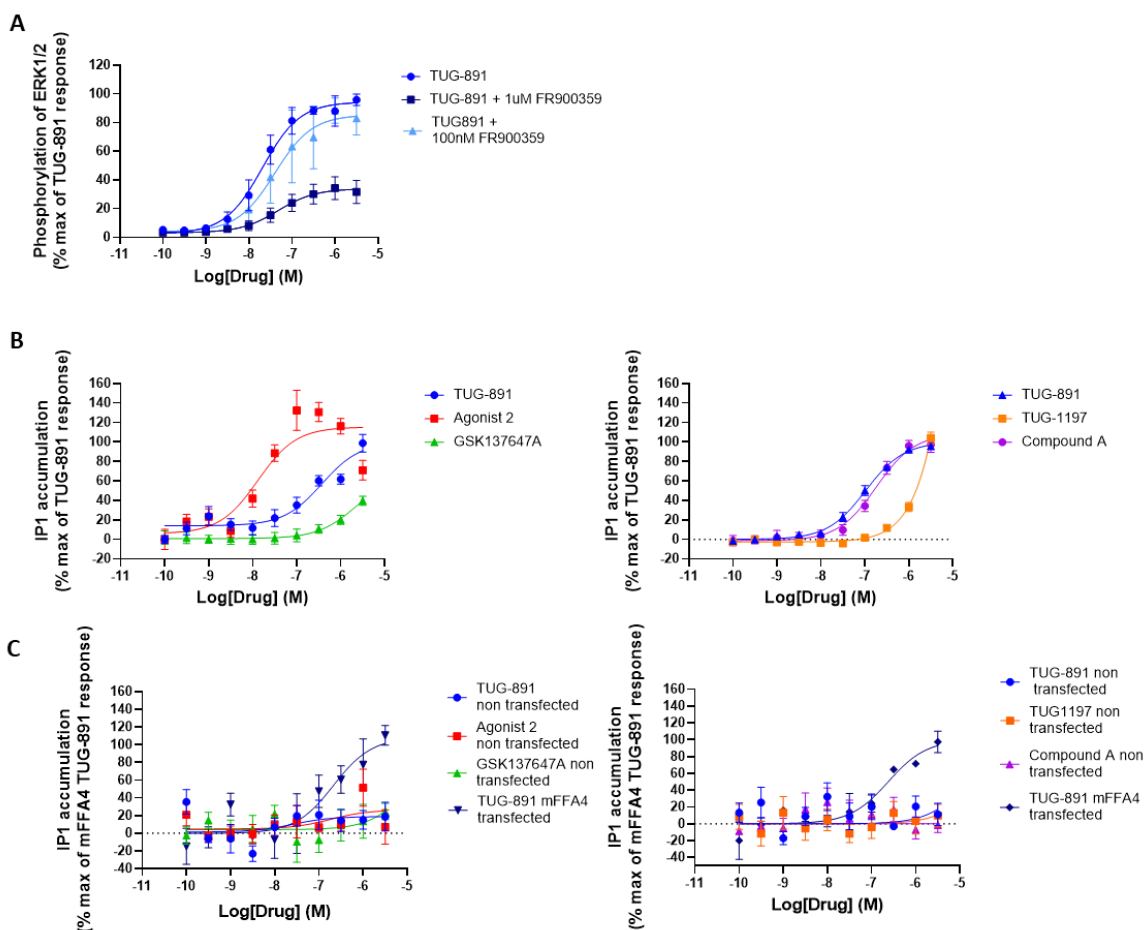
Figure 3-4: FFA4 signalling via Gq coupled pathways
(A) Reduction in TUG-891 induced pERK1/2 response following 30 min pre-treatment of FR900359 Gq inhibitor at either 1 µM or 100 nM concentration. **(B,C)** Agonist-induced IP1 accumulation was measured in **(B)** Flp-In CHO cells stably expressing mFFA4 or **(C)** non-transfected CHO cells following treatment with FFA4 agonists. Cells were stimulated with FFA4 agonist at a range of concentrations for 1 h to produce a concentration-response curve. TUG-891 was used as the reference ligand in all experiments. Results are mean ± S.E.M of three independent experiments (n=3).

Ligand	pEC50		% Emax compared to TUG-891	
	Mean ± S.E.M	P Value	Mean ± S.E.M	P Value
TUG-891	7.7 (± 0.1)		94.4 (±3.7)	
TUG-891 + 100 nM FR900395	7.4 (±0.2)	0.4 (ns)	85.4 (±7.9)	0.4 (ns)
TUG-891 + 1 µM FR900395	7.3 (±0.2)	0.3 (ns)	33.9 (±3.1)	0.0004 (***)

Table 3-2: Potencies and efficacies of FFA4 agonists in pERK1/2 assay following FR900395 Gq inhibitor treatment
Results are mean ± S.E.M of three independent experiments (n=3). Statistical analysis performed was one-way ANOVA (Dunnett's multiple comparisons), ns = non-significant, ***=P<0.001.

Ligand	pEC50		% Emax compared to TUG-891	
	Mean ± S.E.M	P Value	Mean ± S.E.M	P Value
TUG-891	7.1 (±0.1)		100.0 (±10.3)	
Agonist 2	7.9 (±0.2)	0.02 (*)	117.6 (±7.7)	0.4 (ns)
TUG-1197	-		-	
Compound A	6.9 (±0.1)	0.8 (ns)	107.0 (±3.3)	0.9 (ns)
GSK137647A	-		-	

Table 3-3: Potency and efficacy values of FFA4 agonists in Gq signalling
Results are mean ± S.E.M of three independent experiments (n=3). Statistical analysis performed was one-way ANOVA (Dunnett's multiple comparisons), ns= non-significant, *=P<0.05.

Gαs signalling assays were performed to establish whether synthetic FFA4
agonists were able to stimulate Gαs coupled signalling responses, as this has not
been previously reported in literature (Figure 3-5). One method used to assess
Gαs coupled signalling is a cAMP-based assay as Gαs signalling results in cAMP
accumulation. In this assay, treatment of cells with all FFA4 agonists produced a
decreased cAMP accumulation compared to the positive control of forskolin
which directly activates AC to produce cAMP (Figure 3-5A). Results from non-
transfected cells were similar to that of transfected cells, indicating that mFFA4
is indeed not signalling via Gαs coupled pathways when activated by synthetic
FFA4 agonists (Figure 3-5B).
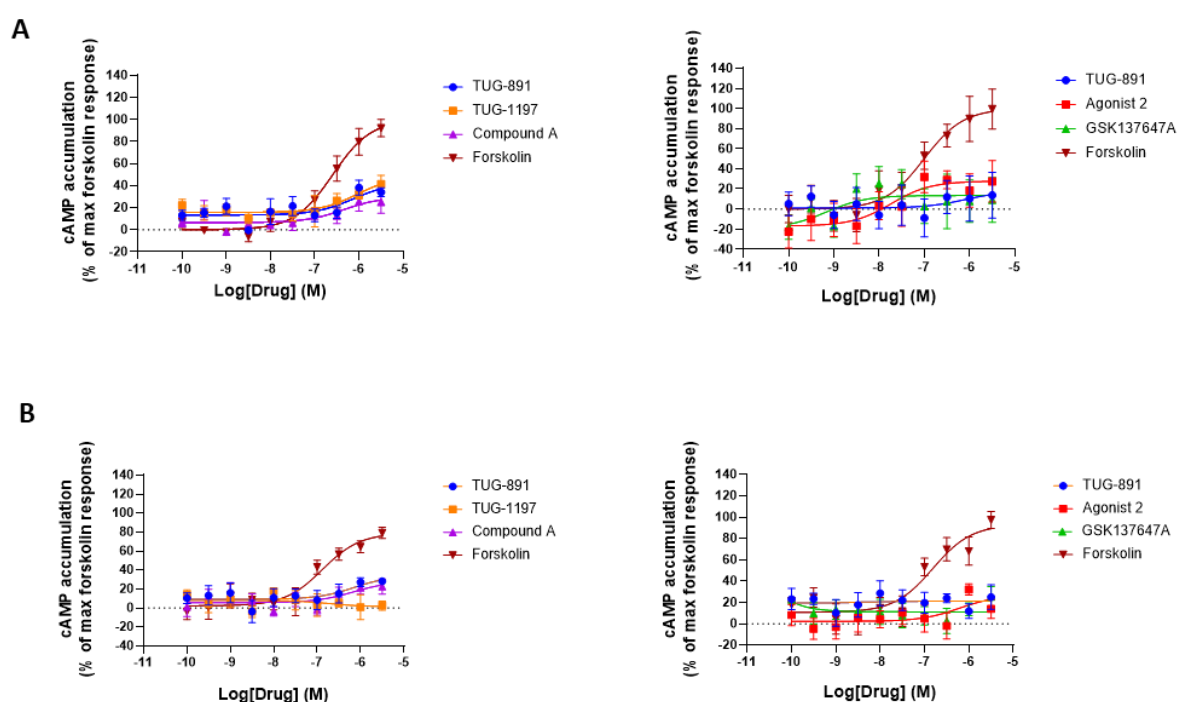
Figure 3-5: FFA4 signalling via Gs coupled pathways
Agonist-induced cAMP accumulation was measured in **(A)** Flp-In CHO cells stably expressing
mFFA4 or **(B)** non-transfected CHO cells following treatment with FFA4 agonists. Cells were
stimulated with FFA4 agonist at a range of concentrations for 1 h 45 min to produce a
concentration-response curve. Forskolin was used as a reference ligand in all experiments.
Results are mean ± S.E.M of three independent experiments (n=3).

Similarly, using a cAMP-based assay, Gαi coupled signalling was assayed. Whilst in Gαs coupled signalling pathways, activation of the FFA4 receptor activates AC to produce cAMP, Gαi coupled signalling acts to inhibit AC activity (Taussig, Iñiguez-Lluhi and Gilman, 1993; Syrovatkina *et al.*, 2016). No reduction of cAMP was observed upon co-incubation of forskolin to activate to AC to produce cAMP accumulation (Figure 3-6A), and FFA4 agonist which if signalled via Gαi signalling pathways would inhibit AC function (Figure 3-6B). This suggests that addition of these FFA4 agonists did not cause signalling events via Gαi pathways in this simple cellular system.
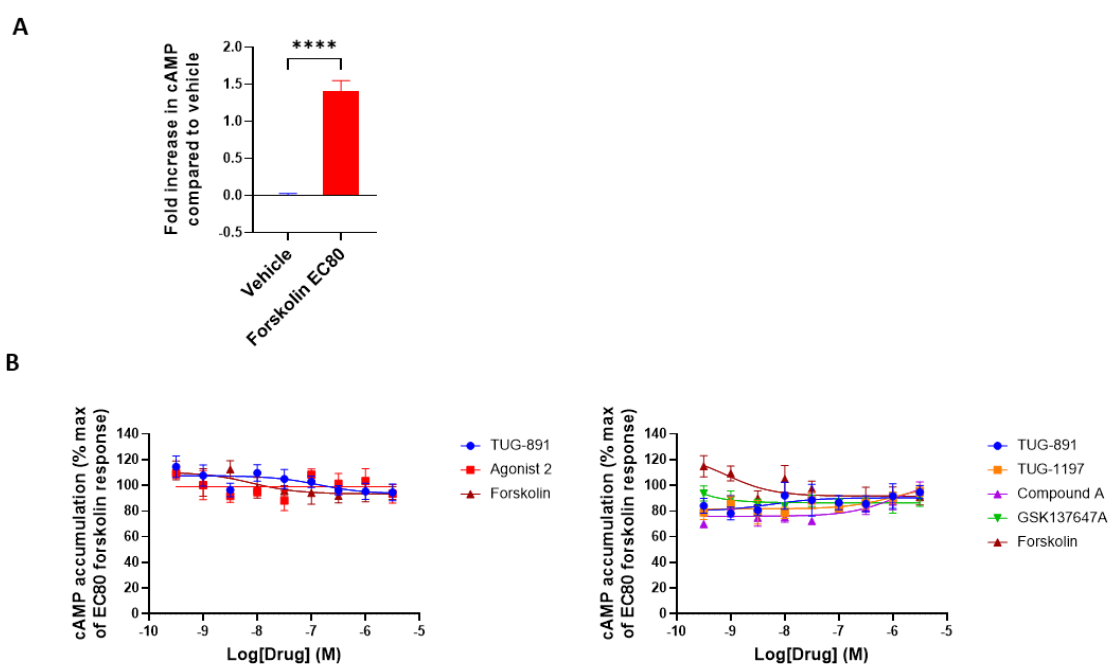
Figure 3-6: FFA4 signalling via Gi coupled pathways
(A) cAMP accumulation following EC80 concentration of forskolin was measured in comparison to a DMSO vehicle. **(B)** Agonist-induced cAMP reduction was measured in Flp-In CHO cells stably transfected with mFFA4. Cells were stimulated with FFA4 agonist at a range of concentrations for 1 h 45 min and EC80 concentration of forskolin simultaneously to produce a concentration-response curve. Forskolin was used as a reference ligand in all experiments. Results are mean ± S.E.M of three independent experiments (n=3). Statistical analysis performed was an unpaired t-test, ****=P<0.0001.

To assess whether WT-mFFA4 cells recruit β-arrestin2 following FFA4 agonist stimulation, BRET assays were performed (Figure 3-7A). All compounds stimulated β-arrestin2 recruitment, demonstrating β-arrestin2 coupling abilities. However, while potencies of compounds were similar to that of TUG-891, efficacies of response varied (Table 3-4). The efficacies of response upon GSK137647A and TUG-1197 stimulation were significantly lower (P=0.03 and 0.01 respectively) than TUG-891, indicating that these agonists may not promote

efficacious coupling of mFFA4 to ß-arrestin2. The efficacy of Agonist 2, however, was statistically increased (P=0.009) in comparison to TUG-891, while the efficacy of Compound A remained similar to that of TUG-891.

As ß-arrestin coupling leads to receptor internalisation in addition to receptor desensitisation, immunocytochemistry was performed after 30 min agonist stimulation to examine whether agonists induced receptor internalisation. Following agonist stimulation, receptor internalisation was observed for all compounds, indicated by the formation of vesicles which move towards the nuclei from the plasma membrane (Figure 3-7B). It should be noted that Agonist 2 looks to promote receptor internalisation particularly well at 30 min as minimal receptor appears to be located at the cell membrane, a result consistent with the promotion of efficacious coupling to ß-arrestin2.

A
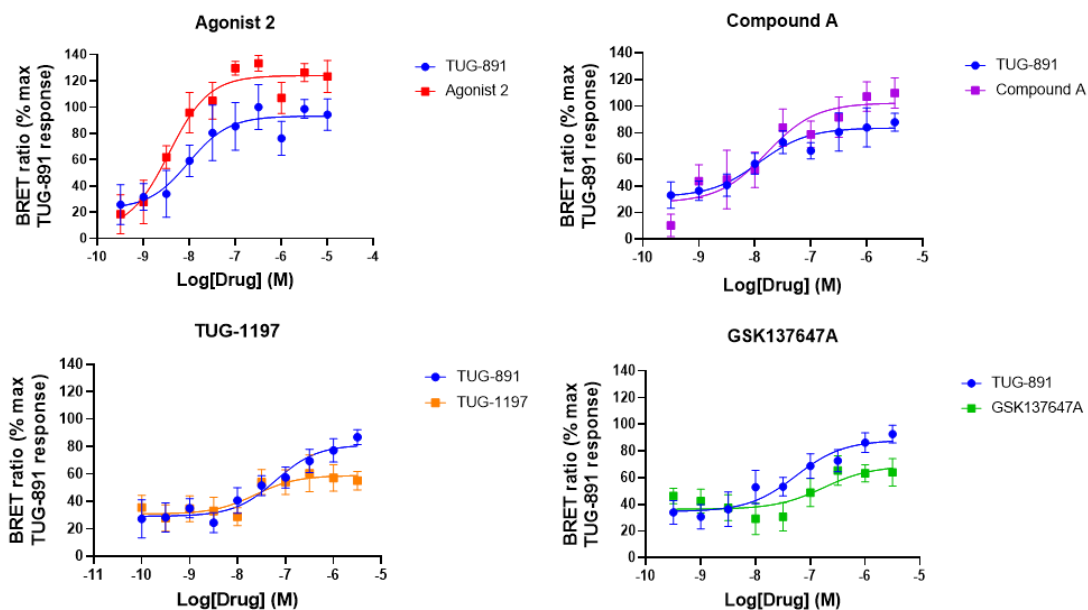
B
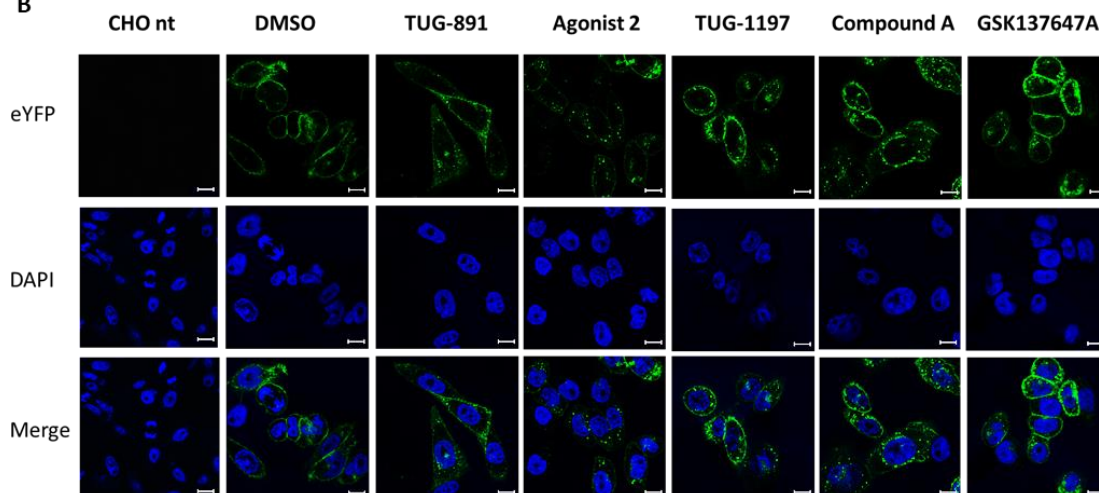
Figure 3-7: FFA4 agonist stimulated β-arrestin2 recruitment and receptor internalisation
(A) Agonist-induced β-arrestin2 recruitment was measured using a BRET based assay in Flp-In CHO cells expressing mFFA4 following treatment with FFA4 agonists. Cells were stimulated with FFA4 agonist at a range of concentrations for 5 min to produce a concentration response curve. Data is displayed as a ratio of 535/475 nm between eYFP and R-luciferase interactions. Results are mean ± S.E.M of three independent experiments (n=3). **(B)** Immunocytochemistry following 30 min stimulation of 10 μM FFA4 agonist on Flp-In CHO cells expressing PD-mFFA4. Merged images show co-localisation of mFFA4 (green, eYFP) with cell nuclei (blue, DAPI). Scale bar represents 10 μm. Images are representative of three independent experiments.

Ligand	pEC50		% Emax compared to TUG-891	
	Mean ± S.E.M	P Value	Mean ± S.E.M	P Value
TUG-891	8.0 (±0.4)		93.2 (±6.9)	
Agonist 2	8.4 (±0.2)	0.9 (ns)	127.9 (±5.2)	0.009 (**)
TUG-1197	7.6 (±0.5)	0.9 (ns)	58.9 (±5.7)	0.01 (**)
Compound A	7.8 (±0.3)	1.0 (ns)	101.2 (±6.6)	0.8 (ns)
GSK137647A	6.9 (±0.6)	0.3 (ns)	64.4 (±6.6)	0.03 (*)

Table 3-4: Potencies and efficacies of FFA4 agonists in β-arrestin2 recruitment assay
Results are mean ± S.E.M of three independent experiments (n=3). Statistical analysis performed was one-way ANOVA (Dunnett's multiple comparisons), ns=non-significant, *=P<0.05, **=P<0.01.

3.3.3 Signalling bias of FFA4 agonists

Bias in signalling pathways downstream of Gαq:receptor coupling was calculated by fitting the concentration–response curves of IP1 accumulation and phosphorylation of ERK1/2 to a model based on the Black and Leff operational model of agonism (Black *et al.*, 1985) to calculate transduction coefficients (τ), previously described by Kenakin *et al.*, (2012). These transduction coefficients were compared with the reference ligand TUG-891, therefore, bias factors for ligands between IP1 accumulation and phosphorylation of ERK1/2 were calculated (Table 3-5). As TUG-1197 and GSK137647A did not reach a maximal response in IP1 accumulation assays, comparisons could not be made for these agonists since the operational model relies on an estimate of functional affinity and efficacy. Agonist 2 displayed bias to IP1 accumulation over phosphorylation of ERK1/2 compared to reference ligand TUG-891, a result which was statistically significant (P=0.01) following unpaired t-test. However, Compound A showed no statistically significant bias compared to TUG-891.

	IP1 Accumulation		ERK1/2 Phosphorylation		Log Bias Factor IP_1 - ERK1/2	Bias Factor IP_1 - ERK1/2	P Value IP_1 - ERK1/2
	$Log_{10}(\tau/K_A)$	$\Delta Log_{10}(\tau/K_A)$	$Log_{10}(\tau/K_A)$	$\Delta Log_{10}(\tau/K_A)$	$\Delta\Delta Log_{10}(\tau/K_A)$	$10^{\wedge}(\Delta\Delta Log_{10}(\tau/K_A)$	
TUG-891	6.39 (±0.07)	0.00 (±0.10)	7.77 (±0.05)	0.00 (±0.07)	0.00 ± 0.12		
Agonist 2	7.61 (±0.07)	1.20 (±0.10)	8.27 (±0.05)	0.51 (±0.07)	0.72 ± 0.12	5.25	0.01 (*)
Compound A	6.23 (±0.07)	-0.16 (±0.10)	7.14 (±0.05)	-0.62 (±0.07)	0.45 ± 0.12	2.81	0.05 (ns)

Table 3-5: Bias factor calculations for IP1 accumulation and phosphorylation of ERK1/2 in WT-mFFA4 cell lines using TUG-891 as reference ligand
Results are mean ± S.E.M of three independent experiments (n=3). Statistical analysis performed was an unpaired t-test, ns=non-significant, *=P<0.05.

Bias factor calculations were also performed to assess bias in relation to Gq-protein and arrestin pathways. Transduction coefficients (τ) for IP1 responses (a Gq coupled response) and ß-arrestin2 recruitment were calculated from concentration responses curves of TUG-891 (reference), Compound A and Agonist 2 (Table 3-6). These data indicated that there was no bias of these ligands in comparison to the reference compound TUG-891. Hence, the only indication of signalling bias was seen between IP1 and pERK1/2 and only for Agonist 2.

	IP1 accumulation		β-arrestin2 recruitment		Log bias factor IP$_1$-βarr2	Bias factor IP$_1$ - βarr2	P value IP$_1$ - βarr2
	Log$_{10}$(τ/ K$_A$)	ΔLog$_{10}$(τ/ K$_A$)	Log$_{10}$(τ/ K$_A$)	ΔLog$_{10}$(τ/ K$_A$)	ΔΔLog$_{10}$(τ/ K$_A$)	10^(ΔΔLog$_{10}$(τ/K$_A$)	
TUG-891	6.39 ± 0.07	0.00 ± 0.10	6.55 ± 0.37	0.00 ± 0.54	0.00 ± 0.56		
Agonist 2	7.61 ± 0.07	1.20 ± 0.10	7.97 ± 0.40	1.42 ± 0.55	-0.20 ± 0.56	-1.58	0.74 (ns)
Compoun d A	6.23 ± 0.07	-0.16 ± 0.10	6.91 ± 0.34	0.36 ± 0.51	-0.52 ± 0.52	-3.31	0.53 (ns)

Table 3-6: Bias factor calculations for IP1 accumulation and β-arrestin2 coupling in WT-mFFA4 cell lines using TUG-891 as reference ligand
Results are mean ± S.E.M of three independent experiments (n=3). Statistical analysis performed was an unpaired t-test, ns=non-significant.

3.3.4 Selectivity of FFA4 agonists

Despite FFA4 and FFA1 sharing low sequence homology, both receptors bind to long chain free fatty acids as well as synthetic ligands. It was therefore of interest to determine if the FFA4 agonists used here might also activate FFA1. To assess this an mFFA1-eYFP fusion protein was expressed in a recombinant HEK-293-cell system in a doxycycline-inducible manner (Hudson *et al.*, 2013). Using the eYFP tag at the C-terminus, the presence of the mFFA1 receptor was confirmed using immunocytochemistry where the receptor can be seen localised to the cell membrane (Figure 3-8A). Following confirmation of mFFA1 receptor within this cell line, agonists were tested in a pERK1/2 assay in a concentration dependent manner (Figure 3-8B). Efficacy of FFA4 agonists TUG-1197, Agonist 2, Compound A and GSK17647A were significantly reduced compared to the positive control TAK-875, an FFA1 selective agonist, suggesting that these compounds are selective for mFFA4 (Table 3-7). However, it is interesting to note that Agonist 2 and GSK137647A may also promote activation of FFA1 at higher concentrations of drug, although as values were significantly decreased from the TAK-875 reference ligand this does indicate greater selectivity for mFFA4. Additionally, TUG-891 did show activity at mFFA1 consistent with TUG-891 being a dual FFA4/FFA1 agonist.

A

B
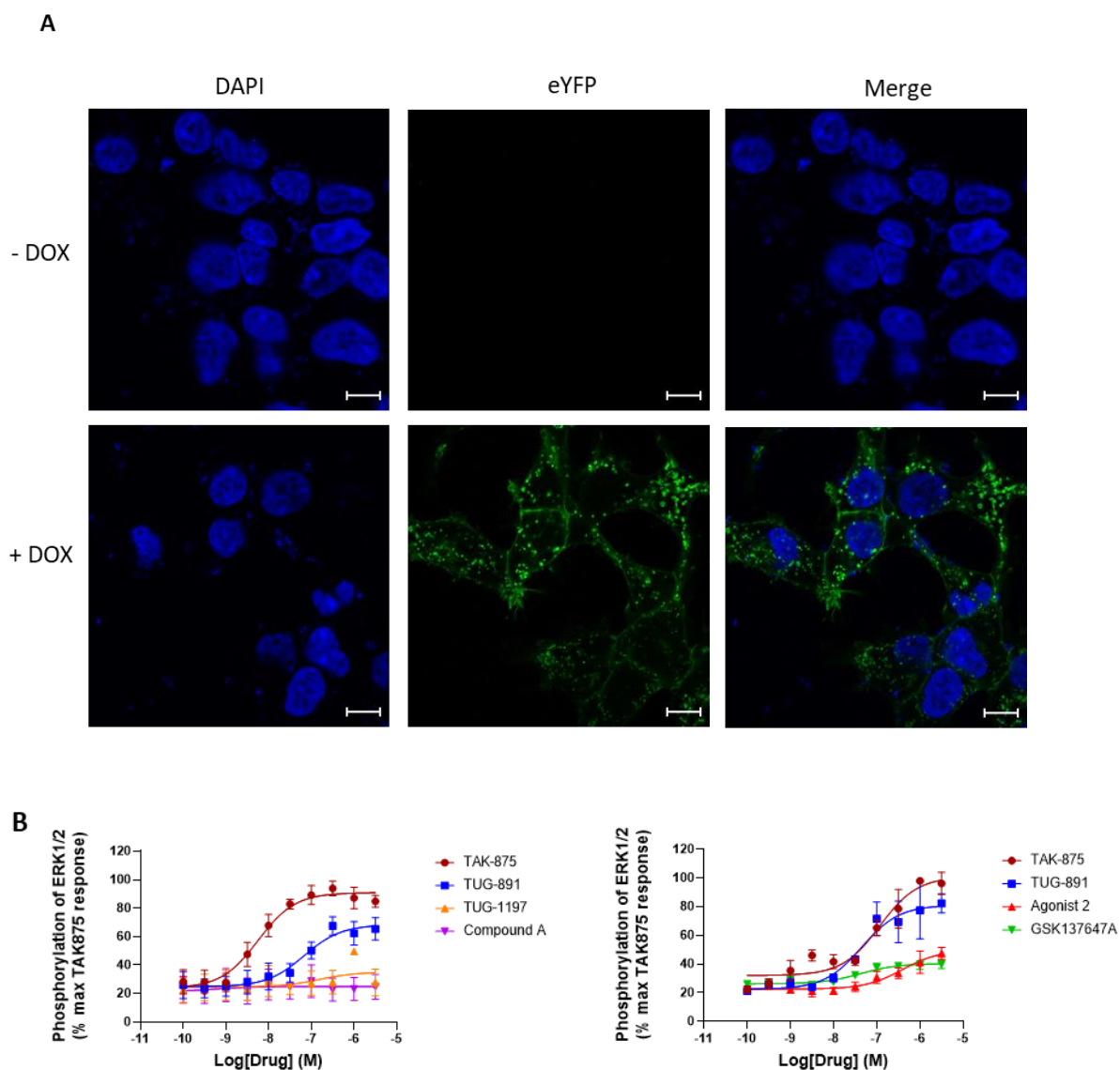
Figure 3-8: Selectivity of FFA4 agonists
(A) Representative images of immunocytochemical staining to show expression of mFFA4-eYFP (green) colocalised with cell nuclei (DAPI, blue). Expression of the constructs was induced by incubating with doxycycline (Dox) overnight at 37°C. Scale bar represents 10 μm, n=3. **(B)** Agonist-induced phosphorylation of ERK1/2 was measured in Flp-In T-rex HEK293 cells stably expressing mFFA1 following treatment with FFA4 agonists. Cells were treated at range of concentrations for 5 min to produce a concentration response curve. FFA1 agonist TAK-875 is used as a reference ligand. Results are mean ± S.E.M of three independent experiments (n=3).

Ligand	% Emax compared to TAK-875	P value
TAK875	100.9 (±5.2)	
TUG-891	81.7 (±6.7)	0.1 (ns)
Agonist 2	49.8 (±5.1)	0.0002 (***)
TUG-1197	35.9 (±8.5)	<0.0001 (****)
Compound A	25.0 (±3.8)	<0.0001 (****)
GSK137647A	40.3 (±1.4)	<0.0001 (****)

Table 3-7: % Emax of pERK1/2 response compared to TAK-875 in mFFA1 HEK293 cells
Results are mean ± S.E.M of three independent experiments (n=3). Statistical analysis performed was one-way ANOVA (Dunnett's multiple comparisons), ns=non-significant, ***=P<0.001, ****=P<0.0001.

3.4 Discussion

In this chapter, I set out to characterise the canonical signalling properties of a range of synthetic FFA4 agonists using the cellular model, Flp-In mFFA4 CHO cells. Following the demonstration of robust expression of mFFA4 in cell lines, agonists were assessed in pERK1/2 assays to determine if stimulation of agonists resulted in mFFA4 activation. Ligand time course experiments reported maximal responses at 5 min for all compounds, agreeing with data by Hudson et al., (2013). Often, pERK1/2 responses relating to G protein signalling are fast occurring, whereas slower and more sustained signals relate to ß-arrestin mediated pathways (Ahn et al., 2004; Shenoy et al., 2006; Herenbrink et al., 2016). Interestingly my results showed that Agonist 2 returned to basal levels slower than other compounds which might indicate a ß-arrestin component. However, ß-arrestin2 is not described to contribute to pERK1/2 signalling in FFA4 (Alvarez-Curto et al., 2016; Prihandoko et al., 2016). Additionally, Agonist 2 showed no signalling bias towards arrestin pathways suggesting that the time course profile should not differ considerably from that of the TUG-891 reference ligand. Therefore, this suggests that Agonist 2 may not be signalling via ß-arrestin2 in assays measuring phosphorylation of ERK1/2 and instead may promote a slower homologous desensitizing effect than other agonists assayed, an event which can occur over seconds to hours (Kelly, Bailey and Henderson, 2008; Rajagopal and Shenoy, 2018).

A range of pharmacological assays were used to assess the coupling properties of mFFA4 following synthetic agonist stimulation. As these were quantitative assays, agonist potencies and efficacies could be characterised. In pERK1/2 assays to determine receptor activation and pERK1/2 signalling capacity, potency values found in my experiments differ from reported values, although these can vary depending on the assay used to determine results (Leroy *et al.*, 2007). Differences in potency are largely down to differences in receptor expression and thereby receptor reserve. Additionally, how the pathways are measured, for example, chosen time points, can also impact upon agonist potencies. Despite a lack of more potent compounds than the TUG-891 reference ligand, efficacy values for all compounds were higher than the TUG-891 reference ligand which suggests that these compounds may be therapeutically effective when moving forth into *in vivo* experiments.

Gαq coupling is described as the primary G protein coupled signalling pathway for FFA4 (Hirasawa *et al.*, 2005; Briscoe *et al.*, 2006; Alvarez-Curto *et al.*, 2016; Milligan *et al.*, 2017) which was recognised also in this thesis by IP1 accumulation in response to FFA4 agonists. While FFA4 agonists TUG-891, Agonist 2 and Compound A were able to produce potent and efficacious responses leading to IP1 accumulation, TUG-1197 and GSK137647A did not. This might suggest that agonists which do not possess a carboxylic group such as TUG-1197 and GSK137647A do not produce potent responses in IP1 accumulation, perhaps explained by their differences in structure. Additionally, the potency of TUG-1197 was around 50x greater in pERK1/2 assays than IP1 and similarly, potency values in ERK1/2 phosphorylation were 3x higher than IP1 accumulation for GSK137647A. In general comparisons of pEC50 values between pERK1/2 signalling assays and IP1 accumulation assays revealed that the pEC50 was around 10-fold greater in pERK1/2 assays than IP1. As ERK1/2 phosphorylation occurs downstream from IP1 accumulation, signal amplification could occur – the number of activated products at each stage of a signalling pathway may increase, thus accounting for the differences in pharmacological values (Seger and Krebs, 1995).

Additionally, there are no reports of FFA4 coupling to Gαs signalling pathways in cell lines, however, G protein coupling can change upon ligand bias (Hauser *et*

al., 2022). To clarify that the FFA4 agonists assayed did not provoke Gαs coupling, cAMP assays were performed. Though FFA4 agonists did not stimulate cAMP accumulation, it is reported that FFA4 couples to Gαi pathways (Engelstoft *et al.*, 2013; Stone *et al.*, 2014). While FFA4 is known to signal via Gαi coupled pathways to reduce levels of somatostatin secretion within the pancreas in periods of elevated glucose levels (Stone *et al.*, 2014) and promotes release of ghrelin from the stomach (Engelstoft *et al.*, 2013), it is possible that this is a tissue specific effect as these results were not replicated in a simple cellular model. It has been shown using bioluminescence resonance energy transfer (BRET) assays, that GPCRs that couple primarily to Gαq G proteins may also couple promiscuously to Gαi G proteins (Okashah *et al.*, 2019). While Okashah *et al.*, used a sensitive BRET assay to detect secondary coupling, weak coupling patterns may not be detectable in some functional assays (including those used in this chapter) and may account for the reason that Gαi coupling was not detected in cell lines in this work. However, weak secondary couplings such as this can still produce physiological outcomes. The Gαs coupled β2AR also couples to Gαi G proteins resulting in reduced cardiac contractility (Xiao, Ji and Lakatta, 1995; Madamanchi, 2007; Okashah *et al.*, 2019).

While FFA4 is reported to couple primarily to Gαq G proteins, FFA4 additionally couples to β-arrestin2. β-arrestin2 coupling to WT-mFFA4 receptors was also investigated with data confirming all agonists promoted mFFA4:β-arrestin2 coupling. Interestingly, while agonist potencies did not differ from TUG-891, both TUG-1197 and GSK137647A displayed much lower efficacy suggesting the promotion of a weak coupling to β-arrestin2. This data is consistent with lower potencies and inability to reach maximal responses in IP1 and pERK1/2 assays. Additionally, internalisation events were observed following stimulation with all compounds by the movement of eYFP tagged receptor into endosomes which move inwards towards the nuclei. This finding is consistent with findings previously reported by Watson, Brown and Holliday, (2012) and Hudson *et al.*, (2013).

Within this chapter, calculations of bias factors downstream of G protein:receptor coupling for FFA4 agonists were performed to assess bias of agonists towards IP1 accumulation and ERK1/2 phosphorylation. Bias factor

values suggested that Agonist 2 showed bias towards IP1 accumulation compared to the TUG-891 reference ligand which has been previously described to show no stimulus bias (Butcher *et al.*, 2014). As described fully in Chapter 4 Part 1.4, Gαq, Gαi and β-arrestin2 pathways can result in ERK1/2 phosphorylation (Eishingdrelo, 2013). Despite this, Alvarez-Curto *et al.*, (2016) and Prihandoko *et al.*, (2016) described that β-arrestin signalling does not contribute to MAPK signalling and phosphorylation of ERK1/2 in FFA4. However, if IP1 and pERK1/2 are both downstream of receptor:Gq/11 coupling then there should be no receptor bias between these pathways. Despite this, in my results there is evidence of bias which does suggest that there is a difference in receptor activation mechanisms between these pathways. Evidently, pERK1/2 signalling is more complex than we suspect, although this is elucidated further in Chapter 4. However, Agonist 2 bias towards IP1 would result in increases in signalling to the downstream Gq coupled signalling associated with this pathway. The product of the Gq signalling pathway in which IP1 is a component is elevations in intracellular calcium which can lead to a whole host of physiological responses such as differentiation, proliferation, contraction, exocytosis and liver cell metabolism (Berridge, 1993). This might be of importance in the preferential activation of physiological responses mediated by FFA4 activated increases in intracellular calcium, such as GLP-1 secretion from enteroendocrine cells which is thought to be promoted by this pathway (examined in Chapter 6) (Hirasawa *et al.*, 2005; Tanaka, Katsuma and Adachi, 2008). Therefore, biased ligands such as Agonist 2 which favour Ca^{2+} elevating pathways could have clinical relevance in areas such as metabolic disease but of course this remains to be investigated. Additionally, no agonist displayed bias for G protein or β-arrestin coupled pathways. As little bias was observed between either IP1 and pERK1/2 or IP1 and β-arrestin pathways, perhaps this alludes to a lack of structural diversity in existing agonists.

A lack of structural diversity in the design of FFA4 ligands can also lead to challenges in agonist selectivity. There is inherent difficulty when studying the FFA4 receptor as despite having low sequence conservation to FFA1, both receptors respond to long chain free fatty acids. This creates a complexity when developing synthetic agonists, as agonists that bind to FFA4 may also be able to bind to FFA1 (Hara *et al.*, 2009). TUG-891 showed activity at FFA1 demonstrating

that this agonist is a dual FFA4/FFA1 agonist, a result that is reported in the mouse ortholog (Hudson, Murdoch and Milligan, 2013). All agonists assayed appeared to be more selective toward mFFA4 in comparison to TUG-891. TUG-1197 and Compound A have been previously reported as highly specific FFA4 agonists in agreement with this data (Oh *et al.*, 2014; Azevedo *et al.*, 2016). Similarly, GSK137647A has been previously reported to be responsive at FFA1 but 50 times more potent at FFA4 receptor (Sparks *et al.*, 2014), in agreement with results in this chapter. This is important to consider when working in systems such as animal models which may express both FFA4 and FFA1.

In conclusion, this chapter has demonstrated that FFA4 agonists are able to activate the mFFA4 receptor and initiate Gαq/11 coupled signalling and β-arrestin2 recruitment. Using a range of pharmacological assays, bias calculations were performed to understand if these agonists can preferentially signal through one pathway over another. Agonist 2 displayed bias towards IP1 pathways whereas Compound A showed no bias. The identification of signal bias downstream of Gq/receptor coupling suggests a complex relationship between pERK1/2 and IP1 signalling mechanisms. Furthermore, in selectivity studies, TUG-891 was a dual FFA4/FFA1 agonist, whereas TUG-1197, Compound A, GSK13647A and Agonist 2 were more selective for mFFA4. This profiling of synthetic agonists is important as it may help us to resolve physiological effects in *ex vivo* and *in vivo* models.

Chapter 4 Pharmacology of phosphorylation deficient mFFA4

4.1 Introduction

Upon binding of an agonist to a GPCR, the equilibrium between inactive (R) state and the activated (R*) state is driven to the (R*) state. Stabilising the receptor in an active conformation results in the interaction of the receptor with G proteins, kinases such as GRKs which phosphorylate intracellular residues on the activated receptor, and adaptor proteins, the most characterised of which are the arrestin family (described in Chapter 1 Part 1.5) (Luttrell and Gesty-Palmer, 2010; Gurevich and Gurevich, 2019). In the case of FFA4, ß-arrestin2 primarily interacts with the receptor following homologous phosphorylation by GRK6, which phosphorylates C-terminal and intracellular serine/threonine residues (Burns *et al.*, 2014; Butcher *et al.*, 2014). Mass-spectrometry analysis has identified five residues on the C-terminus of FFA4 thought to be the primary residues that are phosphorylated upon receptor activation: Thr347, Thr349, Ser350, Ser357 and Ser361 (Prihandoko *et al.*, 2016).

As receptors are multiply phosphorylated at a range of different intracellular sites by kinases including GRKs, a barcode theory has been hypothesised since the complex nature of receptor phosphorylation has indicated that different kinases to the same receptor may result in different phosphorylation patterns. Variances in receptor phosphorylation have the potential to initiate distinct downstream signalling pathways which can result in different functions of the same receptor in different tissues (Tobin, 2008; Butcher *et al.*, 2011). This theory has been supported by phosphorylation studies on mFFA4 where mutation of phospho-acceptor sites within two C-terminal clusters, cluster 1 (Thr347, Thr349, and Ser350) and cluster 2 (Ser357 and Ser361), resulted in the generation of a PD receptor indicating that the vast majority of phosphorylation of this receptor occurred within these C-tail clusters. Mutations at cluster 1 resulted in downregulation of Akt activation whereas mutation of cluster 2 reduced ß-arrestin2 recruitment but did not affect Akt activation (Prihandoko *et al.*, 2016). This differential effect of phosphorylation at clusters 1 and 2 also had an effect on receptor internalisation, with cluster 1 mutations having no effect on receptor internalisation whereas mutations at cluster 2 reduced

internalisation. This is likely due to the fact that cluster 2 is involved in the recruitment of ß-arrestin, whereas cluster 1 is not. The identification of different functions as a result of phosphorylation at different sites supports the barcode theory, suggesting that differential phosphorylation of these sites could lead to activation of different signalling pathways.

This chapter focuses on whether a range of FFA4 agonists were able to induce mFFA4-ß-arrestin2 interaction and canonical G protein signalling in cell lines expressing a PD-mFFA4 variant. It was additionally investigated whether these compounds show signs of preferential signalling for one pathway over another in PD-mFFA4 in comparison to WT-mFFA4. These studies are important as although the functions of phosphorylation and ß-arrestin recruitment are often linked, there is evidence to suggest that agonist induced receptor phosphorylation and ß-arrestin recruitment to FFA4 may have distinct functions. This was highlighted in studies by Alvarez-Curto *et al.*, (2016), where it was discovered that PD-mFFA4 cell lines resulted in an enhanced pERK1/2 signalling which was not evident in arrestin null cell lines. Despite defining the location of phosphorylation sites, little is known about physiological effects of phosphorylation in FFA4 and recognition of the way in which FFA4 agonists behave at PD-mFFA4 receptors creates a strong foundation for understanding effects in primary cells and *in vivo*.

4.2 Aims

The aims of this chapter were to:

- Investigate receptor phosphorylation in WT-mFFA4 and PD-mFFA4 receptors

- Assess coupling to ß-arrestin2 and receptor internalisation in PD-mFFA4 cells

- Assess pERK1/2 and IP1 Gq coupled signalling in PD-mFFA4 cells using FFA4 agonists

4.3 Results

4.3.1 Expression of phosphorylation deficient mFFA4

Mass spectrometry studies from Prihandoko *et al.*, (2016) determined that the mFFA4 receptor is phosphorylated at five key residues in the C-terminus. To study the roles of phosphorylation in FFA4, a PD-mFFA4 cell line was developed where all possible phosphorylation sites on the C-terminal tail were mutated. First, mFFA4-eYFP construct was transfected into CHO cells using Flp-In vector technology. Mutations of serine/threonine residues in the C-terminus to alanine residues were then performed using QuikChange II method (Stratagene, Berkshire, UK). The resulting cell line contained the sequence ADAA-AAA in the C-terminus (Prihandoko *et al.*, 2016) (Figure 4-1).

A

mFFA4-WT C-tail   .....KIFCCFFFPEKGAIF**TDTS**VRRNDL**S**VI**SS**-Ct

B

mFFA4-PD C-tail   .....KIFCCFFFPEKGAIF**A**D**AA**VRRNDL**A**VI**AA**-Ct
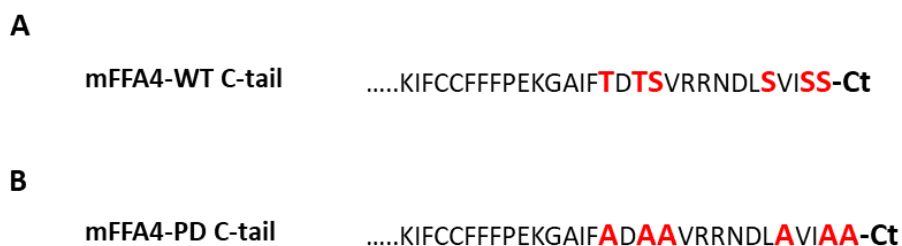
Figure 4-1: C-terminal tail of WT and PD mFFA4
Prihandoko *et al.,* (2016) identified phosphorylation sites on the WT-mFFA4 C-terminus in mass spectrometry experiments (shown in red text) **(A)**. Phosphorylation deficient versions of the mFFA4 receptor were generated by mutation of the phospho-sites to alanine (shown in red text) **(B).**

Firstly, to determine if the in-house phosphorylation specific FFA4 antiserum targeting residues at $pThr^{347}$/$pSer^{350}$ would detect phosphorylation, western blots were performed in Flp-In mFFA4 CHO cells (Figure 4-2A). Bands present at 75kDa following 5 min treatment with all compounds indicated that residues Thr^{347}/Ser^{350} were phosphorylated. In contrast, no phosphorylation was detected in non-transfected cells (Figure 4-2B) confirming the presence of phosphorylated mFFA4 in mFFA4 CHO cells.
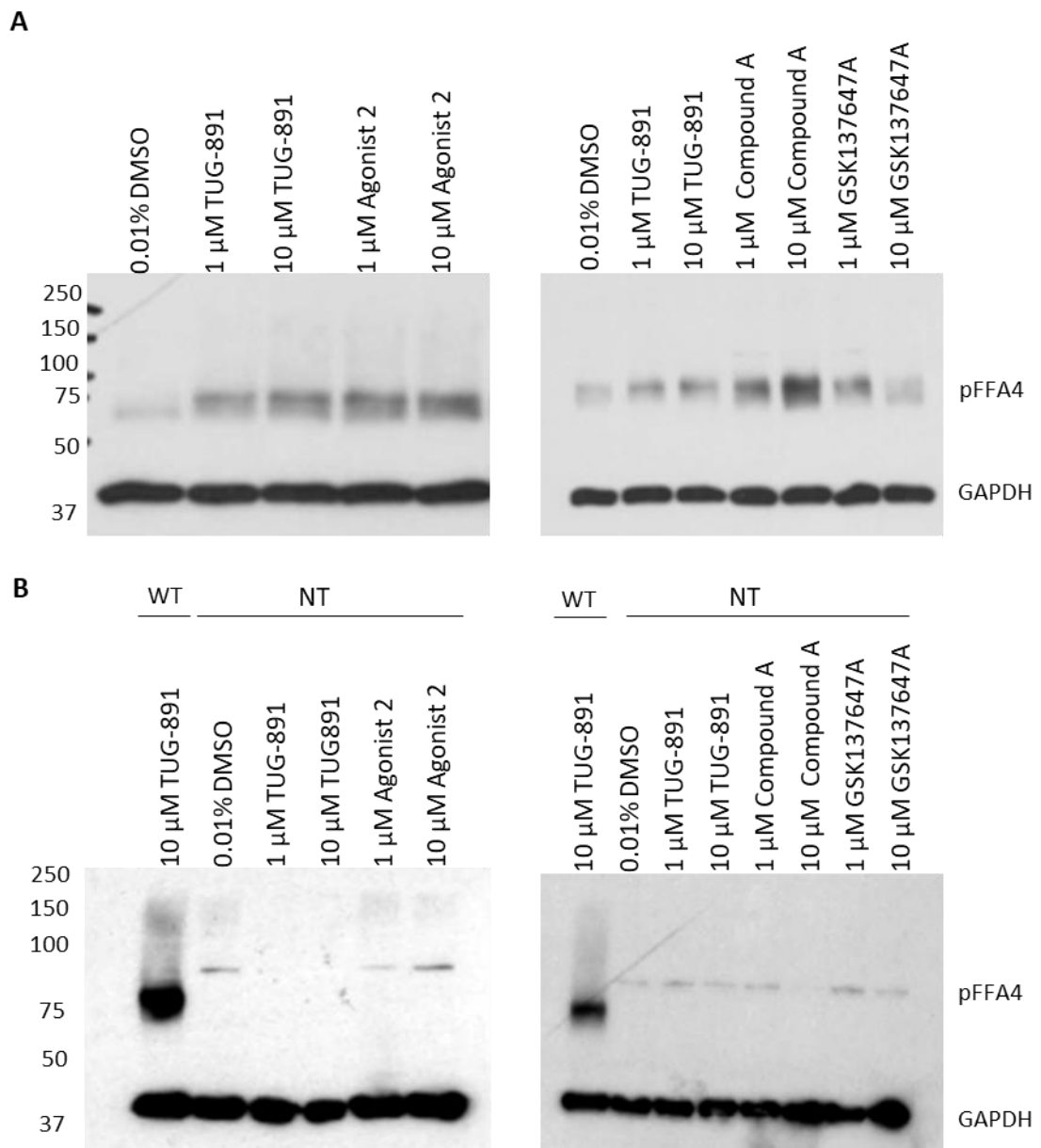
Figure 4-2: Confirmation of pFFA4 in mFFA4 CHO cells
Western blot analysis using in house pFFA4 antiserum to confirm presence of phosphorylated FFA4 following treatment with various FFA4 agonists. **(A)** mFFA4 Flp-In CHO cell lysate (10 µg). **(B)** non-transfected CHO cell lysate (10 µg). Ubiquitously expressed GAPDH was used a loading control. WT = WT mFFA4 Flp-In CHO cells, NT = non-transfected CHO cells. Images are representative of three independent experiments (n=3).

Following confirmation of receptor phosphorylation in WT-mFFA4 cells and functionality of the in-house pFFA4 antiserum, western blots were performed to assess loss of phosphorylation in PD-mFFA4 cell lines (Figure 4-3). Following treatment with all FFA4 agonists, the PD-mFFA4 receptor was not phosphorylated compared to WT-mFFA4 controls, suggesting that mutation of

phospho-acceptor sites resulted in loss of phosphorylation (Figure 4-3A). To validate that the receptor was present within PD-mFFA4 cell lines and that loss of phosphorylation was due to mutation of these phospo-specific sites and not due to loss of receptor expression, western blots were performed with eYPF antibody (Figure 4-3B). Expression of PD-mFFA4-eYFP was detected as indicated with a band at around 75kDa, again representing the molecular weight of FFA4 (45 kDa) in addition to the molecular weight of eYFP (27 kDa).
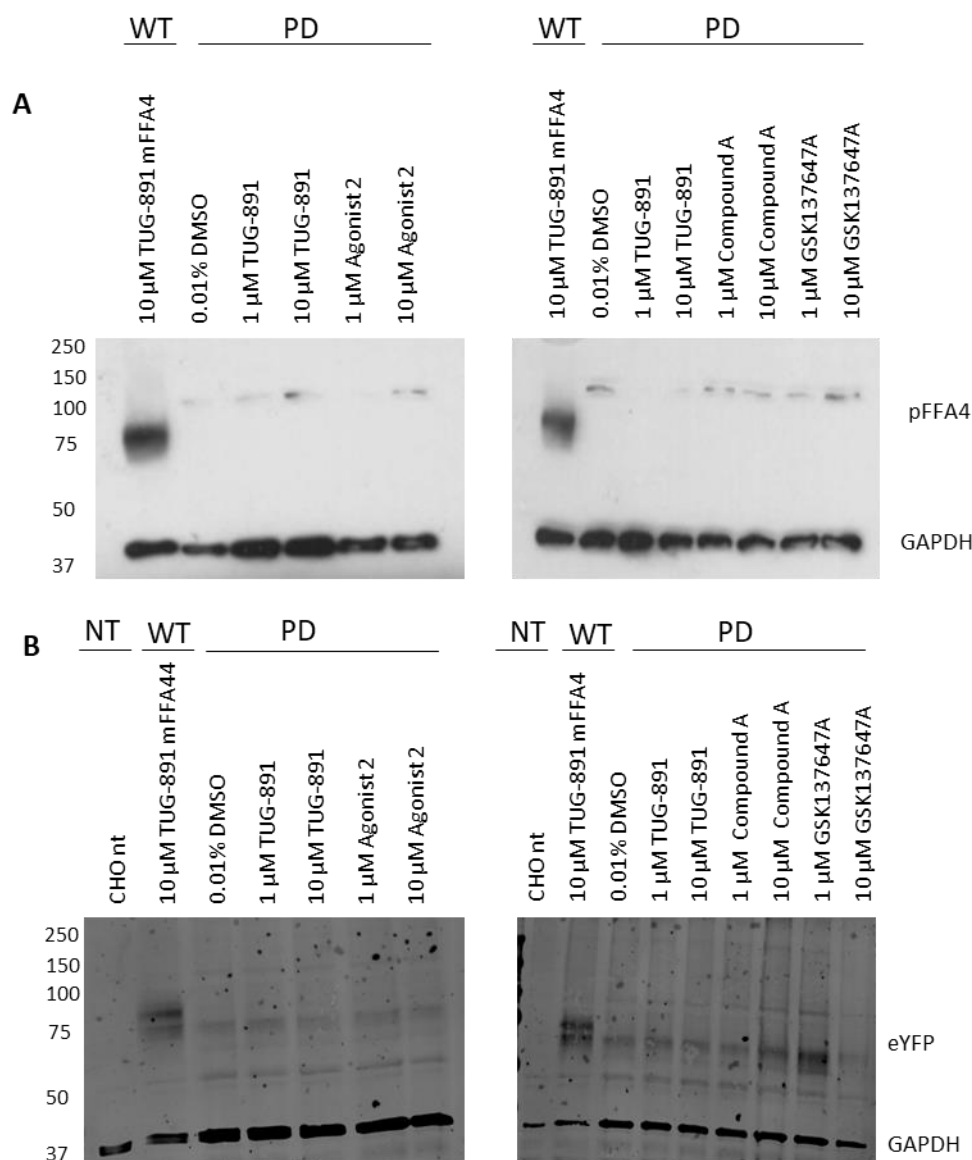
Figure 4-3: Confirmation of loss of phosphorylation in phosphorylation deficient (PD) mFFA4 CHO cells
(A) Western blot analysis using in house pFFA4 antibody to confirm loss of phosphorylation following treatment with various FFA4 agonists in PD -mFFA4 CHO cell lysate (10 µg). (B) Presence of receptor was determined by western blot for eYFP in PD-mFFA4 Flp-In CHO cell lysate (10 µg) following treatment with various FFA4 agonists. Ubiquitously expressed GAPDH was used a loading control. NT= non-transfected CHO cells, WT= wild-type mFFA4 Flp-In CHO

cells, PD= phosphorylation deficient mFFA4 Flp-In CHO cells. Images are representative of three independent experiments (n=3).

4.3.2 β-arrestin signalling in PD-mFFA4 cells

To assess whether the phosphorylation deficient form of mFFA4 was able to induce ß-arrestin recruitment, BRET assays were performed in this cell line. A loss of PD-mFFA4 recruitment of ß-arrestin2 to the cell membrane was detected following stimulation with all agonists compared to agonist profiles in WT-mFFA4 cells (Figure 4-4A). Agonist efficacies were significantly reduced for TUG-891, Agonist 2 and Compound A in PD-mFFA4 cells compared to WT-mFFA4 cells (P=0.003, 0.0004 and 0.001) (Table 4-1). Interestingly, efficacies of TUG-1197 and GSK137647A in PD-mFFA4 cells were not significantly different from values of these agonist treatments in WT-mFFA4 cells, suggesting that these agonists promote poor ß-arrestin2 coupling through C-terminal residues. Reduction of ß-arrestin2 coupling would infer loss of ß-arrestin2 mediated functions in the cell system, including receptor desensitisation.

In addition to a reduction of ß-arrestin2 recruitment following agonist stimulation, it was also evident that PD-mFFA4 lost the capability of receptor internalisation as receptor stayed localised at the plasma membrane and did not internalise and move towards the nuclei (Figure 4-4B).

A
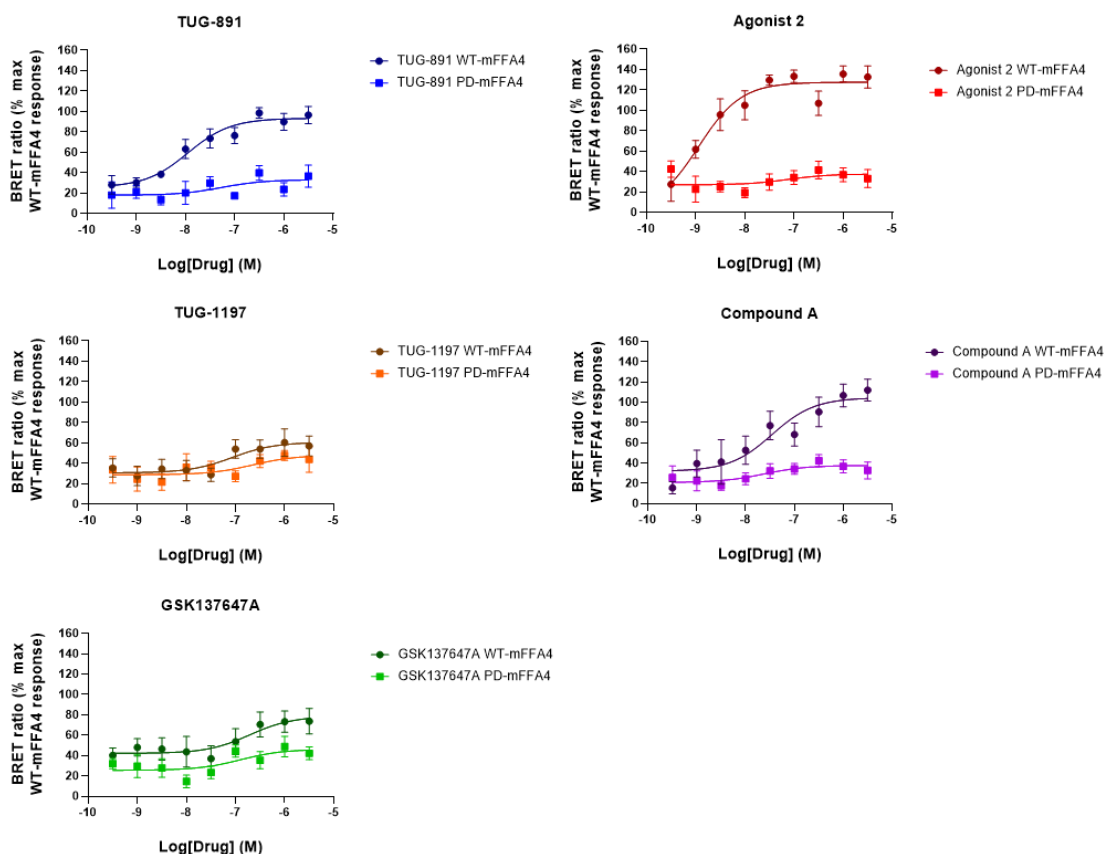
B
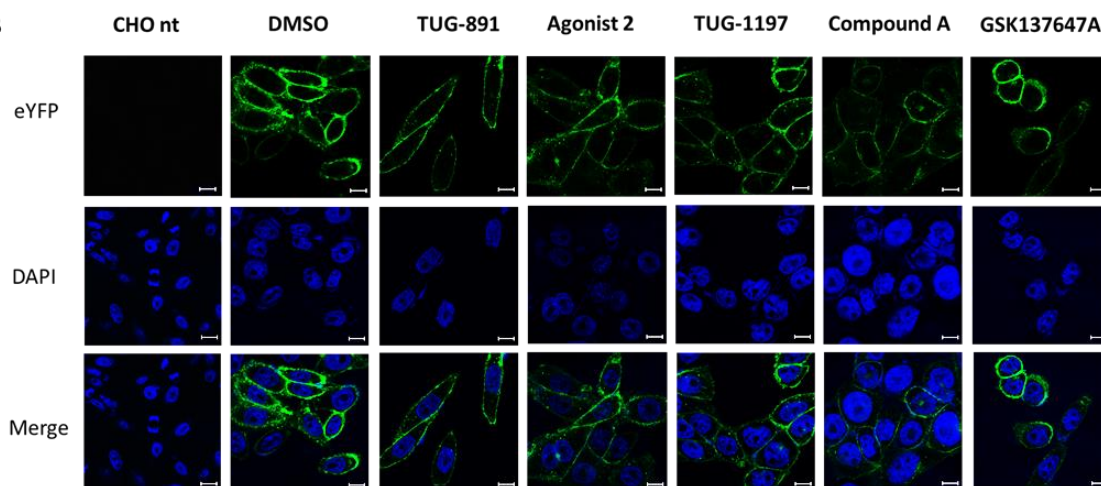
Figure 4-4: FFA4 agonist stimulated β-arrestin2 recruitment and receptor internalisation in PD- mFFA4 CHO cells

(A) Agonist-induced β-arrestin2 recruitment was measured using a BRET based assay in Flp-In CHO cells expressing PD-mFFA4 or WT-mFFA4 following treatment with FFA4 agonists. Cells were stimulated with FFA4 agonist at various concentrations for 5 min to produce a concentration response curve. Data is displayed as a ratio of 535/475 nm emission between eYFP and R-luciferase interactions. Results are mean ± S.E.M of three independent experiments (n=3). **(B)** Immunocytochemistry following 30 min stimulation of 10 µM FFA4 agonist on Flp-In CHO cells expressing PD-mFFA4. Merged images show co-localisation of mFFA4 (green, eYFP) with cell nuclei (blue, DAPI). Scale bar represents 10 µm. Images are representative of three independent experiments (n=3).

Ligand	% Emax		
	WT	PD	P
TUG-891	93.4 (±4.2)	33.2 (±6.1)	0.003 (**)
Agonist 2	127.9 (±5.2)	37.8 (±6.3)	0.0004 (***)
TUG-1197	58.9 (±5.7)	47.8 (±10.8)	0.4 (ns)
Compound A	101.2 (±6.6)	37.8 (±4.3)	0.001 (**)
GSK137647A	64.4 (±6.6)	49.6 (±11.7)	0.3 (ns)

Table 4-1: Efficacy of FFA4 agonists in β-arrestin2 recruitment assay in WT-mFFA4 and PD-mFFA4 cell lines
Results are mean ± S.E.M of three independent experiments (n=3). Statistical analysis performed was an unpaired t-test, ns=non-significant, **=P<0.01, ***=P<0.001.

4.3.3 Canonical signalling in PD-mFFA4 cells

To characterise PD-mFFA4 G protein signalling pathways, pharmacological assays were performed on CHO cells expressing PD-mFFA4. A time course pERK1/2 activation assay was performed on this cell line with an optimum response occurring at 5 min for all compounds (Figure 4-5A) consistent with WT-mFFA4 cells (Chapter 3 part 1.3.2). Interestingly, Agonist 2 returned to basal at the same rate as other compounds in PD-mFFA4 cells in contrast to WT-mFFA4 cells where decline was slower. Overall, decline to basal appeared to occur more slowly in the PD-mFFA4 model in all compounds, however, in comparison to the TUG-891 reference ligand, profiles are similar to TUG-891 with a peak response observed at 5 min followed by a sustained response. This is perhaps attributed to a lack of receptor mediated desensitisation in these cells, resulting in an increase in the number of activated receptors in cells at any one time. Additionally, fold over basal values were plotted for TUG-891 treated WT-mFFA4 cells (Chapter 3 Part 3.3.2) compared to PD-mFFA4 TUG-891, where it was evident that phosphorylation of ERK1/2 was enhanced upon removal of phosphorylation sites (Figure 4-5B).

A
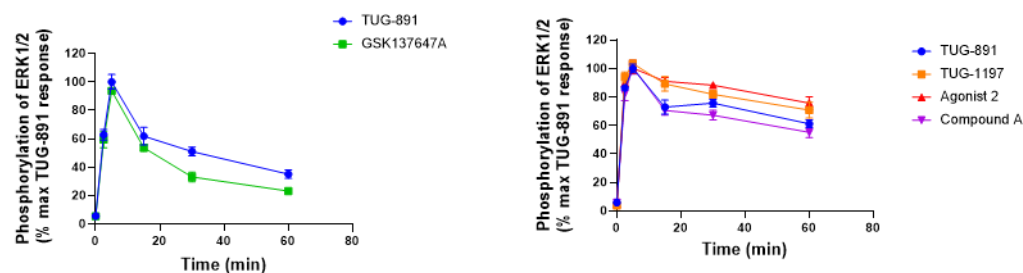
B
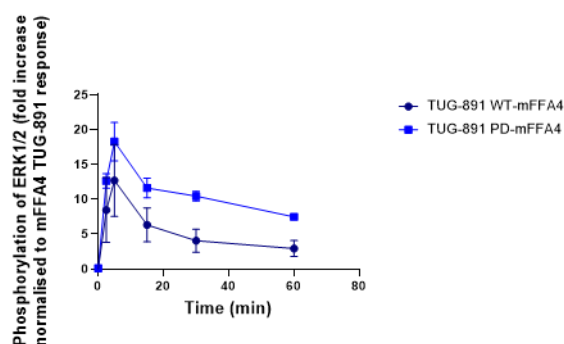
Figure 4-5: PD-mFFA4 pERK1/2 time course studies
Agonist-induced phosphorylation of ERK1/2 was measured using a FRET based assay in Flp-In
CHO cells expressing the PD-mFFA4 following treatment with FFA4 agonists. Cells were
stimulated with constant concentration (10 µM) of FFA4 agonists in 60 min time-course
experiments in PD-mFFA4 Flp-In CHO cells **(A)** or PD-mFFA4 and WT-mFFA4 Flp-In CHO cells
(B). Results are mean ± S.E.M of three independent experiments (n=3).

Concentration response curves to examine phosphorylation of ERK1/2 were also
performed on PD-mFFA4 cell lines, where removal of phosphorylation sites did
not prevent the receptor from stimulating signalling pathways resulting in the
phosphorylation of ERK1/2 (Figure 4-6A). Data indicated that the potencies and
efficacies of FFA4 agonists were not increased in comparison the TUG-891
reference ligand (Table 4-2). However, comparison of agonist potencies and
efficacies in pERK1/2 assays in PD-mFFA4 and WT-mFFA4 cell lines revealed that
agonist potencies and efficacies were significantly increased in PD-mFFA4 cells
in comparison to WT-mFFA4 cells for TUG-891, TUG-1197, Compound A and
GSK137647A (Figure 4-6B, Table 4-3). This again may indicate that this PD-
mFFA4 cell system could have a greater signalling capacity due to the loss of
receptor desensitisation, facilitating increased efficacies of agonists. However,
in the case of Agonist 2, stimulation of PD-mFFA4 did not have increased potency
or efficacy compared to WT-mFFA4, indicating that Agonist 2 acts similarly in
WT-mFFA4 and PD-mFFA4 receptors. This suggests that Agonist 2 may have a
reached a maximal response in WT-mFFA4 cells by occupying a lower number of

active receptors than other agonists, thus explaining why efficacy doesn't differ in PD-mFFA4 cells.
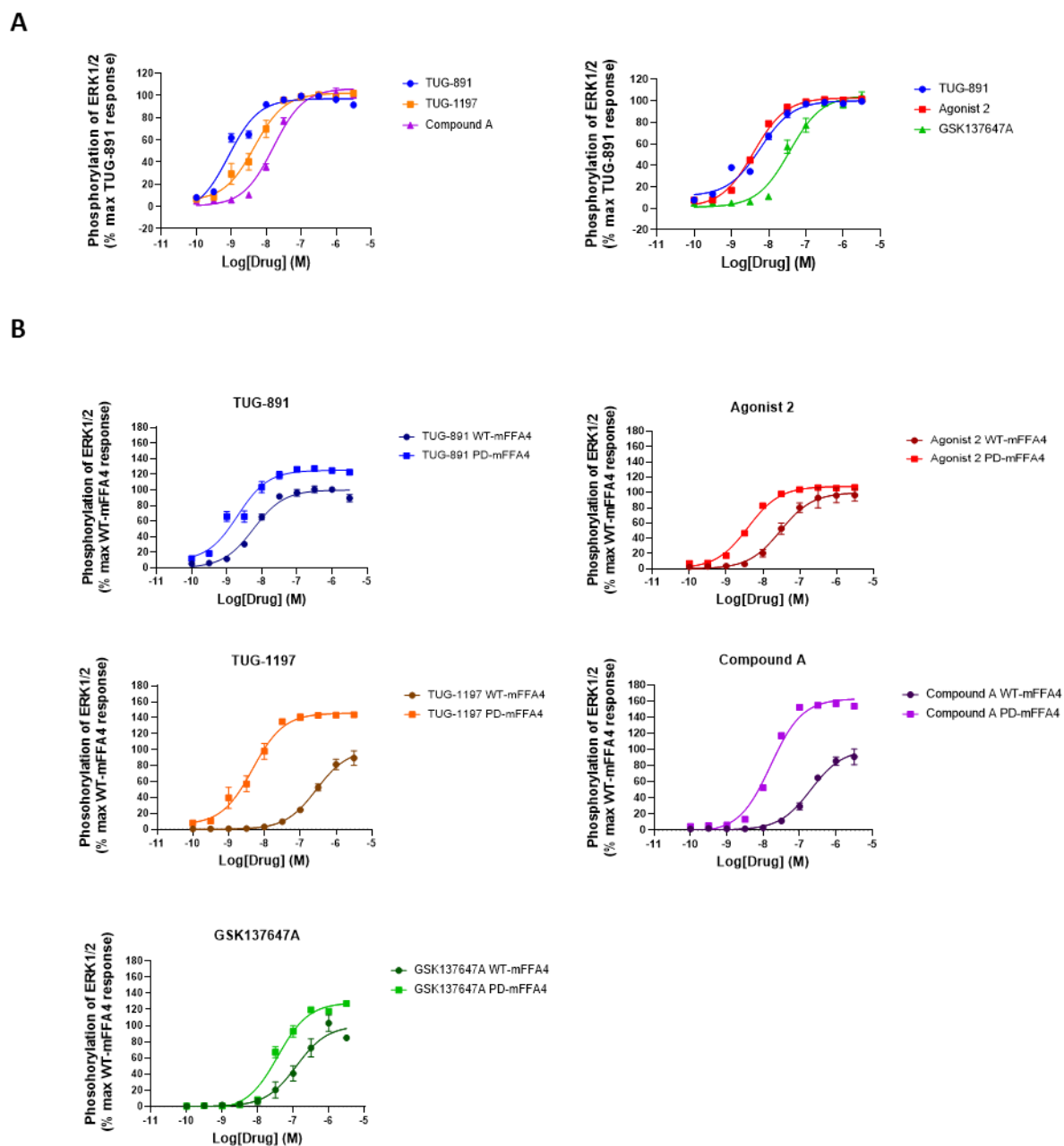
Figure 4-6: FFA4 signalling via pERK1/2 in a PD-mFFA4 cell line
Agonist-induced phosphorylation of ERK1/2 was measured using a FRET based assay in Flp-In CHO cells expressing the PD-mFFA4 following treatment with FFA4 agonists and **(A)** compared to TUG-891 reference ligand or **(B)** Flp-In CHO cells expressing the WT-mFFA4 treated with respective agonist. Cells were stimulated with FFA4 agonist at a range of concentrations for 5 min to produce a concentration-response curve. Results are mean ± S.E.M of three independent experiments (n=3).

Ligand	pERK1/2			
	pEC50		% Emax compared to TUG-891	
	Mean ± S.E.M	P Value	Mean ± S.E.M	P Value
TUG-891	8.7 (±0.1)		100.0 (±1.5)	
Agonist 2	8.4 (±0.0)	0.04 (*)	102.8 (±1.1)	0.7 (ns)
TUG-1197	8.4 (±0.1)	0.04 (*)	102.1 (±2.4)	0.9 (ns)
Compound A	7.8 (±0.0)	<0.0001 (****)	106.3 (±1.7)	0.1 (ns)
GSK137647A	7.4 (±0.1)	<0.0001 (****)	104.9 (±2.7)	0.3 (ns)

Table 4-2: Potencies and efficacies of FFA4 agonists in pERK1/2 assays in PD-mFFA4 cells
Results are mean ± S.E.M of three independent experiments (n=3). One-way ANOVA (Dunnett's multiple comparisons), ns=non-significant, *=P<0.05, ****=P<0.0001.

Ligand	pERK1/2					
	pEC50			% Emax normalised to WT		
	WT	PD	P	WT	PD	P
TUG-891	8.2 (±0.2)	9.1 (±0.1)	0.002 (**)	100.0 (±1.8)	132.7 (±2.2)	<0.0001 (****)
Agonist 2	8.3 (±0.0)	8.4 (±0.0)	0.4 (ns)	100.0 (±3.9)	108.0 (±1.5)	0.2 (ns)
TUG-1197	6.5 (±0.1)	8.3 (±0.1)	<0.0001 (****)	100.0 (±4.1)	145.8 (±3.2)	0.0001 (***)
Compound A	6.8 (±0.1)	7.8 (±0.0)	<0.0001 (****)	100.0 (±3.8)	163.2 (±2.3)	<0.0001 (****)
GSK137647A	6.9 (±0.1)	7.4 (±0.1)	0.004 (**)	100.0 (±6.7)	128.4 (±2.9)	0.003 (**)

Table 4-3: Potencies and efficacies of FFA4 agonists in pERK1/2 assays in PD-mFFA4 and WT-mFFA4 cell lines
Results are mean ± S.E.M of three independent experiments (n=3). Statistical analysis performed was an unpaired t-test, ns=non-significant, **=P<0.01, ***=P<0.001, ****=P<0.0001.

Accumulation of IP1 was assessed as a measure of Gq coupled signalling, where it was evident that removal of phosphorylation sites also did not prevent the receptor from stimulating signalling pathways resulting in IP1 accumulation (Figure 4-7A). While efficacies of response were not improved in comparison to TUG-891, potencies were variable. The potency of Agonist 2 was significantly increased in comparison to TUG-891 (P=0.005), although the potency of Compound A was significantly lower than that of TUG-891 (P=0.003) (Table 4-4). Neither GSK137647A or TUG-1197 reached a maximal response and so potency values could not be reliably calculated here. When comparing agonist potency and efficacy values in WT-mFFA4 and PD-mFFA4 cell lines, potencies and efficacies for TUG-891, Agonist 2 and Compound A were significantly increased in PD-mFFA4 cells in comparison to WT-mFFA4 cells (Figure 4-7B, Table 4-5). As IP1 accumulation did not reach a peak response in WT-mFFA4 cells or PD-mFFA4 cells for GSK137647A and TUG-1197, it was not possible to compare values, although data did show increases in both potency and efficacy. This data implies that in addition to an enhancement of pERK1/2 upon removal of mFFA4 C-terminus phosphorylation sites, IP1 accumulation was also enhanced. This again

suggests a greater signalling capacity in PD-mFFA4 cells which might be due to a loss of receptor desensitisation.

A
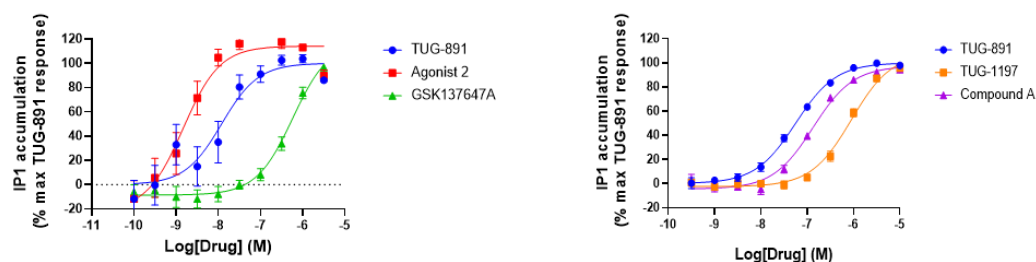
B
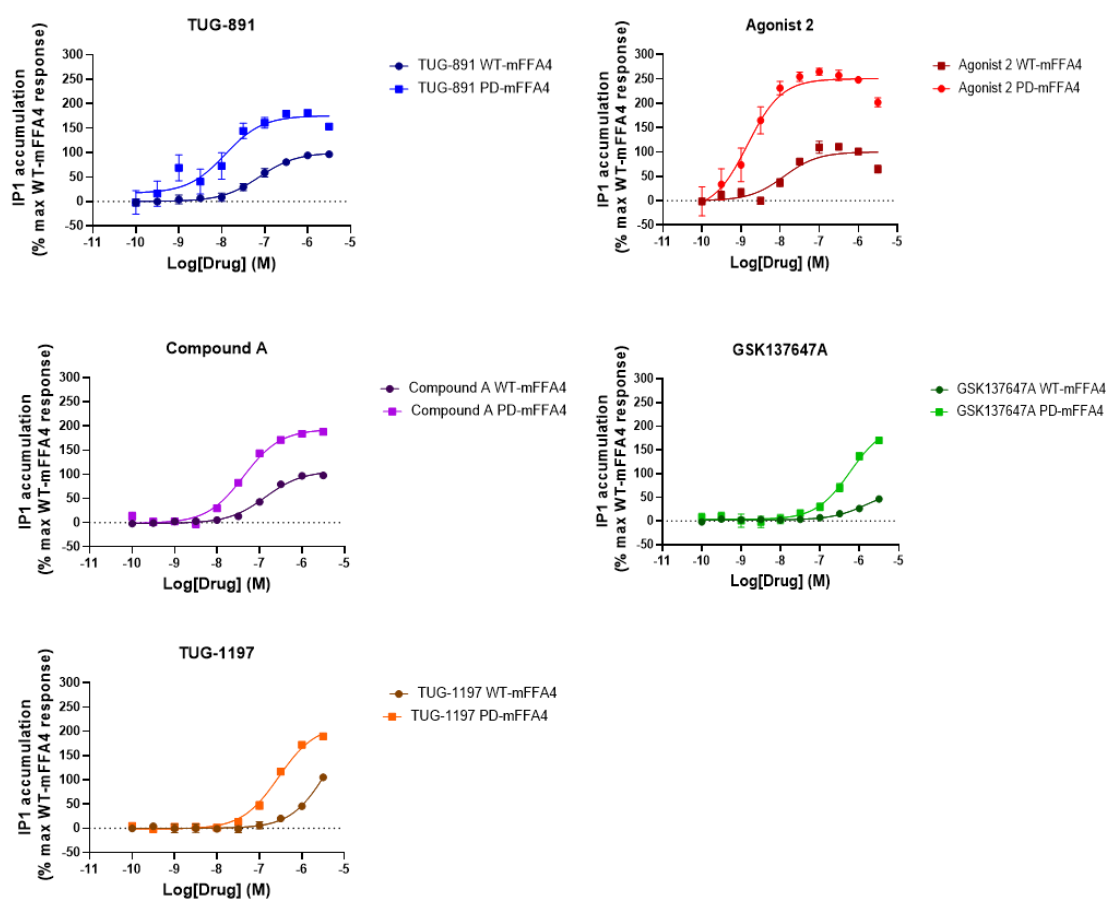
Figure 4-7: FFA4 agonist induced IP1 accumulation in a PD-mFFA4 cell line
Agonist-induced IP1 accumulation was measured using a FRET based assay in Flp-In CHO cells expressing the PD-mFFA4 following treatment with FFA4 agonists and **(A)** compared to TUG-891 reference ligand in PD-mFFA4 cells or **(B)** Flp-In CHO cells expressing the WT-mFFA4 treated with respective agonist. Cells were stimulated with FFA4 agonist at a range of concentrations for 5 min to produce a concentration-response curve. Results are mean ± S.E.M of three independent experiments (n=3).

Ligand	IP1 accumulation			
	pEC50		% Emax compared to TUG-891	
	Mean ± S.E.M	P Value	Mean ± S.E.M	P Value
TUG-891	7.9 (±0.2)		100.0 (±7.0)	
Agonist 2	8.8 (±0.2)	0.005 (**)	110.8 (±5.0)	0.5 (ns)
TUG-1197	-	-	-	-
Compound A	6.9 (±0.1)	0.003 (**)	97.4 (±2.4)	1.0 (ns)
GSK137647A	-	-	-	-

Table 4-4: Potencies and efficacies of FFA4 agonists in IP1 accumulation assays in PD-mFFA4 cells
Results are mean ± S.E.M of three independent experiments (n=3). One-way ANOVA (Dunnett's multiple comparisons), ns=non-significant, **=P<0.01.

Ligand	IP1 accumulation					
	pEC50			% Emax normalised to WT		
	WT	PD	P	WT	PD	P
TUG-891	7.1 (±0.1)	7.9 (±0.2)	0.02 (*)	100.0 (±5.3)	175.4 (±11.2)	0.0005 (***)
Agonist 2	7.9 (±0.2)	8.8 (±0.2)	0.03 (*)	100.0 (±5.7)	250.4 (±9.7)	<0.0001 (****)
TUG-1197	-	-	-	-	-	-
Compound A	6.9 (±0.1)	7.4 (±0.1)	0.004 (**)	108.4 (±3.3)	193.4 (±4.5)	<0.0001 (****)
GSK137647A	-	-	-	-	-	-

Table 4-5: Potencies and efficacies of FFA4 agonists in IP1 assays in PD-mFFA4 and WT-mFFA4 cells
Results are mean ± S.E.M of three independent experiments (n=3). Statistical analysis performed was an unpaired t-test, *=P<0.05, **=P<0.01, ***=P<0.001, ****=P<0.0001.

4.3.4 Biased signalling in PD-mFFA4 cells

Comparisons of bias in signalling pathways downstream of Gαq:receptor coupling in a PD-mFFA4 cell model were calculated by fitting the concentration–response curves of IP1 accumulation and phosphorylation of ERK1/2 to a model based on the Black and Leff operational model of agonism (Black *et al.*, 1985) to calculate transduction coefficients (τ), as previously described by Kenakin *et al.*, (2012). These transduction coefficients were compared with the reference ligand TUG-891, from which bias factors for ligands between IP1 accumulation and phosphorylation of pERK1/2 were calculated (Table 4-6). As TUG-1197 and GSK137647A did not reach a maximal response in IP1 accumulation assays, comparisons could not be made for these agonists since the operational model relies on an estimate of functional affinity and efficacy. Bias factor calculations suggested that Agonist 2 shows significant bias towards IP1 pathways (P<0.0001), consistent with results in WT-mFFA4 cells displayed in Chapter 3 Part 3.3.3. In addition to Agonist 2, Compound A also displayed significant bias in IP1 accumulation pathways in comparison to the TUG-891 reference ligand (P=0.01).

	IP1 Accumulation		ERK1/2 Phosphorylation		Log Bias Factor IP$_1$ - ERK 1/2	Bias Factor	P Value
	$Log_{10}(\tau/K_A)$	$\Delta Log_{10}(\tau/K_A)$	$Log_{10}(\tau/K_A)$	$\Delta Log_{10}(\tau/K_A)$	$\Delta\Delta Log_{10}(\tau/K_A)$	$10\text{\textasciicircum}(\Delta\Delta Log_{10}(\tau/K_A))$	
TUG-891	7.12 ± 0.06	0.00 ± 0.09	8.94 ± 0.04	0.00 ± 0.06	0.00 ± 0.10		
Agonist 2	9.07 ± 0.06	1.95 ± 0.09	8.40 ± 0.04	-0.54 ± 0.06	2.49 ± 0.10	309.03	<0.0001 (****)
Compound A	6.64 ± 0.06	-0.48 ± 0.09	7.82 ± 0.04	-1.12 ± 0.06	0.64 ± 0.10	4.37	0.01 (*)

Table 4-6: Bias factor calculations in PD-mFFA4 cell line compared to TUG-891
Results are mean ± S.E.M of three independent experiments (n=3). Statistical analysis performed was unpaired t-test, ns=non-significant, *=P<0.05, ****=P<0.0001.

4.4 Discussion

Studies on PD mouse models have already proven to be a success in determining physiological roles of phosphorylation in GPCRs, with studies on M1-PD mice demonstrating that phosphorylation/ß-arrestin pathways provide neuroprotective effects in mouse models with neurodegenerative disease (Scarpa *et al.*, 2021) and additionally, M3-PD studies have indicated that M3 muscarinic receptors promote bronchoconstriction via phosphorylation/ß-arrestin-dependent signalling pathways (Bradley *et al.*, 2016). Therefore, in this chapter I wanted to probe the effects of various agonists in a PD cell model to identify mechanisms of agonist mediated receptor activation and signalling cascades in the absence of phosphorylation. As the physiological roles of receptor phosphorylation of FFA4 are largely unknown, characterisation of PD-mFFA4-eYFP cells is important since it may help to elucidate unknown signalling effects in PD animal models.

Changes in coupling patterns between WT-mFFA4 and PD-mFFA4 cells were investigated in a range of pharmacological assays. ß-arrestin2 coupling to PD-mFFA4 receptors was examined, revealing that while synthetic FFA4 agonists induced WT-mFFA4 coupling to ß-arrestin2 and stimulated receptor internalisation, the same effect was not observed in PD-mFFA4 cells where coupling was significantly reduced. This would indicate that mutation of these residues on the mFFA4 C-terminus is responsible for phosphorylation and recruitment of ß-arrestin2. This is consistent with data by Prihandoko *et al.*, (2016) who demonstrated that mutation of all phosphorylation sites on the C-terminal tail resulted in markedly reduced coupling to ß-arrestin2 upon TUG-891

stimulation, more specifically residues Ser357 and Ser361 forming cluster 2. However, in ß-arrestin2 recruitment assays BRET signal was still detected at higher concentrations, particularly visible for GSK137647A, TUG-1197 and Compound A, indicating that there was not a complete loss of ß-arrestin2 recruitment. As GRKs such as GRK6 and other kinases often phosphorylate the receptor at intracellular sites including intracellular loops, it is possible ß-arrestin2 is interacting with mFFA4 at these sites (Gurevich and Gurevich, 2019). Furthermore, it has been previously described that some receptors such as 5-HT2C, ß2AR and vasopressin V1 receptors, can interact with arrestins in a phosphorylation independent manner through interactions with intracellular loops as previously described in Chapter 1 part 1.5.3 (Gurevich and Gurevich, 2006; Marion *et al.*, 2006; Wu *et al.*, 2006). Additionally, some receptors retain interaction with arrestins following mutation of phosphorylation sites through negatively charged residues which mimic the properties of phosphate groups. One such example includes the D6 chemokine receptor which retains ability to bind to arrestin through acidic residues in its C-terminus. The presence of three negatively charged resides Glu341, Asp348, and Asp355 located in close proximity to phosphorylation clusters on the C-terminus of mFFA4 identify an alternative means of coupling (Butcher *et al.*, 2014). While a reduction in arrestin coupling was observed, ß-arrestin2 coupling may occur to some degree on account of the combination of interaction with ICLs and with negatively charged phospho-mimetics. In addition to highlighting other potential ß-arrestin2 coupling mechanisms which are independent from the phosphorylated C-terminus, this assay also indicated that structurally divergent agonists elicited different coupling effects. Mutation of C-terminal residues did not result in significantly reduced coupling to ß-arrestin2 following TUG-1197 and GSK137647A stimulation, with similar coupling observed to the WT-mFFA4 receptor. This reinforced that these compounds may not induce strong coupling to ß-arrestin2 through these C-terminal residues. Since both of these compounds are non-carboxylic compounds, it is interesting to consider that the lack of a carboxylic group may contribute to poor arrestin coupling through the C-terminal tail.

Changes in coupling patterns between WT-mFFA4 and PD-mFFA4 cells in G protein coupled signalling pathways were also investigated and interestingly, my

studies revealed that neither phosphorylation of ERK1/2 nor IP1 accumulation appeared to be phosphorylation dependent pathways as signalling still occurred following removal of C-terminal phosphorylation sites. In many GPCRs, β-arrestin signalling plays a role in phosphorylation of ERK1/2 and associated signalling (Luttrell *et al.*, 2001; Shenoy *et al.*, 2006), however, signalling is more complex in FFA4 where studies in phosphorylation deficient cell lines have shown robust pERK1/2 signalling. This suggested that β-arrestin signalling was not involved in pERK1/2 signalling in FFA4 and rather that it is G protein mediated (Alvarez-Curto *et al.*, 2016; Prihandoko *et al.*, 2016). Consistent with these studies, the phosphorylation of ERK1/2 was enhanced in PD-mFFA4 cells compared to WT-mFFA4 cells and similarly, IP1 assays in PD-mFFA4 cells showed significant increases in efficacy compared to WT-mFFA4 cells. These results are consistent with the idea that phosphorylation and recruitment of arrestins leads to receptor desensitisation and hence removal of phosphorylation sites results in greater signalling capacity because at any one time a greater number of active receptors can signal, since none are inactivated by arrestin-mediated desensitisation. Enhanced signalling capacity following loss of receptor desensitisation has been demonstrated previously in μ-opioid receptors, where an enhanced analgesic response was observed in β-arrestin2 KO mice (Raehal, Walker and Bohn, 2005; Thompson *et al.*, 2015; Bologna *et al.*, 2017). However, this effect was not observed in M1 muscarinic-PD model and so could vary between receptor (Scarpa *et al.*, 2021). However, since receptor expression in WT-mFFA4 and PD-mFFA4 was not measured quantitively and compared, it should also be considered that these effects could be due to increased receptor expression in PD-mFFA4 cells, although this would require to be quantitatively tested for example using qRT-PCR. In addition, it should be noted that experiments to compare WT and PD-mFFA4 were not carried out concurrently in these experiments, which may lead to inconsistencies in reproducibility. For example, experimental differences, such as differences in cell counting or cell viability and health as a result of experiments being performed on different days could lead to inconsistencies and thus should be considered when analysing these results.

Calculations of bias factors downstream of G protein:receptor coupling in IP1 and pERK1/2 pathways highlighted interesting differences in bias factors between WT-mFFA4 and PD-mFFA4 cells. Consistent with results in the WT-

mFFA4 receptor, Agonist 2 displayed bias towards IP1 accumulation in PD-mFFA4, however, Compound A additionally displayed signalling bias in PD-mFFA4 cells. Since Compound A was neutral in the WT-mFFA4 receptor, it was unexpected that this compound would display bias in the PD-mFFA4 receptor as both IP1 accumulation and phosphorylation of ERK1/2 are described to signal via the Gq coupled pathway and these pathways showed greater signalling capacity in the PD-mFFFA4 cell line. Therefore, it is interesting to consider why these ligands preferentially signal through IP1 pathways in the G protein biased form of the receptor. Ligand bias towards IP1 accumulation in PD-mFFA4 suggests that perhaps pERK1/2 signalling may have a phosphorylation dependent component which is absent in the PD-mFFA4 receptor. While pERK1/2 pathways have been shown to be largely Gq regulated, a study by Alvarez-Curto *et al.*, (2016) identified that Gαq/Gα11-null HEK293 expressing PD-mFFA4 elicited a pERK1/2 response which was not reduced upon treatment of Gi inhibitor pertussis toxin, this suggested a Gq/Gi/phosphorylation independent pERK1/2 signalling mechanism. The results presented in this chapter contradict this study by Alvarez-Curto *et al.*, (2016) by suggesting pERK1/2 signalling may have a phosphorylation dependent component which could potentially be masked by loss of receptor desensitisation which resulted in greater signalling capacity and/or the increased expression of PD-mFFA4 in these cell lines. However, it does agree that there is a complex relationship between receptor phosphorylation, ß-arrestin2 and G protein coupling in pERK1/2 pathways in FFA4 and that clearly, there are additional components to the pERK1/2 signalling pathway other than Gq coupled signalling which have yet to been defined.

In conclusion, while previous work in our lab has described that loss of phosphorylation via C-terminus mutation reduces coupling to ß-arrestin2 and subsequently reduces internalisation (Prihandoko *et al.*, 2016), here I have shown that upon stimulation of additional FFA4 agonists Compound A, GSK137647A, TUG-1197 and Agonist 2, similar loss of ß-arrestin2 and internalisation was observed in contrast to WT-mFFA4 receptors. Canonical G protein signalling was also investigated, where it was determined that both phosphorylation of ERK1/2 and IP1 signalling were enhanced upon loss of receptor C-terminus phosphorylation. Additionally, calculations of ligand bias indicated that while only Agonist 2 displayed ligand bias towards IP1 in WT-

mFFA4, Compound A additionally displayed bias in the PD-mFFA4 receptor for IP1 over pERK1/2 pathways. This could give an indication that pERK1/2 signalling is more complex than previously thought and may have a phosphorylation dependent component, despite previous reports suggesting that this is not the case.

Chapter 5   *Ex vivo* evaluation of FFA4 function in the mouse lung

5.1 Introduction

Initially, FFA4 based research was focused on the role of FFA4 within the gut and incretin secretion (described in Chapter 6), however, more recently FFA4 expression within the lung has been investigated, highlighting the possibility of FFA4 as a druggable target for respiratory diseases (Tanaka *et al.*, 2008; Miyauchi *et al.*, 2009; Mizuta *et al.*, 2015; Prihandoko *et al.*, 2020). FFA4 is present in lung resident macrophages which stimulate anti-inflammatory signalling pathways, where disruption of TAB1-TAK1 interactions results in inhibition of pro-inflammatory cytokine production (Oh *et al.*, 2010). Previously we studied FFA4 expression in the lung and we observed that the receptor is not only located in immune cells but is also expressed in lung epithelium and airway smooth muscle layers (Prihandoko *et al.*, 2020).

In our previous studies, FFA4 was shown to be functional within mouse and human airways, and when stimulated with FFA4 agonist, increases in intracellular calcium were detected (Prihandoko *et al.*, 2020). As other Gαq coupled receptors, such as the M3 muscarinic and tachykinin receptors, regulate airway smooth muscle (ASM) contraction following this increase in intracellular calcium (Fryer and Jacoby, 1998; Mizuta *et al.*, 2008; Bradley *et al.*, 2016), our initial hypothesis was that FFA4 may mediate ASM contraction. Changes in airway diameter were monitored in precision cut lung slice experiments following FFA4 agonist addition (Prihandoko *et al.*, 2020) and interestingly we discovered that FFA4 agonists do not mediate smooth muscle contraction but mediate ASM relaxation instead. It was suggested that agonist activated FFA4 might stimulate release of PGE2 which binds to the prostaglandin E2 receptor (EP2), leading to cAMP production, PKA activation and ASM relaxation through a Gαs coupled pathway (Morgan *et al.*, 2014). However, it could not be determined that PGE2 release was as a result of direct activation of FFA4 in ASM and not other lung resident mFFA4. Therefore, while PGE2 release might play a role in mFFA4 mediated ASM relaxation, mechanisms remain largely undefined. As FFA4 is primarily coupled to Gαq G proteins or ß-arrestin2, where Gαq coupled pathways lead to increases in intracellular calcium often associated

with ASM contraction, it was hypothesised that ASM relaxation could be regulated by either phosphorylation or β-arrestin dependent pathways.

Mouse models are a vital tool for studying physiological processes, therefore, to study ASM relaxation in this chapter, mouse models were utilised. A HA-tagged FFA4 C57BL/6 mouse was generated by Genoway by inserting a HA tag sequence upstream of the STOP codon, located in exon 3 of the FFA4 gene. However, this does not disrupt the function of the receptor as it is still expressed under the control of the endogenous FFA4 promoter. This has been validated in studies using cell lines expressing FFA4-HA (Hudson *et al.*, 2013; Prihandoko *et al.*, 2016). Similarly, a mouse line with a phosphorylation deficient mutant version of the FFA4 receptor was also generated by Genoway following phosphorylation studies by our group, described in detail in Chapter 4 (Butcher *et al.*, 2011; Prihandoko *et al.*, 2016). Here, six-point mutations in the C-terminal tail resulting in a phosphorylation deficient mutant (ADAA-AAA, mutations fully described in Chapter 4) and a HA tag were inserted upstream of the STOP codon, located in exon 3 of the FFA4. Lastly, an FFA4-KO mouse was generated by Invitrogen. Here, the gene which encodes for the FFA4 receptor was replaced with the gene coding for β-galactosidase enzyme resulting in a constitutive knock-out animal (Figure 5-1).
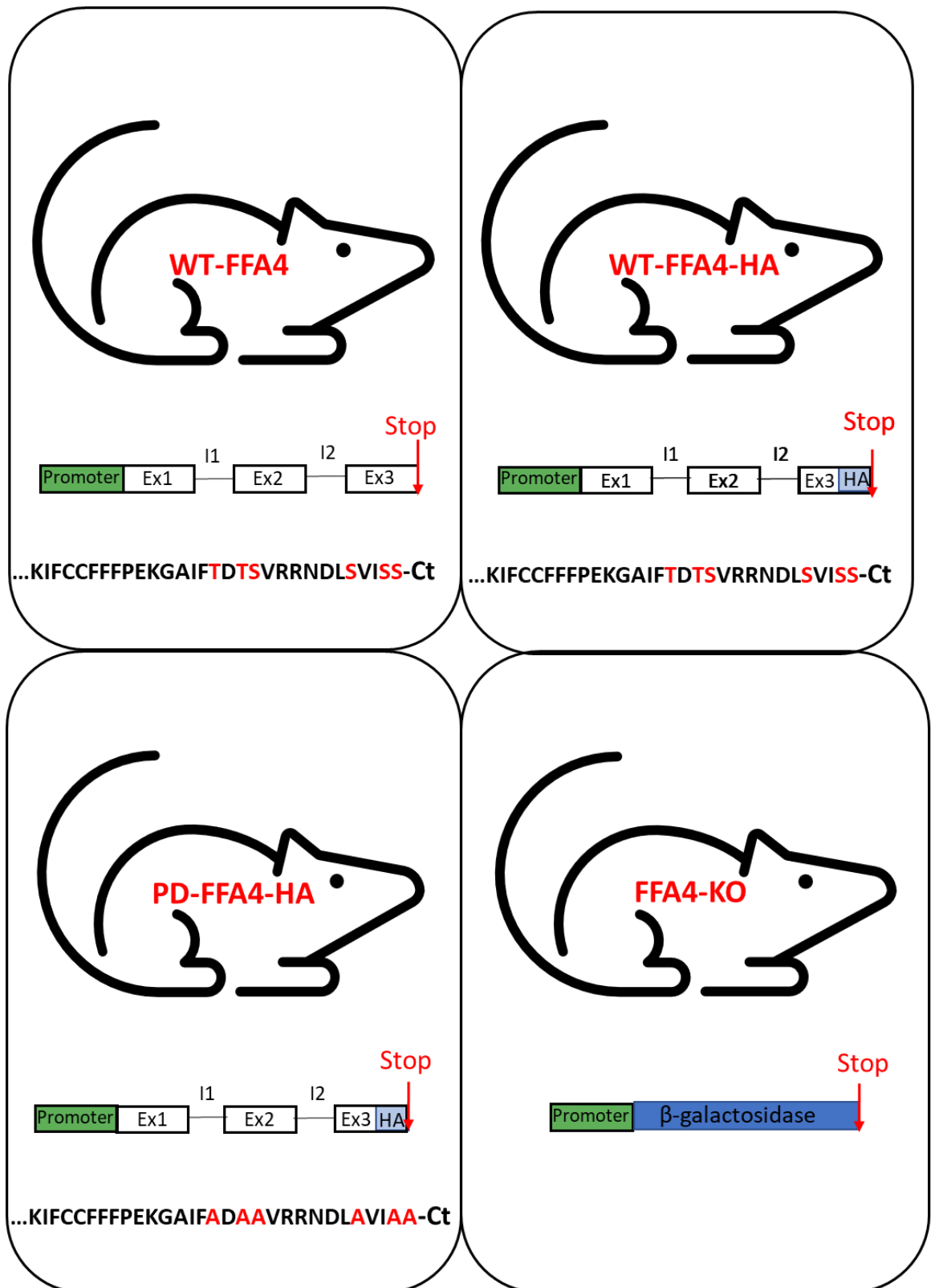
Figure 5-1: Genetically modified FFA4 mouse lines
Genetic modifications of FFA4 mouse lines are shown. The coding region of the WT mouse FFA4 consists of three exons that comprise of the coding regions. In WT-FFA4-HA and PD-FFA4-HA mice, a HA tag is inserted before the stop codon in exon 3. Additionally, PD-FFA4-HA mice have a series of mutations from Threonine/Serine to Alanine in the C-terminal tail, resulting in the inability for these sites to become phosphorylated. In FFA4-KO mice the gene coding for FFA4 is replaced with β-galactosidase enzyme. Ex= exon, I= non-coding intron regions.

This chapter aims to employ the use of genetically modified mice to investigate mFFA4 mediated ASM relaxation using a range of FFA4 agonists. Additionally, potential mechanisms for this ASM relaxation will be investigated, specifically, the potential role of phosphorylation of mFFA4 in ASM relaxation will be considered by use of PD-FFA4-HA animals. The combination of FFA4 presence within the lung and its ability to inhibit production of pro-inflammatory cytokines and promote ASM relaxation highlights FFA4 as a novel drug target for inflammatory respiratory diseases such as asthma and COPD.

5.2 Aims

The aims of this chapter were to:

- Confirm presence of mFFA4 within mouse lung tissues and compare to expression levels of PD-FFA4-HA lung tissues

- Investigate mFFA4 agonist induced ASM relaxation in PCLS

- Investigate whether phosphorylation of mFFA4 plays a role in FFA4 agonist induced ASM relaxation in PCLS experiments

5.3 Results

5.3.1 Expression of FFA4 within mouse lung tissue

mFFA4 expression has been reported within lung epithelium in previous studies within our lab (Prihandoko *et al.*, 2020) and this finding was first confirmed by performing q-PCR on cDNA samples prepared from mouse lung tissues. Studies were performed using HA-tagged animals as the HA tag is a particularly powerful tool in detecting the receptor in this context because the tag allows detection of proteins without the need for a protein specific antibody/serum and many commercially available anti-GPCR antisera, including for FFA4 have been poorly characterised. mFFA4-HA expression was confirmed in WT-FFA4-HA and PD-FFA4-HA mouse lung but not in WT-FFA4 C57BL/6 mice as expected (Figure 5-2A). Interestingly, PD-mFFA4-HA expression was significantly higher than that of WT-mFFA4-HA. However, PD-mFFA4 expression was not significantly increased from WT-mFFA4 levels when examining global mFFA4 expression (Figure 5-2B). Here,

mFFA4 was found to be expressed in the mouse lungs of WT-FFA4, WT-FFA4-HA and PD-FFA4-HA C57BL/6 mice but not present in FFA4-KO mice. Additionally, mFFA1 levels of transcript were analysed as there is a possibility that dual FFA4/FFA1 agonists could activate mFFA1, however, it is evident that mFFA1 is expressed at low levels within these mouse lines, with the exception of FFA4-KO animals (Figure 5-2C).
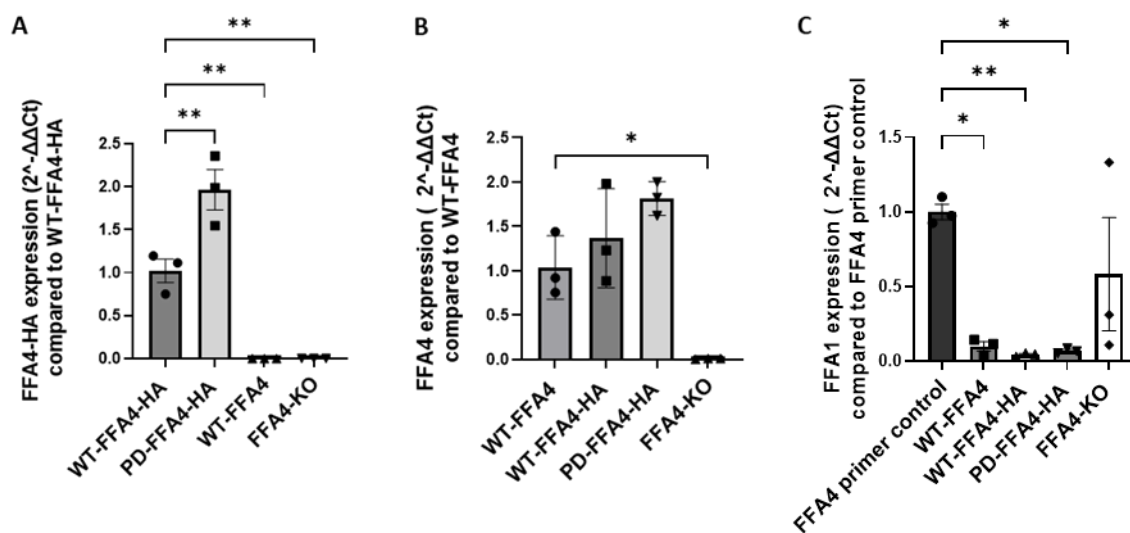
Figure 5-2: Expression of FFA4 and FFA1 in mouse lung
Lung tissue was isolated from WT-FFA4 C57BL/6 mice, WT-FFA4-HA C57BL/6 mice, FFA4-KO C57BL/6 mice and PD-FFA4-HA C57BL/6 mice, RNA isolated and cDNA prepared. q-PCR analysis on cDNA was performed using **(A)** FFA4-HA primers **(B)** FFA4 primers **(C)** FFA1 primers. Expression using FFA1 primer pairs are normalised to FFA4 expression using FFA4 primer pairs. Results are mean ± S.E.M of three independent experiments (n=3). Statistical analysis performed is ordinary one-way ANOVA (Dunnett's multiple comparisons), *=P<0.05, **=P<0.01.

mFFA4-HA expression was next examined using immunohistochemistry. Sections of mouse lung tissue were stained with an anti-HA rat antibody followed by Alexa-fluor 647 far red antibody to detect mFFA4-HA. Alexa-fluor 647 produces less overlap in emission spectrums when used in combination with other secondary antibodies and may reduce background staining. Therefore, this antibody was seen as an optimal choice for experiment. Expression of mFFA4-HA was confirmed in WT-FFA4-HA and not in FFA4-KO mouse tissues (Figure 5-3). Additionally in a novel finding, expression of HA was detected in PD-FFA4-HA mouse tissues, suggesting that the PD mutations of mFFA4 did not disrupt receptor expression. Furthermore, mFFA4 in these lung samples colocalised with epithelial clara cell marker CC10, suggesting mFFA4 presence in these cells, with

secondary controls displaying minimal background staining confirming these results.
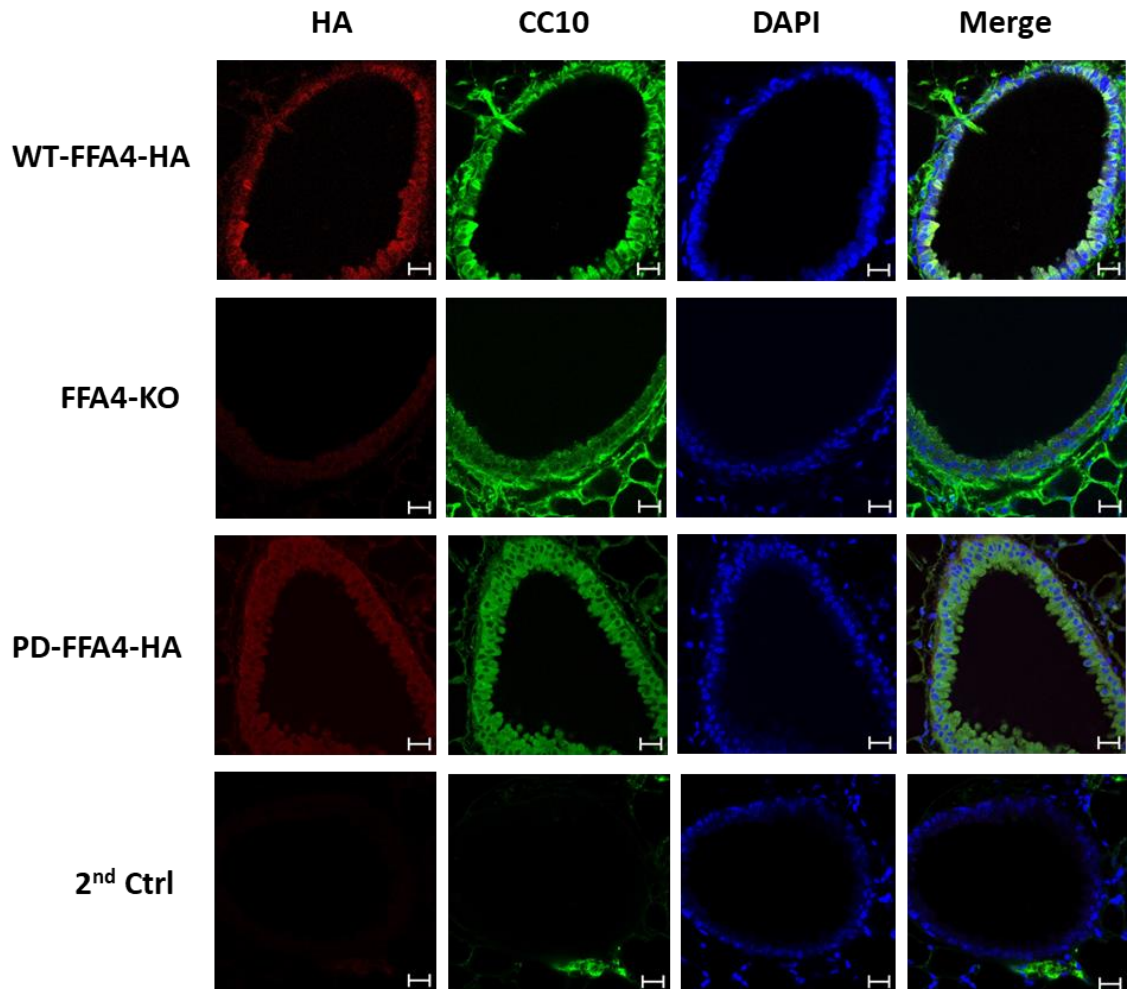
Figure 5-3: Co-localisation of mFFA4 with lung epithelium
Lung tissue sections from WT-FFA4-HA C57BL/6 mice, FFA4-KO C57BL/6 mice or PD-FFA4-HA C57BL/6 mice were processed for immunohistochemistry and stained using rat HA primary antibody and CC10 primary antibody, which is a marker for lung epithelium, before imaging on a confocal microscope at 40x objective. Images are representative of n=3, scale bar represents 20 μm.

In addition to mFFA4 presence in epithelial clara cells, co-localisation of mFFA4 with smooth muscle actin was also detected in WT-FFA4-HA lung sections, indicating that mFFA4 was also present within smooth muscle layers of the lung airways (Figure 5-4). Furthermore, this finding was replicated in PD-FFA4-HA lung samples, again suggesting that these PD mutations in the C-terminus did not affect receptor expression.
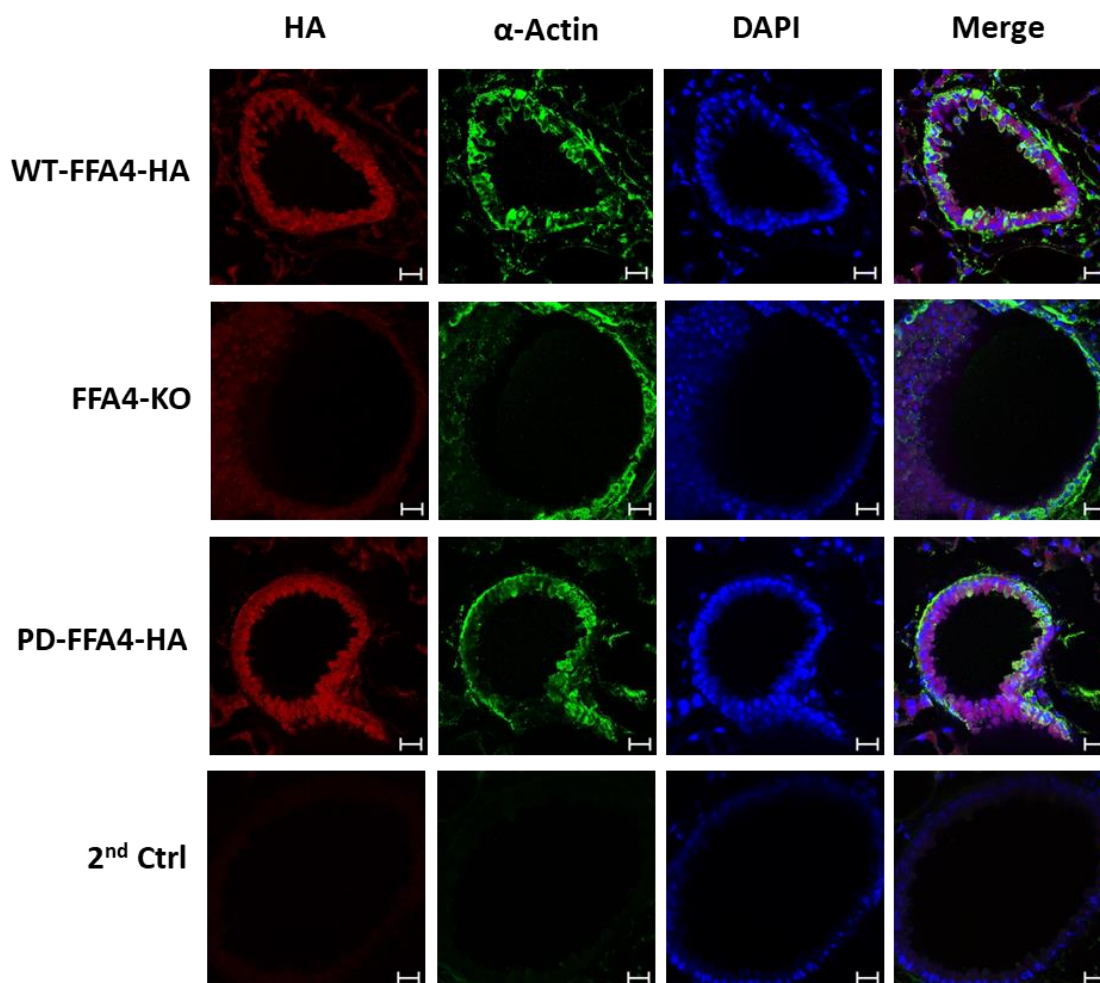
Figure 5-4: Co-localisation of FFA4 with lung airway smooth muscle
Lung tissue sections from WT-FFA4-HA C57BL/6 mice, FFA4-KO C57BL/6 or PD-FFA4-HA C57BL/6 mice were processed for immunohistochemistry and stained using rat HA primary antibody and α-Actin smooth muscle primary antibody which is a marker for airway smooth muscle before imaging on a confocal microscope at 40x objective. Images are representative of n=3, scale bar represents 20 µm.

With the finding that PD-mFFA4 was expressed in lung epithelium and airway smooth muscle, similarly to WT-mFFA4, PD-mFFA4 expression patterns were further investigated. To understand whether there was any differential mFFA4 expression pattern between WT-FFA4-HA and PD-FFA4-HA animals, images were taken at a higher magnification (63x objective) (Figure 5-5). However, from these images it did not appear that there were differences in distribution of mFFA4 inside each cell.
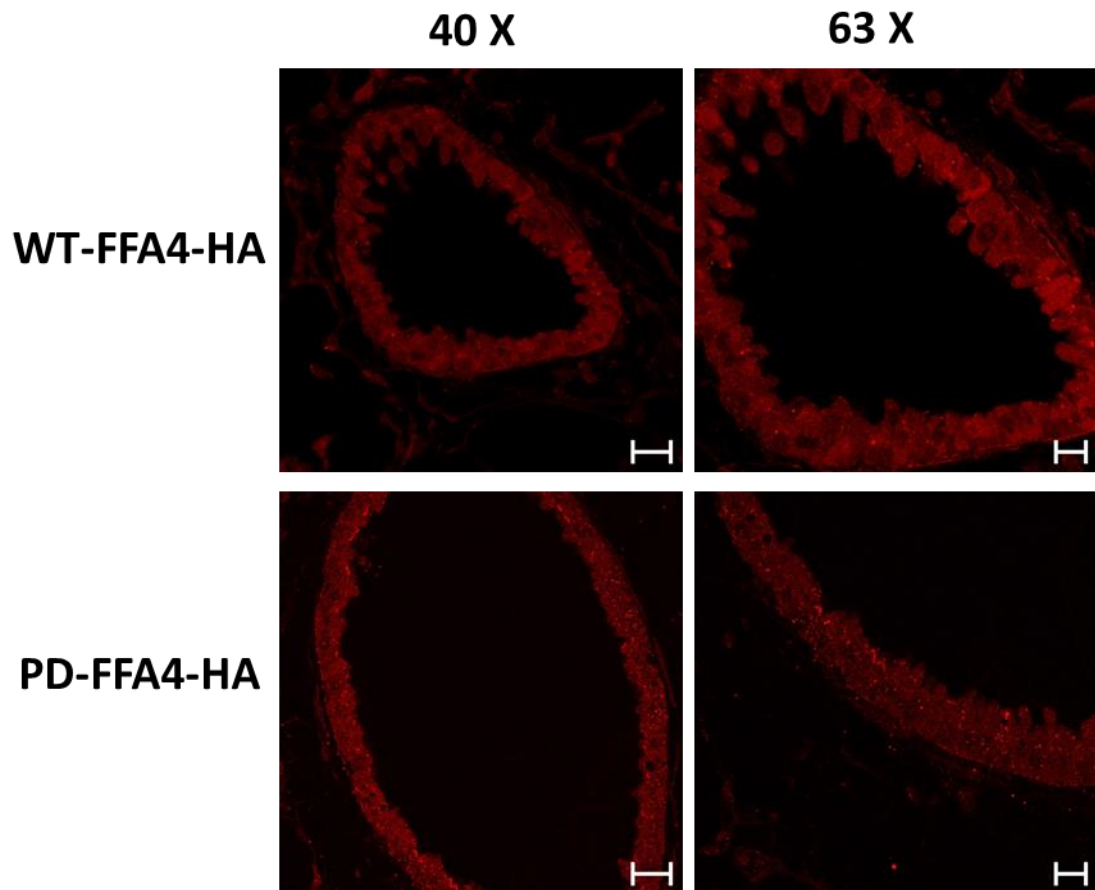
Figure 5-5: Distribution of mFFA4 within WT-FFA4-HA and PD-FFA4-HA airways
Lung tissue sections from WT-FFA4-HA C57BL/6 mice or PD-FFA4-HA C57BL/6 mice were
processed for immunohistochemistry and stained using rat HA primary antibody before imaging on
a confocal microscope at either 40x or 63x objective to assess distribution of mFFA4. Images are
representative of n=3. Scale bar represents 20 μm at 40x objective and 10 μm at 63x objective.

5.3.2 *Ex vivo* analysis of synthetic FFA4 agonist mediated airway smooth muscle relaxation

With the knowledge that WT-mFFA4 and PD-mFFA4 were present in mouse lung
epithelium and ASM layers, *ex vivo* experiments to determine whether FFA4
agonists stimulate bronchodilation were performed. *Ex vivo* PCLS experiments
were performed by monitoring the area of airway lumen over a time course
following FFA4 agonist addition. Carbachol was used as a pre-contraction agent
as carbachol is a muscarinic agonist, which induces Ca^{2+} dependent contraction
upon binding and activation of muscarinic receptors (Protas, Shen and Pappano,
1998; Bradley *et al.*, 2016). First, concentration response curves were performed
to determine appropriate concentrations of carbachol and FFA4 agonist for
experiment. Airways were maximally contracted at 100 μM carbachol (Figure
5-6A,B) and maximally relaxed at 50 μM TUG-891 (Figure 5-6C,D). Therefore,
these concentrations were used in subsequent *ex vivo* experiments. Additionally,

previous experiments within our group (Prihandoko *et al.*, 2020) found maximal airway contraction and relaxation at a 20 min incubation time point and so this time period was used in experimentation.
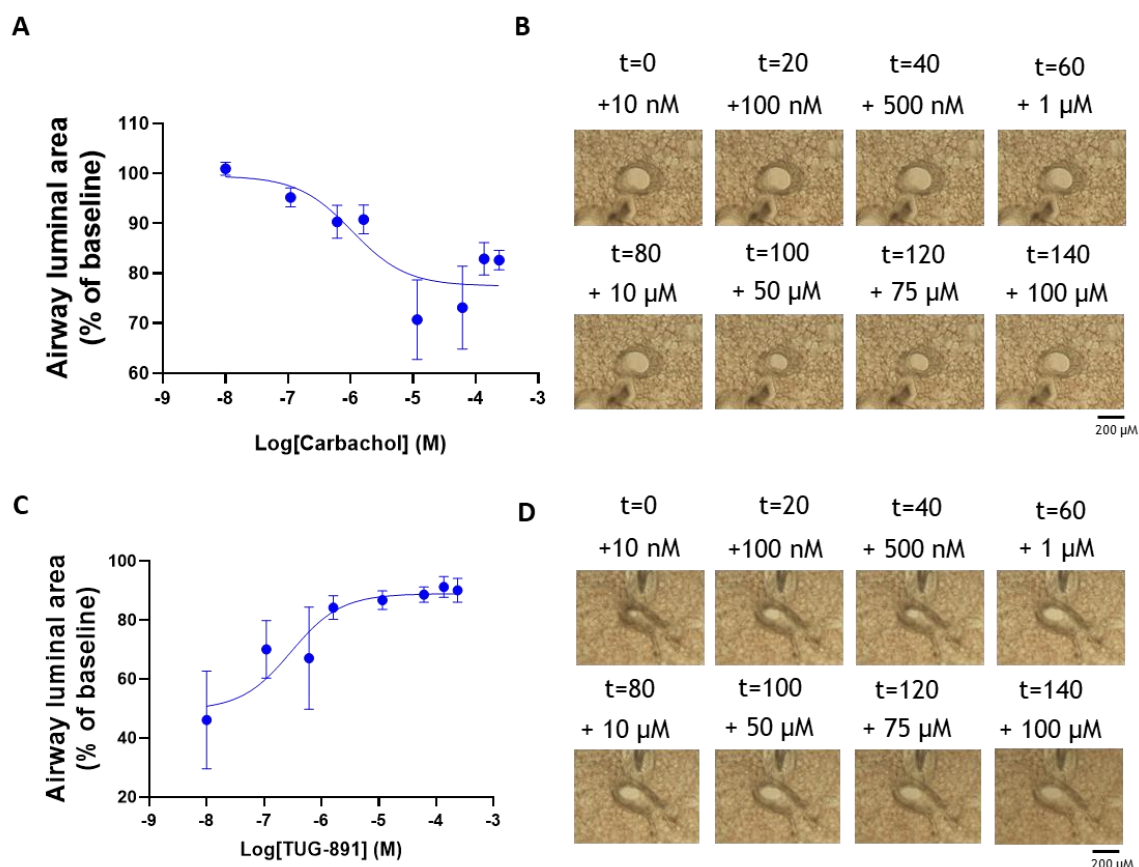
Figure 5-6: Precision cut lung slice concentration curves
Concentration response curves of **(A)** carbachol and **(C)** TUG-891 on precision cut lung slices from WT-FFA4-HA mouse lung. In a time-course experiment, increasing concentrations of compound were added every 20 min for 140 min and airway luminal area was quantified at each time point. Results are mean ± S.E.M of three independent experiments (n=3). Representative images of **(B)** carbachol and **(D)** TUG-891 are shown (n=3).

Precision-cut lung slice experiments were performed by addition of carbachol to fully pre-contract airways. Following full ASM contraction after 20 min, FFA4 agonist was added to the lung section to determine whether the FFA4 agonist would stimulate airway relaxation. Changes in airway luminal area were calculated to quantify contraction and relaxation. Upon agonist treatment following carbachol contraction, WT-FFA4-HA lung airways were significantly relaxed following treatment of TUG-891, Agonist 2 and Compound A. GSK137647A showed a trend of relaxation which may be significant upon repeat.

Conversely, TUG-1197 did not produce a significant relaxation (Figure 5-7, Table 5-1).

Conducting similar experiments in FFA4-KO PCLS revealed that Compound A still showed a significant relaxation response (P= 0.04) indicating that this agent has off-target activity. In addition, Agonist 2 showed a trend of relaxation. In contrast, the relaxation response to TUG-891 and trend of relaxation for GSK137647A was not evident in the FFA4-KO PCLS preparations indicating that it was likely these agents were acting through mFFA4, although repetition of this experiment would be further needed to define these preliminary results (Figure 5-8,Table 5-2).

A

B

Figure 5-7: WT-FFA4-HA *ex vivo* precision cut lung slice experiments
Lungs were dissected from WT-FFA4-HA C57BL/6 mice and sliced into 200 µm slices before culturing overnight. Slices were imaged on EVOS microscope in a 40 min time course. Lung slices were treated with 100 µM carbachol and after 20 min lung slices were treated with 50 µM compound or 0.1% DMSO. Experiments were terminated at 40 min. **(A)** Images shown represent an n=3. **(B)** Quantification of airway luminal area in images shown in A. Results are mean ± S.E.M of three independent experiments (n=3). Statistical analysis performed is paired t-test, *=P<0.05, **=P<0.01.

Ligand	% Baseline Luminal Area	% Airway Luminal Area After Cch Treatment	% Airway Luminal Area After Compound Treatment	% Difference	P Value
TUG-891	100	35.1 (±7.4)	74.8 (±8.9)	39.7 (± 13.2)	0.04 (*)
Agonist 2	100	32.3 (±18.0)	77.3 (±10.2)	45.0 (± 11.3)	0.02 (*)
TUG-1197	100	45.8 (±10.3)	50.1 (±12.5)	4.4 (± 6.4)	0.4 (ns)
Compound A	100	41.1 (±6.3)	90.4 (±2.8)	49.3 (± 3.7)	0.002 (**)
GSK137647A	100	31.8 (±14.2)	69.0 (±12.4)	37.2 (±26.2)	0.06 (ns)
DMSO	100	33.5 (±9.0)	41.8 (±15.2)	8.3 (± 6.5)	0.2 (ns)

Table 5-1: Airway relaxation following FFA4 agonist treatment on WT-FFA4-HA precision cut lung slices
Results are mean ± S.E.M of three independent experiments (n=3). Statistical analysis performed is paired t-test, ns= non-significant, *=$P<0.05$, **=$P<0.01$.

A

B
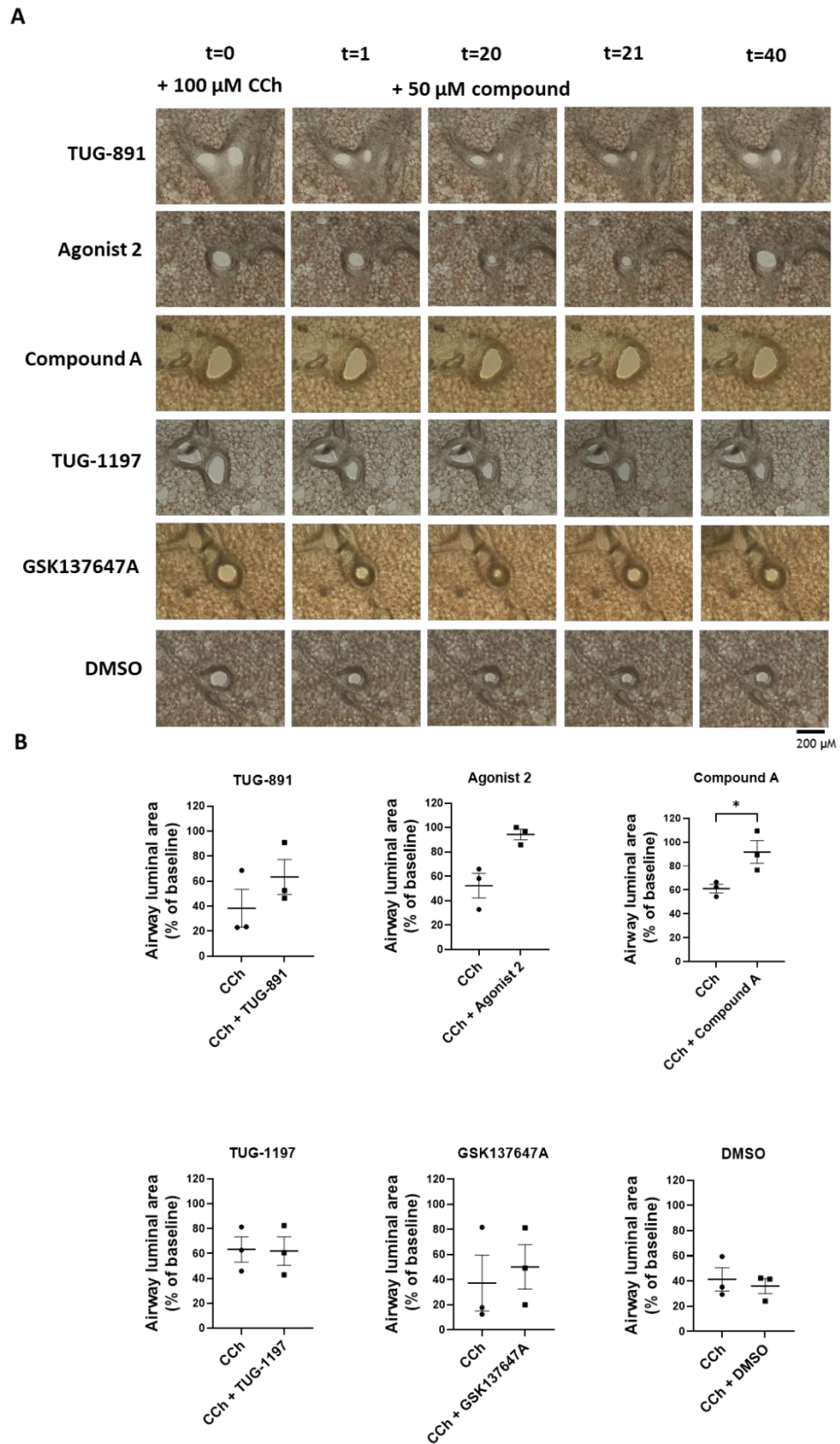
Figure 5-8: FFA4-KO *ex vivo* precision cut lung slice experiments
Lungs were dissected from FFA4-KO C57BL/6 mice and sliced into 200 µm slices before culturing overnight. Slices were imaged on EVOS microscope in a 40 min time course. Lung slices were treated with 100 µM carbachol at 1 min and at 20 min lung slices were treated with 50 µM compound or 0.1% DMSO. Experiments were terminated at 40 min. **(A)** Images shown represent an n=3. **(B)** Quantification of airway luminal area in images shown in A. Results are mean ± S.E.M of three independent experiments (n=3). Statistical analysis performed is paired t-test, *=P<0.05.

Ligand	% Baseline Luminal Area	% Airway Luminal Area After Cch Treatment	% Airway Luminal Area After Compound Treatment	% Difference	P Value
TUG-891	100	38.3 (± 26.1)	63.3 (± 24.1)	25.0 (± 3.5)	0.4 (ns)
Agonist 2	100	52.0 (± 18.8)	95.0 (± 8.4)	43.0 (± 24.6)	0.08 (ns)
Compound A	100	61.1 (± 6.2)	91.8 (± 16.5)	30.7 (± 10.8)	0.03 (*)
GSK137647A	100	37.3 (±38.6)	50.2 (±30.8)	12.9 (±20.7)	0.4 (ns)
TUG-1197	100	63.4 (± 25.0)	62.7 (± 27.8)	-1.0 (± 2.9)	0.4 (ns)
DMSO	100	41.4 (± 15.9)	36.0 (± 10.3)	-5.3 (± 11.6)	0.5 (ns)

Table 5-2: Airway relaxation following FFA4 agonist treatment on FFA4-KO precision cut lung slices
Results are mean ± S.E.M of three independent experiments (n=3). Statistical analysis performed is paired t-test, ns=non-significant, *=$P<0.05$.

Experiments were also performed on PCLS from PD-FFA4-HA mice to determine if phosphorylation of mFFA4 may play a role in ASM relaxation. While TUG-891 previously stimulated a significant increase in airway relaxation, in PD-FFA4-HA PCLS this compound no longer promoted a significant relaxation, indicating that this agonist was driving relaxation in an mFFA4 phosphorylation dependent manner (Figure 5-9,Table 5-3). These results not only confirmed PD-mFFA4 to be functional in an *ex vivo* mouse model in agreement with data from pharmacological assays in cell lines in Chapter 4, but indicated phosphorylation of FFA4 also had a physiological function.

Interestingly, Agonist 2 and Compound A, that potentially act via mechanisms independent of FFA4, mediated relaxation in PCLS prepared from PD-FFA4-HA mice as well as WT-FFA4-HA and FFA4-KO mice. These findings reiterated the suggestion that these compounds elicited off-target effects.
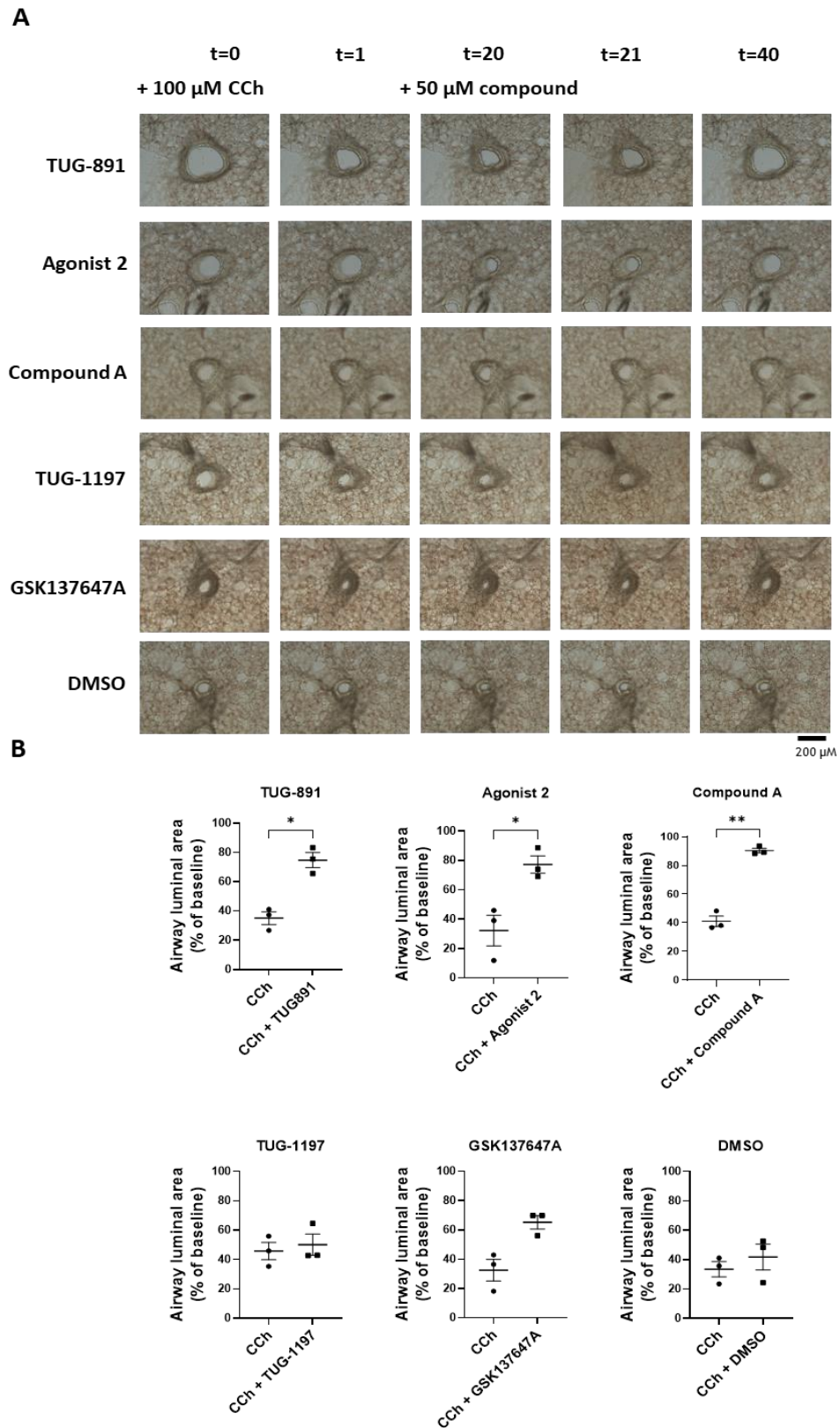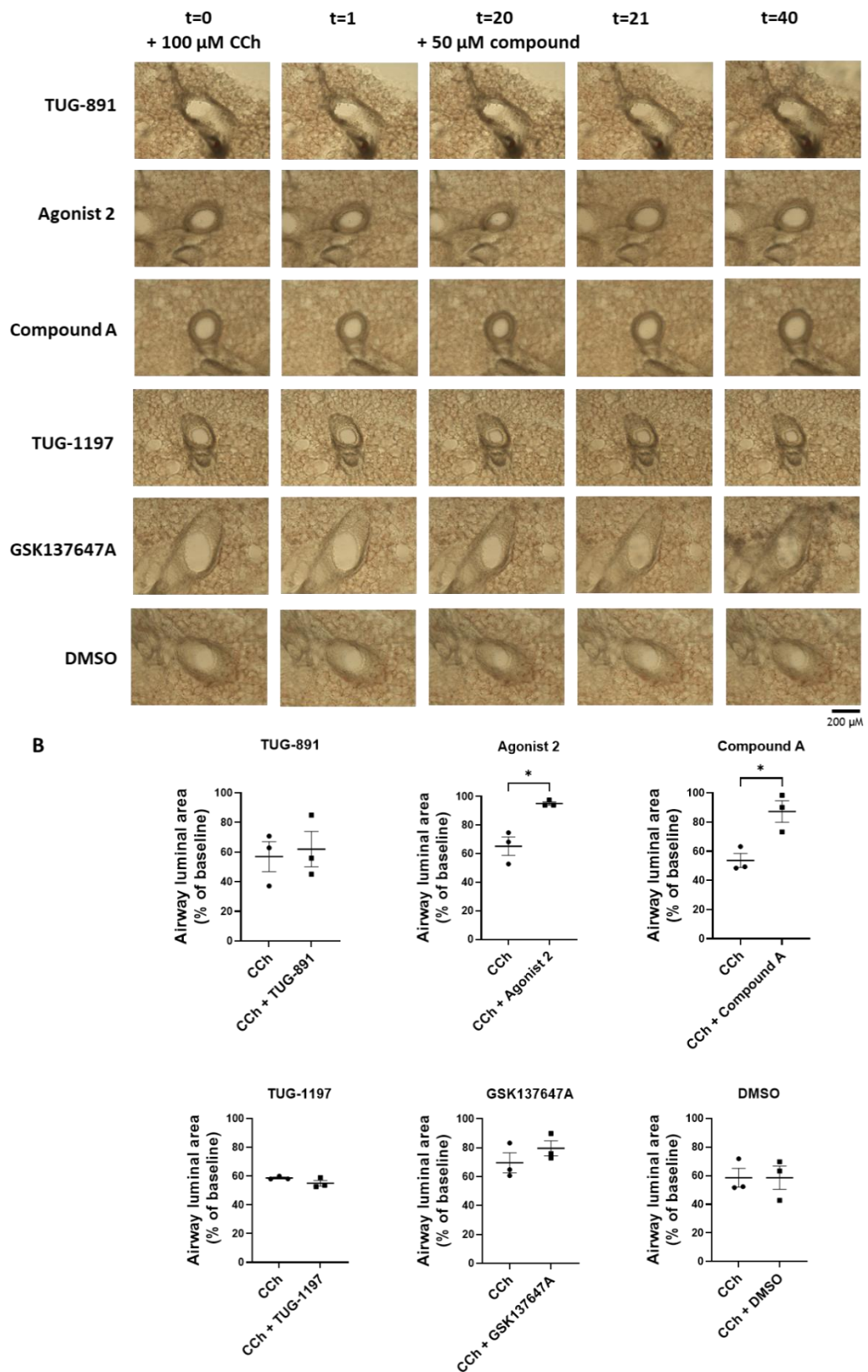
Figure 5-9: PD-FFA4-HA *ex vivo* precision cut lung slice experiments
Lungs were dissected from PD-FFA4-HA C57BL/6 mice and sliced into 200 µm slices before culturing overnight. Slices were imaged on EVOS microscope in a 40 min time course. Lung slices were treated with 100 µM carbachol after 20 min lung slices were treated with 50 µM compound or 0.1% DMSO. Experiments were terminated at 40 min. **(A)** Images shown represent an n=3. **(B)** Quantification of airway luminal area in images shown in A. Results are mean ± S.E.M of three independent experiments (n=3). Statistical analysis performed is paired t-test, *=P<0.05.

Ligand	% Baseline Luminal Area	% Airway Luminal Area After Cch Treatment	% Airway Luminal Area After Compound Treatment	% Difference	P Value
TUG-891	100	55.2 (±33.1)	71.9 (±29.5)	16.6 (±4.7)	0.5 (ns)
Agonist 2	100	65.2 (±11.2)	95.2 (±2.1)	29.9 (±6.2)	0.03 (*)
Compound A	100	53.7 (±8.3)	87.3 (±10.3)	30.4 (±17.9)	0.05 (*)
TUG-1197	100	58.7 (±1.1)	55.1 (±3.4)	3.6 (±3.9)	0.2 (ns)
GSK137647A	100	69.6 (±12.0)	79.6 (±9.0)	10.0 (±3.0)	0.06 (ns)
DMSO	100	58.6 (±11.4)	58.6 (±14.1)	0.02 (±10.1)	1.0 (ns)

Table 5-3: Airway relaxation following FFA4 agonist treatment on PD-FFA4-HA precision cut lung slices
Results are mean ± S.E.M of three independent experiments (n=3). Statistical analysis performed is paired t-test, ns=non-significant, *=P<0.05.

5.4 Discussion

While the role of FFA4 in tissues such as the colon, associated with metabolic diseases including diabetes have gathered interest since Hirasawa *et al.*, published their initial paper in 2005, the expression of FFA4 in other tissues has led to the hypotheses that FFA4 may be a broader therapeutic target. Consistent with reports that FFA4 is expressed in the lung, expression of mFFA4 in the lung was detected in this chapter at both RNA transcript level and at the protein level (Tanaka *et al.*, 2008; Miyauchi *et al.*, 2009; Prihandoko *et al.*, 2020). Low levels of mFFA1 expression in comparison to mFFA4 may indicate that there is a high probability that dual FFA4/FFA1 agonists such as TUG-891 activate mFFA4 as opposed to mFFA1, however as this experiment measured relative expression levels between mFFA1 and mFFA4, we cannot conclude that there is no expression. Additionally, it was interesting to note that mFFA1 mRNA expression showed an indication of increased expression in FFA4-KO lung tissue in comparison to WT-FFA4 lung. While it is possible that mFFA1 may provide a compensatory mechanism in the absence of mFFA4, there is no literature

evidence for this and since data was spread and did not show significance, more experiments are required to be performed before confirmation of this observation. It should however be noted that these experiments are reliant on specificity of primers and while melt curves were performed to test specificity, it is possible that primers may have had some specificity for one another, which could be determined by performing standard curves. Amplification of different amounts of DNA to create a standard curve can test primer efficiency which is assumed to be comparable between genes in the ΔΔCt method to measure gene expression (Ma, Bell and Loker, 2021).

At the protein level, mFFA4 was observed within lung epithelium and α-actin smooth muscle in agreement with previous work carried out by our lab (Prihandoko *et al.*, 2020). Furthermore, PD-mFFA4 receptor expression was also detected in lung epithelium and α-actin smooth muscle, suggesting that the PD mutation does not affect receptor localisation. This is consistent with results in Chapter 4, where PD-mFFA4 was able to retain pERK1/2 and IP1 signalling in stably transfected cell lines, despite the loss of phosphorylation, ß-arrestin2 coupling and receptor internalisation. However, images magnified at a 63x objective could not determine whether receptor distribution was different between the WT-mFFA4 and PD-mFFA4 receptors, which might be expected following the loss of receptor internalisation. While the limit of magnification of the confocal microscope was reached, potentially the distribution of the receptors may be better observed by more sensitive techniques such as super-resolution microscopy. Additionally, quantification of images by using software such as ImageJ to identify intensity values at potential sites of accumulation in images taken from WT-mFFA4 mouse lung sections compared to PD-mFFA4 mouse lung sections may be able to deduce differences in protein localisation in future studies.

With the knowledge that WT-mFFA4 and PD-mFFA4 were present within lung epithelium and ASM layers, *ex vivo* experiments were performed to determine contributions of FFA4 agonists on ASM relaxation. In *ex vivo* PCLS experiments in WT-FFA4-HA lung slices, TUG-1197 did not show a significant relaxation, although previous work from our lab show that while TUG-891 promotes optimal airway relaxation at 50 µM, effects with TUG-1197 on airway relaxation are

minimal at 61.11 µM and they are not completely evident until 161.11 µM (Prihandoko *et al.*, 2020). Therefore, 50 µM of TUG-1197 may not be an optimal concentration in the promotion of airway relaxation. Furthermore, while TUG-1197 showed responses in pharmacological assays in Chapter 3 and Chapter 4, the potencies and/or efficacies of TUG-1197 were low and in some assays did not reach a maximum response. Therefore, results may be difficult to reproduce, and given the inherent variability associated with PCLS experiments it was difficult to confirm the activity of TUG-1197. However, in contrast to TUG-1197, TUG-891, Agonist 2 and Compound A promoted ASM relaxation in WT-FFA4-HA PCLS. GSK137647A showed a trend of relaxation but due to data spread, this result was not significant. Analysis in FFA4-KO lung slices determined that TUG-891 was shown to mediate its relaxation effects selectively through mFFA4. Additionally, GSK137647A showed no indication of relaxation, in contrast to WT-FFA4-HA mice. However, Compound A still showed a significant response suggesting that this elicited off-target effects and may broadly activate other receptors involved in smooth muscle relaxation. Additionally, Agonist 2 showed a trend of relaxation which brings forth the question of whether this agonists also elicits off-target effects. PCLS experiments are inherently variable for a number of reasons, mainly differences in airway area between mice and differences in the extent of contraction between airways which can lead to spread in collected data. Power calculation analysis revealed that to achieve the desired power value in PCLS assays, 4 experimental animals would be necessary and therefore, this preliminary data requires to be repeated an additional time to confirm the significance of these results.

A previous publication by Mizuta *et al.*, (2015) suggested that FFA1 is involved in the regulation of ASM contraction, but did not see a purpose for FFA4 in ASM contraction. The data presented in this chapter is consistent with this observation suggesting that mFFA4 mediates ASM relaxation and not contraction. However, previous data in our lab conflicts the data presented by Mizuta *et al.*, (2015) suggesting that dual FFA4/FFA1 agonists potentiate ASM relaxation significantly more in human tissues than FFA4 selective agonists, indicating that FFA1 may play a role in ASM relaxation and not contraction (Prihandoko *et al.*, 2020). Since in our previous study the effects of TUG-891 were compared to TUG-1197 which had a lower potency, additional testing of this wider range of

FFA4 agonists in human tissues may clarify these effects further. Additionally, the use of FFA1 specific antagonist GW1100 may be able to refine a role of FFA1 in airway smooth muscle relaxation.

Receptors involved in smooth muscle relaxation elicit effects in a variety of ways, including through a PGE2 mediated pathway in receptors such as protease-activated receptor-2 (PAR-2) and EP2 receptors, or cAMP increases in Gαs coupled pathways in GPCRs including β2AR (Johnson, 1998; Fortner, Breyer and Paul, 2001; Chambers *et al.*, 2003; Tanaka, Horinouchi and Koike, 2005). While PGE2 release might contribute to an FFA4 mediated relaxation effect, as previously described in Part 5.1, the full mechanisms still are not defined (Prihandoko *et al.*, 2020). Additionally, FFA4 has not demonstrated Gαs coupling abilities, therefore, it is unlikely that FFA4 would promote relaxation in the same manner as the β2AR. As phosphorylation of GPCRs has previously been implicated in ASM control where Bradley *et al.*, (2016) demonstrated that phosphorylation of the muscarinic M3 receptor regulates ASM contraction, it was hypothesised that phosphorylation of mFFA4 and/or β-arrestin coupling could play a role in ASM relaxation. Data showed promising results in PCLS experiments for PD-FFA4-HA animals and interestingly, results for PD-FFA4-HA PCLS were similar to FFA4-KO data. The reduction in airway smooth muscle relaxation following TUG-891 treatment demonstrated a novel finding that while this compound mediates smooth muscle relaxation in WT-FFA4-HA mice, ASM relaxation may also be also phosphorylation dependent. However, it should be considered that while experiments on WT-FFA4-HA and FFA4-KO mouse *ex vivo* tissue were performed in parallel, PD-FFA4-HA experiments preceded these which may lead to some experimental inconsistencies which should be considered in future experiments.

In conclusion, FFA4 agonist TUG-891 promoted an mFFA4 mediated relaxation of airway smooth muscle, indicating potential benefits in the treatment of respiratory diseases such as asthma and COPD. Furthermore, analysis of PCLS from PD-FFA4-HA animals indicated a novel finding that phosphorylation of FFA4 could be involved in FFA4 mediated ASM relaxation demonstrating that receptor phosphorylation or arrestin signalling might be a mechanism by which FFA4 mediates ASM relaxation. However, repeated experiments are required to

confirm this preliminary data. Following confirmation by repetition, validation *in vivo* may be performed by measuring lung resistance as a measure of lung function in healthy mice and diseased mice, for example those which have been subject to ozone exposure such as experiments performed by Prihandoko *et al.*, (2020). While these previous experiments in our lab proved that TUG-891 was able to selectively mediate a reduction of airway resistance, further characterising this in PD-mFFA4 mice may define a role for phosphorylation *in vivo*. Additionally, as described in Chapter 4, while receptor phosphorylation and ß-arrestin signalling are often linked, there is evidence of distinct signalling from both pathways (Alvarez-Curto *et al.*, 2016). Therefore, it is not possible to tell if ASM relaxation is dependent on phosphorylation or rather ß-arrestin pathways, but this would be possible to examine with the use of ß-arrestin-KO mice in the absence and presence of phosphorylation. Furthermore, as the PD-mFFA4 receptor is G protein biased (Butcher *et al.*, 2014), perhaps an arrestin biased agonist may be beneficial in the treatment of respiratory diseases. However, no agonists tested showed arrestin signalling bias (Chapter 3), and therefore, the development of novel arrestin biased ligands may provide respiratory relief through airway relaxation.

Chapter 6 Evaluation of FFA4 activation in primary colonic crypts

6.1 Introduction

In 2005, Hirasawa *et al*., indicated that FFA4 was expressed within the intestinal secretin tumour cell line (STC-1) in addition to human and mouse colon tissues. Epithelial layers are present in mucosal layers of the colon and within these epithelial layers are invaginations called colonic crypts (Fre, 2015). Colonic crypts are made up of a variety of different cell types including stem cells, enterocytes, goblet cells, enteroendocrine cells and transit amplifying or progenitor cells (Figure 6-1) (Humphries and Wright, 2008; Fre, 2015; Meneses *et al*., 2016). It is the enteroendocrine cells, which include L cells, within the colonic crypt structure that secrete peptide hormones such as GLP-1 and PYY (Spreckley and Murphy, 2015).
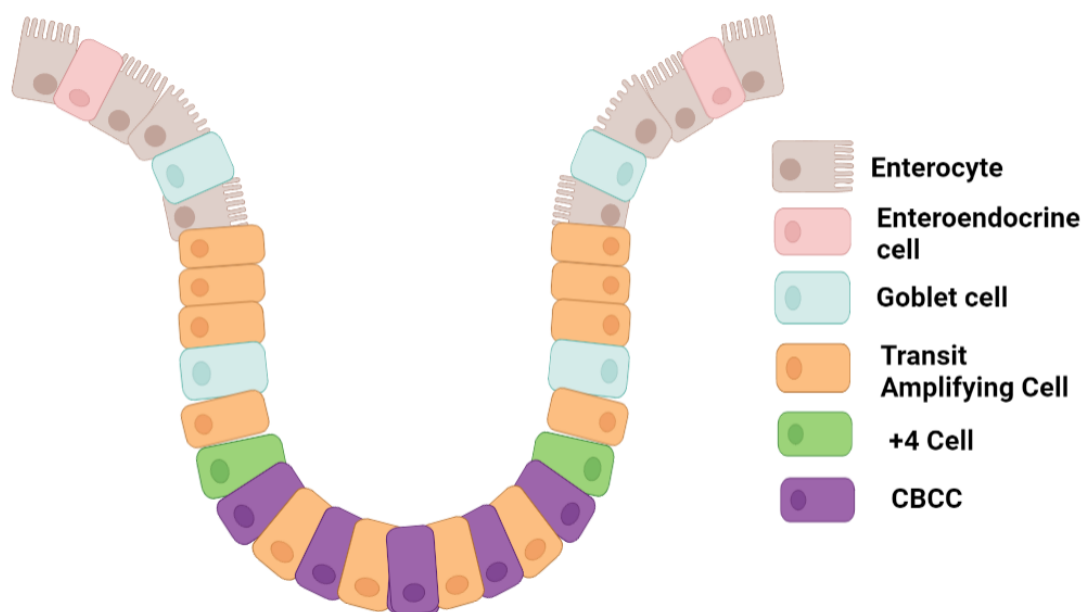
Figure 6-1: Cell types within colonic crypts
Colonic crypts are made up of a variety of cell types. The role of the colonic crypt is to renew the intestinal lining and so crypt-based columnar cells (CBCC) and +4 stem cells are present. These stem cells give rise to undifferentiated transit amplifying cells which proliferate and form other cell types. These cell types include enterocytes which are the absorptive cells, enteroendocrine cells which secrete hormones and goblet cells which secrete mucus (Meneses *et al.,* 2016). Image created using Biorender.

Later, the specific cell populations within the intestines that contain FFA4 were characterised. Expression of FFA4 has been found in various locations within the intestines including the K cells of the small intestines that contain gastric inhibitory peptide (GIP) and the D and A cells in the stomach containing somatostatin and ghrelin respectively (Parker *et al.*, 2009; Lu *et al.*, 2012; Engelstoft *et al.*, 2013; Egerod *et al.*, 2015). Additionally, FFA4 is expressed in intestinal I cells containing CCK, however, within the colon the highest level of expression is seen within L cells of the descending colon from which PYY and GLP-1 are released (Reimann *et al.*, 2008).

GLP-1 is an incretin hormone released in response to food intake (Mojsov *et al.*, 1986; Reimann *et al.*, 2008). Upon an increase in glucose concentration, glucose is converted into ATP through cellular respiration. ATP is a substrate for adenylyl cyclase production of cAMP and increase in cAMP levels results in inhibition of K_{ATP} channels, membrane depolarisation and opening of voltage-dependent calcium channels (VDCC's), leading to an increase in Ca^{2+} concentration (Ashcroft and Rorsman, 1989; MacDonald *et al.*, 2002; Seino, Fukushima and Yabe, 2010). GLP-1 enhances these effects by binding to GLP-1 receptors and activating Gαs coupled G protein pathways, resulting in adenylyl cyclase activation, cAMP production and activating protein kinase A (PKA)-dependent signalling and exchange protein directly activated by cAMP (EPAC) (Drucker *et al.*, 1987; Seino, Fukushima and Yabe, 2010; Islam, 2015). GLP-1 stimulated activation of PKA and EPAC potentiates glucose-stimulated insulin secretion by various mechanisms including preventing repolarisation of cells by inhibition of both the K^{+}_{ATP} and the K_{v} channels and release of intracellular calcium (Britsch *et al.*, 1995; Light *et al.*, 2002; Kang *et al.*, 2005; Seino, Fukushima and Yabe, 2010). The resulting calcium influx triggers insulin release from the β cells of the pancreatic islets (Figure 6-2).
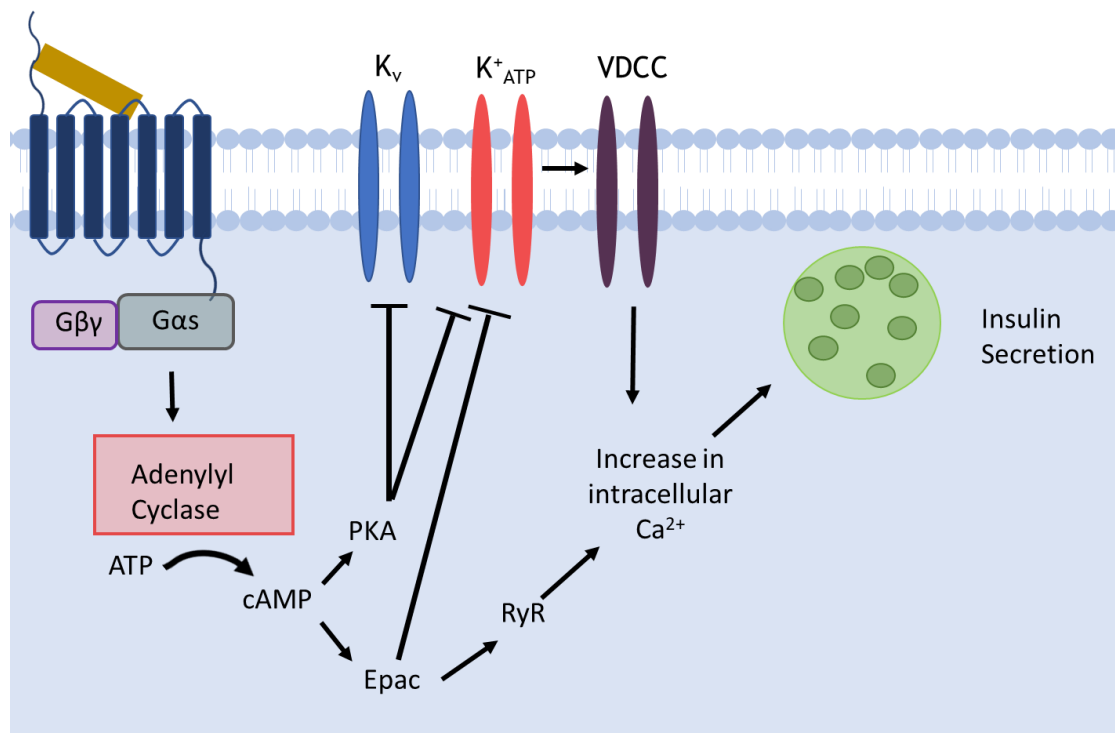
Figure 6-2: GLP-1 mediated insulin secretion
Following binding of GLP-1 (yellow) to GLP-1R (dark blue), adenylyl cyclase is activated by Gαs G proteins. Adenylyl cyclase stimulates the production of cAMP from ATP, which activates protein kinase A (PKA) and exchange protein directly activated by cAMP (EPAC) pathways. Both PKA and EPAC sensitise K_{ATP} channels resulting in channel closure and cell depolarisation. Cell depolarisation opens voltage-dependent calcium channels (VDCCs) and results in increase of intracellular calcium. PKA also prevents repolarisation of cells by inhibition of K_v channels. Additionally, EPAC stimulates opening of ryanodine receptors (RyR) leading to increase of intracellular calcium. Increase of intracellular calcium stimulates insulin release.

There are varying reports on the roles of FFA4 in the release of GLP-1 from enteroendocrine cells within the colon. Initial papers by Hirasawa *et al.*, (2005) noted that the endogenous ligand α-linolenic acid promoted the release of GLP-1 *in vitro* from the STC-1 mouse intestinal enteroendocrine cell line and also *in vivo* by measuring levels of GLP-1 in mouse blood plasma following oral administration of α-linolenic acid. While these studies were performed using endogenous ligand α-linolenic acid which is non-specific and can activate FFA1, studies have also been performed using FFA4 specific agonists. Sundstrom *et al.*, (2017) reported the release of GLP-1 in STC-1 cell lines and measured elevated levels in blood plasma following oral administration of the FFA4 specific agonists Metabolex-36 and AZ13581837. However in experiments performed by other groups, this finding was not replicated. Xiong *et al.*, (2013) failed to find a role of FFA4 in GLP-1 secretion when examining blood plasma from WT and FFA4-KO mice following oral-gavage administration of corn oil. Oh *et al.*, (2014) also observed that the synthetic FFA4 selective agonist Compound A did not result in

an increase in the levels of GLP-1 in blood plasma during oral glucose challenge. Similarly, Paulsen *et al.,* (2014) performed a study in rats where α-linolenic acid and octanoic acid were administered orally and GLP-1 levels in blood plasma measured. This study also could not confirm a role for FFA4 in GLP-1 secretion.

Enteroendocrine cells are also known to secrete PYY. There are two isoforms of PYY, PYY1-36 and PYY3-36, the most common of which is PYY3-36 (Grandt *et al.,* 1994; Karra, Chandarana and Batterham, 2009). PYY is most well known for its role as a satiety hormone, with the lowest levels of PYY observed in a fasting state, and subsequently elevating after a meal (Adrian *et al.,* 1985; Small *et al.,* 2002). Furthermore, PYY3-36 has demonstrated an ability to reduce feeding in both obese rodents and humans (Batterham *et al.,* 2003). PYY acts by slowing gastric emptying and intestinal transit time, mediating ileal and colon brakes (Savage *et al.,* 1987; Lin *et al.,* 1996; Chelikani, Haver and Reidelberger, 2004; Persaud and Bewick, 2014) and is released following glucose ingestion, exerting its effects by binding to the Y type receptor. In both human and mouse distal colon, PYY effects are facilitated by the Y1 receptor type of six Y receptor subtypes (Tough *et al.,* 2011). With FFA4 also being present in L cells of the distal colon, it is highly possible that FFA4 could regulate these effects. One study by Moodaley *et al.,* (2017) demonstrated that incubation of FFA4 agonist Metbolex-36 in *ex vivo* isolated mouse colon slowed gastric transit and similarly, the same agonist also slowed colonic transit *in vivo* following oral gavage through PYY mediated effects.

Both GLP-1 and PYY have been highlighted as potential therapies for metabolic diseases. There are many approved GLP-1 receptor agonists currently available: xenatide, liraglutide, albiglutide, dulaglutide, lixisenatid and semaglutidein are available as injectable short acting drugs in Europe and the US, and more recently semaglutide has also been approved for oral ingestion as a long acting drug (Prasad-Reddy and Isaacs, 2015; Nauck *et al.,* 2021). These agonists act to mimic previously outlined effects of GLP-1. PYY has also shown promise in therapies for obesity. Studies performed by Batterham *et al.,* (2003) demonstrated that upon administration of PYY to both mice and humans, food intake was decreased. However, there is a lack of FFA4 agonists which have progressed to clinical trials in these areas to date. Therefore, through

investigation of FFA4 mediated GLP-1 and PYY secretion within the colon, we may validate FFA4 agonists with appropriate drug-like characteristics as viable therapies for metabolic diseases such as diabetes and obesity.

Because of varying results around the role of FFA4 in GLP-1 release in the colon, this chapter aims to re-investigate potential effects and roles further using different experimental methods. Agonists TUG-891 and GSK137647A, previously characterised in Chapters 3 and 4, were investigated and while TUG-891 has been previously used to investigate GLP-1 secretion (Hudson *et al.*, 2013), GSK137647A an FFA4 selective agonist has not been previously characterised in this context. Additionally, the effects of FFA4 agonists on PYY, also present within colonic L cells, will be investigated. In this chapter, isolated primary colonic crypts were utilised as previous studies on FFA1 (Hauge *et al.*, 2015) and FFA2 (Psichas *et al.*, 2015; Bolognini *et al.*, 2019) receptors indicated GLP-1 release following agonist stimulation.

6.2 Aims

The aims of this chapter were to:

- Confirm presence of mFFA4 within mouse colon tissue

- Investigate the functionality of the mFFA4 receptor within colonic crypts

- Investigate GLP-1 release from primary colonic crypts following stimulation of FFA4 synthetic agonists

- Investigate PYY release from primary colonic crypts following synthetic FFA4 agonist stimulation

6.3 Results

6.3.1 Expression of mFFA4 in mouse colon tissue

FFA4 is reportedly expressed within the distal colon, largely within enteroendocrine L cells which are known to regulate the release of many hormones involved in metabolism. Confirmation of mFFA4 in mouse colon tissue was needed as a pre-requisite for further study, therefore, knock-in transgenic mice containing HA-tagged mFFA4 (WT-FFA4-HA) on a C57BL/6 background and FFA4-KO mice previously described in Chapter 5, were examined in experiments.

Firstly, mFFA4 expression was detected as mRNA using qRT-PCR (Figure 6-3). In experiments performed using mFFA4-HA primers, mFFA4-HA was detected in WT-FFA4-HA tagged mice but not in WT-FFA4 or FFA4-KO mice (Figure 6-3A). When evaluating expression of mFFA4 globally and not targeting a HA tag, mFFA4 was detected in WT-FFA4 and WT-FFA4-HA mice, confirming expression in these animals, but was not detected in FFA4-KO animals (Figure 6-3B). Given that FFA4 agonist TUG-891 activates both mFFA4 and mFFA1, it was important to compare the levels of expression of both receptors in the colon (Figure 6-3C). Expression levels of mFFA1 in mouse colon were significantly lower than the mFFA4 control, similar results were seen in lung tissue in Chapter 5. Although as previously described in Chapter 5, these experiments measure relative gene expression and so it cannot be assumed that there is no mFFA1 expression.
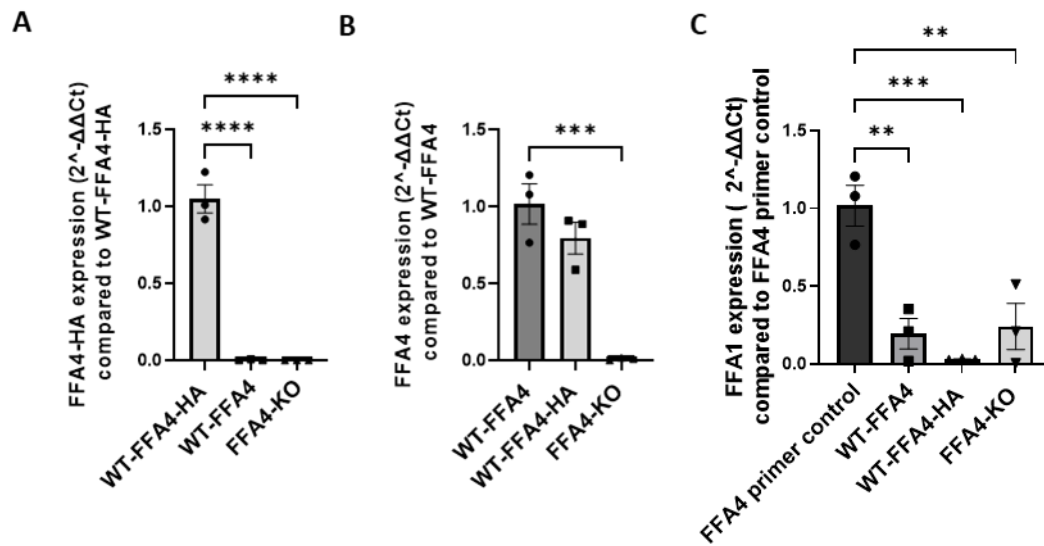
Figure 6-3: Expression of FFA4 and FFA1 in mouse colon
Colon tissue was isolated from WT-FFA4 C57BL/6 mice, WT-FFA4-HA tagged C57BL/6 mice and FFA4-KO C57L/6 mice. q-PCR analysis on cDNA was performed using **(A)** FFA4-HA primers **(B)** FFA4 primers **(C)** FFA1 primers. Expression using FFA1 primer pairs are normalised to FFA4 expression using FFA4 primer pairs. Results are mean ± S.E.M of three independent experiments (n=3). Statistical analysis performed was one-way ANOVA (Dunnett's multiple comparisons), **=P<0.01, ***=P<0.001, ****=P<0.0001.

mFFA4-HA protein expression was examined using immunohistochemistry, using both in-house FFA4 antisera and commercial HA antibodies, in methods validated in lung immunohistochemistry (Chapter 5 Part 5.3.1), however levels of expression were too low to detect mFFA4-HA. This was unsurprising since enteroendocrine comprise of less than 1% of the cells in the colon epithelium (Latorre *et al.*, 2016). Therefore, further experiments were carried out under the knowledge that FFA4 was present at the mRNA level and the assumption that FFA4 was present in mouse colon as reported by Rubbino *et al.*, (2022).

6.3.2 Isolation of primary colonic crypts

Based on the fact that mFFA4 was present in the colon at the mRNA level, experiments were performed to determine whether this mFFA4 had any functional responses within the colon. Primary colonic crypts were isolated from mouse colon tissue for use in Ca^{2+} imaging, GLP-1 and PYY secretion assays. Figure 6-4A depicts an image of an isolated colonic crypt using a brightfield microscope whereas images in Figure 6-4B show a DAPI stained colonic crypt imaged by confocal microscopy. The image in Figure 6-4C shows the morphology

of colonic crypts in intact colon sections. It is evident that colonic crypts are made up of a variety of different cell types as explained in Part 6.1.
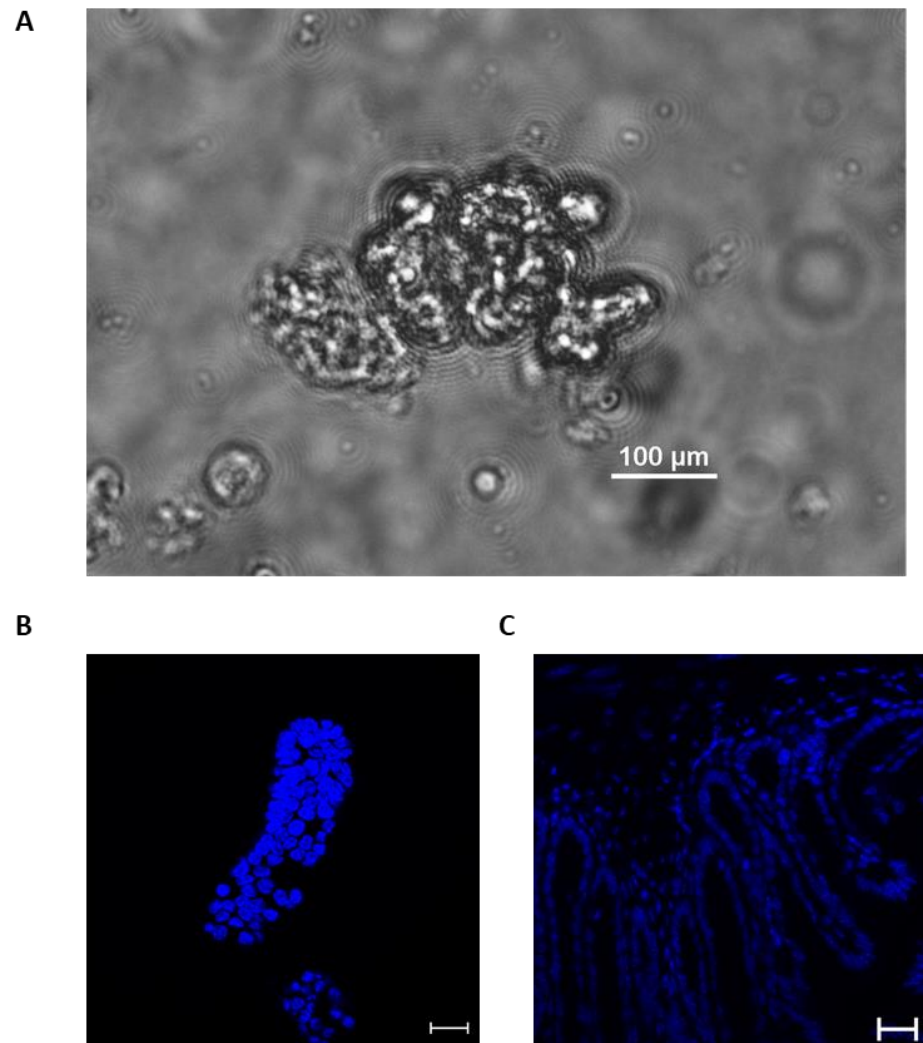
Figure 6-4: Isolated colonic crypts
WT-FFA4-HA C57BL/6 mouse colon was digested using collagenase and isolated colonic crypts were plated into 24 well plates and then imaged **(A)** on a brightfield microscope at 20x objective or **(B)** on a confocal microscope using DAPI stain at a 40x objective, scale bar = 20 μm. **(C)** Whole colon sectioned to 40 μm thick was stained with DAPI before imaging at 40x objective on a confocal microscope, scale bar =20 μm. Images are representative of three independent experiments (n=3).

6.3.3 Activation of mFFA4 within the colon

Based on the fact that FFA4 is primarily a Gq coupled receptor, calcium imaging assays were used to determine whether mFFA4 was functional in colonic crypts and able to produce a physiological increase in intracellular calcium following TUG-891 synthetic agonist activation. In these calcium assays, ratio-metric calcium indicator dye, Fura-8 AM, was used as a measure of intracellular calcium. Fura-8 AM works on the principle that upon entrance to the cytosol,

esterases convert Fura-8 AM into Fura-8. Fura-8 binds to Ca^{2+}, producing a fluorescent substance, shifting the emission wavelength of 525 nm to 355 and 415 nm. Therefore, the emissions at these wavelengths are directly related to the levels of intracellular calcium.

Following TUG-891 addition to isolated colonic crypts from WT-FFA4-HA and FFA4-KO mice, an increase in intracellular Ca^{2+} was observed (Figure 6-5A,C). Once intracellular calcium levels had returned to basal following TUG-891 addition, cells were treated with ionomycin, a calcium ionophore which acts to increase intracellular calcium levels (Figure 6-5B,D). While an increase in intracellular calcium was observed following ionomycin treatment, the response was not as characteristically rapid and robust as reported (Mason *et al.*, 1999). For this reason, the differences in Fura-8 ratio, before TUG-891 addition during the stable baseline and after TUG-891 treatment at the peak calcium response, were calculated instead of comparing values to a peak ionomycin response. As FFA4 is not expressed in every cell within the crypt, % of cells responding to TUG-891 were calculated using these ratios. The % of cells responding to TUG-891 was significantly increased (P=0.005) in WT-FFA4-HA colonic crypts compared to FFA4-KO colonic crypts (Figure 6-5E). To ensure that addition of TUG-891 was mediating this response, a HEPES buffer negative control was performed (Figure 6-5F) which showed a slight change in ratio upon addition, returning to normal following addition. The changes in Fura-8 ratio and thereby increases in intracellular calcium upon addition of TUG-891 are visually shown in Figure 6-5G,H. Taken together, this data indicates that 50 µM TUG-891 activates mFFA4 in the colon, leading to a functional Ca^{2+} response.
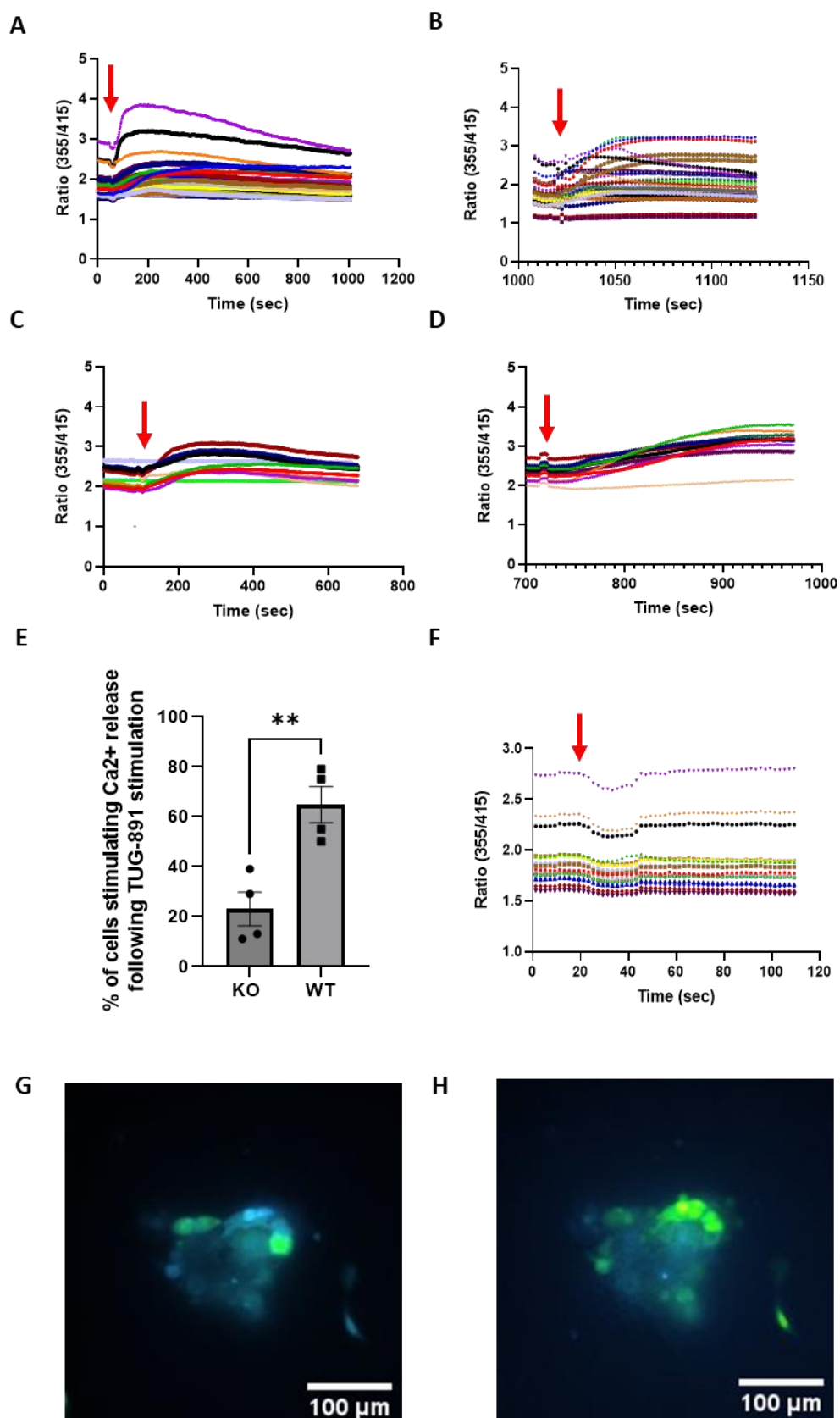
Figure 6-5: Calcium imaging of colonic crypts following 50 µM TUG-891 treatment
A stable baseline of 355/415 nm ratio of Fura-8 calcium indicator dye was established for at least
60 sec in primary colonic crypts isolated from WT-FFA4-HA C57BL/6 mice **(A,B)** or FFA4-KO
C57BL/6 mice **(C,D)**. Crypts were then stimulated with 50 µM TUG-891 at time points indicated by
red arrows and increases in ratio were measured in real-time **(A**, **C)**. After the calcium response
had returned to a stable baseline, 5 µM ionomycin was added to cells as a positive control **(B,D).**
The 355/415 nm Fura-8 ratio was determined at basal levels before TUG-891 addition, and also at

peak responses following TUG-891 addition in WT-FFA4-HA and FFA4-KO colonic crypts. Differences in these two ratios were calculated to determine responsive cells. % of responding cells were calculated for each mouse and values compared between WT-FFA4-HA and FFA4-KO mice to assess release of calcium in response to TUG-891 **(E)**. Addition of HEPES buffer at the time point indicated by the red arrow was used to negatively control for the Fura-8 ratio changes in A-D **(F)**. Images representing crypts at stable baseline **(G)** and at peak calcium responses following TUG-891 addition **(H)** show visually the ratio-metric changes in Fura-8 wavelengths relating to calcium increases. Images are representative of four independent experiments. Results are mean ± S.E.M (N=4, n=54, 87, where N = number of mice and n = number of cells) Statistical analysis performed is unpaired t-test on average values for each independent mouse, **=P<0.01.

While 50 µM TUG-891 activated mFFA4 in WT-FFA4-HA colonic crypts and promoted intracellular calcium release, this was also observed in FFA4-KO crypts although the response was significantly reduced. Additionally, TUG-891 produced a response greater than that of ionomycin, suggesting that at this concentration TUG-891 could have resulted in receptor desensitisation or resulted in depletion of intracellular calcium stores which had not fully restored before ionomycin addition. To try and reduce these effects, the same experiments were carried out using a lower concentration of TUG-891 (10 µM) (Figure 6-6). Here, an increase in intracellular calcium upon 10 µM TUG-891 treatment in WT-FFA4-HA colonic crypts was observed, and to a reduced effect in FFA4-KO crypts (Figure 6-6A,C). Additionally, robust ionomycin responses were seen following 10 µM TUG-891 stimulation, unlike those seen at 50 µM (Figure 6-6B,D). Calculation of % cells responding to TUG-891, by measurement of ratio of increases between basal measurements before TUG-891 addition and at peak calcium responses following TUG-891 addition, indicated that 10 µM TUG-891 resulted in a significant increase (P=0.01) of intracellular calcium in WT-FFA4-HA crypts compared to FFA4-KO crypts (Figure 6-6E). Increases in Fura-8 ratio corresponding to increases in intracellular calcium upon addition of TUG-891 are shown visually in Figure 6-6F,G. These results indicated that 10 µM TUG-891 in addition to 50 µM TUG-891, activated mFFA4 in the colon leading to a functional Ca^{2+} response.
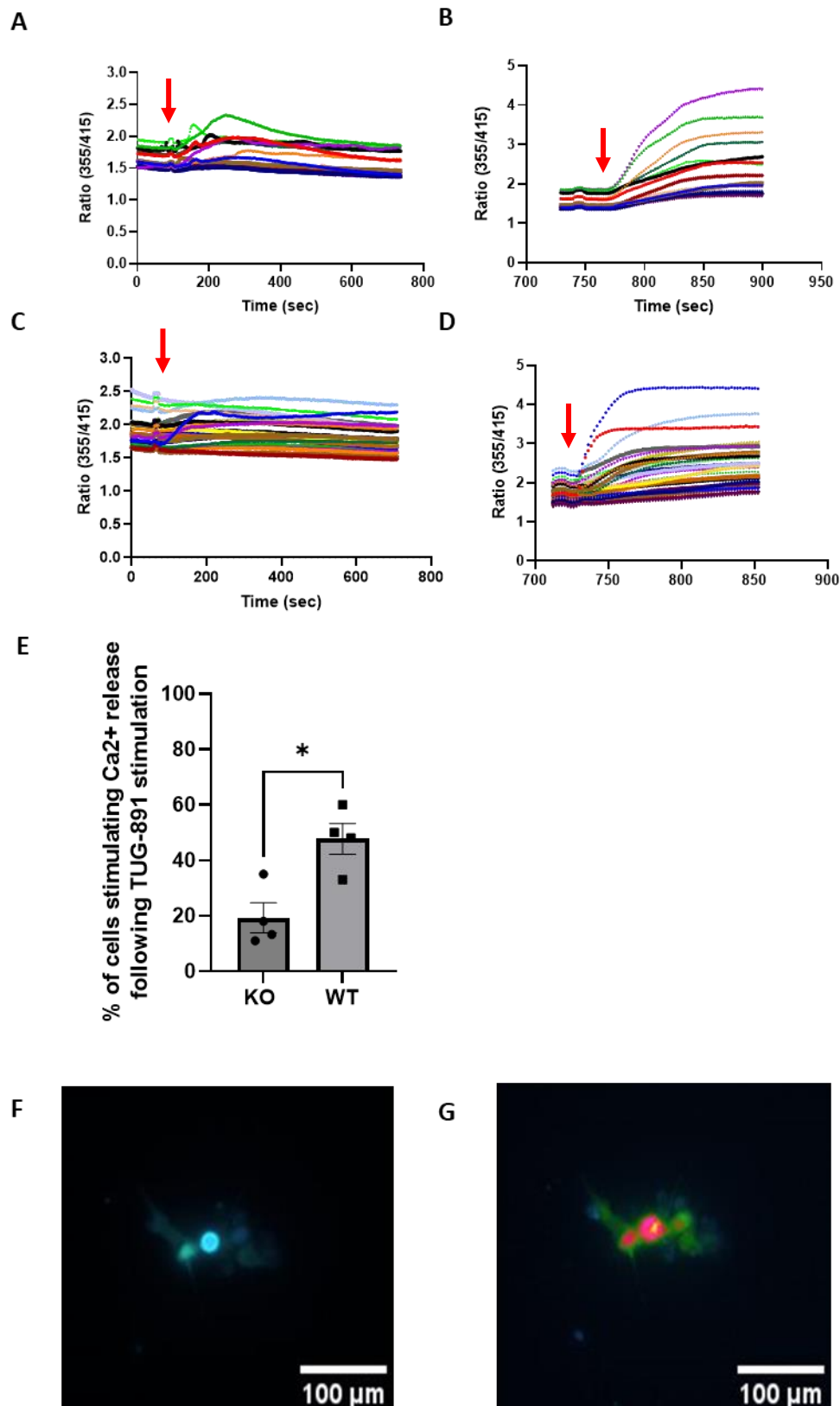
Figure 6-6: Calcium imaging of colonic crypts following 10 µM TUG-891 stimulation
A stable baseline of 355/415 nm ratio of Fura-8 calcium indicator dye was established for at least 60 sec in primary colonic crypts isolated from WT-FFA4-HA C57BL/6 mice **(A,B)** or FFA4-KO C57BL/6 mice **(C,D)**. Crypts were then stimulated with 10 µM TUG-891 at time points indicated by red arrows and increases in ratio were measured in real-time **(A**, **C)**. After the calcium response had returned to a stable baseline, 5 µM ionomycin was added to cells as a positive control **(B,D).** The 355/415 nm Fura-8 ratio was determined at basal levels before TUG-891 addition, and also at

peak responses following TUG-891 addition in WT-FFA4-HA and FFA4-KO colonic crypts. Differences in these two ratios were calculated to determine responsive cells. % of responding cells were calculated for each mouse and values compared between WT-FFA4-HA and FFA4-KO mice to assess release of calcium in response to TUG-891 **(E).** Images representing crypts at stable baseline **(F)** and at peak calcium responses following TUG-891 addition **(G)** show visually the ratio-metric changes in Fura-8 wavelengths relating to calcium increases. Images are representative of four independent experiments. Results are mean ± S.E.M (N=4, n=38, 41, where N = number of mice and n = number of cells) Statistical analysis performed is unpaired t-test on average values for each independent mouse, *=P<0.05.

6.3.4 FFA4 synthetic agonist stimulated GLP-1 release from primary colonic crypts

To determine a physiological function of this active mFFA4 in colonic crypts, GLP-1 secretion assays were performed on colonic crypts (Figure 6-7). Agonists were assayed at 10 μM as intracellular calcium responses were detected at this concentration and additionally, maximal responses were elicited at this concentration in cellular assays in Chapters 3 and 4. The data displayed is broken down so that individual values for the concentration of GLP-1 in cell supernatant and cell lysate are shown. However, GLP-1 secretion from cells is dependent on the number of cells present prior to cell lysis, and therefore the concentration of GLP-1 in cell lysate may vary. Secretion of GLP-1 from cells (concentration of GLP-1 in supernatant) must consequently be normalised to the concentration of GLP-1 in cell lysates as experiments are inherently variable. I have hence expressed GLP-1 secretion as a % secretion compared to concentration of cell lysate and then normalised to the DMSO vehicle control. A C3 positive control was also included as C3 has been shown to activate FFA2, resulting in a robust secretion of GLP-1 (Psichas *et al.*, 2015; Bolognini *et al.*, 2019). Compared to the C3 control, neither 10 μM dual FFA4/FFA1 agonist TUG-891 nor specific FFA4 agonist GSK137647A caused a significant % GLP-1 secretion in colonic crypts from any mouse line assayed, indicating that at 10 μM concentrations these drugs did not promote GLP-1 release. Here, GSK137647A was used instead of the other well characterised FFA4 specific agonists, as TUG-1197 showed poor physiological effects in Chapter 5, while other agonists displayed off-target effects.

A

B

Figure 6-7: GLP-1 release from colonic crypts following 10 µM agonist treatment
Colonic crypts were isolated from colon tissues from **(A)** WT-FFA4-HA C57BL/6 mice and **(B)** FFA4-KO C57BL/6 mice before 2 h treatment with compound (10 µM C3, TUG-891 and GSK137647A, DMSO 0.1%). Cell lysates and supernatants were assayed on GLP-1 ELISA. Results are mean ± S.E.M of three independent experiments (n=3). Statistical analysis performed was repeated measures one-way ANOVA (Geisser-Greenhouse multiple comparisons), *=P<0.05.

However, as both 50 µM and 10 µM TUG-891 led to functional calcium responses despite GLP-1 secretion not being observed at 10 µM TUG-891 colonic crypts, it was hypothesised this could have been due to a reduction in agonist potency owing to the inclusion of BSA in the secretion buffer of the GLP-1 assay, which acts as a natural carrier for free fatty acids (Spector, John and Fletcher, 1969; Vusse, 2009). Therefore, a higher concentration of TUG-891 was applied to isolated colonic crypts so that potency of agonist was increased. It was evident that 50 µM TUG-891 caused a robust secretion of GLP-1 (Figure 6-8A) in contrast to results seen for 10 µM TUG-891 (Figure 6-7). Additionally, colonic crypts isolated from FFA4-KO mice showed no significant increase in GLP-1 secretion (P>0.05) suggesting that 50 µM TUG-891 treatment selectively activated mFFA4 to mediate GLP-1 secretion (Figure 6-8B). GSK137647A was not assayed in this experiment as results from Chapter 3 indicated a lower potency than TUG-891 and given the hypothesis of a reduced potency due to BSA inclusion, it was

thought that a compound with poor potency would not be appropriate in this setting.
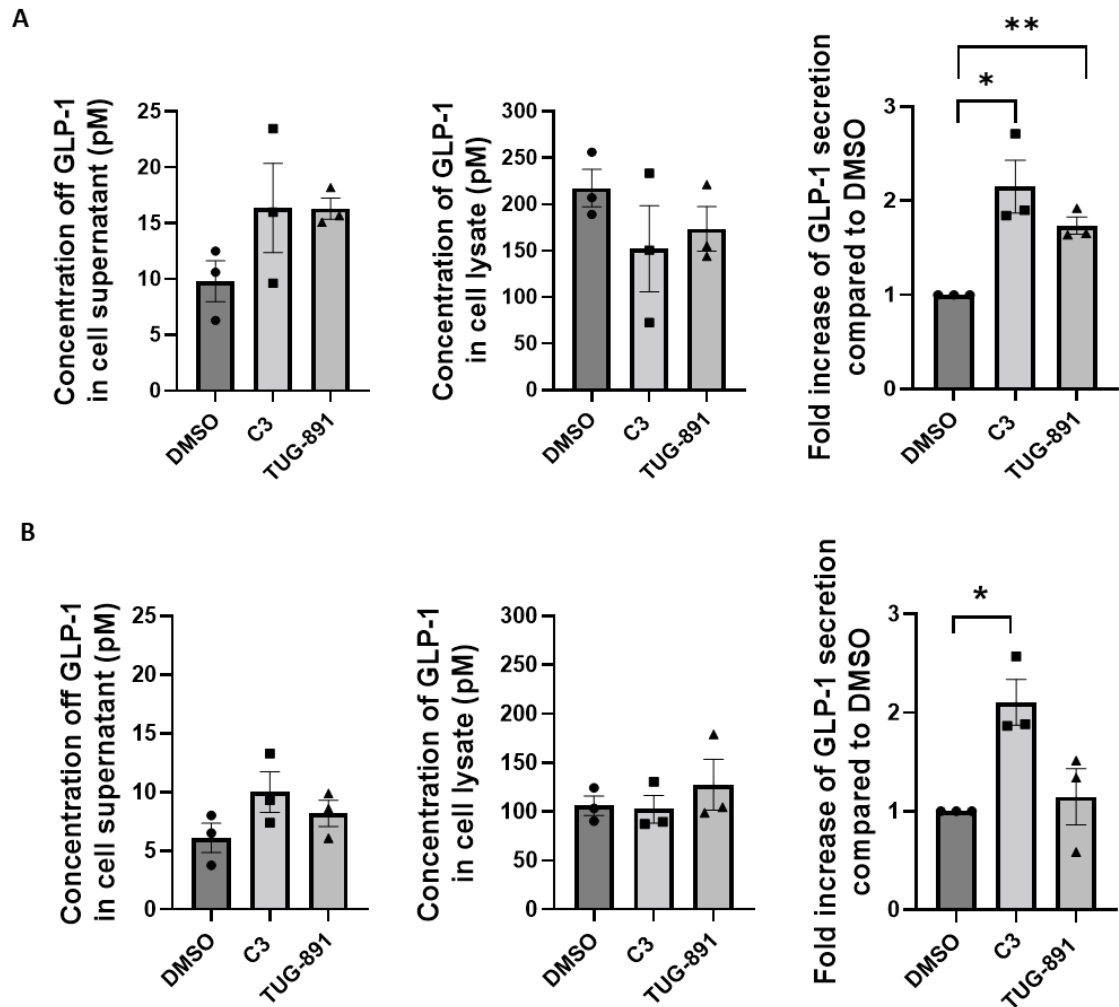
Figure 6-8: GLP-1 release from colonic crypts following 50 µM TUG-891 treatment
Colonic crypts were isolated from colon tissues from **(A)** WT-FFA4-HA C57BL/6 mice or **(B)** FFA4-KO C57BL/6 mice, before 2 h treatment with compound (10 µM C3, 50 µM TUG-891 and DMSO 0.1%). Cell lysates and supernatants were assayed on GLP-1 ELISA. Results are mean ± S.E.M of three independent experiments (n=3). Statistical analysis performed was repeated measures one-way ANOVA (Geisser-Greenhouse multiple comparisons), *=P<0.05, **=P<0.01.

6.3.5 FFA4 synthetic agonist stimulated PYY release from primary colonic crypts

PYY release was also assayed after synthetic agonist stimulation of primary colonic crypts (Figure 6-9). Consistent with GLP-1 data in Figure 6-7 and 8, C3 was used as a positive control, as C3 activation of FFA2 results in a robust

secretion of PYY (Psichas *et al.*, 2015). Data is again broken down into individual values for the concentration of PYY in cell supernatant and cell lysate, along with the % secretion normalised to the DMSO vehicle control. Consistent with results from GLP-1 assays, no significant increase in PYY secretion was detected for FFA4 agonists at 10 μM compared to the vehicle control in any mouse line used (Figure 6-9A, B). It is interesting to note that GSK137647A showed a trend of reduction of PYY secretion to levels below basal.
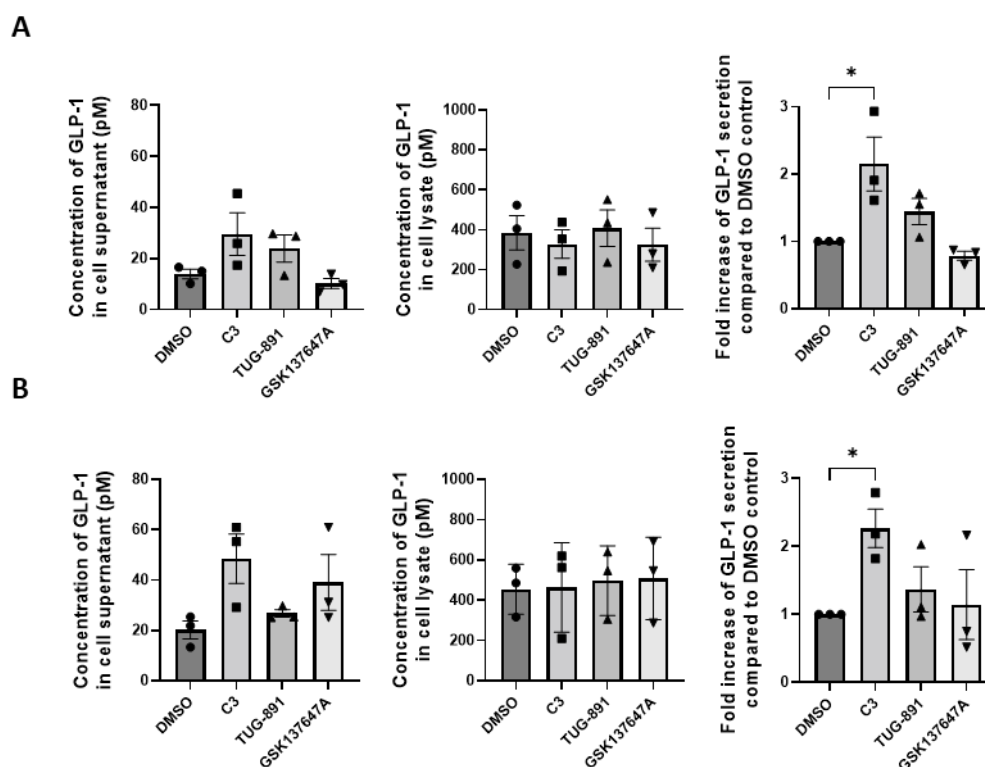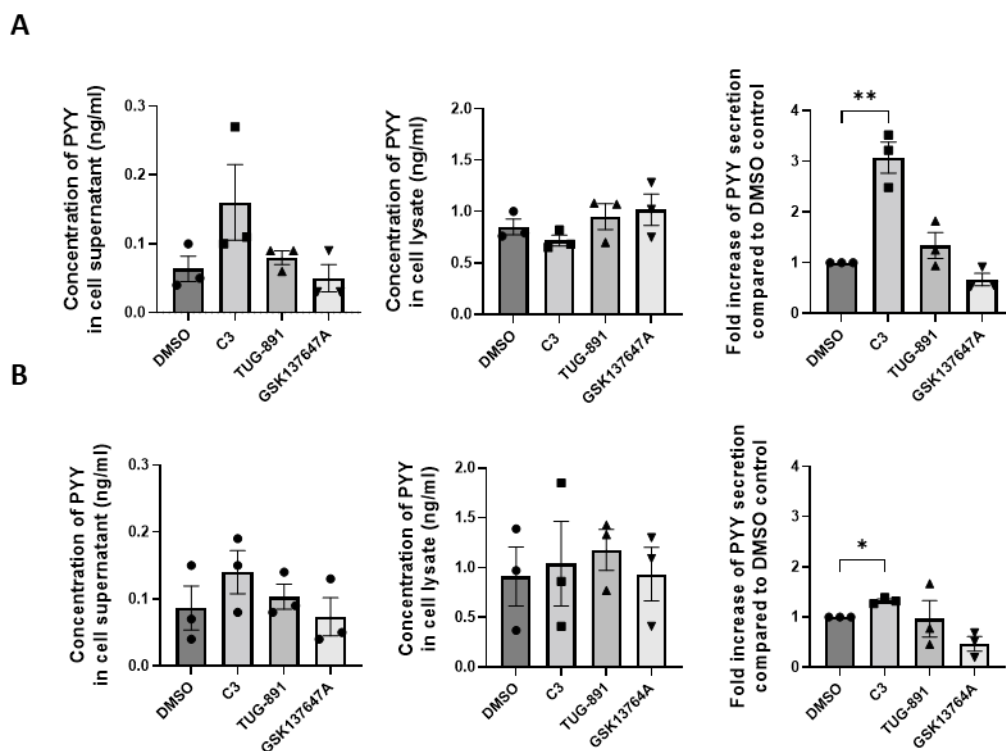

Figure 6-9: PYY release from colonic crypts following 10 μM FFA4 agonist treatment
Colonic crypts were isolated from **(A)** WT-FFA4-HA C57BL/6 mice and **(B)** FFA4-KO C57BL/6 mice before 2 h treatment with compound (10 μM C3, TUG-891 and GSK137647A, DMSO 0.1%). Cell lysates and supernatants were assayed on PYY ELISA. Results are mean ± S.E.M of three independent experiments (n=3). Statistical analysis performed was repeated measures one-way ANOVA (Geisser-Greenhouse multiple comparisons), *=P<0.05, **=P<0.01.

Additionally, PYY secretion from colonic crypts was measured following 50 μM TUG-891 treatment as both a functional calcium response and GLP-1 release was detected at this concentration (Figure 6-10). While there was a trend of PYY secretion in WT-FFA4-HA mouse colonic crypts following TUG-891 stimulation, this was not significant (P>0.05), likely because the results were highly variable (Figure 6-10A). Therefore, it was not possible to reliably show that 10 μM or 50 μM TUG-891 promoted PYY secretion from colonic crypts. Repeated experiments

are required to be performed to determine whether this result is statistically significant. Power calculations revealed that a total sample size of 51 would be required to correctly power experiments. However, to keep in line with the principles of the 3Rs, there is no justification for the use of inappropriately high numbers of animals that may result in false positive values, and therefore a fewer number of repeats would be more justifiable.
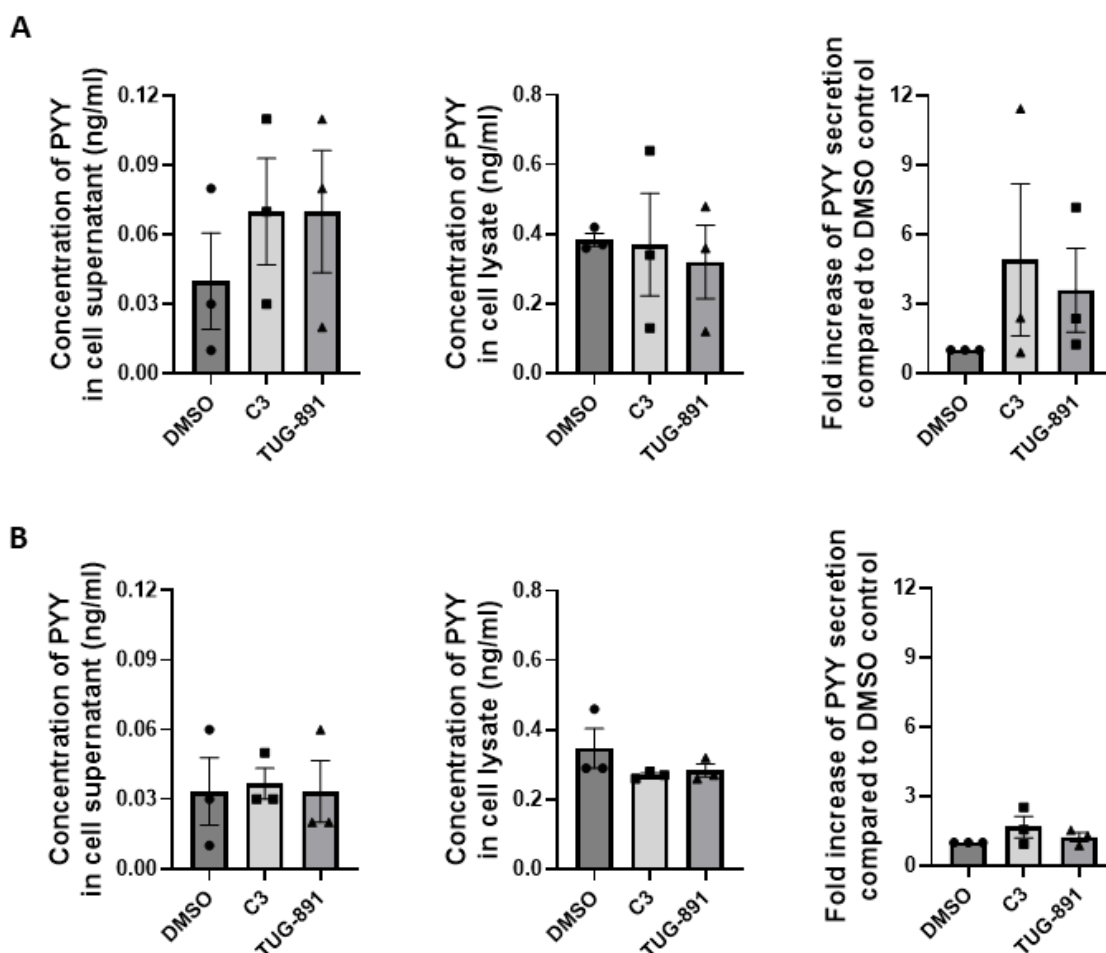
Figure 6-10: PYY release from colonic crypts following 50 µM TUG-891 treatment
Colonic crypts were isolated from **(A)** WT-FFA4-HA C57BL/6 mice, **(B)** FFA4-KO C57BL/6 mice before 2 h treatment with compound (10 µM C3, 50 µM TUG-891 and DMSO 0.1%). Cell lysates and supernatants were assayed on PYY ELISA. Results are mean ± S.E.M of three independent experiments (n=3). Statistical analysis performed was repeated measures one-way ANOVA (Geisser-Greenhouse multiple comparisons).

6.4 Discussion

While the colocalization of FFA4 and metabolic hormones such as GLP-1 and PYY led to a hypothesis that FFA4 is involved in the secretion of such hormones, conflicting evidence on the topic has led to some uncertainty in the role of FFA4

within the colon (Hirasawa *et al.*, 2005; Xiong *et al.*, 2013; Oh *et al.*, 2014; Paulsen *et al.*, 2014; Sundström *et al.*, 2017). This chapter set out to define whether mFFA4 was functional in the colon and to investigate the action of mFFA4 agonist mediated GLP-1 and PYY secretion.

Previously, the role of FFA4 within the colon was uncertain, however, here mFFA4 was shown to be functionally active in the colon in calcium imaging studies at 50 μM and 10 μM concentrations of TUG-891. However, the reduced responses to ionomycin observed following 50 μM TUG-891 were interesting and may suggest that stimulation with TUG-891 at high concentrations could have resulted in receptor desensitisation. Although, these experiments were sufficiently short lived and receptor desensitisation is unlikely within this time period, therefore, an alternative explanation is that this concentration of TUG-891 could have resulted in depletion of intracellular calcium stores and the cells may take a longer period of time to recover from Ca^{2+} release from intracellular stores. Therefore, it is possible that the time allowed for cell recovery in experiments using 50 μM TUG-891 was simply not long enough.

Though GLP-1 secretion was not detected by Xiong *et al.*, (2013), Oh *et al.*, (2014) and Paulsen *et al.*, (2014), it is possible that GLP-1 could have been degraded in the experimental procedure before sample collection (Sharma *et al.*, 2018). GLP-1 is rapidly broken down and inactivated by the enzyme dipeptidyl peptidase IV (DPP-4) which cleaves dipeptides from the N-terminus but is also degraded by neutral endopeptidase 24.11 (NEP24.11) (Mentlein, Gallwitz and Schmidt, 1993; Plamboeck *et al.*, 2005; Cho, Wideman and Kieffer, 2013). Therefore, as GLP-1 has a short half-life of 1.5 minutes, it can be difficult to determine when the agonist has reached the colon following agonist administration, and when GLP-1 has been released to determine which time-point samples should be collected to accurately measure GLP-1 levels. To understand whether GLP-1 could have broken down before sample collection, alternative studies using colonic crypts were performed, as agonist stimulation on colonic crypts followed by a GLP-1 ELISA to measure output provides a greater level of control on GLP-1 release and degradation. Preliminary results from GLP-1 ELISA on cell lysate and supernatant from primary colonic crypts suggested dual FFA4/FFA1 agonist TUG-891 and FFA4 specific agonist

GSK137647A did not stimulate GLP-1 secretion at concentrations of 10 µM. These results were in agreement with data from Xiong *et al.*, (2013), Oh *et al.*, (2014) and Paulsen *et al.*, (2014) suggesting mFFA4 did not mediate GLP-1 release. However, colonic crypts treated at 50 µM TUG-891 promoted FFA4 mediated GLP-1 secretion, demonstrating a novel finding that 50 µM but not 10 µM TUG-891 results in GLP-1 secretion in primary colonic crypts. However, it is interesting that 10 µM TUG-891 led to a response in Ca^{2+} assays but GLP-1 secretion was not observed at this concentration. It was thought the presence of fatty acid free BSA in the medium could have reduced the potency of FFA4 agonists in GLP-1 assays. BSA is a natural carrier protein for fatty acids and thus FFA4 agonists may have bound to BSA (Spector, John and Fletcher, 1969; Vusse, 2009). Previously, BSA has been shown to bind to added free fatty acids and reduce Ca^{2+} signalling for FFA1 and so it is possible that addition of this BSA in the secretion buffer to prevent non-specific binding, increase stability of reagents and prevent binding to experimental materials, might have actually reduced availability of agonist (Stoddart, Brown and Milligan, 2007; Peña and Domínguez, 2010). Therefore, we may see an effect at 50 µM TUG-891 but not at 10 µM as a higher concentration would be required to occupy receptors and produce a response. To determine if this was the case, this should be assessed in a cell line assay similar to those described by Stoddart, Brown and Milligan (2007). In calcium imaging assays, BSA was not present in the medium and so the potency may not be affected, thus accounting for the response at 10 µM in this assay. Additionally, as the two concentrations used were only 5-fold different and resulted in different outcomes, this suggests that these concentrations are at the bottom of the concentration-response curve in this assay. Therefore, more potent FFA4 agonists are required to address the roles of GLP-1 secretion in colonic crypts. However, agonists investigated in Chapters 3 and 4 had similar or reduced potency in comparison to TUG-891, suggesting that these agonists may not be appropriate to fully understand these effects. While not commercially available, characterisation of agonists based on the structure of TUG-891 and chemically diverse agonists have been synthesised (Carullo *et al.*, 2021). One series of chromane propionic acid-based agonist demonstrated good potency and selectivity for both mouse and human FFA4, and therefore, the availability of novel agonists such as these could prove to be beneficial in

furthering research on FFA4 in metabolic diseases (Adams *et al.*, 2017; Carullo *et al.*, 2021).

Another hormone which is secreted from enteroendocrine cells of the colon is PYY (Reimann *et al.*, 2008). Neither 10 µM nor 50 µM TUG-891 sustained a significant increase in PYY secretion. While Moodaley *et al.*, (2017) demonstrated that incubation of FFA4 agonist Metbolex-36 slowed gastric transit in *ex vivo* isolated mouse colon and colonic transit *in vivo* following oral gavage, this study did not measure concentrations of PYY secreted and instead measured changes in short-circuit current to study colonic transit, proving it to be a PYY mediated effect by application of PYY Y1 and Y2 receptor inhibitors. Though the results displayed in this thesis are not in agreement with this study, these studies are not comparable and while it was hypothesised that FFA4 agonists could stimulate PYY release, there is not yet evidence for that in this thesis and further studies would be needed to confirm this.

In this chapter, it was demonstrated that following synthetic FFA4 agonist treatment of primary colonic crypts, activation of mFFA4 in colonic crypts did result in an increase in intracellular calcium. This suggests that not only is mFFA4 active within the mouse colon but it may function through a Gq/11 coupled pathway. GLP-1 release was also detected at 50 µM but not 10 µM TUG-891 demonstrating that not only is mFFA4 active but may also function to stimulate the release of GLP-1. Further characterising the effects of other FFA4 agonists within the colon may validate these FFA4 agonists as viable and novel therapies for metabolic diseases such as diabetes, however, studies are currently hindered by a lack of potent FFA4 agonists.

Chapter 7   Final discussion

GPCRs account for around 30% of drug targets, largely due to their ability to respond to a wide variety of different stimuli and involvement in many physiological processes in the body (Zhang and Xie, 2012; Nejat *et al.*, 2022). However, there are still many GPCRs to be exploited for their therapeutic potential. Amongst these is the FFA4 receptor, which has been identified as a potential drug target for the treatment of metabolic diseases such as type 2 diabetes mellitus since its deorphanisation and expression profile was revealed in 2005 (Hirasawa *et al.*, 2005). FFA4 provides a novel therapeutic target for type 2 diabetes mellitus based on its involvement in regulation of glucose stimulated insulin release and glucagon secretion (Moran *et al.*, 2014; Suckow *et al.*, 2014; Sundström *et al.*, 2017; McCloskey *et al.*, 2020; Croze *et al.*, 2021). However, FFA4 is widely expressed in tissues and functions of FFA4 in the lung, the organ which shows the highest level of FFA4 expression, has only recently been considered (Prihandoko *et al.*, 2020). Researching the roles of FFA4 in different tissues may define novel roles of FFA4 and identify novel therapeutic opportunities of the receptor.

However, to date there has been a significant lack of FFA4 compounds progressing from pre-clinical studies to in-human clinical trials for a variety of reasons, including issues with selectivity of FFA4 over FFA1 leading to challenges in assessing FFA4 receptor function, issues with compound solubility, pharmacokinetic and dynamic properties (Hudson *et al.*, 2013; Sparks *et al.*, 2014; Milligan *et al.*, 2017). There are also only a handful of commercially available agonists which consequently limits studies. One of the aims of this thesis was to test FFA4 compounds in pharmacological assays to characterise ligand properties and directly compare to one another. While different agonists have been tested by different groups in a variety of assays, there is a lack of consistency across the pharmacological data collected for FFA4 ligands resulting in different reported potencies and efficacies (Hudson *et al.*, 2013; Oh *et al.*, 2014; Sparks *et al.*, 2014). Although it has been previously characterised that FFA4 primarily couples to Gαq G proteins, testing a variety of agonists allowed the direct comparisons of agonist potencies and efficacies. This pharmacological

data enabled the calculation of bias factors for IP1 and pERK1/2 /ß-arrestin2 pathways using a model based on the Black and Leff operational model of agonism. Biased agonism delivers considerable promise in regard to preferentially activating physiological responses (Michel and Charlton, 2018). However little calculable bias was detected, and no agonists biased towards arrestin signalling were identified, meaning it is currently not possible to exploit potential anti-inflammatory properties of the FFA4 receptor which may have a therapeutic basis in inflammatory based diseases. However, the identification that Agonist 2 displayed signalling bias was encouraging suggesting that it may be possible to exploit beneficial effects resulting from Ca^{2+} mediated Gq signalling, such as release of metabolic hormones including GLP-1 which may be regulated by this pathway.

Following on from testing this range of FFA4 agonists in pharmacological assays, agonists were also used to probe the activity of FFA4 in a range of physiological tissues in a variety novel mouse models. These models included FFA4-HA tagged mice, FFA4-KO mice and FFA4 mice containing PD mutations leading to the uncoupling phosphorylation dependent signalling including ß-arrestin pathways. Using these tools, the on-target activity of agonists in mouse tissues such as lung and colon were defined. Interestingly, receptor expression in these tissues did correlate to functional activity, revealing that agonists working on-target at FFA4 were promoting novel physiological effects. Using these mouse models, it was discovered bronchorelaxation effects were observed in airways from WT-FFA4-HA PCLS following FFA4 agonist treatment. It was important to understand the coupling mechanisms by which this physiological response occurred as FFA4 was observed to couple to Gαq and ß-arrestin2 pathways in cell line assays. This was explored in the lung by using the PD mouse model, where preliminary data indicated that TUG-891 treatment was shown to promote airway relaxation through phosphorylation dependent signalling pathways.

Although the contributions of FFA4 anti-inflammatory properties in the lung was not considered in this thesis, our group has previously characterised TUG-891 and/or TUG-1197 compounds in disease models such as cigarette smoking, ozone and house dust mites (Prihandoko et al., 2020). These disease models demonstrated an increase in inflammatory markers, often seen in respiratory

diseases such as asthma and COPD, while TUG-891 and/or TUG-1197 acted to decrease immune responses. As FFA4-mediated anti-inflammatory signalling is described to function through ß-arrestin coupled pathways (Oh *et al.*, 2014), perhaps analysis of a PD-mutant disease model may be of importance in understanding the anti-inflammatory contributions that FFA4 may have in respiratory disease. Although, as previously described in Chapter 4 and 5, there is evidence of distinct functions of receptor phosphorylation and ß-arrestin signalling (Alvarez-Curto *et al.*, 2016), so PD mutants might not necessarily portray the action of ß-arrestin signalling and so ß-arrestin null FFA4 containing mice might help to differentiate the effects of receptor phosphorylation and ß-arrestin2 recruitment.

Since FFA4 agonists examined in pharmacological assays did not display bias toward G protein or arrestin pathways, development of agonists which display ß-arrestin2 bias may be beneficial in preferentially promoting relaxation of airways. Arrestin biased ligands may therefore be beneficial in treatment of respiratory diseases such as asthma and COPD, which involve the bronchoconstriction of airways and infiltration of inflammatory molecules, as FFA4 possesses both bronchorelaxation and anti-inflammatory properties which may act through ß-arrestin pathways. The data presented in this thesis indicate that FFA4 synthetic agonists represent novel therapeutic opportunities in this field. Clearly there is a great need for novel clinical therapies in this area, as despite development of different therapeutic interventions, increasing numbers of patients suffer from these respiratory diseases year on year (Vos *et al.*, 2016; Abbafati *et al.*, 2020). This highlights that while therapies might be effective on populations of patients, disease is not effectively controlled in many and disease progression and mortality remains an issue (Gross and Barnes, 2017).

In addition to inducing physiological effects in the lung, TUG-891 also promoted GLP-1 secretion in mouse colonic crypts. Here mFFA4 was shown to be coupled to calcium mobilisation, suggesting that this may be the mechanism by which GLP-1 is secreted. Furthers studies using PD mouse model tools or Gq inhibitors, such as those characterised in pharmacological assays, might reveal the definitive mechanism by which GLP-1 release occurs.

GLP-1 is often found at low levels in T2DM patients, and increase in GLP-1 levels results in increases in insulin secretion, stimulating the reduction of blood glucose levels (Nadkarni, Chepurny and Holz, 2014; Müller *et al.*, 2019). Despite the improvements in diabetes therapeutics in recent years, the prevalence of T2DM is increasing (International Diabetes Federation, 2021). Additionally, carcinogens have been found in the most commonly prescribed drug therapy for T2DM, metformin and other therapies can provoke side effects including vomiting, diarrhoea, weight gain, pancreatitis and increased risk of heart failure (Miller *et al.*, 2014; Bailey and Day, 2018; Carullo *et al.*, 2021; Kanwal *et al.*, 2022). This highlights the need for the development of safer, more effective drug therapies in diabetes, where FFA4 agonists might provide a novel mechanism for the restoration of glucose homeostasis by promoting the secretion of GLP-1.

The confirmation that mFFA4 has a role in GLP-1 secretion and regulation of glucose stimulated insulin release confirms FFA4 as a valid target for the treatment of metabolic diseases such as type 2 diabetes metillus and furthermore, the combination of proven anti-inflammatory effects and airway smooth muscle relaxation gives FFA4 agonists a potential setting as a drug target in respiratory diseases. However, there are still clear limitations to further studies. Agonists had poor potency in these studies, displaying off-target effects and demonstrated little signalling bias. However, the future of FFA4 based research is promising, with two physiological responses of FFA4 activation demonstrated here in the lung and colon. The use of the novel physiological PD mouse model might also identify roles of receptor phosphorylation in other tissues expressing FFA4 such as the colon, pancreas and adipose tissues, allowing the characterisation of distinct phosphorylation dependent and independent pathways such as those described in the M1 and M3 muscarinic receptors using similar mouse models (Bradley *et al.*, 2016, 2020; Scarpa *et al.*, 2021). Additionally, with the availability of more potent and biased agonists, we might be able to exploit beneficial effects such as airway relaxation and anti-inflammatory effects.

List of References

Abbafati, C., Abbas, K.M., Abbasi-Kangevari, M., Abd-Allah, F., Abdelalim, A., Abdollahi, M., Abdollahpour, I., Abegaz, K.H., Abolhassani, H., Aboyans, V., Abreu, L.G., Abrigo, M.R.M., Abualhasan, A., Abu-Raddad, L.J., Abushouk, A.I., Adabi, M., Adekanmbi, V., Adeoye, A.M., Adetokunboh, O.O., *et al.* (2020) 'Global burden of 369 diseases and injuries in 204 countries and territories, 1990–2019: a systematic analysis for the Global Burden of Disease Study 2019', *The Lancet*, 396(10258), pp. 1204–1222. doi:10.1016/S0140-6736(20)30925-9.

Adams, G.L., Velazquez, F., Jayne, C., Shah, U., Miao, S., Ashley, E.R., Madeira, M., Akiyama, T.E., Salvo, J. Di, Suzuki, T., Wang, N., Truong, Q., Gilbert, E., Zhou, D., Verras, A., Kirkland, M., Pachanski, M., Powles, M., Yin, W., *et al.* (2017) 'Discovery of Chromane Propionic Acid Analogues as Selective Agonists of GPR120 with in Vivo Activity in Rodents', *ACS Medicinal Chemistry Letters*, 8(1), pp. 96–101. doi:10.1021/acsmedchemlett.6b00394.

Adrian, T.E., Ferri, G.L., Bacarese-Hamilton, A.J., Fuessl, H.S., Polak, J.M. and Bloom, S.R. (1985) 'Human distribution and release of a putative new gut hormone, peptide YY', *Gastroenterology*, 89(5), pp. 1070–1077. doi:10.1016/0016-5085(85)90211-2.

Agostino, M., Pohl, S.Ö.G. and Dharmarajan, A. (2017) 'Structure-based prediction of Wnt binding affinities for frizzled-type cysteine-rich domains', *Journal of Biological Chemistry*, 292(27), pp. 11218–11229. doi:10.1074/jbc.M117.786269.

Alexander, S.P.H., Christopoulos, A., Davenport, A.P., Kelly, E., Mathie, A., Peters, J.A., Veale, E.L., Armstrong, J.F., Faccenda, E., Harding, S.D., Pawson, A.J., Sharman, J.L., Southan, C., Davies, J.A., Abbracchio, M.P., Alexander, W., Al-hosaini, K., Bäck, M., Beaulieu, J.M., *et al.* (2019) 'THE CONCISE GUIDE TO PHARMACOLOGY 2019/20: G protein-coupled receptors', *British Journal of Pharmacology*, 176(S1), pp. S21–S141. doi:10.1111/bph.14748.

Alvarez-Curto, E., Inoue, A., Jenkins, L., Raihan, S.Z., Prihandoko, R., Tobin, A.B. and Milligan, G. (2016) 'Targeted elimination of G proteins and arrestins

defines their specific contributions to both intensity and duration of G protein-coupled receptor signaling', *Journal of Biological Chemistry*, 291(53), pp. 27147–27159. doi:10.1074/jbc.M116.754887.

Alvarez-Curto, E. and Milligan, G. (2016) 'Metabolism meets immunity: The role of free fatty acid receptors in the immune system', *Biochemical Pharmacology*, 114, pp. 3–13. doi:10.1016/j.bcp.2016.03.017.

Araç, D., Boucard, A.A., Bolliger, M.F., Nguyen, J., Soltis, S.M., Südhof, T.C. and Brunger, A.T. (2012) 'A novel evolutionarily conserved domain of cell-adhesion GPCRs mediates autoproteolysis', *EMBO Journal*, 31(6), pp. 1364–1378. doi:10.1038/emboj.2012.26.

Ashcroft, F.M. and Rorsman, P. (1989) 'Electrophysiology of the pancreatic ß-cell', *Progress in Biophysics and Molecular Biology*, 54(2), pp. 87–143. doi:10.1016/0079-6107(89)90013-8.

Attramadal, H., Arriza, J.L., Aoki, C., Dawson, T.M., Codina, J., Kwatra, M.M., Snyder, S.H., Caron, M.G. and Lefkowitz, R.J. (1992) 'ß-Arrestin2, a novel member of the arrestin/ß-arrestin gene family', *Journal of Biological Chemistry*, 267(25), pp. 17882–17890. doi:10.1016/S0021-9258(19)37125-X.

Attwood, T.K. and Findlay, J.B.C. (1994) 'Fingerprinting g-protein-coupled receptors', *Protein Engineering, Design and Selection*, 7(2), pp. 195-203. doi:10.1093/protein/7.2.195.

Azevedo, C.M.G., Watterson, K.R., Wargent, E.T., Hansen, S.V.F., Hudson, B.D., Kępczyńska, M.A., Dunlop, J., Shimpukade, B., Christiansen, E., Milligan, G., Stocker, C.J. and Ulven, T. (2016) 'Non-Acidic Free Fatty Acid Receptor 4 Agonists with Antidiabetic Activity', *Journal of Medicinal Chemistry*, 59(19), pp. 8868–8878. doi:10.1021/acs.jmedchem.6b00685.

Bailey, C.J. and Day, C. (2018) 'Treatment of type 2 diabetes: future approaches', *British Medical Bulletin*, (April), pp. 123–137. doi:10.1093/bmb/ldy013.

Barki, N., Bolognini, D., Börjesson, U., Jenkins, L., Riddell, J., Hughes, D.I., Ulven, T., Hudson, B.D., Ulven, E.R., Dekker, N., Tobin, A.B. and Milligan, G. (2022) 'Chemogenetics defines a short-chain fatty acid receptor gut–brain axis', *eLife*, 11, pp. 1–23. doi:10.7554/eLife.73777.

Barnes, J.P., Rodger, I.W. and Thomson., N.C. (2009) *Asthma: Basic Mechanisms and Clinical Management*. 2nd edn. Edited by N.C.T. Peter J. Barnes, Jeffrey M. Drazen, Stephen I. Rennard. London: London Academic Press.

Barnes, P.J. (2008) 'Immunology of asthma and chronic obstructive pulmonary disease', *Nature Reviews Immunology*, 8(3), pp. 183–192. doi:10.1038/nri2254.

Barnes, P.J. (2016) 'Inflammatory mechanisms in patients with chronic obstructive pulmonary disease', *Journal of Allergy and Clinical Immunology*, 138(1), pp. 16-27. doi:10.1016/j.jaci.2016.05.011.

Barnes, P.J. (2018) 'Targeting cytokines to treat asthma and chronic obstructive pulmonary disease', *Nature Reviews Immunology*, 18(7), pp. 454–466. doi:10.1038/s41577-018-0006-6.

Barnes, P.J. (2019) 'Inflammatory endotypes in COPD', *Allergy: European Journal of Allergy and Clinical Immunology*, 74(7), pp. 1249–1256. doi:10.1111/all.13760.

Basith, S., Cui, M., Macalino, S.J.Y., Park, J., Clavio, N.A.B., Kang, S. and Choi, S. (2018) 'Exploring G protein-coupled receptors (GPCRs) ligand space via cheminformatics approaches: Impact on rational drug design', *Frontiers in Pharmacology*, 9(MAR), pp. 1–26. doi:10.3389/fphar.2018.00128.

Batterham, R.L., Cohen, M.A., Ellis, S.M., Le Roux, C.W., Withers, D.J., Frost, G.S., Ghatei, M.A. and Bloom, S.R. (2003) 'Inhibition of Food Intake in Obese Subjects by Peptide YY 3–36', *New England Journal of Medicine*, 349(10), pp. 941–948. doi:10.1056/nejmoa030204.

Benovic, J.L., Deblasi, A., Stone, W.C., Caron, M.G. and Lefkowitz, R.J. (1989) 'ß-Adrenergic Receptor Kinase: Primary Structure Delineates a Multigene

Family', *Science*, 246(4927), pp. 235–240. doi:10.1126/science.2552582.

Berridge, M.J. (1993) 'Inositol trisphosphate and calcium signalling', *European Journal of Endocrinology*, 361(6410), pp. 315–325. doi:10.1530/eje.0.130s0004.

Bhatia, R. and Fromer, L. (2011) 'Diagnosing and treating COPD: understanding the challenges and finding solutions', *International Journal of General Medicine*, 4, pp. 129-139. doi:10.2147/ijgm.s21387.

Billington, C.K., Ojo, O.O., Penn, R.B. and Ito, S. (2013) 'cAMP regulation of airway smooth muscle function', *Pulmonary Pharmacology and Therapeutics*, 26(1), pp. 112–120. doi:10.1016/j.pupt.2012.05.007.

Black, J.W., Leffl, P., Shankley, N.P., Wood, J. and Court, L. (1985) 'An operational model of pharmacological agonism : the effect of E /[A] curve shape on agonist dissociation constant estimation', *British Journal of Pharmacology*, 84, pp. 561–571.

Bologna, Z., Teoh, J.P., Bayoumi, A.S., Tang, Y. and Kim, I.M. (2017) 'Biased g protein-coupled receptor signaling: New player in modulating physiology and pathology', *Biomolecules and Therapeutics*, 25(1), pp. 12–25. doi:10.4062/biomolther.2016.165.

Bolognini, D., Barki, N., Butcher, Adrian J., Hudson, B.D., Sergeev, E., Molloy, C., Moss, C.E., Bradley, S.J., Le Gouill, C., Bouvier, M., Tobin, A.B. and Milligan, G. (2019) 'Chemogenetics defines receptor-mediated functions of short chain free fatty acids', *Nature Chemical Biology*, 15(5), pp. 489–498. doi:10.1038/s41589-019-0270-1.

Bonapersona, V., Hoijtink, H., Sarabdjitsingh, R.A. and Joëls, M. (2020) 'RePAIR: a power solution to animal experimentation', *bioRxiv*, (December), p. 864652. doi:10.1101/864652.

Bond, R.A., Lucero Garcia-Rojas, E.Y., Hegde, A. and Walker, J.K.L. (2019) 'Therapeutic Potential of Targeting ß-Arrestin', *Frontiers in Pharmacology*, 10(March). doi:10.3389/fphar.2019.00124.

Bosnjak, B., Stelzmueller, B., Erb, K.J. and Epstein, M.M. (2011) 'Treatment of allergic asthma: Modulation of Th2 cells and their responses', *Respiratory Research*, 12, pp. 1–17. doi:10.1186/1465-9921-12-114.

Bradley, S.J., Molloy, C., Valuskova, P., Dwomoh, L., Scarpa, M., Rossi, M., Finlayson, L., Svensson, K.A., Chernet, E., Barth, V.N., Gherbi, K., Sykes, D.A., Wilson, C.A., Mistry, R., Sexton, P.M., Christopoulos, A., Mogg, A.J., Rosethorne, E.M., Sakata, S., *et al.* (2020) 'Biased M1-muscarinic-receptor-mutant mice inform the design of next-generation drugs', *Nature Chemical Biology*, 16(3), pp. 240–249. doi:10.1038/s41589-019-0453-9.

Bradley, S.J., Wiegman, C.H., Iglesias, M.M., Kong, K.C., Butcher, A.J., Plouffe, B., Goupil, E., Bourgognon, J.M., Macedo-Hatch, T., Legouill, C., Russell, K., Laporte, S.A., König, G.M., Kostenis, E., Bouvier, M., Chung, K.F., Amrani, Y. and Tobin, A.B. (2016) 'Mapping physiological G protein-coupled receptor signaling pathways reveals a role for receptor phosphorylation in airway contraction', *Proceedings of the National Academy of Sciences of the United States of America*, 113(16), pp. 4524–4529. doi:10.1073/pnas.1521706113.

Bridges, T.M. and Lindsley, C.W. (2008) 'G-protein-coupled receptors: From classical modes of modulation to allosteric mechanisms', *ACS Chemical Biology*, 3(9), pp. 530–541. doi:10.1021/cb800116f.

Briscoe, C.P., Peat, A.J., McKeown, S.C., Corbett, D.F., Goetz, A.S., Littleton, T.R., McCoy, D.C., Kenakin, T.P., Andrews, J.L., Ammala, C., Fornwald, J.A., Ignar, D.M. and Jenkinson, S. (2006) 'Pharmacological regulation of insulin secretion in MIN6 cells through the fatty acid receptor GPR40: Identification of agonist and antagonist small molecules', *British Journal of Pharmacology*, 148(5), pp. 619–628. doi:10.1038/sj.bjp.0706770.

Briscoe, C.P., Tadayyon, M., Andrews, J.L., Benson, W.G., Chambers, J.K., Eilert, M.M., Ellis, C., Elshourbagy, N.A., Goetz, A.S., Minnick, D.T., Murdock, P.R., Sauls, H.R., Shabon, U., Spinage, L.D., Strum, J.C., Szekeres, P.G., Tan, K.B., Way, J.M., Ignar, D.M., *et al.* (2003) 'The orphan G protein-coupled receptor GPR40 is activated by medium and long chain fatty acids', *Journal of Biological Chemistry,* 278(13), pp.11303-11311. doi:10.1074/jbc.M211495200.

Britsch, S., Krippeit-Drews, P., Lang, F., Gregor, M. and Drews, G. (1995) 'Glucagon-like peptide-1 modulates Ca2+ current but not K+ATP current in intact mouse pancreatic B-cells', *Biochemical and Biophysical Research Communications*, 207(1), pp. 33–39. doi:10.1006/bbrc.1995.1149.

Brown, A.J., Goldsworthy, S.M., Barnes, A.A., Eilert, M.M., Tcheang, L., Daniels, D., Muir, A.I., Wigglesworth, M.J., Kinghorn, I., Fraser, N.J., Pike, N.B., Strum, J.C., Steplewski, K.M., Murdock, P.R., Holder, J.C., Marshall, F.H., Szekeres, P.G., Wilson, S., Ignar, D.M., *et al.* (2003) 'The orphan G protein-coupled receptors GPR41 and GPR43 are activated by propionate and other short chain carboxylic acids', *Journal of Biological Chemistry*, 278(13), pp. 11312–11319. doi:10.1074/jbc.M211609200.

Burns, R.N., Singh, M., Senatorov, I.S. and Moniri, N.H. (2014) 'Mechanisms of homologous and heterologous phosphorylation of FFA receptor 4 (GPR120): GRK6 and PKC mediate phosphorylation of Thr347, Ser 350, and Ser357 in the C-terminal tail', *Biochemical Pharmacology*, 87(4), pp. 650–659. doi:10.1016/j.bcp.2013.12.016.

Butcher, A.J., Hudson, B.D., Shimpukade, B., Alvarez-Curto, E., Prihandoko, R., Ulven, T., Milligan, G. and Tobin, A.B. (2014) 'Concomitant action of structural elements and receptor phosphorylation determines arrestin-3 interaction with the free fatty acid receptor FFA4', *Journal of Biological Chemistry*, 289(26), pp. 18451–18465. doi:10.1074/jbc.M114.568816.

Butcher, A.J., Prihandoko, R., Kong, K.C., McWilliams, P., Edwards, J.M., Bottrill, A., Mistry, S. and Tobin, A.B. (2011) 'Differential G-protein-coupled receptor phosphorylation provides evidence for a signaling bar code', *Journal of Biological Chemistry*, 286(13), pp. 11506–11518. doi:10.1074/jbc.M110.154526.

Bylund, D.B., Eikenberg, D.C., Hieble, J.P., Langer, S.Z., Lefkowitz, R.J., Minneman, K.P., Molinoff, P.B., Ruffolo Jr, R.R. and Trendelenburg, U. (1994) 'International Union of Pharmacology nomenclature of adrenoceptors.', *Pharmacological Reviews*, 46(2), pp. 121–136. doi:10.1016/0165-6147(85)90003-3.

Cahill, T.J., Thomsen, A.R.B., Tarrasch, J.T., Plouffe, B., Nguyen, A.H., Yang, F., Huang, L.Y., Kahsai, A.W., Bassoni, D.L., Gavino, B.J., Lamerdin, J.E., Triest, S., Shukla, A.K., Berger, B., Little, J., Antar, A., Blanc, A., Qu, C.X., Chen, X., *et al.* (2017) 'Distinct conformations of GPCR-ß-arrestin complexes mediate desensitization, signaling, and endocytosis', *Proceedings of the National Academy of Sciences of the United States of America*, 114(10), pp. 2562–2567. doi:10.1073/pnas.1701529114.

Carullo, G., Mazzotta, S., Vega-holm, M., Iglesias-guerra, F., Vega-p, M., Aiello, F. and Brizzi, A. (2021) 'GPR120 / FFAR4 Pharmacology : Focus on Agonists in Type 2 Diabetes Mellitus Drug Discovery', *Journal of Medicinal Chemistry*, 6(48), pp. 4312–4332. doi:10.1021/acs.jmedchem.0c01002.

Carvajal, J.A., Germain, A.M., Huidobro-Toro, J.P. and Weiner, C.P. (2000) 'Molecular mechanism of cGMP-mediated smooth muscle relaxation', *Journal of Cellular Physiology*, 184(3), pp. 409–420. doi:10.1002/1097-4652(200009)184:3<409::AID-JCP16>3.0.CO;2-K.

Chambers, L.S., Black, J.L., Ge, Q., Carlin, S.M., Au, W.W., Poniris, M., Thompson, J., Johnson, P.R. and Burgess, J.K. (2003) 'PAR-2 activation, PGE2, and COX-2 in human asthmatic and nonasthmatic airway smooth muscle cells', *American Journal of Physiology - Lung Cellular and Molecular Physiology*, 285(3 29-3), pp. 619–627. doi:10.1152/ajplung.00416.2002.

Charan, J. and Kantharia, N. (2013) 'How to calculate sample size in animal studies?', *Journal of Pharmacology and Pharmacotherapeutics*, 4(4), pp. 303–306. doi:10.4103/0976-500X.119726.

Chaudhry, R. and Bordoni., B. (2021) *Anatomy, Thorax, Lungs*. Treasure Island (FL): StatPearls Publishing [Internet]. Available at: https://www.ncbi.nlm.nih.gov/books/NBK470197/?report=classic.

Chelikani, P.K., Haver, A.C. and Reidelberger, R.D. (2004) 'Comparison of the inhibitory effects of PYY (3-36) and PYY (1-36) on gastric emptying in rats', *American Journal of Physiology*, 68105(151), pp. 1064–1070. doi:10.1152/ajpregu.00376.2004.

Chen, L., Magliano, D.J. and Zimmet, P.Z. (2012) 'The worldwide epidemiology of type 2 diabetes mellitus - Present and future perspectives', *Nature Reviews Endocrinology*, pp. 228–236. doi:10.1038/nrendo.2011.183.

Cho, Y.M., Wideman, R.D. and Kieffer, T.J. (2013) 'Clinical Application of Glucagon-Like Peptide 1 Receptor Agonists for the Treatment of Type 2 Diabetes Mellitus', *Endocrinology and Metabolism*, 28(4), p. 262. doi:10.3803/enm.2013.28.4.262.

Choi, I.S., Ki, W.J., Kim, T.O., Han, E.R. and Seo, I.K. (2012) 'Seasonal factors influencing exercise-induced asthma', *Allergy, Asthma and Immunology Research*, 4(4), pp. 192–198. doi:10.4168/aair.2012.4.4.192.

Christopoulos, A. (2014) 'Advances in G protein-coupled receptor allostery: From function to structure', *Molecular Pharmacology*, 86(5), pp. 463–478. doi:10.1124/mol.114.094342.

Coope, A., Torsoni, A.S. and Velloso, L.A. (2016) 'Mechanisms in endocrinology metabolic and inflammatory pathways on the pathogenesis of type 2 diabetes', *European Journal of Endocrinology*, 174(5), pp. R175–R187. doi:10.1530/EJE-15-1065.

Cornall, L.M., Mathai, M.L., Hryciw, D.H. and McAinch, A.J. (2014) 'GPR120 agonism as a countermeasure against metabolic diseases', *Drug Discovery Today*, 19(5), pp. 670–679. doi:10.1016/j.drudis.2013.11.021.

Craft, C.M., Whitmore, D.H. and Wiechmann, A.F. (1994) 'Cone arrestin identified by targeting expression of a functional family', *Journal of Biological Chemistry*, 269(6), pp. 4613–4619. doi:10.1016/s0021-9258(17)41820-5.

Croze, M.L., Flisher, M.F., Guillaume, A., Tremblay, C., Noguchi, G.M., Granziera, S., Vivot, K., Castillo, V.C., Campbell, S.A., Ghislain, J., Huising, M.O. and Poitout, V. (2021) 'Free fatty acid receptor 4 inhibitory signaling in delta cells regulates islet hormone secretion in mice', *Molecular Metabolism*, 45(January), p. 101166. doi:10.1016/j.molmet.2021.101166.

Dann, C.E., Hsieh, J., Rattner, A. and Sharma, D. (2001) 'Insights into Wnt binding and signalling from the structures of two Frizzled cysteine-rich domains', *Letters to Nature*, 412(July), pp. 86–90.

Davenport, A.P., Alexander, S.P.H., Sharman, J.L., Pawson, A.J., Benson, H.E., Monaghan, A.E., Liew, W.C., Mpamhanga, C.P., Bonner, T.I., Neubig, R.R., Pin, J.P., Spedding, M. and Harmar, A.J. (2013) 'International union of basic and clinical pharmacology. LXXXVIII. g protein-coupled receptor list: Recommendations for new pairings with cognate Ligands', *Pharmacological Reviews*, 65(3), pp. 967–986. doi:10.1124/pr.112.007179.

Deepesh, K. and Anis, R. (2021) *Pathophysiology of Obesity*. Treasure Island (FL): StatPearls Publishing [Internet]. Available at: https://www.ncbi.nlm.nih.gov/books/NBK572076/.

Defossa, E. and Wagner, M. (2014) 'Recent developments in the discovery of FFA1 receptor agonists as novel oral treatment for type 2 diabetes mellitus', *Bioorganic and Medicinal Chemistry Letters*, 24(14), pp. 2991-3000. doi:10.1016/j.bmcl.2014.05.019.

Drucker, D.J., Philippe, J., Mojsov, S., Chick, W.L. and Habener, J.F. (1987) 'Glucagon-like peptide I stimulates insulin gene expression and increases cyclic AMP levels in a rat islet cell line', *Proceedings of the National Academy of Sciences of the United States of America*, 84(10), pp. 3434–3438. doi:10.1073/pnas.84.10.3434.

Dupré, D.J., Robitaille, M., Rebois, R.V. and Hébert, T.E. (2009) 'The role of Gβγ subunits in the organization, assembly, and function of GPCR signaling complexes', *Annual Review of Pharmacology and Toxicology*, 49, pp. 31–56. doi:10.1146/annurev-pharmtox-061008-103038.

Egerod, K.L., Engelstoft, M.S., Lund, M.L., Grunddal, K. V, Zhao, M., Barir-Jensen, D., Nygaard, E.B., Petersen, N., Holst, J.J. and Schwartz, T.W. (2015) 'Transcriptional and functional characterization of the G protein-coupled receptor repertoire of gastric somatostatin cells', *Endocrinology (United States)*, 156(11), pp. 3909-3923. doi:10.1210/EN.2015-1388.

Eishingdrelo, H. (2013) 'Minireview: Targeting GPCR Activated ERK Pathways for Drug Discovery', *Current Chemical Genomics and Translational Medicine*, 7, pp. 9–15. doi:10.2174/2213988501307010009.

Engelking, L.R. (2015) 'Fatty Acid Biosynthesis', in *Textbook of Veterinary Physiological Chemistry*, pp. 358–364. doi:10.1016/b978-0-12-391909-0.50056-6.

Engelstoft, M.S., Park, W. mee, Sakata, I., Kristensen, L. V., Husted, A.S., Osborne-Lawrence, S., Piper, P.K., Walker, A.K., Pedersen, M.H., Nøhr, M.K., Pan, J., Sinz, C.J., Carrington, P.E., Akiyama, T.E., Jones, R.M., Tang, C., Ahmed, K., Offermanns, S., Egerod, K.L., *et al.* (2013) 'Seven transmembrane G protein-coupled receptor repertoire of gastric ghrelin cells', *Molecular Metabolism*, 2(4), pp. 376–392. doi:10.1016/j.molmet.2013.08.006.

Exton, J.H. (1996) 'Regulation of phosphoinositide phospholipases by hormones, neurotransmitters, and other agonists linked to G proteins', *Annual Review of Pharmacology and Toxicology*, 36, pp. 481–509. doi:10.1146/annurev.pa.36.040196.002405.

Finlin, B.S., Zhu, B., Kok, B.P., Godio, C., Westgate, P.M., Grayson, N., Sims, R., Bland, J.S., Saez, E. and Kern, P.A. (2017) 'The influence of a KDT501, a novel isohumulone, on adipocyte function in humans', *Frontiers in Endocrinology*, 8(SEP), pp. 1–11. doi:10.3389/fendo.2017.00255.

Flanagan, C.A. and Manilall, A. (2017) 'Gonadotropin-releasing hormone (GnRH) receptor structure and GnRH binding', *Frontiers in Endocrinology*, 8(OCT), pp. 1–14. doi:10.3389/fendo.2017.00274.

Fortner, C.N., Breyer, R.M. and Paul, R.J. (2001) 'EP2 receptors mediate airway relaxation to substance P, ATP, and PGE2', *American Journal of Physiology - Lung Cellular and Molecular Physiology*, 281(2 25-2), pp. 469–474. doi:10.1152/ajplung.2001.281.2.l469.

Fre, S. (2015) 'Intestinal stem cells', *Stem Cell Biology and Regenerative Medicine*, 12(5), pp. 455–475. doi:10.5937/mckg47-3311.

Fredriksson, R., Lagerström, M.C., Lundin, L.G. and Schiöth, H.B. (2003) 'The G-protein-coupled receptors in the human genome form five main families. Phylogenetic analysis, paralogon groups, and fingerprints', *Molecular Pharmacology*, 63(6), pp. 1256-1272. doi:10.1124/mol.63.6.1256.

Fromm, C., Coso, O.A., Montaner, S., Xu, N. and Gutkind, J.S. (1997) 'The small GTP-binding protein Rho links G protein-coupled receptors and Gα12 to the serum response element and to cellular transformation', *Proceedings of the National Academy of Sciences of the United States of America*, 94(19), pp. 10098–10103. doi:10.1073/pnas.94.19.10098.

Fronik, P., Gaiser, B.I. and Sejer Pedersen, D. (2017) 'Bitopic Ligands and Metastable Binding Sites: Opportunities for G Protein-Coupled Receptor (GPCR) Medicinal Chemistry', *Journal of Medicinal Chemistry*, 60(10), pp. 4126–4134. doi:10.1021/acs.jmedchem.6b01601.

Fryer, A.D. and Jacoby, D.B. (1998) 'Muscarinic receptors and control of airway smooth muscle', *American Journal of Respiratory and Critical Care Medicine*, 158(5 III), pp. 154–160. doi:10.1164/ajrccm.158.supplement_2.13tac120.

Fujiwara, K., Maekawa, F. and Yada, T. (2005) ' Oleic acid interacts with GPR40 to induce Ca 2+ signaling in rat islet β-cells: mediation by PLC and L-type Ca 2+ channel and link to insulin release ', *American Journal of Physiology-Endocrinology and Metabolism*. 289(4). doi:10.1152/ajpendo.00035.2005.

Galindo, M.M., Voigt, N., Stein, J., Van lengerich, J., Raguse, J.D., Hofmann, T., Meyerhof, W. and Behrens, M. (2012) 'G protein-coupled receptors in human fat taste perception', *Chemical Senses*, 37(2), pp. 123–139. doi:10.1093/chemse/bjr069.

Galli, C. and Risé, P. (2006) 'Origin of fatty acids in the body: Endogenous synthesis versus dietary intakes', *European Journal of Lipid Science and Technology*, 108(6), pp. 521–525. doi:10.1002/ejlt.200600056.

Gao, Z.G. and Jacobson, K.A. (2013) 'Allosteric modulation and functional selectivity of G protein-coupled receptors', *Drug Discovery Today: Technologies*,

10(2), pp. e237–e243. doi:10.1016/j.ddtec.2012.08.004.

Gautam, N., Downes, G.B., Yan, K. and Kisselev, O. (1998) 'The G-protein βγ complex', *Cellular Signalling*, 10(7), pp. 447–455. doi:10.1016/S0898-6568(98)00006-0.

Ghislain, J. and Poitout, V. (2017) 'The Role and Future of FFA1 as a Therapeutic Target', in *Handb Exp Pharmacol*, pp. 159–180.

Gilman, A.G. (1987) 'G proteins: transducers of receptor-generated signals.', *Annual review of biochemistry*, pp. 615–649. doi:10.1146/annurev.bi.56.070187.003151.

Gohla, A., Harhammer, R. and Schultz, G. (1998) 'The G-protein G13 but not G12 mediates signaling from lysophosphatidic acid receptor via epidermal growth factor receptor to Rho', *Journal of Biological Chemistry*, 273(8), pp. 4653–4659. doi:10.1074/jbc.273.8.4653.

Goodman, O., Krupnick, J.G., Santini, F., Gurevich, V. V, Penn, R.B., Gagnon, A.W., Keen, J.H. and Benovic, J.L. (1996) 'β-Arrestin acts as a clathrin adaptor in endocytosis of the β2-adrenergic receptor', *Nature*, 383(October), pp. 447–450.

Gosens, R., Zaagsma, J., Meurs, H. and Halayko, A.J. (2006) 'Muscarinic receptor signaling in the pathophysiology of asthma and COPD', *Respiratory Research*, 7, pp. 1–15. doi:10.1186/1465-9921-7-73.

Grandt, D., Schimiczek, M., Beglinger, C., Layer, P., Goebell, H., Eysselein, V.E. and Reeve, J.R. (1994) 'Two molecular forms of Peptide YY (PYY) are abundant in human blood: characterization of a radioimmunoassay recognizing PYY 1-36 and PYY 3-36', *Regulatory Peptides*, 51(2), pp. 151–159. doi:10.1016/0167-0115(94)90204-6.

Gross, N.J. and Barnes, P.J. (2017) 'New Therapies for Asthma and Chronic Obstructive Pulmonary Disease', *American Journal of Respiratory and Critical Care Medicine*, 195(2), pp. 159–166. doi:10.1164/rccm.201610-2074PP.

Grygiel-Górniak, B. (2014) 'Peroxisome proliferator-activated receptors and their ligands: Nutritional and clinical implications - A review', *Nutrition Journal*, 13(1), pp. 1–10. doi:10.1186/1475-2891-13-17.

Guilherme, A., Virbasius, J. V., Puri, V. and Czech, M.P. (2008) 'Adipocyte dysfunctions linking obesity to insulin resistance and type 2 diabetes', *Nature Reviews Molecular Cell Biology*, 9(5), pp. 367–377. doi:10.1038/nrm2391.Adipocyte.

Guo, P., Tai, Y., Wang, M., Sun, H., Zhang, L., Wei, W., Xiang, Y.K. and Wang, Q. (2022) 'Gα12 and Gα13: Versatility in Physiology and Pathology', *Frontiers in Cell and Developmental Biology*, 10(February), pp. 1–19. doi:10.3389/fcell.2022.809425.

Gurevich, E. V., Tesmer, J.J.G., Mushegian, A. and Gurevich, V. V. (2012) 'G protein-coupled receptor kinases: More than just kinases and not only for GPCRs', *Pharmacology and Therapeutics*, 133(1), pp. 40–69. doi:10.1016/j.pharmthera.2011.08.001.

Gurevich, V. V. and Gurevich, E. V. (2006) 'The structural basis of arrestin-mediated regulation of G-protein-coupled receptors', *Pharmacology and Therapeutics*, 110(3), pp. 465–502. doi:10.1016/j.pharmthera.2005.09.008.

Gurevich, V. V. and Gurevich, E. V. (2008) 'How and why do GPCRs dimerize?', *Trends in Pharmacological Sciences*, 29(5), pp. 234–240. doi:10.1016/j.tips.2008.02.004.

Gurevich, V. V. and Gurevich, E. V. (2019) 'The structural basis of the arrestin binding to GPCRs', *Molecular and Cellular Endocrinology*, 484(January), pp. 34–41. doi:10.1016/j.mce.2019.01.019.

Hafen, B. and Burns, B. (2022) *Physiology, Smooth Muscle*. Treasure Island (FL): StatPearls Publishing [Internet]. Available at: https://www.ncbi.nlm.nih.gov/books/NBK526125/.

Hara, T., Hirasawa, A., Sun, Q., Sadakane, K., Itsubo, C., Iga, T., Adachi, T.,

Koshimizu, T.A., Hashimoto, T., Asakawa, Y. and Tsujimoto, G. (2009) 'Novel selective ligands for free fatty acid receptors GPR120 and GPR40', *Naunyn-Schmiedeberg's Archives of Pharmacology*, 380(3), pp. 247–255. doi:10.1007/s00210-009-0425-9.

Hara, T., Kashihara, D., Ichimura, A., Kimura, I., Tsujimoto, G. and Hirasawa, A. (2014) 'Role of free fatty acid receptors in the regulation of energy metabolism', *Biochimica et Biophysica Acta - Molecular and Cell Biology of Lipids,* 1841(9), pp. 1292-1300. doi:10.1016/j.bbalip.2014.06.002.

Harmar, A.J. (2001) 'Family-B G-protein-coupled receptors', *Genome Biology*, 2(12), pp. 1–10. doi:10.1186/gb-2001-2-12-reviews3013.

Hassani, M. and Koenderman, L. (2018) 'Immunological and hematological effects of IL-5(Rα)-targeted therapy: An overview', *Allergy: European Journal of Allergy and Clinical Immunology*, 73(10), pp. 1979–1988. doi:10.1111/all.13451.

Hatting, M., Tavares, C.D.J., Sharabi, K., Rines, A.K. and Puigserver, P. (2018) 'Insulin regulation of gluconeogenesis', *Annals of the New York Academy of Sciences*, 1411(1), pp. 21–35. doi:10.1111/nyas.13435.

Hauge, M., Vestmar, Marie A, Husted, A.S., Ekberg, J.P., Wright, M.J., Di Salvo, J., Weinglass, A.B., Engelstoft, M.S., Madsen, A.N., Lückmann, M., Miller, M.W., Trujillo, M.E., Frimurer, T.M., Holst, B., Howard, A.D. and Schwartz, T.W. (2015) 'GPR40 (FFAR1) - Combined Gs and Gq signaling invitro is associated with robust incretin secretagogue action ex vivo and in vivo', *Molecular Metabolism*, 4(1), pp. 3–14. doi:10.1016/j.molmet.2014.10.002.

Hauser, A.S., Attwood, M.M., Rask-Andersen, M., Schiöth, H.B. and Gloriam, D.E. (2017) 'Trends in GPCR drug discovery: New agents, targets and indications', *Nature Reviews Drug Discovery*, 16(12), pp. 829–842. doi:10.1038/nrd.2017.178.

Hauser, A.S., Avet, C., Normand, C., Mancini, A., Inoue, A., Bouvier, M. and Gloriam, D.E. (2022) 'Common coupling map advances GPCR-G protein selectivity', *eLife*, 11, pp. 1–22. doi:10.7554/eLife.74107.

Hermans, E. (2003) 'Biochemical and pharmacological control of the multiplicity of coupling at G-protein-coupled receptors', *Pharmacology and Therapeutics*, 99(1), pp. 25–44. doi:10.1016/S0163-7258(03)00051-2.

Hirasawa, A., Tsumaya, K., Awaji, T., Katsuma, S., Adachi, T., Yamada, M., Sugimoto, Y., Miyazaki, S. and Tsujimoto, G. (2005) 'Free fatty acids regulate gut incretin glucagon-like peptide-1 secretion through GPR120', *Nature Medicine*, 11(1), pp. 90–94. doi:10.1038/nm1168.

Hodavance, S.Y., Gareri, C., Torok, R.D. and Rockman, H.A. (2016) 'G protein-coupled receptor biased agonism', *Journal of Cardiovascular Pharmacology*, 67(3), pp. 193–202. doi:10.1097/FJC.0000000000000356.

Hoffmann, C., Zürn, A., Bünemann, M. and Lohse, M.J. (2008) 'Conformational changes in G-protein-coupled receptors - The quest for functionally selective conformations is open', *British Journal of Pharmacology*, 153(SUPPL. 1), pp. 358–366. doi:10.1038/sj.bjp.0707615.

Holdcroft, C. (1994) 'Salmeterol_ A Long-Acting β 2 -Agonist For Asthma.pdf', *The Nurse Practitioner*, 19(7), pp. 9–10.

Hudson, B.D., Christiansen, E., Tikhonova, I.G., Grundmann, M., Kostenis, E., Adams, D.R., Ulven, T. and Milligan, G. (2012) 'Chemically engineering ligand selectivity at the free fatty acid receptor 2 based on pharmacological variation between species orthologs', *FASEB Journal*, 26(12), pp. 4951–4965. doi:10.1096/fj.12-213314.

Hudson, B.D., Murdoch, H. and Milligan, G. (2013) 'Minireview: The effects of spcies ortholog and SNP variation on receptors for free fatty acids', *Molecular Endocrinology*, 27(8), pp. 1177–1187. doi:10.1210/me.2013-1085.

Hudson, B.D., Shimpukade, B., Mackenzie, A.E., Butcher, A.J., Pediani, J.D., Christiansen, E., Heathcote, H., Tobin, A.B., Ulven, T. and Milligan, G. (2013) 'The pharmacology of TUG-891, a potent and selective agonist of the free fatty acid receptor 4 (FFA4/GPR120), demonstrates both potential opportunity and possible challenges to therapeutic agonism', *Molecular Pharmacology*, 84(5), pp.

710-725. doi:10.1124/mol.113.087783.

Hudson, B.D., Shimpukade, B., Milligan, G. and Ulven, T. (2014) 'The molecular basis of ligand interaction at free fatty acid receptor 4 (FFA4/GPR120)', *Journal of Biological Chemistry*, 289(29), pp. 20345–20358. doi:10.1074/jbc.M114.561449.

Hudson, B.D., Smith, N.J. and Milligan, G. (2011) *Experimental Challenges to Targeting Poorly Characterized GPCRs. Uncovering the Therapeutic Potential for Free Fatty Acid Receptors*, *Advances in Pharmacology*. doi:10.1016/B978-0-12-385952-5.00006-3.

Humphries, A. and Wright, N.A. (2008) 'Colonic crypt organization and tumorigenesis', *Nature Reviews Cancer*, pp. 415–424. doi:10.1038/nrc2392.

Ichimura, A., Hasegawa, S., Kasubuchi, M. and Kimura, I. (2014) 'Free fatty acid receptors as therapeutic targets for the treatment of diabetes', *Frontiers in Pharmacology*, 5(NOV), pp. 1–6. doi:10.3389/fphar.2014.00236.

Ichimura, A., Hirasawa, A., Poulain-Godefroy, O., Bonnefond, A., Hara, T., Yengo, L., Kimura, I., Leloire, A., Liu, N., Iida, K., Choquet, H., Besnard, P., Lecoeur, C., Vivequin, S., Ayukawa, K., Takeuchi, M., Ozawa, K., Tauber, M., Maffeis, C., *et al.* (2012) 'Dysfunction of lipid sensor GPR120 leads to obesity in both mouse and human', *Nature*, 483(7389), pp. 350–354. doi:10.1038/nature10798.

International Diabetes Federation (2021) *IDF Diabetes Atlas 2021*, *International Diabetes Federation*. doi:10.1016/j.diabres.2013.10.013.

Islam, S. (2015) *Islets of langerhans, second edition*, *Islets of Langerhans, Second Edition*. doi:10.1007/978-94-007-6686-0.

Itoh, Y., Kawamata, Y., Harada, M., Kobayashi, M., Fujii, R., Fukusumi, S., Ogi, K., Hosoya, M., Tanaka, Y., Uejima, H., Tanaka, H., Maruyama, M., Satoh, R., Okubo, S., Kizawa, H., Komatsu, H., Matsumura, F., Noguchi, Y., Shinohara, T., *et al.* (2003) 'Free fatty acids regulate insulin secretion from pancreatic β cells

through GPR40', *Nature,* 422(6928), pp. 173-176. doi:10.1038/nature01478.

Jarpe, M.B., Knall, C., Mitchell, F.M., Buhl, A.M., Duzic, E. and Johnson, G.L. (1998) '[D-Arg1,d-Phe5,d-Trp(7,9),Leu11]substance P acts as a biased agonist toward neuropeptide and chemokine receptors', *Journal of Biological Chemistry*, 273(5), pp. 3097–3104. doi:10.1074/jbc.273.5.3097.

Jensen, J., Rustad, P.I., Kolnes, A.J. and Lai, Y.C. (2011) 'The role of skeletal muscle glycogen breakdown for regulation of insulin sensitivity by exercise', *Frontiers in Physiology*, 2 DEC(December 2011). doi:10.3389/fphys.2011.00112.

Johnson, M. (1998) 'The B2-Adrenoceptor', *American Journal of Respiratory and Critical Care Medicine*, 158(2), pp. 146–153.

Kahsai, A.W., Pani, B. and Lefkowitz, R.J. (2018) 'GPCR signaling: conformational activation of arrestins', *Cell Research,* (July), pp. 3–4. doi:10.1038/s41422-018-0067-x.

Kaku, K., Araki, T. and Yoshinaka, R. (2013) 'Randomized, double-blind, dose-ranging study of TAK-875, a novel GPR40 agonist, in Japanese patients with inadequately controlled type 2 diabetes', *Diabetes Care*, 36(2), pp. 245-250. doi:10.2337/dc12-0872.

Kamato, D., Thach, L., Bernard, R., Chan, V., Zheng, W., Kaur, H., Brimble, M., Osman, N. and Little, P.J. (2015) 'Structure, Function, Pharmacology, and Therapeutic Potential of the G Protein, Gα/q,11', *Frontiers in Cardiovascular Medicine*, 2(June). doi:10.3389/fcvm.2015.00014.

Kang, G., Chepurny, O.G., Rindler, M.J., Collis, L., Chepurny, Z., Li, W.H., Harbeck, M., Roe, M.W. and Holz, G.G. (2005) 'A cAMP and Ca2+ coincidence detector in support of Ca2+-induced Ca2+ release in mouse pancreatic β cells', *Journal of Physiology*, 566(1), pp. 173–188. doi:10.1113/jphysiol.2005.087510.

Kang, Y., Zhou, X.E., Gao, X., He, Y., Liu, W., Ishchenko, A., Barty, A., White, T.A., Yefanov, O., Han, G.W., Xu, Q., De Waal, P.W., Ke, J., Tan, M.H.E., Zhang, C., Moeller, A., West, G.M., Pascal, B.D., Van Eps, N., *et al.* (2015)

'Crystal structure of rhodopsin bound to arrestin by femtosecond X-ray laser', *Nature*, 523(7562), pp. 561–567. doi:10.1038/nature14656.

Kanwal, A., Kanwar, N., Bharati, S., Srivastava, P., Singh, S.P. and Amar, S. (2022) 'Exploring New Drug Targets for Type 2 Diabetes: Success, Challenges and Opportunities', *Biomedicines*, 10(2), pp. 1–18. doi:10.3390/biomedicines10020331.

Karageorgos, V., Venihaki, M., Sakellaris, S., Pardalos, M., Kontakis, G., Matsoukas, M.T., Gravanis, A., Margioris, A. and Liapakis, G. (2018) 'Current understanding of the structure and function of family B GPCRs to design novel drugs', *Hormones*, 17(1), pp. 45–59. doi:10.1007/s42000-018-0009-5.

Karaki, S.I., Tazoe, H., Hayashi, H., Kashiwabara, H., Tooyama, K., Suzuki, Y. and Kuwahara, A. (2008) 'Expression of the short-chain fatty acid receptor, GPR43, in the human colon', *Journal of Molecular Histology*, 39(2), pp. 135–142. doi:10.1007/s10735-007-9145-y.

Karra, E., Chandarana, K. and Batterham, R.L. (2009) 'The role of peptide YY in appetite regulation and obesity', 1, pp. 19–25. doi:10.1113/jphysiol.2008.164269.

Katritch, V., Cherezov, V. and Stevens, R.C. (2012) 'Diversity and modularity of G protein-coupled receptor structures', *Trends in Pharmacological Sciences*, 33(1), pp. 17–27. doi:10.1016/j.tips.2011.09.003.

Kebede, M.A., Alquier, T., Latour, M.G. and Poitout, V. (2009) 'Lipid receptors and islet function: Therapeutic implications?', *Diabetes, Obesity and Metabolism*, 11(SUPPL. 4), pp. 10–20. doi:10.1111/j.1463-1326.2009.01114.x.

Kelly, E., Bailey, C.P. and Henderson, G. (2008) 'Agonist-selective mechanisms of GPCR desensitization', *British Journal of Pharmacology*, 153(SUPPL1), pp. 379–388. doi:10.1038/sj.bjp.0707604.

Kenakin, T., Watson, C., Muniz-Medina, V., Christopoulos, A. and Novick, S. (2012) 'A simple method for quantifying functional selectivity and agonist bias',

ACS Chemical Neuroscience, 3(3), pp. 193–203. doi:10.1021/cn200111m.

Kenakin, T.P. and Miller, L.J. (2010) 'Seven transmembrane receptors as shapeshifting proteins: The impact of allosteric modulation and functional selectivity on new drug discovery', *Pharmacological Reviews*, 62(2), pp. 265–304. doi:10.1124/pr.108.000992.

Kenakin, T.P. and Morgan, P.H. (1989) 'Theoretical effects of single and multiple transducer receptor coupling proteins on estimates of the relative potency of agonists', *Molecular Pharmacology*, 35(2), pp. 214–222.

Khan., Y.S. and Lynch., D.T. (2022) *Histology, Lung*. Treasure Island (FL): StatPearls Publishing [Internet]. Available at: https://www.ncbi.nlm.nih.gov/books/NBK534789/.

Khan, M.A.B., Hashim, M.J., King, J.K., Govender, R.D., Mustafa, H. and Kaabi, J. Al (2020) 'Epidemiology of Type 2 Diabetes – Global Burden of Disease and Forecasted Trends', *Journal of Epidemiology and Global Health*, 10, pp. 107–111.

Kia'i, N. and Bajaj, T. (2022) *Histology, Respiratory Epithelium*. Treasure Island (FL): StatPearls Publishing [Internet]. Available at: https://www.ncbi.nlm.nih.gov/books/NBK541061/

Kieffer, P. and Epstein, K. (2022) *Small Colon Enterolith, Comparative Veterinary Anatomy*. Elsevier Inc. doi:10.1016/b978-0-323-91015-6.00059-5.

Kiela, P.R. and Ghishan, F.K. (2016) 'Physiology of intestinal absorption and secretion', *Best Practice and Research: Clinical Gastroenterology*, 30(2), pp. 145–159. doi:10.1016/j.bpg.2016.02.007.

Kim, R.Y., Rae, B., Neal, R., Donovan, C., Pinkerton, J., Balachandran, L., Starkey, M.R., Knight, D.A., Horvat, J.C. and Hansbro, P.M. (2016) 'Elucidating novel disease mechanisms in severe asthma', *Clinical & Translational Immunology*, 5(7), p. e91. doi:10.1038/cti.2016.37.

Kimura, I., Ichimura, A., Ohue-Kitano, R. and Igarashi, M. (2020) 'Free fatty acid receptors in health and disease', *Physiological Reviews*, 100(1), pp. 171–210. doi:10.1152/physrev.00041.2018.

Konda, V.R., Desai, A., Darland, G., Grayson, N. and Bland, J.S. (2014) 'KDT501, a derivative from hops, normalizes glucose metabolism and body weight in rodent models of diabetes', *PLoS ONE*, 9(1). doi:10.1371/journal.pone.0087848.

Kotarsky, K., Nilsson, N.E., Flodgren, E., Owman, C. and Olde, B. (2003) 'A human cell surface receptor activated by free fatty acids and thiazolidinedione drugs', *Biochemical and Biophysical Research Communications,* 301(2), pp. 406-410. doi:10.1016/S0006-291X(02)03064-4.

Kunishima, N., Shimada, Y., Tsuji, Y., Sato, T., Yamamoto, M., Kumasaka, T., Nakanishi, S., Jingami, H. and Morikawa, K. (2000) 'Structural basis of glutamate recognition by a dimeric metabotropic glutamate receptor', *Nature*, 407(6807), pp. 971–977. doi:10.1038/35039564.

Lambrecht, B.N., Hammad, H. and Fahy, J. V. (2019) 'The Cytokines of Asthma', *Immunity*, 50(4), pp. 975–991. doi:10.1016/j.immuni.2019.03.018.

Lambright, D.G., Sondek, J., Bohm, A., Skiba:J:, N.P., Hamm, H.E., Be, : and Sigler, P.B. (1996) 'The 2.0 A crystal structure of a heterotrimeric G protein The sites of post-translational modification on G Structure determination and refinement', *Nature*, 379(January), pp. 311–319. Available at: https://www.nature.com/articles/379311a0.pdf.

Lane, J.R., Sexton, P.M. and Christopoulos, A. (2013) 'Bridging the gap: Bitopic ligands of G-protein-coupled receptors', *Trends in Pharmacological Sciences*, 34(1), pp. 59–66. doi:10.1016/j.tips.2012.10.003.

Lankatillake, C., Huynh, T. and Dias, D.A. (2019) 'Understanding glycaemic control and current approaches for screening antidiabetic natural products from evidence-based medicinal plants', *Plant Methods*, 15(1), pp. 1–36. doi:10.1186/s13007-019-0487-8.

Laporte, S.A., Oakley, R.H., Zhang, J., Holt, J.A., Ferguson, S.S.G., Caron, M.G. and Barak, L.S. (1999) 'The ß2-adrenergic receptor/ßarrestin complex recruits the clathrin adaptor AP-2 during endocytosis', *Proceedings of the National Academy of Sciences of the United States of America*, 96(7), pp. 3712–3717. doi:10.1073/pnas.96.7.3712.

Larsen, S.B., Cowley, C.J. and Fuchs, E. (2020) 'Epithelial cells: liaisons of immunity', *Current Opinion in Immunology*, 62, pp. 45–53. doi:10.1016/j.coi.2019.11.004.

Latorraca, N.R., Venkatakrishnan, A.J. and Dror, R.O. (2017) 'GPCR dynamics: Structures in motion', *Chemical Reviews*, 117(1), pp. 139–155. doi:10.1021/acs.chemrev.6b00177.

Latorre, Rocco, Huynh, J., Mazzoni, M., Gupta, A., Bonora, E., Clavenzani, P., Chang, L., Mayer, E.A., De Giorgio, R. and Sternini, C. (2016) 'Expression of the Bitter taste receptor, T2R38, in enteroendocrine cells of the colonic mucosa of overweight/obese vs. Lean subjects', *PLoS ONE*, 11(2), pp. 1–16. doi:10.1371/journal.pone.0147468.

Latorre, R., Sternini, C., De Giorgio, R. and Greenwood-Van Meerveld, B. (2016) 'Enteroendocrine cells: A review of their role in brain-gut communication', *Neurogastroenterology and Motility*, 28(5), pp. 620–630. doi:10.1111/nmo.12754.

Lee, K.P., Park, S.J., Kang, S., Koh, J.M., Sato, K., Chung, H.Y., Okajima, F. and Im, D.S. (2017) 'ω-3 polyunsaturated fatty acids accelerate airway repair by activating FFA4 in club cells', *American Journal of Physiology - Lung Cellular and Molecular Physiology*, 312(6), pp. L835–L844. doi:10.1152/ajplung.00350.2016.

León, B. and Ballesteros-Tato, A. (2021) 'Modulating Th2 Cell Immunity for the Treatment of Asthma', *Frontiers in Immunology*, 12(February), pp. 1–14. doi:10.3389/fimmu.2021.637948.

Leroy, D., Missotten, M., Waltzinger, C., Martin, T. and Scheer, A. (2007) 'G

protein-coupled receptor-mediated ERK1/2 phosphorylation: Towards a generic sensor of GPCR activation', *Journal of Receptors and Signal Transduction*, 27(1), pp. 83–97. doi:10.1080/10799890601112244.

Levoye, A., Dam, J., Ayoub, M.A., Guillaume, J.L. and Jockers, R. (2006) 'Do orphan G-protein-coupled receptors have ligand-independent functions? New insights from receptor heterodimers', *EMBO Reports,* 7(11), pp. 1094-1098. doi:10.1038/sj.embor.7400838.

Li, L., Homan, K.T., Vishnivetskiy, S.A., Manglik, A., Tesmer, J.J.G., Gurevich, V. V. and Gurevich, E. V. (2015) 'G protein-coupled receptor kinases of the GRK4 protein subfamily phosphorylate inactive G protein-coupled receptors (GPCRs)', *Journal of Biological Chemistry*, 290(17), pp. 10775–10790. doi:10.1074/jbc.M115.644773.

Liddle, R.A. (2018) 'Interactions of Gut Endocrine Cells with Epithelium and Neurons', *Comprehensive Physiology*, 8(3), pp. 1019–1030. doi:10.1002/cphy.c170044.Interactions.

Light, P.E., Manning Fox, J.E., Riedel, M.J. and Wheeler, M.B. (2002) 'Glucagon-like peptide-1 inhibits pancreatic ATP-sensitive potassium channels via a protein kinase A- and ADP-dependent mechanism', *Molecular Endocrinology*, 16(9), pp. 2135–2144. doi:10.1210/me.2002-0084.

Lin, H.C., Zhao, X.T., Wang, L. and Wong, H. (1996) 'Fat-induced ileal brake in the dog depends on peptide YY', *Gastroenterology*, 110(5), pp. 1491–1495. doi:10.1053/gast.1996.v110.pm8613054.

Liu, Y., Chen, L.Y., Sokolowska, M., Eberlein, M., Alsaaty, S., Martinez-Anton, A., Logun, C., Qi, H.Y. and Shelhamer, J.H. (2014) 'The fish oil ingredient, docosahexaenoic acid, activates cytosolic phospholipase A2 via GPR120 receptor to produce prostaglandin E2 and plays an anti-inflammatory role in macrophages', *Immunology,* 143(1), pp. 81–95. doi:10.1111/imm.12296.

Lohse, M.J., Benovic, J.L., Codina, J., Caron, M.G. and Lefkowitz, R.J. (1990) 'β-Arrestin : A Protein That Regulates β-Adrenergic Function', *Science*, (7), pp.

1–4.

Lohse, M.J. and Hoffmann, C. (2014) *Not just signal Shutoff: The protective role of arrestin-1 in rod cells, Arrestin Interactions with G Protein-Coupled Receptors. In: Gurevich, V. (eds) Arrestins - Pharmacology and Therapeutic Potential. Handbook of Experimental Pharmacology.* doi:10.1007/978-3-642-41199-1_5.

Lu, X., Zhao, X., Feng, J., Liou, A.P., Anthony, S., Pechhold, S., Sun, Y., Lu, H. and Wank, S. (2012) 'Postprandial inhibition of gastric ghrelin secretion by long-chain fatty acid through GPR120 in isolated gastric ghrelin cells and mice', *American Journal of Physiology - Gastrointestinal and Liver Physiology*, 303(3), pp. 367–376. doi:10.1152/ajpgi.00541.2011.

Luttrell, L.M. (2008) 'Reviews in molecular biology and biotechnology: Transmembrane signaling by G protein-coupled receptors', *Molecular Biotechnology*, 39(3), pp. 239–264. doi:10.1007/s12033-008-9031-1.

Luttrell, L.M. and Gesty-Palmer, D. (2010) 'Beyond desensitization: Physiological relevance of arrestin-dependent signaling', *Pharmacological Reviews*, 62(2), pp. 305–330. doi:10.1124/pr.109.002436.

Luttrell, L.M., Roudabush, F.L., Choy, E.W., Miller, W.E., Field, M.E., Pierce, K.L. and Lefkowitz, R.J. (2001) 'Activation and targeting of extracellular signal-regulated kinases by β-arrestin scaffolds', *Proceedings of the National Academy of Sciences of the United States of America*, 98(5), pp. 2449–2454. doi:10.1073/pnas.041604898.

Ma, H., Bell, K.N. and Loker, R.N. (2021) 'qPCR and qRT-PCR analysis: Regulatory points to consider when conducting biodistribution and vector shedding studies', *Molecular Therapy - Methods and Clinical Development*, 20(March), pp. 152–168. doi:10.1016/j.omtm.2020.11.007.

MacDonald, P.E., El-kholy, W., Riedel, M.J., Salapatek, A.M.F., Light, P.E. and Wheeler, M.B. (2002) 'The multiple actions of GLP-1 on the process of glucose-stimulated insulin secretion', *Diabetes*, 51(SUPPL. 3).

doi:10.2337/diabetes.51.2007.s434.

Madamanchi, A. (2007) 'B-Adrenergic Receptor Signaling in Cardiac Function and Heart Failure', *McGill Journal of Medicine*, 10(2), pp. 99–104. doi:10.26443/mjm.v10i2.458.

Majumdar, S.K. and Inzucchi, S.E. (2013) 'Investigational anti-hyperglycemic agents: The future of type 2 diabetes therapy?', *Endocrine*, 44(1), pp. 47–58. doi:10.1007/s12020-013-9884-3.

Mancini, A.D., Bertrand, G., Vivot, K., Carpentier, É., Tremblay, C., Ghislain, J., Bouvier, M. and Poitout, V. (2015) 'ß-arrestin recruitment and biased agonism at free fatty acid receptor 1', *Journal of Biological Chemistry*, 290(34), pp. 21131-21140. doi:10.1074/jbc.M115.644450.

Mantas, I., Saarinen, M., Xu, Z.Q.D. and Svenningsson, P. (2022) 'Update on GPCR-based targets for the development of novel antidepressants', *Molecular Psychiatry*, 27(1), pp. 534–558. doi:10.1038/s41380-021-01040-1.

Marín-Peñalver, J.J., Martín-Timón, I., Sevillano-Collantes, C. and Cañizo-Gómez, F.J. del (2016) 'Update on the treatment of type 2 diabetes mellitus', *World Journal of Diabetes*, 7(17), p. 354. doi:10.4239/wjd.v7.i17.354.

Marion, S., Oakley, R.H., Kim, K.M., Caron, M.G. and Barak, L.S. (2006) 'A ß-arrestin binding determinant common to the second intracellular loops of rhodopsin family G protein-coupled receptors', *Journal of Biological Chemistry*, 281(5), pp. 2932–2938. doi:10.1074/jbc.M508074200.

Marsango, S., Jenkins, L., Pediani, J. and Bradley, S. (2022) 'The M 1 muscarinic receptor is present in situ as a ligand-regulated mixture of monomers and oligomeric complexes ligand-regulated mixture of monomers and', *Proceedings of the National Academy of Sciences of the United States of America*, 119(94). doi:10.1073/pnas.2201103119.

Mason, W.T., Dempster, J., Hoyland, J., Mccann, T.J., Somasundaram, B. and O'brien, W. (1999) 'Quantitative Digital Imaging of Biological Activity in Living

Cells with Ion-sensitive Fluorescent Probes', *Fluorescent and Luminescent Probes for Biological Activity*, pp. 175–195. doi:10.1016/b978-012447836-7/50014-2.

May, R.D. and Fung, M. (2015) 'Strategies targeting the IL-4/IL-13 axes in disease', *Cytokine*, 75(1), pp. 89–116. doi:10.1016/j.cyto.2015.05.018.

McCauley, H.A. (2020) 'Enteroendocrine Regulation of Nutrient Absorption', *Journal of Nutrition*, 150(1), pp. 10–21. doi:10.1093/jn/nxz191.

De Mendoza, A., Sebé-Pedrós, A. and Ruiz-Trillo, I. (2014) 'The evolution of the GPCR signaling system in eukaryotes: Modularity, conservation, and the transition to metazoan multicellularity', *Genome Biology and Evolution*, 6(3), pp. 606–619. doi:10.1093/gbe/evu038.

Meneses, A.M.C., Schneeberger, K., Kruitwagen, H.S., Penning, L.C., van Steenbeek, F.G., Burgener, I.A. and Spee, B. (2016) 'Intestinal organoids-Current and future applications', *Veterinary Sciences*, 3(4), pp. 1–12. doi:10.3390/vetsci3040031.

Mentlein, R., Gallwitz, B. and Schmidt, W. (1993) 'and Is Responsible for Their Degradation in Human Serum', *European journal of biochemistry / FEBS*, 0215(3), pp. 829–835.

Michel, M.C. and Charlton, S.J. (2018) 'Biased agonism in drug discovery-is it too soon to choose a path?', *Molecular Pharmacology*, 93(4), pp. 259–265. doi:10.1124/mol.117.110890.

Miller, B.R., Nguyen, H., Hu, C.J.H., Lin, C. and Nguyen, Q.T. (2014) 'New and emerging drugs and targets for type 2 diabetes: Reviewing the evidence', *American Health and Drug Benefits*, 7(8), pp. 452–461.

Milligan, G. (2009) 'G protein-coupled receptor hetero-dimerization: Contribution to pharmacology and function', *British Journal of Pharmacology*, 158(1), pp. 5–14. doi:10.1111/j.1476-5381.2009.00169.x.

Milligan, G., Alvarez-Curto, E., Hudson, B.D., Prihandoko, R. and Tobin, A.B. (2017) 'FFA4/GPR120: Pharmacology and Therapeutic Opportunities', *Trends in Pharmacological Sciences*, 38(9), pp. 809–821. doi:10.1016/j.tips.2017.06.006.

Milligan, G., Shimpukade, B., Ulven, T. and Hudson, B.D. (2017) 'Complex pharmacology of free fatty acid receptors', *Chemical Reviews*, 117(1), pp. 67–110. doi:10.1021/acs.chemrev.6b00056.

Miyauchi, S., Hirasawa, A., Iga, T., Liu, N., Itsubo, C., Sadakane, K., Hara, T. and Tsujimoto, G. (2009) 'Distribution and regulation of protein expression of the free fatty acid receptor GPR120', *Naunyn-Schmiedeberg's Archives of Pharmacology*, 379(4), pp. 427–434. doi:10.1007/s00210-008-0390-8.

Mizuta, K., Gallos, G., Zhu, D., Mizuta, F., Goubaeva, F., Xu, D., Panettieri, R.A., Yang, J. and Emala, C.W. (2008) 'Expression and coupling of neurokinin receptor subtypes to inositol phosphate and calcium signaling pathways in human airway smooth muscle cells', *American Journal of Physiology - Lung Cellular and Molecular Physiology*, 294(3), pp. 523–534. doi:10.1152/ajplung.00328.2007.

Mizuta, K., Zhang, Y., Mizuta, F., Hoshijima, H., Shiga, T., Masaki, E. and Emala, C.W. (2015) 'Novel identification of the free fatty acid receptor FFAR1 that promotes contraction in airway smooth muscle', *American Journal of Physiology - Lung Cellular and Molecular Physiology*. doi:10.1152/ajplung.00041.2015.

Mojsov, S., Heinrich, G., Wilson, I.B., Ravazzola, M., Orci, L. and Habener, J.F. (1986) 'Preproglucagon gene expression in pancreas and intestine diversifies at the level of post-translational processing', *Journal of Biological Chemistry*, 261(25), pp. 11880–11889. doi:10.1016/s0021-9258(18)67324-7.

Moniri, N.H. (2016) 'Free-fatty acid receptor-4 (GPR120): Cellular and molecular function and its role in metabolic disorders', *Biochemical Pharmacology*, 110–111, pp. 1–15. doi:10.1016/j.bcp.2016.01.021.

Moodaley, R., Smith, D.M., Tough, I.R., Schindler, M. and Cox, H.M. (2017) 'Agonism of free fatty acid receptors 1 and 4 generates peptide YY-mediated

inhibitory responses in mouse colon', *British Journal of Pharmacology*, 174(23), pp. 4508–4522. doi:10.1111/bph.14054.

Moore, K., Zhang, Q., Murgolo, N., Hosted, T. and Duffy, R. (2009) 'Cloning, expression, and pharmacological characterization of the GPR120 free fatty acid receptor from cynomolgus monkey: Comparison with human GPR120 splice variants', *Comparative Biochemistry and Physiology - B Biochemistry and Molecular Biology*, 154(4), pp. 419–426. doi:10.1016/j.cbpb.2009.08.005.

Morgan, S.J., Deshpande, D.A., Tiegs, B.C., Misior, A.M., Yan, H., Hershfeld, A. V, Rich, T.C., Panettieri, R.A., An, S.S. and Penn, R.B. (2014) 'ß-agonist-mediated relaxation of airway smooth muscle is protein kinase A-dependent', *Journal of Biological Chemistry*, 289(33), pp. 23065–23074. doi:10.1074/jbc.M114.557652.

Mukherjee, S., Gurevich, V. V., Preninger, A., Hamm, H.E., Bader, M.F., Fazleabas, A.T., Birnbaumer, L. and Hunzicker-Dunn, M. (2002) 'Aspartic acid 564 in the third cytoplasmic loop of the luteinizing hormone/choriogonadotropin receptor is crucial for phosphorylation-independent interaction with arrestin2', *Journal of Biological Chemistry*, 277(20), pp. 17916–17927. doi:10.1074/jbc.M110479200.

Müller, T.D., Finan, B., Bloom, S.R., Alessio, D.D., Drucker, D.J., Flatt, P.R. and Fritsche, A. (2019) 'Glucagon-like peptide 1 (GLP-1)', *Molecular Metabolism*, 30(September), pp. 72–130. doi:10.1016/j.molmet.2019.09.010.

Nadkarni, P., Chepurny, O.G. and Holz, G.G. (2014) *Regulation of Glucose Homeostasis by GLP-1*. 1st edn, *Glucose Homeostatis and the Pathogenesis of Diabetes Mellitus*. 1st edn. Elsevier Inc. doi:10.1016/B978-0-12-800101-1.00002-8.

Nauck, M.A., Quast, D.R., Wefers, J. and Meier, J.J. (2021) 'GLP-1 receptor agonists in the treatment of type 2 diabetes – state-of-the-art', *Molecular Metabolism*, 46(October 2020), p. 101102. doi:10.1016/j.molmet.2020.101102.

Neer, E.J. (1995) 'Heterotrimeric G Proteins: Organizers of Transmembrane

Signals Review', *Cell*, 80(Jan), pp. 249–257.

Neer, E.J. and Clapham, D.E. (1988) 'Roles of G protein subunits in transmembrane signalling', *Nature*, 333(6169), pp. 129–134. doi:10.1038/333129a0.

Nejat, R., Sadr, A.S., Torshizi, M.F. and Najafi, D.J. (2022) 'GPCRs of Diverse Physiologic and Pathologic Effects with Fingerprints in COVID-19', p. 19. doi:10.3390/ecb2021-10261.

Nichols, A.S., Floyd, D.H., Bruinsma, S.P., Narzinski, K. and Baranski, T.J. (2013) 'Frizzled receptors signal through G proteins', *Cellular Signalling*, 25(6), pp. 1468–1475. doi:10.1016/j.cellsig.2013.03.009.

Nilsson, N.E., Kotarsky, K., Owman, C. and Olde, B. (2003) 'Identification of a free fatty acid receptor, FFA2R, expressed on leukocytes and activated by short-chain fatty acids', *Biochemical and Biophysical Research Communications*, 303(4), pp. 1047–1052. doi:10.1016/S0006-291X(03)00488-1.

Nobles, K.N., Xiao, K., Ahn, S., Shukla, A.K., Lam, C.M., Rajagopal, S., Strachan, R.T., Huang, T.Y., Bressler, E.A., Hara, M.R., Shenoy, S.K., Gygi, S.P. and Lefkowitz, R.J. (2011) 'Distinct phosphorylation sites on the β 2-adrenergic receptor establish a barcode that encodes differential functions of β-arrestin', *Science Signaling*, 4(185), pp. 1–11. doi:10.1126/scisignal.2001707.

Nomiyama, H. and Yoshie, O. (2015) 'Functional roles of evolutionary conserved motifs and residues in vertebrate chemokine receptors', *Journal of Leukocyte Biology*, 97(1), pp. 39–47. doi:10.1189/jlb.2ru0614-290r.

Nordström, K.J.V., Lagerström, M.C., Wallér, L.M.J., Fredriksson, R. and Schiöth, H.B. (2009) 'The Secretin GPCRs descended from the family of Adhesion GPCRs', *Molecular Biology and Evolution*, 26(1), pp. 71–84. doi:10.1093/molbev/msn228.

Oakley, R.H., Laporte, S.A., Holt, J.A., Caron, M.G. and Barak, L.S. (2000) 'Differential affinities of visual arrestin, βarrestin1, and βarrestin2 for G protein-

coupled receptors delineate two major classes of receptors', *Journal of Biological Chemistry*. doi:10.1074/jbc.M910348199.

Oh, D.Y., Talukdar, S., Bae, E.J., Imamura, T., Morinaga, H., Fan, W.Q., Li, P., Lu, W.J., Watkins, S.M. and Olefsky, J.M. (2010) 'GPR120 Is an Omega-3 Fatty Acid Receptor Mediating Potent Anti-inflammatory and Insulin-Sensitizing Effects', *Cell*, 142(5), pp. 687–698. doi:10.1016/j.cell.2010.07.041.

Oh, D.Y., Walenta, E., Akiyama, T.E., Lagakos, W.S., Lackey, D., Pessentheiner, A.R., Sasik, R., Hah, N., Chi, T.J., Cox, J.M., Powels, M.A., Di Salvo, J., Sinz, C., Watkins, S.M., Armando, A.M., Chung, H., Evans, R.M., Quehenberger, O., McNelis, J., *et al.* (2014) 'A Gpr120-selective agonist improves insulin resistance and chronic inflammation in obese mice', *Nature Medicine*. doi:10.1038/nm.3614.

Okashah, N., Wan, Q., Ghosh, S., Sandhu, M., Inoue, A., Vaidehi, N. and Lambert, N.A. (2019) 'Variable G protein determinants of GPCR coupling selectivity', *Proceedings of the National Academy of Sciences of the United States of America*, 116(24), pp. 12054–12059. doi:10.1073/pnas.1905993116.

Oldham, W.M. and Hamm, H.E. (2008) 'Heterotrimeric G protein activation by G-protein-coupled receptors', *Nature Reviews Molecular Cell Biology*, 9(1), pp. 60–71. doi:10.1038/nrm2299.

Otieno, M.A., Snoeys, J., Lam, W., Ghosh, A., Player, M.R., Pocai, A., Salter, R., Simic, D., Skaggs, H., Singh, B. and Lim, H.K. (2018) 'Fasiglifam (TAK-875): Mechanistic investigation and retrospective identification of hazards for drug induced liver injury', *Toxicological Sciences*, 163(2), pp. 374–384. doi:10.1093/toxsci/kfx040.

Page, C. and Cazzola, M. (2014) 'Bifunctional drugs for the treatment of asthma and chronic obstructive pulmonary disease', *European Respiratory Journal*, 44(2), pp. 475–482. doi:10.1183/09031936.00003814.

Parker, H.E., Habib, A.M., Rogers, G.J., Gribble, F.M. and Reimann, F. (2009) 'Nutrient-dependent secretion of glucose-dependent insulinotropic polypeptide

from primary murine K cells', *Diabetologia*, 52(2), pp. 289–298. doi:10.1007/s00125-008-1202-x.

Paulsen, S.J., Larsen, L.K., Hansen, G., Chelur, S., Larsen, P.J. and Vrang, N. (2014) 'Expression of the fatty acid receptor GPR120 in the gut of diet-induced-obese rats and its role in GLP-1 secretion', *PLoS ONE*, 9(2), pp. 2–7. doi:10.1371/journal.pone.0088227.

Peiris, M., Aktar, R., Reed, D., Cibert-Goton, V., Zdanaviciene, A., Halder, W., Robinow, A., Corke, S., Dogra, H., Knowles, C.H. and Blackshaw, A. (2022) 'Decoy bypass for appetite suppression in obese adults: role of synergistic nutrient sensing receptors GPR84 and FFAR4 on colonic endocrine cells', *Gut*, 71(5), pp. 928–937. doi:10.1136/gutjnl-2020-323219.

Peña, I. and Domínguez, J.M. (2010) 'Thermally denatured BSA, a surrogate additive to replace BSA in buffers for high-throughput screening', *Journal of Biomolecular Screening*, 15(10), pp. 1281–1286. doi:10.1177/1087057110379768.

Perez-Zoghbi, J.F., Bai, Y. and Sanderson, M.J. (2010) 'Nitric oxide induces airway smooth muscle cell relaxation by decreasing the frequency of agonist-induced Ca2+ oscillations', *Journal of General Physiology*, 135(3), pp. 247–259. doi:10.1085/jgp.200910365.

Perez, J.F. and Sanderson, M.J. (2005) 'The frequency of calcium oscillations induced by 5-HT, ACH, and KCl determine the contraction of smooth muscle cells of intrapulmonary bronchioles', *Journal of General Physiology*, 125(6), pp. 535–553. doi:10.1085/jgp.200409216.

Persaud, S.J. and Bewick, G.A. (2014) 'Peptide YY: More than just an appetite regulator', *Diabetologia*, 57(9), pp. 1762–1769. doi:10.1007/s00125-014-3292-y.

Plamboeck, A., Holst, J.J., Carr, R.D. and Deacon, C.F. (2005) 'Neutral endopeptidase 24.11 and dipeptidyl peptidase IV are both mediators of the degradation of glucagon-like peptide 1 in the anaesthetised pig', *Diabetologia*, 48(9), pp. 1882–1890. doi:10.1007/s00125-005-1847-7.

Le Poul, E., Loison, C., Struyf, S., Springael, J.Y., Lannoy, V., Decobecq, M.E., Brezillon, S., Dupriez, V., Vassart, G., Van Damme, J., Parmentier, M. and Detheux, M. (2003) 'Functional characterization of human receptors for short chain fatty acids and their role in polymorphonuclear cell activation', *Journal of Biological Chemistry*, 278(28), pp. 25481–25489. doi:10.1074/jbc.M301403200.

Prasad-Reddy, L. and Isaacs, D. (2015) 'A clinical review of GLP-1 receptor agonists: Efficacy and safety in diabetes and beyond', *Drugs in Context*, pp. 1–19. doi:10.7573/dic.212283.

Prentki, M. and Nolan, C.J. (2006) 'Islet β cell failure in type 2 diabetes', *Journal of Clinical Investigation*, 116(7), pp. 1802–1812. doi:10.1172/JCI29103.

Prihandoko, R., Alvarez-Curto, E., Hudson, B.D., Butcher, A.J., Ulven, T., Miller, A.M., Tobin, A.B. and Milligan, G. (2016) 'Distinct phosphorylation clusters determine the signaling outcome of free fatty acid receptor 4/g protein-coupled receptor 120', *Molecular Pharmacology*, 89(5), pp. 505–520. doi:10.1124/mol.115.101949.

Prihandoko, R., Kaur, D., Wiegman, C.H., Alvarez-Curto, E., Donovan, C., Chachi, L., Ulven, T., Tyas, M.R., Euston, E., Dong, Z., Alharbi, A.G.M., Kim, R.Y., Lowe, J.G., Hansbro, P.M., Chung, K.F., Brightling, C.E., Milligan, G. and Tobin, A.B. (2020) 'Pathophysiological regulation of lung function by the free fatty acid receptor FFA4', *Science Translational Medicine*, 12(557), pp. 1–14. doi:10.1126/SCITRANSLMED.AAW9009.

Prömel, S., Langenhan, T. and Araç, D. (2013) 'Matching structure with function: The GAIN domain of Adhesion-GPCR and PKD1-like proteins', *Trends in Pharmacological Sciences*, 34(8), pp. 470–478. doi:10.1016/j.tips.2013.06.002.

Pronin, A.N., Tang, H., Connor, J. and Keung, W. (2004) 'Identification of ligands for two human bitter T2R receptors', *Chemical Senses*, 29(7), pp. 583–593. doi:10.1093/chemse/bjh064.

Protas, L., Shen, J.B. and Pappano, A.J. (1998) 'Carbachol increases contractions and intracellular Ca++ transients in guinea pig ventricular

myocytes', *Journal of Pharmacology and Experimental Therapeutics*, 284(1), pp. 66–74.

Psichas, A., Sleeth, M.L., Murphy, K.G., Brooks, L., Bewick, G.A., Hanyaloglu, A.C., Ghatei, M.A., Bloom, S.R. and Frost, G. (2015) 'The short chain fatty acid propionate stimulates GLP-1 and PYY secretion via free fatty acid receptor 2 in rodents', *International Journal of Obesity*, 39(3), pp. 424-429. doi:10.1038/ijo.2014.153.

Raehal, K.M., Walker, J.K.L. and Bohn, L.M. (2005) 'Morphine side effects in β-arrestin 2 knockout mice', *Journal of Pharmacology and Experimental Therapeutics*, 314(3), pp. 1195–1201. doi:10.1124/jpet.105.087254.

Rajagopal, S. and Shenoy, S.K. (2018) 'GPCR desensitization: Acute and prolonged phases', *Cellular Signalling*, 41, pp. 9–16. doi:10.1016/j.cellsig.2017.01.024.

Rao, J. and Wang, J. (2010) 'Intestinal Architecture and Development.', in *Regulation of Gastrointestinal Mucosal Growth*. San Rafael (CA): Morgan & Claypool Life Sciences. Available at: https://www.ncbi.nlm.nih.gov/books/NBK54098.

Rask-Andersen, M., Masuram, S. and Schiöth, H.B. (2014) 'The Druggable Genome: Evaluation of Drug Targets in Clinical Trials Suggests Major Shifts in Molecular Class and Indication', *Annual Review of Pharmacology and Toxicology*. doi:10.1146/annurev-pharmtox-011613-135943.

Redinger, R.N. (2007) 'The Pathophysiology of Obesity and Its Clinical Manifestations', *Gastroenterology and Hepatology*, 3(11), pp. 856–863. Available at: http://dx.doi.org/10.1016/j.brat.2010.04.003%0Ahttp://dx.doi.org/10.1016/j.jad.2013.04.028%0Ahttps://doi.org/10.1016/j.jad.2018.01.030%0Ahttp://dx.doi.org/10.1007/s00125-016-4062-9%0Ahttp://dx.doi.org/10.1016/S0140-6736(11)60602-8%0Ahttp://dx.doi.org/10.1.

Reimann, F., Habib, A.M., Tolhurst, G., Parker, H.E., Rogers, G.J. and Gribble,

F.M. (2008) 'Glucose Sensing in L Cells: A Primary Cell Study', *Cell Metabolism*, 8(6), pp. 532–539. doi:10.1016/j.cmet.2008.11.002.

Ring, J., Klimek, L. and Worm, M. (2018) 'Adrenaline in the acute treatment of anaphylaxis', *Deutsches Arzteblatt International*, 115(31–32), pp. 528–534. doi:10.3238/arztebl.2018.0528.

Roche, D., Gil, D. and Giraldo, J. (2013) 'Mechanistic analysis of the function of agonists and allosteric modulators: Reconciling two-state and operational models', *British Journal of Pharmacology*, 169(6), pp. 1189–1202. doi:10.1111/bph.12231.

Romanet-Manent, S., Charpin, D., Magnan, A., Lanteaume, A. and Vervloet, D. (2002) 'Allergic vs nonallergic asthma: What makes the difference?', *Allergy: European Journal of Allergy and Clinical Immunology*, 57(7), pp. 607–613. doi:10.1034/j.1398-9995.2002.23504.x.

Rosenbaum, D.M., Rasmussen, S.G.F. and Kobilka, B.K. (2009) 'The structure and function of G-protein-coupled receptors', *Nature*, 459(7245), pp. 356–363. doi:10.1038/nature08144.

Rosenkilde, M.M. and Schwartz, T.W. (2000) 'Potency of ligands correlates with affinity measured against agonist and inverse agonists but not against neutral ligand in constitutively active chemokine receptor', *Molecular Pharmacology*, 57(3), pp. 602–609. doi:10.1124/mol.57.3.602.

Rovati, G.E., Capra, V. and Neubig, R.R. (2007) 'The highly conserved DRY motif of class A G protein-coupled receptors: Beyond the ground state', *Molecular Pharmacology*, 71(4), pp. 959–964. doi:10.1124/mol.106.029470.

Ruan, Y.C., Zhou, W. and Chan, H.C. (2011) 'Regulation of smooth muscle contraction by the epithelium: role of prostaglandins.', *Physiology (Bethesda, Md.)*, 26(3), pp. 156–170. doi:10.1152/physiol.00036.2010.

Rubbino, F., Garlatti, V., Garzarelli, V., Massimino, L., Spanò, S., Iadarola, P., Cagnone, M., Giera, M., Heijink, M., Guglielmetti, S., Arena, V., Malesci, A.,

Laghi, L., Danese, S. and Vetrano, S. (2022) 'GPR120 prevents colorectal adenocarcinoma progression by sustaining the mucosal barrier integrity', *Scientific Reports*, 12(1), pp. 1–18. doi:10.1038/s41598-021-03787-7.

Russkamp, D., Aguilar-Pimentel, A., Alessandrini, F., Gailus-Durner, V., Fuchs, H., Ohnmacht, C., Chaker, A., de Angelis, M.H., Ollert, M., Schmidt-Weber, C.B. and Blank, S. (2019) 'IL-4 receptor α blockade prevents sensitization and alters acute and long-lasting effects of allergen-specific immunotherapy of murine allergic asthma', *Allergy: European Journal of Allergy and Clinical Immunology*, 74(8), pp. 1549–1560. doi:10.1111/all.13759.

Saisho, Y. (2015) 'ß-cell dysfunction: Its critical role in prevention and management of type 2 diabetes', *World Journal of Diabetes*, 6(1), p. 109. doi:10.4239/wjd.v6.i1.109.

Salahudeen, M.S. and Nishtala, P.S. (2017) 'An overview of pharmacodynamic modelling, ligand-binding approach and its application in clinical practice', *Saudi Pharmaceutical Journal*, 25(2), pp. 165–175. doi:10.1016/j.jsps.2016.07.002.

Sanches, J.M., Zhao, L.N., Salehi, A., Wollheim, C.B. and Kaldis, P. (2021) 'Pathophysiology of type 2 diabetes and the impact of altered metabolic interorgan crosstalk', *FEBS Journal*, pp. 1–29. doi:10.1111/febs.16306.

Santos, R., Ursu, O., Gaulton, A., Bento, A.P., Donadi, R.S., Bologa, C.G., Karlsson, A., Al-Lazikani, B., Hersey, A., Oprea, T.I. and Overington, J.P. (2016) 'A comprehensive map of molecular drug targets', *Nature Reviews Drug Discovery*, 16(1), pp. 19–34. doi:10.1038/nrd.2016.230.

Savage, A.P., Adrian, T.E., Carolan, G., Chatterjee, V.K. and Bloom, S.R. (1987) 'Effects of peptide YY (PYY) on mouth to caecum intestinal transit time and on the rate of gastric emptying in healthy volunteers', *Gut*, 28(2), pp. 166–170. doi:10.1136/gut.28.2.166.

Sawzdargo, M., George, S.R., Nguyen, T., Xu, S., Kolakowski, L.F. and O'dowd, B.F. (1997) 'A cluster of four novel human G protein-coupled receptor genes occurring in close proximity to CD22 gene on chromosome 19q13.1', *Biochemical*

and Biophysical Research Communications. doi:10.1006/bbrc.1997.7513.

Scarpa, M., Molloy, C., Jenkins, L., Strellis, B., Budgett, R.F., Hesse, S., Dwomoh, L., Marsango, S., Tejeda, G.S., Rossi, M., Ahmed, Z., Milligan, G., Hudson, B.D., Tobin, A.B. and Bradley, S.J. (2021) 'Biased M1 muscarinic receptor mutant mice show accelerated progression of prion neurodegenerative disease', *Proceedings of the National Academy of Sciences of the United States of America,* 118(50). doi:10.1073/pnas.2107389118.

Schiöth, H.B. and Fredriksson, R. (2005) 'The GRAFS classification system of G-protein coupled receptors in comparative perspective', *General and Comparative Endocrinology,* 142(1-2 SPEC. ISS.), pp. 94–101. doi:10.1016/j.ygcen.2004.12.018.

Schrage, R., Schmitz, A.-L., Evelyn Gaffal, S., Annala, S.K., Wenzel, D., M., K., Büllesbach, T.B., Inoue, A., Shinjo, Y., Galandrin, S., Shridhar, N., Hesse, M., Grundmann, M., Merten, N., Charpentier, T.H., Martz, M., Butcher, A.J., Slodczyk, T., Armando, S., *et al.* (2015) 'The experimental power of FR900359 to study Gq-regulated biological processes', *Nature Communications*, 6, pp. 1–7. doi:10.1038/ncomms10156.

Seger, R. and Krebs, E.G. (1995) 'The MAPK signaling cascade', *The FASEB Journal*, 9(9), pp. 726–735. doi:10.1096/fasebj.9.9.7601337.

Seino, Y., Fukushima, M. and Yabe, D. (2010) 'GIP and GLP-1, the two incretin hormones: Similarities and differences', *Journal of Diabetes Investigation*, 1(1–2), pp. 8–23. doi:10.1111/j.2040-1124.2010.00022.x.

Seumois, G., Chavez, L., Gerasimova, A., Lienhard, M., Omran, N., Kalinke, L., Vedanayagam, M., Ganesan, A.P. V., Chawla, A., Djukanović, R., Ansel, K.M., Peters, B., Rao, A. and Vijayanand, P. (2014) 'Epigenomic analysis of primary human T cells reveals enhancers associated with TH2 memory cell differentiation and asthma susceptibility', *Nature Immunology*, 15(8), pp. 777–788. doi:10.1038/ni.2937.

Shapiro, H., Shachar, S., Sekler, I., Hershfinkel, M. and Walker, M.D. (2005)

'Role of GPR40 in fatty acid action on the β cell line INS-1E', *Biochemical and Biophysical Research Communications*. doi:10.1016/j.bbrc.2005.07.042.

Sharma, D., Verma, S., Vaidya, S., Kalia, K. and Tiwari, V. (2018) 'Recent updates on GLP-1 agonists: Current advancements & challenges', *Biomedicine and Pharmacotherapy*, pp. 952–962. doi:10.1016/j.biopha.2018.08.088.

Shavadia, J.S., Sharma, A., Gu, X., Neaton, J., DeLeve, L., Holmes, D., Home, P., Eckel, R.H., Watkins, P.B. and Granger, C.B. (2019) 'Determination of fasiglifam-induced liver toxicity: Insights from the data monitoring committee of the fasiglifam clinical trials program', *Clinical Trials*, 16(3), pp. 253–262. doi:10.1177/1740774519836766.

Shenoy, S.K., Drake, M.T., Nelson, C.D., Houtz, D.A., Xiao, K., Madabushi, S., Reiter, E., Premont, R.T., Lichtarge, O. and Lefkowitz, R.J. (2006) 'β-arrestin-dependent, G protein-independent ERK1/2 activation by the β2 adrenergic receptor', *Journal of Biological Chemistry*, 281(2), pp. 1261–1273. doi:10.1074/jbc.M506576200.

Shimabukuro, M., Zhou, Y.T., Levi, M. and Unger, R.H. (1998) 'Fatty acid-induced β cell apoptosis: A link between obesity and diabetes', *Proceedings of the National Academy of Sciences of the United States of America*, 95(5), pp. 2498–2502. doi:10.1073/pnas.95.5.2498.

Shimpukade, B., Hudson, B.D., Hovgaard, C.K., Milligan, G. and Ulven, T. (2012) 'Discovery of a potent and selective GPR120 agonist', *Journal of Medicinal Chemistry*, 55(9), pp. 4511–4515. doi:10.1021/jm300215x.

Shukla, A.K., Westfield, G.H., Xiao, K., Reis, R.I., Huang, L.Y., Tripathi-Shukla, P., Qian, J., Li, S., Blanc, A., Oleskie, A.N., Dosey, A.M., Su, M., Liang, C.R., Gu, L.L., Shan, J.M., Chen, X., Hanna, R., Choi, M., Yao, X.J., *et al.* (2014) 'Visualization of arrestin recruitment by a G-protein-coupled receptor', *Nature*, 512(7513), pp. 218–222. doi:10.1038/nature13430.

Sieber, J. and Jehle, A.W. (2014) 'Free fatty acids and their metabolism affect function and survival of podocytes', *Frontiers in Endocrinology*, 5(OCT), pp. 1–7.

doi:10.3389/fendo.2014.00186.

Siehler, S. (2009) 'Regulation of RhoGEF proteins by G 12/13-coupled receptors', *British Journal of Pharmacology*, 158(1), pp. 41–49. doi:10.1111/j.1476-5381.2009.00121.x.

Small, C.J., Herzogk, H., Cohen, M.A., Dakin, C.L., Wren, A.M., Brynes, A.E., Ghatei, M.A. and Bloom, S.R. (2002) 'Gut hormone PYY 3-36 physiologically inhibits food intake', *Nature*, 418(August), pp. 728–730. Available at: https://idp.nature.com/authorize/casa?redirect_uri=https://www.nature.com/articles/nature00887&casa_token=3AU8AVRKV3YAAAAA:QFBFVbrr987mRQljNGqf NxoX_wDM413EBMsL8jsUfZYuXoJc7t9fyeNetRtZA0RvgtLmx3F1XAne86jXZA.

Smith, N.J., Stoddart, L.A., Devine, N.M., Jenkins, L. and Milligan, G. (2009) 'The action and mode of binding of thiazolidinedione ligands at free fatty acid receptor 1', *Journal of Biological Chemistry*, 284(26), pp. 17527–17539. doi:10.1074/jbc.M109.012849.

Sojka, A.C., Brennan, K.M., Maizels, E.T. and Young, C.D. (2017) 'The Science Behind G Protein-Coupled Receptors (GPCRs) and Their Accurate Visual Representation in Scientific Research', *Journal of Biocommunication*, 41(1). Available at: http://firstmonday.org/ojs/index.php/jbc/article/view/7309/6067.

Somers, R.L. and Klein, D.C. (1984) 'Rhodopsin kinase activity in the mammalian pineal gland and other tissues', *Science*, 226(4671), pp. 184–187. doi:10.1126/science.6091271.

Somlyo, A.P. and Somlyo, A. V (2003) 'Ca2+ sensitivity of smooth muscle and nonmuscle myosin II: Modulated by G proteins, kinases, and myosin phosphatase', *Physiological Reviews*, pp. 1325–1358. doi:10.1152/physrev.00023.2003.

Song, T., Peng, Jie, Ren, J., Wei, H.K. and Peng, Jian (2015) 'Cloning and characterization of spliced variants of the porcine G protein coupled receptor 120', *BioMed Research International*, 2015(L). doi:10.1155/2015/813816.

Sparks, S.M., Chen, G., Collins, J.L., Danger, D., Dock, S.T., Jayawickreme, C., Jenkinson, S., Laudeman, C., Leesnitzer, M.A., Liang, X., Maloney, P., McCoy, D.C., Moncol, D., Rash, V., Rimele, T., Vulimiri, P., Way, J.M. and Ross, S. (2014a) 'Identification of diarylsulfonamides as agonists of the free fatty acid receptor 4 (FFA4/GPR120)', *Bioorganic and Medicinal Chemistry Letters*, 24(14), pp. 3100–3103. doi:10.1016/j.bmcl.2014.05.012.

Spector, A.A., John, K. and Fletcher, J.E. (1969) 'Binding of long-chain fatty acids to bovine serum albumin.', *Journal of Lipid Research*, 10(1), pp. 56–67. doi:10.1016/s0022-2275(20)42649-5.

Spreckley, E. and Murphy, K.G. (2015) 'The L-cell in nutritional sensing and the regulation of appetite', *Fronteirs in Nutrition*, 2(July), pp. 1–17. doi:10.3389/fnut.2015.00023.

Sriram, K. and Insel, P.A. (2018) 'G protein-coupled receptors as targets for approved drugs: How many targets and how many drugs?', *Molecular Pharmacology*, 93(4), pp. 251–258. doi:10.1124/mol.117.111062.

Stanford, K.I. and Goodyear, L.J. (2014) 'Exercise and type 2 diabetes: Molecular mechanisms regulating glucose uptake in skeletal muscle', *Advances in Physiology Education*, 38(4), pp. 308–314. doi:10.1152/advan.00080.2014.

Stoddart, L.A., Brown, A.J. and Milligan, G. (2007) 'Uncovering the pharmacology of the G protein-coupled receptor GPR40: High apparent constitutive activity in guanosine 5′-O-(3-[35S]thio) triphosphate binding studies reflects binding of an endogenous agonist', *Molecular Pharmacology*, 71(4), pp. 994–1005. doi:10.1124/mol.106.031534.

Stoddart, L.A., Smith, N.J. and Milligan, G. (2008) 'International union of pharmacology. LXXI. Free fatty acid receptors FFA1, -2, and -3: Pharmacology and pathophysiological functions', *Pharmacological Reviews*, 60(4), pp. 405–417. doi:10.1124/pr.108.00802.

Stone, V.M., Dhayal, S., Brocklehurst, K.J., Lenaghan, C., Sörhede Winzell, M., Hammar, M., Xu, X., Smith, D.M. and Morgan, N.G. (2014) 'GPR120 (FFAR4) is

preferentially expressed in pancreatic delta cells and regulates somatostatin secretion from murine islets of Langerhans', *Diabetologia*, 57(6), pp. 1182–1191. doi:10.1007/s00125-014-3213-0.

Strange, P.G. (2008) 'Agonist binding, agonist affinity and agonist efficacy at G protein-coupled receptors', *British Journal of Pharmacology*, 153(7), pp. 1353–1363. doi:10.1038/sj.bjp.0707672.

Suckow, A.T., Polidori, D., Yan, W., Chon, S., Ma, J.Y., Leonard, J. and Briscoe, C.P. (2014) 'Alteration of the glucagon axis in GPR120 (FFAR4) knockout mice: A role for gpr120 in glucagon secretion', *Journal of Biological Chemistry*, 289(22), pp. 15751–15763. doi:10.1074/jbc.M114.568683.

Sundström, L., Myhre, S., Sundqvist, M., Ahnmark, A., McCoull, W., Raubo, P., Groombridge, S.D., Polla, M., Nyström, A.C., Kristensson, L., Någård, M. and Winzell, M.S. (2017) 'The acute glucose lowering effect of specific GPR120 activation in mice is mainly driven by glucagon-like peptide 1', *PLoS ONE*, 12(12), pp. 1–22. doi:10.1371/journal.pone.0189060.

Suzuki, T., Igari, S.I., Hirasawa, A., Hata, M., Ishiguro, M., Fujieda, H., Itoh, Y., Hirano, T., Nakagawa, H., Ogura, M., Makishima, M., Tsujimoto, G. and Miyata, N. (2008) 'Identification of G protein-coupled receptor 120-selective agonists derived from PPARγ agonists', *Journal of Medicinal Chemistry*, 51(23), pp. 7640–7644. doi:10.1021/jm800970b.

Syrovatkina, V., Alegre, K.O., Dey, R. and Huang, X.Y. (2016) 'Regulation, Signaling, and Physiological Functions of G-Proteins', *Journal of Molecular Biology*, 428(19), pp. 3850–3868. doi:10.1016/j.jmb.2016.08.002.

Szczepek, M., Beyrière, F., Hofmann, K.P., Elgeti, M., Kazmin, R., Rose, A., Bartl, F.J., Von Stetten, D., Heck, M., Sommer, M.E., Hildebrand, P.W. and Scheerer, P. (2014) 'Crystal structure of a common GPCR-binding interface for G protein and arrestin', *Nature Communications*, 5(4801). doi:10.1038/ncomms5801.

Tanaka, T., Katsuma, S. and Adachi, T. (2008) 'Free fatty acids induce

cholecystokinin secretion through GPR120', *Naunyn Schmiedebergs Arch Pharmacol*, 377(4–6), pp. 523–527. doi:10.1007/s00210-007-0200-8.

Tanaka, T., Yano, T., Adachi, T., Koshimizu, T.A., Hirasawa, A. and Tsujimoto, G. (2008) 'Cloning and characterization of the rat free fatty acid receptor GPR120: In vivo effect of the natural ligand on GLP-1 secretion and proliferation of pancreatic β cells', in *Naunyn-Schmiedeberg's Archives of Pharmacology*, pp. 515–522. doi:10.1007/s00210-007-0250-y.

Tanaka, Y., Horinouchi, T. and Koike, K. (2005) 'New insights into β-adrenoceptors in smooth muscle: Distribution of receptor subtypes and molecular mechanisms triggering muscle relaxation', *Clinical and Experimental Pharmacology and Physiology*, 32(7), pp. 503–514. doi:10.1111/j.1440-1681.2005.04222.x.

Tang, X.L., Wang, Y., Li, D.L., Luo, J. and Liu, M.Y. (2012) 'Orphan G protein-coupled receptors (GPCRs): Biological functions and potential drug targets', *Acta Pharmacologica Sinica*, pp. 363–371. doi:10.1038/aps.2011.210.

Tate, K.M., Briend-Sutren, M. -M, Emorine, L.J., Delavier-Klutchko, C., Marullo, S. and Strosberg, A.D. (1991) 'Expression of three human β-adrenergic-receptor subtypes in transfected chinese hamster ovary cells', *European Journal of Biochemistry*, 196(2), pp. 357–361. doi:10.1111/j.1432-1033.1991.tb15824.x.

Taussig, R., Iñiguez-Lluhi, J.A. and Gilman, A.G. (1993) 'Inhibition of adenylyl cyclase by Giα', *Science*, 261(5118), pp. 218–221. doi:10.1126/science.8327893.

Tazoe, H., Otomo, Y., Karaki, S.I., Kato, I., Fukami, Y., Terasaki, M. and Kuwahara, A. (2009) 'Expression of short-chain fatty acid receptor GPR41 in the human colon', *Biomedical Research*, 30(3), pp. 149–156. doi:10.2220/biomedres.30.149.

Tesmer, V.M., Kawano, T., Shankaranarayanan, A., Kozasa, T. and Tesmer, J.J.G. (2005) 'Structural biology: Snapshot of activated G proteins at the membrane: The Gαq-GRK2-Gβγ complex', *Science*, 310(5754), pp. 1686–1690. doi:10.1126/science.1118890.

Thompson, G.L., Kelly, E., Christopoulos, A. and Canals, M. (2015) 'Novel GPCR paradigms at the μ-opioid receptor', *British Journal of Pharmacology*, 172(2), pp. 287–296. doi:10.1111/bph.12600.

Thomsen, A.R.B., Plouffe, Bianca, Cahill Iii, T.J., Shukla, A.K., Tarrasch, J.T., Dosey, A.M., Kahsai, A.W., Strachan, R.T., Pani, Biswaranjan, Mahoney, J.P., Huang, L., Breton, B., Heydenreich, F.M., Sunahara, R.K., Skiniotis, G., Bouvier, M., Lefkowitz, R.J., Conceptualization, A.R.B.T., Plouffe, B, *et al.* (2016) 'GPCR-G Protein-β-Arrestin Super-Complex Mediates Sustained G Protein Signaling HHS Public Access In Brief Megaplexes containing a GPCR simultaneously engaged with a G protein and β-arrestin sustain G protein signaling following internalization into endoso', *Cell*, 166(4), pp. 907–919. doi:10.1016/j.cell.2016.07.004.GPCR-G.

Tobin, A.B. (2008) 'G-protein-coupled receptor phosphorylation: Where, when and by whom', in *British Journal of Pharmacology*, pp. 167–176. doi:10.1038/sj.bjp.0707662.

Tolhurst, G., Heffron, H., Lam, Y.S., Parker, H.E., Habib, A.M., Diakogiannaki, E., Cameron, J., Grosse, J., Reimann, F. and Gribble, F.M. (2012) 'Short-chain fatty acids stimulate glucagon-like peptide-1 secretion via the G-protein-coupled receptor FFAR2', *Diabetes*, 61(2), pp. 364–371. doi:10.2337/db11-1019.

Torrecilla, I., Spragg, E.J., Poulin, B., McWilliams, P.J., Mistry, S.C., Blaukat, A. and Tobin, A.B. (2007) 'Phosphorylation and regulation of a G protein-coupled receptor by protein kinase CK2', *Journal of Cell Biology*, 177(1), pp. 127–137. doi:10.1083/jcb.200610018.

Tough, I.R., Forbes, S., Tolhurst, R., Ellis, M., Herzog, H., Bornstein, J.C. and Cox, H.M. (2011) 'Endogenous peptide YY and neuropeptide y inhibit colonic ion transport, contractility and transit differentially via Y 1 and Y 2 receptors', *British Journal of Pharmacology*, 164(2 B), pp. 471–484. doi:10.1111/j.1476-5381.2011.01401.x.

Traves, S.L., Culpitt, S. V., Russell, R.E.K., Barnes, P.J. and Donnelly, L.E. (2002) 'Increased levels of the chemokines GROα and MCP-1 in sputum samples

from patients with COPD', *Thorax*, 57(7), pp. 590–595. doi:10.1136/thorax.57.7.590.

Trivedi, M. and Denton, E. (2019) 'Asthma in children and adults—what are the differences and what can they tell us about asthma?', *Frontiers in Pediatrics*, 7(JUN), pp. 1–15. doi:10.3389/fped.2019.00256.

Upadhyaya, J., Singh, N., Bhullar, R.P. and Chelikani, P. (2015) 'The structure-function role of C-terminus in human bitter taste receptor T2R4 signaling', *Biochimica et Biophysica Acta - Biomembranes*, 1848(7), pp. 1502–1508. doi:10.1016/j.bbamem.2015.03.035.

Valant, C., Robert Lane, J., Sexton, P.M. and Christopoulos, A. (2012) 'The best of both worlds? bitopic orthosteric/allosteric ligands of g proteincoupled receptors', *Annual Review of Pharmacology and Toxicology*, 52, pp. 153–178. doi:10.1146/annurev-pharmtox-010611-134514.

Varga, T., Czimmerer, Z. and Nagy, L. (2011) 'PPARs are a unique set of fatty acid regulated transcription factors controlling both lipid metabolism and inflammation', *Biochimica et Biophysica Acta - Molecular Basis of Disease*, 1812(8), pp. 1007–1022. doi:10.1016/j.bbadis.2011.02.014.

Venter, C.J., Adams, M.D., Myers, E.W., Li, P.W., Mural, R.J., Sutton, G.G., Smith, H.O., Yandell, M., Evans, C.A., Holt, R.A., Gocayne, J.D., Amanatides, P., Ballew, R.M., Huson, D.H., Wortman, J.R., Zhang, Q., Kodira, C.D., Zheng, X.H., Chen, L., *et al.* (2001) 'The sequence of the human genome', *Science*, 291(5507), pp. 1304–1351. doi:10.1126/science.1058040.

Vizurraga, A., Adhikari, R., Yeung, J., Yu, M. and Tall, G.G. (2020) 'Mechanisms of adhesion G protein–coupled receptor activation', *Journal of Biological Chemistry*, 295(41), pp. 14065–14083. doi:10.1074/jbc.REV120.007423.

Vos, T., Allen, C., Arora, M., Barber, R.M., Brown, A., Carter, A., Casey, D.C., Charlson, F.J., Chen, A.Z., Coggeshall, M., Cornaby, L., Dandona, L., Dicker, D.J., Dilegge, T., Erskine, H.E., Ferrari, A.J., Fitzmaurice, C., Fleming, T., Forouzanfar, M.H., *et al.* (2016) 'Global, regional, and national incidence,

prevalence, and years lived with disability for 310 diseases and injuries, 1990–2015: a systematic analysis for the Global Burden of Disease Study 2015', *The Lancet*. doi:10.1016/S0140-6736(16)31678-6.

Vusse, G.J. van der (2009) 'Albumin as Fatty Acid Transporter', *Drug Metabolism and Pharmacokinetics*, 24(4), pp. 300–307. Available at: https://www.jstage.jst.go.jp/article/dmpk/24/4/24_4_300/_pdf.

Watson, S.J., Brown, A.J.H. and Holliday, N.D. (2012) 'Differential signaling by splice variants of the human free fatty acid receptor GPR120', *Molecular Pharmacology*, 81(5), pp. 631–642. doi:10.1124/mol.111.077388.

Watterson, K.R., Hansen, S.V.F., Hudson, B.D., Alvarez-Curto, E., Raihan, S.Z., Azevedo, C.M.G., Martin, G., Dunlop, J., Yarwood, S.J., Ulven, T. and Milligan, G. (2017) 'Probe-dependent negative allosteric modulators of the long-chain free fatty acid receptor FFA4', *Molecular Pharmacology,* 91(6), pp. 630-641. doi:10.1124/mol.116.107821.

Watterson, K.R., Hudson, B.D., Ulven, T. and Milligan, G. (2014) 'Treatment of type 2 diabetes by free fatty acid receptor agonists', *Frontiers in Endocrinology*, 5(137). doi:10.3389/fendo.2014.00137.

Weatherall, M. (1966) 'The meaning and importance of drug potency in medicine', *Clinical Pharmacology and Therapeutics*, 7(5), pp. 577–582. doi:10.1002/cpt196675577.

Webb, R.C. (2003) 'Smooth muscle contraction and relaxation', *American Journal of Physiology - Advances in Physiology Education*, 27(1–4), pp. 201–206. doi:10.1152/advan.00025.2003.

Weis, W.I. and Kobilka, B.K. (2018) 'The Molecular Basis of G Protein-Coupled Receptor Activation', *Annual Review of Biochemistry*, 87(June), pp. 897–919. doi:10.1146/annurev-biochem-060614-033910.The.

Weiss, E.R., Ducceschi, M.H., Horner, T.J., Li, A., Craft, C.M. and Osawa, S. (2001) 'Species-specific differences in expression of G-protein-coupled receptor

kinase (GRK) 7 and GRK1 in mammalian cone photoreceptor cells: Implications for cone cell phototransduction', *Journal of Neuroscience*, 21(23), pp. 9175–9184. doi:10.1523/jneurosci.21-23-09175.2001.

Wendell, S.G., Fan, H. and Zhang, C. (2020) 'G protein–coupled receptors in asthma therapy: Pharmacology and drug actions', *Pharmacological Reviews*, 72(1), pp. 1–49. doi:10.1124/pr.118.016899.

Wenzel-Seifert, K. and Siefert, R. (2000) 'Molecular Analysis of b2-Adrenoceptor Coupling to Gs-, Gi -, and Gq-Proteins', *Molecular Pharmacology*, 58(5), pp. 954–966. doi:10.1016/j.mce.2019.02.006.

Wettschureck, N. and Offermanns, S. (2005) 'Mammalian G proteins and their cell type specific functions', *Physiological Reviews*, 85(4), pp. 1159–1204. doi:10.1152/physrev.00003.2005.

Wilden, U., Hall, S.W. and Kuhn, H. (1986) 'Phosphodiesterase activation by photoexcited rhodopsin is quenched when rhodopsin is phosphorylated and binds the intrinsic 48-kDa protein of rod outer segments', *Proceedings of the National Academy of Sciences of the United States of America*, 83(5), pp. 1174–1178. doi:10.1073/pnas.83.5.1174.

Wootten, D., Christopoulos, A., Marti-Solano, M., Babu, M.M. and Sexton, P.M. (2018) 'Mechanisms of signalling and biased agonism in G protein-coupled receptors', *Nature Reviews Molecular Cell Biology*, 19(10), pp. 638–653. doi:10.1038/s41580-018-0049-3.

Wu, H., Wang, C., Gregory, K.J., Han, G.W., Cho, H.P., Xia, Y., Niswender, C.M., Katritch, V., Meiler, J., Cherezov, V., Conn, P.J. and Stevens, R.C. (2014) 'Structure of a class C GPCR metabotropic glutamate receptor 1 bound to an allosteric modulator', *Science*, 344(6179), pp. 58–64. doi:10.1126/science.1249489.

Wu, N., Macion-Dazard, R., Nithianantham, S., Xu, Z., Hanson, S.M., Vishnivetskiy, S.A., Gurevich, V. V., Thibonnier, M. and Shoham, M. (2006) 'Soluble mimics of the cytoplasmic face of the human V1-vascular vasopressin

receptor bind arrestin2 and calmodulin', *Molecular Pharmacology*, 70(1), pp. 249–258. doi:10.1124/mol.105.018804.

Xiao, R.P., Ji, X. and Lakatta, E.G. (1995) 'Functional coupling of the β2-adrenoceptor to a pertussis toxin- sensitive G protein in cardiac myocytes', *Molecular Pharmacology*, 47(2), pp. 322–329.

Xiong, Y., Swaminath, G., Cao, Q., Yang, L., Guo, Q., Salomonis, H., Lu, J., Houze, J.B., Dransfield, P.J., Wang, Y., Liu, J.J., Wong, S., Schwandner, R., Steger, F., Baribault, H., Liu, L., Coberly, S., Miao, L., Zhang, J., *et al.* (2013) 'Activation of FFA1 mediates GLP-1 secretion in mice. Evidence for allosterism at FFA1', *Molecular and Cellular Endocrinology*, 369(1–2), pp. 119–129. doi:10.1016/j.mce.2013.01.009.

Yang, L.K., Hou, Z.S. and Tao, Y.X. (2021) 'Biased signaling in naturally occurring mutations of G protein-coupled receptors associated with diverse human diseases', *Biochimica et Biophysica Acta - Molecular Basis of Disease*, 1867(1), p. 165973. doi:10.1016/j.bbadis.2020.165973.

Zamarbide, M., Etayo-Labiano, I., Ricobaraza, A., Martínez-Pinilla, E., Aymerich, M.S., Luis Lanciego, J., Pérez-Mediavilla, A. and Franco, R. (2014) 'GPR40 activation leads to CREB and ERK phosphorylation in primary cultures of neurons from the mouse CNS and in human neuroblastoma cells', *Hippocampus*, 27(7), pp. 733-739. doi:10.1002/hipo.22263.

Zatterale, F., Longo, M., Naderi, J., Raciti, G.A., Desiderio, A., Miele, C. and Beguinot, F. (2020) 'Chronic Adipose Tissue Inflammation Linking Obesity to Insulin Resistance and Type 2 Diabetes', *Frontiers in Physiology*, 10(January), pp. 1–20. doi:10.3389/fphys.2019.01607.

Zhang, D., Zhao, Q. and Wu, B. (2015) 'Structural studies of G protein-coupled receptors', *Molecules and Cells*, 38(10), pp. 836–842. doi:10.14348/molcells.2015.0263.

Zhang, R. and Xie, X. (2012) 'Tools for GPCR drug discovery', *Acta Pharmacologica Sinica*, 33(3), pp. 372–384. doi:10.1038/aps.2011.173.

Zhao, X., Yokoyama, K., Whitten, M.E., Huang, J., Gelb, M.H. and Palczewski, K. (1999) 'A novel form of rhodopsin kinase from chicken retina and pineal gland', *FEBS Letters*, 454(1–2), pp. 115–121. doi:10.1016/S0014-5793(99)00764-4.

Zhou, G., Myers, R., Li, Y., Chen, Y., Shen, X., Fenyk-Melody, J., Wu, M., Ventre, J., Doebber, T., Fujii, N., Musi, N., Hirshman, M.F., Goodyear, L.J. and Moller, D.E. (2001) 'Role of AMP-activated protein kinase in mechanism of metformin action', *Journal of Clinical Investigation*, 108(8), pp. 1167–1174. doi:10.1172/JCI13505.